

6-25-2020

Studies of Quaternary Depositional Systems of the Coastal Plain and Inner Continental Shelf along the Georgia Bight: South Carolina and Georgia, U.S.A.

Joshua H. Long
Coastal Carolina University

Follow this and additional works at: <https://digitalcommons.coastal.edu/etd>



Part of the [Geology Commons](#), [Oceanography Commons](#), and the [Sedimentology Commons](#)

Recommended Citation

Long, Joshua H., "Studies of Quaternary Depositional Systems of the Coastal Plain and Inner Continental Shelf along the Georgia Bight: South Carolina and Georgia, U.S.A." (2020). *Electronic Theses and Dissertations*. 117.

<https://digitalcommons.coastal.edu/etd/117>

This Dissertation is brought to you for free and open access by the College of Graduate Studies and Research at CCU Digital Commons. It has been accepted for inclusion in Electronic Theses and Dissertations by an authorized administrator of CCU Digital Commons. For more information, please contact commons@coastal.edu.

Studies of Quaternary Depositional Systems of the Coastal Plain and Inner
Continental Shelf along the Georgia Bight: South Carolina and Georgia, U.S.A.

by
Joshua H. Long
Ph.D. Dissertation

Bachelor of Science, Geology
University of Maryland, College Park, 2004

Master of Science, Geology
Northern Arizona University, 2008

Submitted to the faculty at Coastal Carolina University in partial fulfillment of the requirements
for the degree of Doctor of Philosophy in Marine Science

Department of Coastal and Marine Systems Science
School of the Coastal Environment
Coastal Carolina University
2020

Ph.D. Advisor

Till Hanebuth, Ph.D.

Committee:

Andrea Hawkes, Ph.D.

University of North Carolina, Wilmington

Scott Howard, Ph.D.

South Carolina Geological Survey

Richard Viso, Ph.D.

Coastal Carolina University

Thomas Lüdmann, Ph.D.

University of Hamburg, Germany

Zhixiong Shen, Ph.D.

Coastal Carolina University

Dedication

This project is dedicated to my girls Ashley, Amelia, and Eva Long for their continuous motivation, inspiration, and support over the last few years and to my parents, Janet and Jerry Long, for their love and support.

Acknowledgements

I thank my advisor, Dr. Till Hanebuth, and committee members for their guidance and involvement throughout the writing process.

Thanks to the South Carolina Geological Survey for both technical and financial support particularly Dr. Scott Howard, Katherine Luciano, and Dr. William Doar III. Captain James Phillips, Evan Roberts, Ashley Long, and Dr. Jenna Hill from Coastal Carolina University (CCU) helped immensely with data acquisition and processing. The manuscripts included as part of this document benefitted from input by Dr. Clark Alexander and Claudia Venherm (Skidaway Institute of Oceanography), and Dr. John Wehmiller (University of Delaware).

I very much appreciate the help in the field provided by students in the Coastal Geosystems Research Group at CCU, particularly John Durica.

Table of Contents

Chapter 1: Introduction.....	4
Chapter 2: The Quaternary Stratigraphic Architecture of a Low-Accommodation, Passive-Margin Continental Shelf (Santee Delta Region, South Carolina, U.S.A.)	22
Chapter 3: Depositional Environments Preserved within Quaternary Paleochannel Systems Offshore of the Georgia Bight, Southeastern U.S.A	83
Chapter 4: Late Holocene Stratigraphy and Facies Distributions of an Anthropogenically-modified Delta Plain (Santee Delta, SC, U.S.A.)	132
Chapter 5: Summary of Results and Conclusions	183
Chapter 6: Future Work.....	193
References.....	202
Appendices	
A. Sediment Core Inventory.....	230
B. Associated Reports and Summaries.....	232
C. Related Conference Presentations.....	233

Chapter 1

Introduction

Research Topics and Structure of Dissertation

The research presented here consists of three component studies. These studies focus on understanding the sedimentary successions deposited in a range of non-marine, paralic, and offshore environments along the modern coastal plain and inner shelf offshore of South Carolina and Georgia to better understand how this region has evolved since the beginning of the Quaternary Period. While these studies share common objectives and methodologies, they are focused on neighboring geographic areas (Fig. 1.1) and attempt to resolve paleoenvironmental change over different temporal and spatial scales. Collectively, these three studies contribute to the understanding of how local and regional, as well as natural and anthropogenic forcing mechanisms have influenced non-marine, coastal, and marine depositional systems across the Georgia Bight throughout the Quaternary.

While temporal and spatial scales vary from one topic to another, each study poses the same basic questions: how can we use the stratigraphy of the area to reconstruct its geological history and how has this history been influenced by various forcing mechanisms? The technical flowchart summarizes the common approach taken in all studies to address these questions (Fig. 1.2) Using both geological and geophysical input data I interpret lithofacies, key bounding surfaces, and seismic facies to define the stratigraphic architecture within the study areas. Both newly-acquired and existing geological data including sediment cores, borehole logs, and surface sediment samples provide the foundation for sedimentological, paleontological, and geochemical analyses. Geophysical data bathymetric data provide information about the geometry and distribution of subsurface stratigraphic units as well as surface morphology. When calibrated with

geochronological data, including AMS-¹⁴C and Amino Acid Racemization analyses, this stratigraphic framework yields valuable information about the geologic history on both local and regional scales. The development and evolution of depositional systems within the study areas associated with piedmont-draining and coastal plain rivers, estuaries, barrier islands, deltas, and offshore environments are related to changes in sediment supply and accommodation driven by climate, sea level, and tectonics over long time periods, and by autogenic processes and anthropogenic influences over shorter time periods (Fig. 1.2).

A central focus of two out of the three integrated studies presented here is the Santee River and its delta. The Santee is the largest river within the Georgia Bight, is the second largest on the U.S. east coast in terms of drainage area and water discharge and has been a significant sediment source to the coastal plain and inner continental shelf throughout the Quaternary (Colquhoun et al. 1972; USGS, 1991; Weems et al. 1994). Currently in a destructive phase, the Santee Delta is small by comparison to other Holocene deltas, however its size and lack of modern infrastructure make it an ideal laboratory for studying fluvial, deltaic, estuarine, and marine processes and products.

Research Topic 1 is the thematically broadest of the three proposed studies and focuses on the regional Quaternary evolution of the Santee River delta and surrounding areas with the overall goal of building a coherent stratigraphic framework as tool for understanding the geologic evolution of this region. This study covers an approximate area of 7,500 km² across the coastal plain and continental shelf of central South Carolina and incorporates both new and existing borehole, sediment core, and high-resolution seismo-acoustic (Chirp) data.

The focus of Research Topic 2 is on the distribution, morphology, and sedimentology of paleochannel networks preserved along the inner shelf of South Carolina and Georgia using a dense set of newly-acquired geophysical and geological data. These data were acquired as part of

a BOEM sand resource assessment and distributed across eight discrete focus areas from the norther border of South Carolina to the southern border of Georgia. From these data I reconstruct the planform and cross-sectional morphology and describe the sedimentary successions associated with complex networks of paleoincisions. Additionally, I have attempted to quantify the distribution of paleochannel types and use this distribution to define a regional trend in both paleochannel development and preservation.

Research Topic 3 focuses on the later Holocene stratigraphy and modern depositional environments of the Santee delta plain. The goal of this study is to evaluate the paleoenvironmental variability of the Santee delta plain throughout the Holocene and compare the modern anthropogenically-modified delta plain to the depositional environments of the pre-human environments as they are preserved in the subsurface.

These three studies benefited greatly from collaboration with scientists from several organizations and universities including the South Carolina Geological Survey; University of North Carolina, Wilmington; University of Hamburg, Germany; University of Delaware; and the University of Georgia Skidaway Institute of Oceanography.

Regional Setting

Throughout the Quaternary period high-frequency fluctuations in relative sea level driven primarily by glacioeustacy have exerted a primary control on the nature and distribution of coastal depositional systems along continental shelf and coastal plain of the southeastern United States (Cooke, 1936; Colquhoun, 1961; Colquhoun, 1995; Gayes et al., 1992; Denny et al., 2013; Doar, 2014). Although the continental shelf of central South Carolina is situated along a passive margin, syn- and post-depositional modifications have been affected by dynamic topography, neotectonics, glacioisostacy, and hydroisostacy. These modifications have altered not only the original

elevations of these deposits but they may also have influenced accommodation and regional topographic and bathymetric gradients throughout the Quaternary (Colquhoun, 1995; Baldwin et al., 2006; Weems & Lewis, 2002; Bartholomew & Rich, 2012; Rovere et al., 2014; Moucha et al., 2008; Rowley et al., 2013; Englehart et al., 2011). Regional climatic fluctuations at the millennial to decadal scale influence storm frequency and intensity, vegetation patterns, sediment supply, and precipitation (Cronin et al., 1981; Leigh, 2006; Wright et al., 2017). In addition to these allogenic forcing mechanisms, autogenic processes, those that are intrinsic to the depositional setting (Reading and Levell, 2006; Hajek and Straub, 2017), within these complex systems strongly influence the stratigraphic record and act to modulate allogenic signals. Processes such as channel avulsion, spit and bar migration, as well as storm-related deposition occur over much shorter time scales compared to allogenic processes. They exert a significant influence on the geomorphology, and as a product, the stratigraphy, associated with depositional systems (Kim et al., 2006; Hajek and Straub, 2017).

The relatively stable, broad, low-gradient continental shelf of the southeastern United States is an overall low accommodation setting. Accommodation, as used here, adheres to Jervey's (1988) definition as the space below base level, above the depositional surface, and it represents an estimation of the potential preservation space available for sediment. Base level refers to a dynamic, largely conceptual, surface of equilibrium between erosion and deposition (Cross, 1991; Catuneanu, 2006). In offshore settings, accommodation is approximately the height between the seafloor and the regional wave base (Catuneanu, 2006). The across-shelf migration of shoreline and associated environments in response to changes in relative sea level within an overall low accommodation setting has resulted in a complex modern onshore stratigraphy that consists of a series of seaward-stepping scarps and terraces that were deposited during Pliocene and Pleistocene

relative sea level (RSL) highstands (Cooke, 1936). These scarps and terraces decrease in both age and elevation towards the coast and preserve highstand barrier and backbarrier systems deposited above a composite transgressive erosional surface (Doar and Kendall, 2014). Their current elevations are a product of post-depositional regional isostatic and tectonic uplift (Doar, 2014).

Applications and Relevance

In addition to a detailed understanding of the long-term natural history of this region, there are societal and economic benefits to defining the surficial and subsurface geology. The composition, diagenetic history, and distribution of subsurface stratigraphic units influence socioeconomic and engineering efforts including understanding coastal morphodynamics, coastal management, and resource management. These resources include sand for beach renourishment, detrital industrial mineral distribution, as well as aquifer and hydrocarbon reservoir distribution and connectivity. The geologic framework of a region can also exert a significant influence on modern nearshore systems in terms of sediment sources and coastal erosion (Riggs et al., 1995, Harris et al., 2005). Issues related to coastal erosion and beach replenishment are economically significant along the coast of South Carolina. Between 1980 – 2010, an estimated 30.1 million m³ of sand was added to the 161 km of developed shoreline in the state (Kana et al., 2013). Identifying new sand resources along the inner continental shelf is the subject of ongoing research in the region (Luciano et al., 2019).

MATERIALS AND METHODS

All three component studies presented here rely on common data types and methods as their foundation. Integrated sediment core and seismic facies analysis combined with geochronological and micropaleontological data provide the basis of the sedimentological and stratigraphic interpretations presented here.

Geological Data and Analyses

Subsurface sediment samples include vibracores, push cores, hand augers, and shallow trenches and are used to define the physical stratigraphy, composition, age, and environment of deposition of local subsurface successions. Sediment cores are correlated to subsurface seismic data to help define the physical characteristics of seismic units on a larger scale. Sixty-seven sediment cores with a cumulative length of more than 210 m were described in detail (cm-scale); graphic logs and detailed core descriptions are presented in Appendix A. Twenty-seven of these cores were recovered from the Santee delta plain (Chapter 4) while the remaining cores were recovered from offshore as part of the 2015 Bureau of Ocean Energy Management (BOEM) Atlantic Sand Assessment Project (ASAP) (Chapter 3).

Core Descriptions and Interpretations

Physical core descriptions were completed for all cores and consist of detailed observation and documentation of color, grain size, sorting, physical and biological structures, composition, bed thickness, and bed contacts found within each core. These characteristics are described at cm-scale resolution and recorded in combination written and graphic logs. Compositionally, sediments within all samples consist of four main components: (1) sand, (2) mud, (3) organic detritus, and (4) shell material. Sand is comprised of clastic (mineral and lithic) grains between 64 and 2000 μm (Wentworth, 1922). Mud consists of both clay and silt-sized particles since distinguishing clay-sized ($<4 \mu\text{m}$) from silt-sized particles using mesoscopic methods is difficult. Lithofacies are defined on the basis of sediment composition, color, and grain size and are used in the interpretation of depositional conditions and settings.

Descriptive lithofacies for vibracores, push cores, hand augers, and grab samples have been defined on the basis of composition, grain size, physical structures, degree and types of

bioturbation, and color. These descriptive lithofacies are grouped into lithofacies associations which, when combined with other data, represent an interpretation of depositional conditions that constrain paleoenvironmental settings. Where possible, interpretation of paleoenvironmental conditions are compared to modern, surficial samples from grab samples and the upper sections of sediment cores. The application of modern conditions and sediment distributions as analogues is fundamental to understanding the depositional conditions preserved within subsurface sedimentary successions.

Surface Samples

Surface-sediment samples including subaqueous and subaerial grab samples as well as shallow trenches were collected to determine sediment composition and shallow sedimentary architecture within the modern system. One hundred and twenty-five subaqueous grab samples, 20 subaerial grab samples, and 10 trenches (up to 30 m long) provide the foundation for understanding the distribution of facies in the modern Santee delta plain and river as well as the shallow subsurface (Chapter 4).

Borehole Data

Lithological descriptions from more than 400 boreholes drilled onshore by the South Carolina Geological Survey, South Carolina Department of Health and Environmental Control and United States Geological Survey (Weems et al., 1985a, b; Weems et al., 1987a, b, and c) over the last 30 years were reviewed in detail. These data provide a relatively low vertical resolution (~meter-scale) but they extend (10's of meters) the record of the onshore subsurface stratigraphy. These data utilized in Chapter 2 and helped to define the location and rough morphology of the Bulls paleovalley onshore.

Micropaleontology

Twenty samples were acquired from two cores (SOU-01-V01 and CAN-01-V01) recovered from the Santee delta plain for micropaleontological analysis (*Chapter 4*). The purpose of this analysis is to identify the tests of various microorganisms, primarily forams, diatoms, and testate amoebae, whose distribution is controlled by environmental conditions. The species diversity as well as the ratio of agglutinated to calcareous microfossils is a function of salinity, alkalinity, carbonate saturation, and preservation potential (Leckie and Olson, 2013). This information is then used to constrain environmental conditions at the time of deposition for discrete stratigraphic intervals. Samples were acquired from several cores at CCU and analysis and interpretation of these samples was completed by Dr. Andrea Hawkes at the University of North Carolina, Wilmington. The results of these analyses were incorporated into core descriptions to provide the sedimentological context necessary for paleoenvironmental interpretation.

Geochronology

A total of 96 samples were analyzed for both AMS-¹⁴C (Chapters 2, 3, and 4) dates and amino acid racemization (AAR) age estimates (Chapter 3). Twenty-five samples chosen from 11 sediment cores for AMS-¹⁴C analysis to resolve the ages of lithofacies observed in sediment cores and Chirp data acquired from the Santee delta plain (Chapter 4). AMS-¹⁴C analysis was completed at the Poznań Radiocarbon Laboratory in Poznań, Poland. An additional 28 samples were taken from 11 offshore cores for AMS-¹⁴C dating (Chapters 2 and 3). These samples were analyzed at the University of Georgia Center for Applied Isotope Studies in Athens, Georgia, USA as part of the BOEM ASAP project (Luciano et al., 2019). Seven AAR samples from 4 offshore cores were analyzed at Northern Arizona University's Amino Acid Geochronology Lab and interpreted as part of the BOEM regional assessment project (Luciano et al. 2019).

Geophysical Data and Analyses

In total, over ~1,200 km of seismo-acoustic data were used to map and interpret regional and local stratigraphy as part of all three studies presented here. This includes approximately 300 km of Chirp data from the channels of the Santee delta, 250 km of Chirp offshore of the Santee delta, and 250 km of Bubble Gun data that were specifically acquired for this research. In addition to these newly-acquired data, existing seismic reflection data from several NOAA cruises, in conjunction with Coastal Carolina University, as well as data acquired by BOEM during the 2015 ASAP evaluation have been incorporated into these studies. High-resolution (Chirp) data were acquired using an EdgeTech 3200 subbottom profiler combined with EdgeTech SB-0512i and SB-424 towfish with bandwidths of 0.5 - 12 kHz and 4 – 24 kHz, respectively. The Hegg Marine Solutions HMS-620 Bubble Gun operates at a bandwidth of 70-1500 Hz. When combined, these tools provide for decimeter- to meter-scale vertical resolution and penetration of up to 80 m in the resulting processed data.

In Chapters 2 and 3, seismo-acoustic data were interpreted with the purpose of defining the nature and distribution of the stratigraphic units that make up the regional stratigraphic framework. Key stratigraphic surfaces were defined and mapped. Seismic facies were then described using a methodology similar to that proposed by Mitchum et al. (1977) and were defined on the basis of geometry, amplitude, frequency, continuity, and terminations of internal seismic reflectors. External characteristics including cross-sectional geometry and bounding surface morphology also were used to describe and interpret stratigraphic units. The result of this classification is a framework defined by seismic facies separated by a bounding surfaces.

Historical Data

In addition to the data mentioned above, historical maps of the Santee delta plain and surrounding areas provide valuable information regarding the geomorphology of the delta plain

and coastal line and how these systems have changed over the past few hundred years. Detailed maps from 1775 and 1883 along with nautical charts and bathymetric surveys from 1910, 1929, and 1935 help to constrain changes that have occurred within the Santee system, particularly those associated with anthropogenic modifications as presented in Chapter 4.

Geological Maps

Surface geological maps in key areas have also been included in the regional interpretations associated with Chapters 2 and 3, particularly with reference to mapping of the paleovalleys of the Santee River (Chapter 2). Geologic maps were completed by both the South Carolina and United States Geological Surveys (Weems and Lemon, 1999; Weems et al., 2014).

RESEARCH OBJECTIVES AND HYPOTHESES

Research Topic 1: The Quaternary Stratigraphic Architecture of a Low-Accommodation, Passive-Margin Continental Shelf (Santee Delta Region, South Carolina, U.S.A.)

Coauthors: Hanebuth, T.J.J.

Objectives- The three primary goals of this study are: 1) to utilize high-resolution geological and geophysical data sets to define the temporal and spatial distribution of key stratigraphic elements and surfaces offshore of the Santee Delta and establish a stratigraphic framework for the Quaternary section of this region, 2) to combine this offshore framework with the established onshore stratigraphy to elucidate the Quaternary evolution of the region, and 3) to understand how the deposition and preservation of stratigraphic units are influenced by regional trends in accommodation and sediment supply.

Hypotheses- Two hypotheses are related to the preservation of Quaternary stratigraphy offshore: 1) While the highstand components of Quaternary depositional sequences are well preserved onshore, offshore equivalent deposits have been extensively re-worked leaving only

thin, discontinuous Quaternary stratigraphic units resting unconformably upon Mesozoic and early Cenozoic basement rocks. 2) Due to the nature of the Santee River as a significant sediment source, and the location of the study area near the southern extent of the structural influence of the Cape Fear Arch, this region is characterized by both higher sediment supply, sourced by the Santee River, and structurally-enhanced accommodation and therefore should preserve a more complete stratigraphic succession.

Research Topic 2: Depositional Environments Preserved within Quaternary Paleochannel Systems Offshore of the Georgia Bight, Southeastern U.S.A.

Coauthors: Hanebuth, T.J.J., Alexander, C., Wehmiller, J.

Objectives- The primary goal of this study is to define the depositional facies, seismic facies, and planform morphologies of paleochannel and paleovalley systems preserved along the inner continental shelf, within 25 km of the coast, of South Carolina and Georgia. To better understand the regional distribution of paleochannels and paleovalleys, we also document the spatial and temporal distribution of these features from the northern border of South Carolina to the southern border of Georgia (Fig. 1.1).

Hypotheses- Three hypotheses are related to the morphology and connectivity of paleochannels and paleovalleys: 1) There are systematic trends in paleochannel architecture, morphology, and distribution which allow for high-confidence correlation of discrete paleochannels and paleovalleys; 2) Paleochannel networks are similar in morphology to those of modern coastal systems which range in orientation from shore-normal to shore-oblique to shore-parallel; or 3) Paleochannel networks in this area more closely resemble previous estimations of channel morphologies which are dominated by shore-normal orientations. Two additional hypotheses focus on the sedimentary successions that are part of paleochannel systems and state

that: 1) basal portions should include a coarse-grained fraction deposited as bedload overlain by a finer, mud-rich, fraction reflecting a vertical transition from traction deposition into lower energy suspension deposition associated with channel abandonment; and 2) these sediments should preserve indications of deposition in both fluvial (e.g. minimal tidal influence) and estuarine (e.g. strong tidal influence) environments.

Research Topic 3: Late Holocene Stratigraphy and Facies Distributions within an Anthropogenically-modified Delta Plain, Santee Delta, SC USA

Coauthors: Hanebuth, T.J.J., Durica, J.T., Hawkes, A.D.

Objectives- The main objectives of this research are to: 1) define and map the distribution of modern depositional facies of the Santee delta plain; 2) use these depositional facies to inform an interpretation of the Holocene stratigraphy; and 3) define the roles that anthropogenic modifications may have had on both the distribution of modern facies and the late Holocene stratigraphy.

Hypotheses- The hypotheses developed here address the third research objective listed above, namely which is the dominant forcing mechanism that is responsible for Holocene depositional systems observed within the subsurface of the Santee delta plain. First, considering the dynamic nature of combined fluvial and estuarine systems, it is possible that the accessible portion of the sedimentary record is dominated by local, diachronous, event-related erosion and sedimentation which are not directly a product of regional (i.e. allogenic) processes. Rather the shallow depositional architecture is a product of autogenic processes such as channel migration, avulsion, barrier spit growth and migration, and storm-related deposition/erosion. Second, while there is significant local variability, deposition within the Santee delta plain is largely driven by Holocene sea-level rise. Third, the anthropogenic modifications to the Santee River and the Santee

delta have resulted in significant, recognizable changes to the natural system. Changes including the clearing of lowland forests for rice cultivation; the dredging of large canals connecting the North Santee River, the South Santee River, and Winyah Bay; and the construction of a series of large dams have altered channel-floodplain morphodynamics, sediment storage, sediment supply, and inshore hydrodynamics in a significant and measurable way.

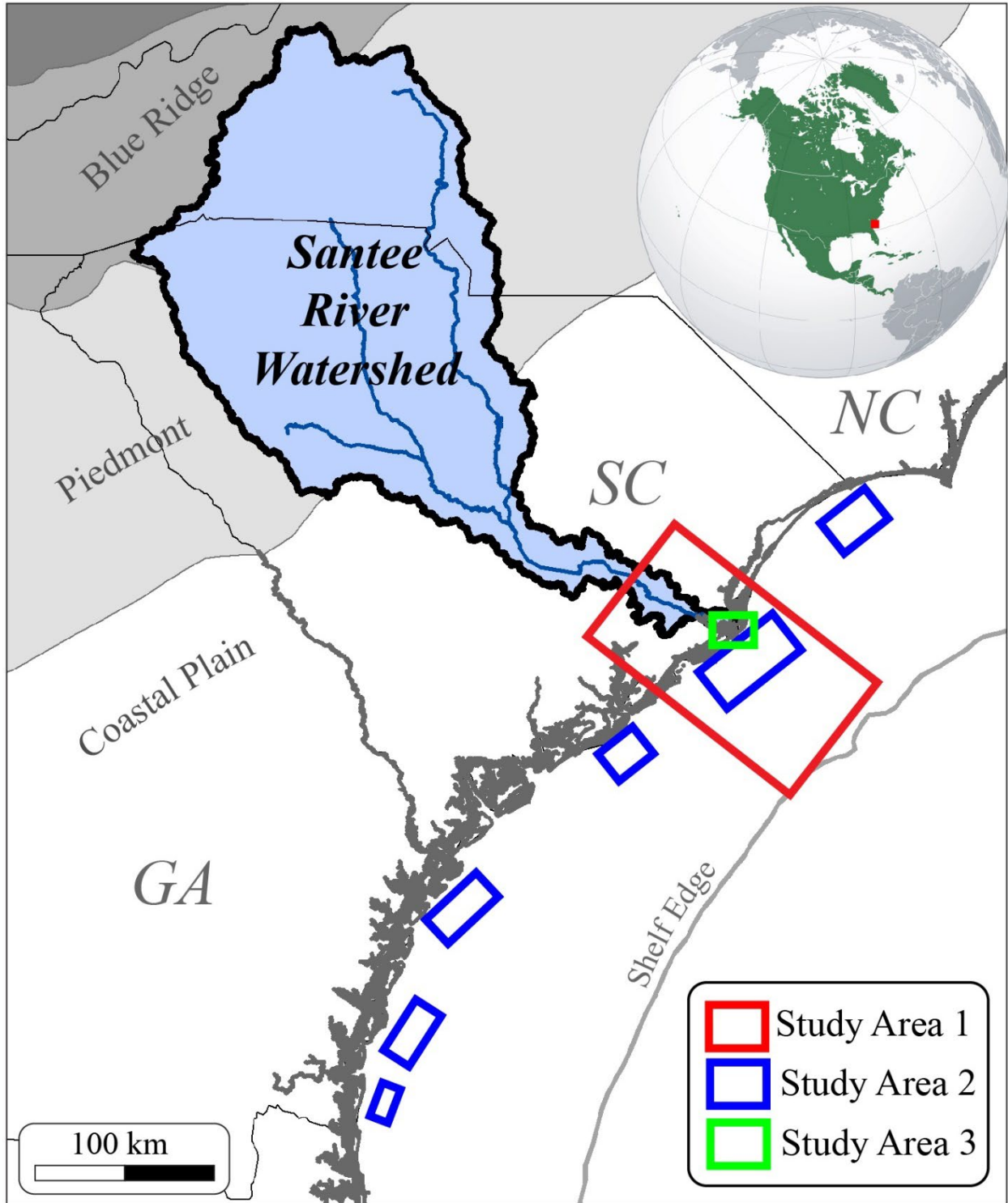


Figure 1.1. Base map showing the locations of study areas associated with all three research topics.

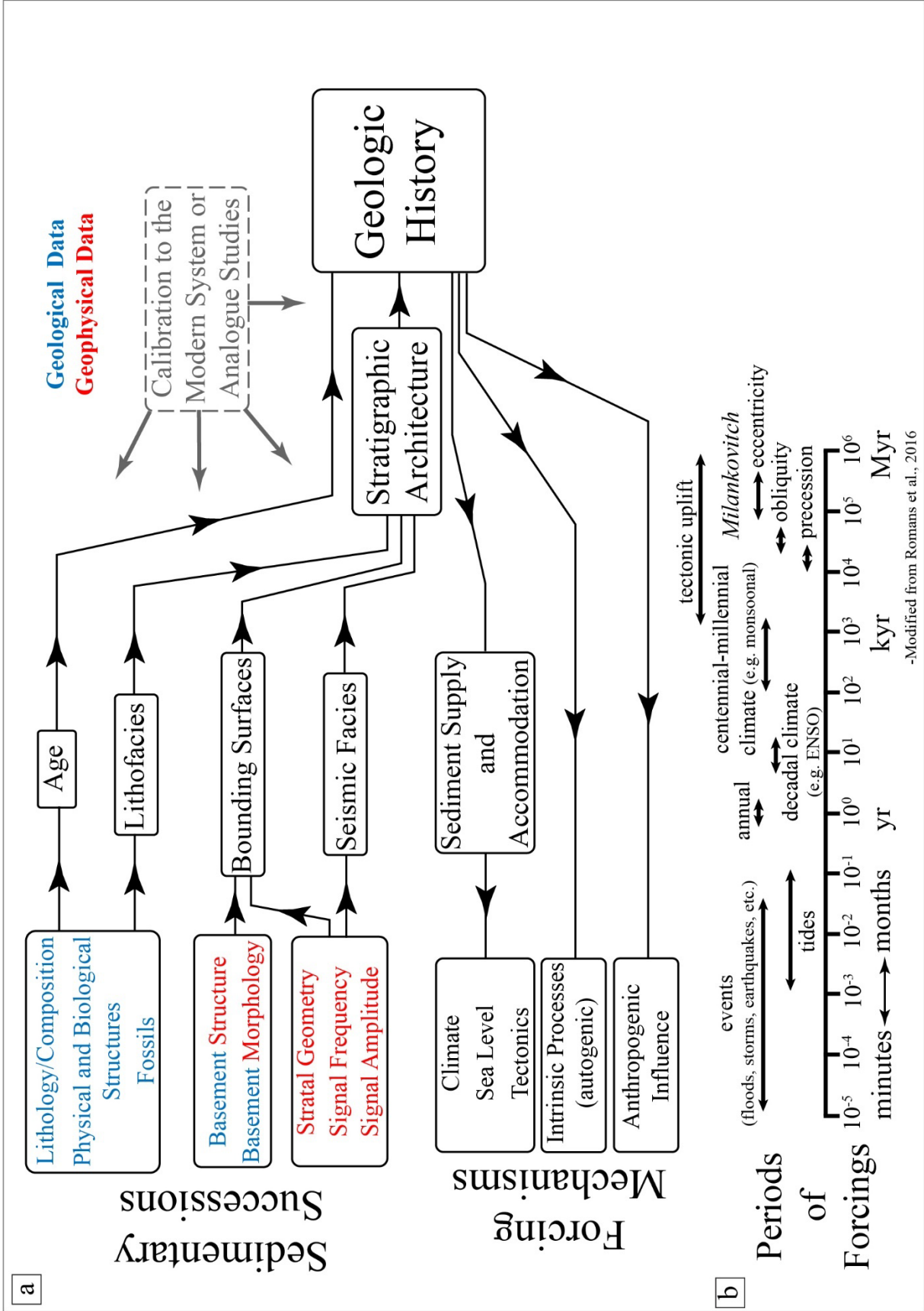


Figure 1.2. Summary chart of input data, methods and objectives of stratigraphic interpretation, and the periods of major forcing mechanisms. **a)** Stratigraphic analysis begins with the integration of both geological (i.e. sediment cores and surface samples) and geophysical (Chirp, HRS, Bathymetry, etc.) data to define the stratigraphic architecture for the region. Once this architecture, or framework, is calibrated with both absolute and relative ages, we can begin to interpret the geologic history of the area. This history is a result of both allogenic forcing (climate, sea level, and tectonics), autogenic forcing (intrinsic to the depositional system, i.e. river avulsions), or, in the latest Holocene, human modifications. **b)** is a modified scale depicting the periodicity of various forcing mechanisms from Romans et al. (2016).

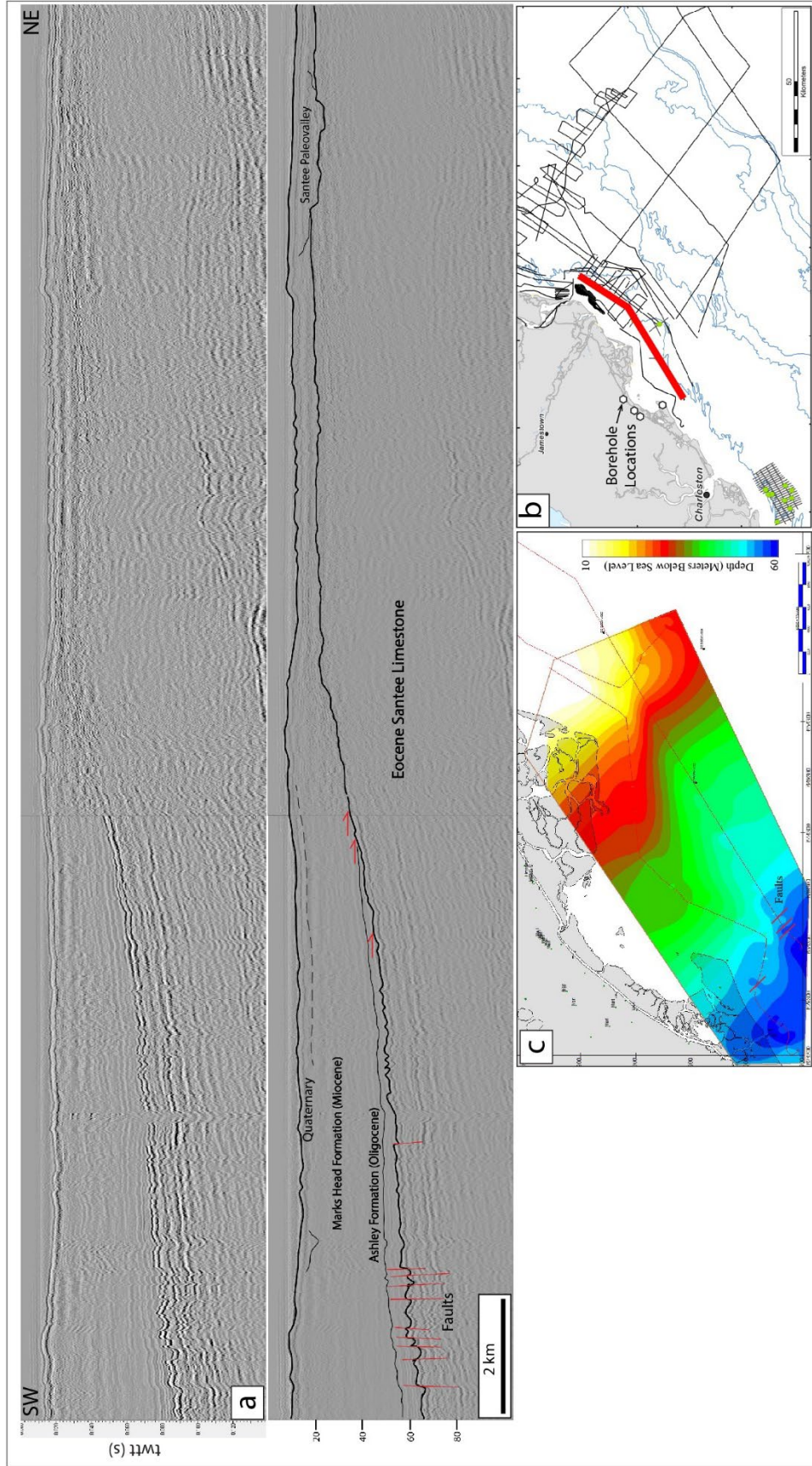


Figure 1.3. Shore-parallel HRS (bubble gun) profile offshore of Bulls Bay. **a)** HRS profile and interpretation showing the top of the Eocene section as a high-impedance surface showing multiple, small-offset (~5 m) faults and a structural dip to the south. The stratigraphic section that overlies the Eocene consists of two discrete onlapping units that, based on correlation to onshore borehole data, are Oligocene and Miocene age. A major unconformity separates these older units from the Quaternary section near the top of the profile. **b)** Location map showing the profile in A as well as the location of onshore boreholes used to define the age of the units along the HRS profile. **c)** Structure contour map on the Eocene surface. A constant seismic velocity of 1500 m/s was used to convert time to depth, so the true depth is probably a bit deeper than what is shown.

Chapter 2

The Quaternary Stratigraphic Architecture of a Low-Accommodation, Passive-Margin Continental Shelf (Santee Delta Region, South Carolina, U.S.A.)

ABSTRACT

The Quaternary stratigraphy of the continental shelf offshore of South Carolina consists of stratigraphic units deposited in coastal plain, shallow marine, and shelfal environments bound by composite erosional surfaces that developed in response to numerous glacioeustatic cycles and overprinted by regional uplift. These units are commonly distributed laterally rather than stacked vertically, a function of the long-term, low shelf gradient and the resulting lack of accommodation.

This study integrates high-resolution geological and geophysical data sets acquired offshore and onshore with existing data onshore into a comprehensive conceptual model describing the Quaternary geologic evolution of the coastal plain and continental shelf within a study area of approximately 8,000 km². We use seismic facies and core analysis to define stratigraphic units associated with transgressive, regressive, and lowstand systems offshore. Regressive systems include progradational wave- and river-dominated deltaic and shoreface deposits. Lowstand systems consist of a complex network of paleo-incisions produced by regional, Piedmont-draining fluvial systems and smaller coastal-plain rivers. Transgressive systems include paleochannel-fill successions dominated by mud-rich, tidally-influenced backbarrier deposits, cusped and linear shelf sand ridges; and transgressive sand sheets and shoals.

The low-accommodation setting of the continental shelf influences the stratigraphic record in several key ways: 1) the geometry of progradational coastal lithosomes; 2) the development of

composite allogenic erosional surfaces; 3) the deposition of widespread, thin transgressive sand sheets; and 4) the restriction of thicker transgressive deposits to paleo-incisions. In this setting, the use of a hierarchical bounding surface scheme is preferable to the more common sequence stratigraphic or allostratigraphic conventions for several reasons: 1) major erosional bounding surfaces are commonly amalgamated; 2) lower-order surfaces capture internal variability which is key to the genetic interpretation of stratigraphic units; and 3) stratal stacking patterns typically used to define a sequence stratigraphic framework are rare.

INTRODUCTION

The stratigraphy of coastal plain and neighboring continental shelf of the southeastern United States is a complex succession of Cretaceous through Holocene sedimentary units (Cooke 1936; Colquhoun 1962; Weems et al. 1994; Colquhoun 1995; Denny et al. 2007). These units, both active and relict, were deposited and modified by terrigenous and marine processes during numerous, high-frequency glacioeustatic sea-level cycles (Cooke 1936; Colquhoun et al. 1991; Doar 2014). The stratigraphy of this region preserves a long-term record of environmental change on the scale of 10^2 to 10^6 years, but this record is replete with gaps related to periods of regressive, subaerial, and transgressive erosion. Weems et al. (1994) described the onshore stratigraphy of the Charleston area, SC, post-Oligocene deposits as a “mosaic” of remnant stratigraphic units that are “distributed [preserved] more commonly side by side than in superposition”. While the coastal plain and adjacent portions of the inner shelf are well-studied (Cooke 1936; Colquhoun 1962; Hoyt and Henry 1971; Gayes et al. 1992; Weems et al. 1994; Colquhoun 1995; Denny et al. 2007; Denny et al. 2013; Doar 2014; Doar and Kendall 2014), the region offshore of the Santee Delta and Cape Romain (Fig. 2.1) is relatively understudied, with just a few studies focused on the surficial deposits of the inner shelf and shoreface (Swift 1972; Sexton et al. 1992; Denny et al. 2013). This

area is unique in that the Santee River, a Piedmont-draining fluvial system, forms the only river-fed delta on the US east coast and has served as a significant source of sediment throughout the Quaternary (Colquhoun et al. 1972; Weems et al. 1994).

Although the continental shelf of central South Carolina is situated along a passive margin, post- and syn-depositional modifications due to dynamic topography, neotectonics, glacio-isostasy, and hydro-isostasy have altered not only the original elevations of pre-Holocene deposits, but may have also influenced accommodation dynamics and regional topographic and bathymetric gradients throughout the Quaternary (Richards 1967; Hathaway et al. 1976; Cronin et al. 1981; Colquhoun 1995; Peltier 1999; Weems and Lewis 2002; Baldwin et al. 2006; Moucha et al. 2008; Englehart et al. 2011; Bartholomew and Rich 2012; Rowley et al. 2013; Rovere et al. 2014). Regional uplift and local faulting have been mechanisms that exert a significant influence on Quaternary depositional systems (LeGrand 1961; Marple and Talwani 2000; Weems and Lewis 2002).

There are three primary goals of this study: 1) to utilize high-resolution geological and geophysical data sets to define the temporal and spatial distribution of key stratigraphic elements and surfaces offshore of the Santee Delta and establish a stratigraphic framework for the Quaternary section of this region, 2) to combine this offshore framework with the established onshore stratigraphy to elucidate the Quaternary evolution of the region, and 3) to understand how the deposition and preservation of stratigraphic units are influenced by regional trends in accommodation and sediment supply.

PHYSICAL SETTING

Geomorphic Setting

The Coastal Plain of central and northern South Carolina is drained by several coastal plain rivers and two major piedmont-draining rivers, the Pee Dee and Santee Rivers (Fig. 2.1). The headwaters of the Santee system are located in the Blue Ridge Mountains of western North Carolina, a drainage path that was established prior to the Quaternary Period (Cooke 1936; Weems et al. 1994). The Santee River begins at the confluence of the Congaree and Wateree Rivers in central South Carolina and flows 160 km to the Atlantic coast, where it forms the only river-fed delta on the US east coast (Fig. 2.1) (Eckard et al. 1986; Hughes 1994). With a drainage basin area of 37,000 km² and an average annual discharge of 400 m³/s, the Santee River system is the second largest river system along the US east coast (Hughes 1994; Patterson et al. 1996; McCarney-Castle et al. 2010).

The Santee Delta has an area of 100 km², modest in size by global standards (Abruwi 1968; Payne 1970; Eckard et al. 1986). The modern geomorphological configuration indicates that the Santee Delta is a mixed-energy delta and is dominated by wave and tidal processes (Galloway 1975; Hayes 1989). Twenty-two km inland from the coast, the Santee River branches into its two main distributary channels, the North and South Santee Rivers of the delta plain (Fig. 2.1). Within the lower delta plain, the North Santee River bifurcates where the northern channel forms the wide and shallow North Santee Bay (Fig. 2.1). This channel configuration has been static for at least the last 245 yrs owing in part to anthropogenic stabilization (Cook 1775). Since the early 18th century, the Santee River, and its delta, have been extensively modified by human activity including major dam construction, canal diversions, and complete clearing of the tidelands for rice cultivation (Lewis 1979; Anderson et al. 1982). With an estimated suspended sediment discharge for the Santee River ranging from the modern rate of 825,000 tons/yr to pre-European discharge of 2.24 Mt/yr, the Santee is a major source of sediment to the barrier-island coasts of South Carolina and

Georgia (Abuwi 1968; Payne 1970; Eckard et al. 1986; Hayes 1989; Sexton et al. 1992; Hayes et al. 1993; Patterson et al. 1996; McCarney-Castle et al. 2010).

Less than 10 km to the north, another Piedmont-draining river system, the Pee Dee, enters the Atlantic Ocean through Winyah Bay (Fig. 2.1c), providing an additional 0.43 to 1.45 Mt/yr of suspended sediment under modern conditions, a rate that has not significantly changed since pre-European times (Patchineelam et al. 1999; McCarney-Castle et al. 2010). This modern configuration is a result of the southerly migration of the Pee Dee River throughout the Pleistocene (Soller 1988; Baldwin et al. 2006).

The study area lies within a section of the US Atlantic coast referred to as the Georgia Bight (Fig. 2.1a), a large, basement-influenced coastal embayment that stretches from North Carolina to Florida (LeGrand 1961; Hayes 1994). The coastline and shelf along the central part of the Bight experience microtidal conditions and mean significant wave heights from 0.5 to 1 m (Nummedal and Fischer 1978; Hayes 1994). While circulation, and sediment transport, along the inner shelf varies with meteorological conditions (i.e. cold fronts, warm fronts, and low-pressure systems), net sediment transport is directed to the southwest (Warner et al. 2012); a pattern that has persisted since at least the late Oligocene (Weems et al. 1994; Colquhoun 1995).

The continental shelf offshore of the Santee Delta, in some literature referred to as the Carolina Platform (Hutchinson et al. 1981; Pinet and Popenoe 1985), extends 80 km offshore to a depth of approximately 60 m (Fig. 2.1). The shelf-margin slope defines the transition from the shelf down to the Blake Plateau (Fig. 2.1d), a broad platform of Cretaceous through Oligocene carbonate-rich rocks that extends to a distance of 150 km from the shelf edge (Maher 1971; Pinet and Popenoe 1985). With an estimated average slope of 0.05° , the continental shelf within the study area is classified as a low-gradient shelf (Field and Trincardi 1991). This configuration can

exert a primary influence on the deposition and preservation of marine deposits (Field and Trincardi 1991; Muto and Steel 1997; Zecchin 2007; Zecchin et al. 2019). Accommodation in this setting can control shoreline progradation rates, preservation potential, frequency of autogenic processes such as distributary channel avulsions and delta mouth-bar abandonment, efficiency of transgressive erosion, as well as the stratigraphic architecture of shoreface and shelfal deposits (Field and Trincardi 1991; Van Yperen et al. 2019).

Geologic Setting

Throughout the Quaternary, high-frequency fluctuations in sea-level, driven primarily by glacioeustasy, have exerted a primary control on the nature and distribution of coastal depositional systems across the coastal plain of the southeastern United States (Cooke 1936; Colquhoun 1961; Colquhoun et al. 1972; Gayes et al. 1992; Colquhoun 1995; Doar 2014). Additionally, regional basement-involved tectonics and near-surface fault systems have influenced Quaternary depositional systems (Marple and Talwani 2000; Baldwin et al. 2006; Bartholomew and Rich 2012; Van De Plassche et al. 2014).

Various studies have focused on the regional subsidence associated with the composite structural high located in the vicinity of southern North Carolina and northern South Carolina referred to as the Cape Fear Arch or Mid-Carolina Platform High (Fig. 2.1) (Richards 1967; Baldwin et al. 2006; Van De Plassche et al. 2014). Uplift along the arch has resulted in lower rates of relative sea level rise (RSL) rise over the crest of this feature in southern North Carolina during the past 4 kyr relative to our study area (Van De Plassche et al. 2014), evidence of ongoing regional uplift. Baldwin et al. (2006) concluded that regional uplift along the Cape Fear Arch (Fig. 2.1) has been a contributing factor in the southerly migration of the Pee Dee River since the late Pliocene.

Local structural trends and their associated fault networks have influenced the morphology of modern fluvial systems across the coastal plain. Marple and Talwani (2000) and Bartholomew and Rich (2012) attributed both local and regional trends in fluvial channel morphology to vertical movement along segments of regional fault systems throughout the Quaternary. These movements have resulted in discrete zones of river deflection that trend NNE-SSW and has influenced all major fluvial systems between the Edisto and Pee Dee Rivers in South Carolina (Marple and Talwani 2000). Another series of basement-involved, NW-SE trending faults have compartmentalized segments of the coastline between North Carolina and Georgia and have been active since the early Pleistocene (Bartholomew and Rich 2012).

The onshore Quaternary stratigraphy of the coastal plain of the southeastern United States consists of a series of seaward-stepping scarps and terraces deposited as a succession of coupled barrier-island and backbarrier systems during Plio-Pleistocene glacioeustatic sea-level highstands (Cooke 1936; Colquhoun 1961; Dubar et al. 1974; Willis 2006; Rovere et al. 2014; Doar 2014). These scarps are prominent morphological features across the coastal lowland of South Carolina and most of the southeastern US coastal plain (Cooke 1936). Unconsolidated Quaternary deposits lie unconformably atop Cretaceous to Eocene rocks and are internally bound by numerous composite erosional surfaces that are likely amalgamated sequence boundaries and transgressive erosional surfaces that formed in response to multiple glacioeustatic sea-level cycles (Cooke 1936; Colquhoun 1995; Doar 2014; Doar and Kendall 2014).

In addition to the preserved surficial shallow-marine deposits, two paleovalleys of the ancestral Santee River have been partially mapped in the subsurface from borehole data by Weems (1994) and Colquhoun et al. (1972). The southern-most, and oldest paleovalley, referred to here as the Four Hole Paleovalley, was active during the latest Pliocene to early Pleistocene and lies

beneath Four Hole Swamp and the Edisto River in southeastern South Carolina (Weems et al. 1994). The second, and younger onshore paleovalley was mapped by Colquhoun et al. (1972) near Jamestown, South Carolina adjacent to the Bethera Scarp. On the basis of regional mapping by Weems et al. (2014), the base of this paleovalley intersects the modern coastline at Bulls Bay (Fig. 2.1) and is referred to here as the Bulls Bay Paleovalley. Paleovalley-fill sediment belongs to the Ladson Formation and which was deposited between 730-240 ka (Weems et al. 1994). Colquhoun et al. (1972) mapped a highstand delta of the Santee River as part of the Bethera Scarp and suggested that the avulsion of the Santee River from the Bulls Bay Paleovalley into the modern Santee incised valley occurred during the deposition of the Bethera coastal system around 200 ka. Eckard (1986) used borehole and sediment core data to define the morphology of the Santee River incised valley within the modern Santee delta plain. The base of this incised valley is as deep as 20 mbsl and contains a sedimentary succession consisting of basal, coarse-grained fluvial deposits overlain by fluvial and estuarine floodplain and channel deposits of Holocene age (Eckard 1986).

While the onshore stratigraphy is well documented, the offshore stratigraphy of this region is considerably less so (Hoyt and Henry 1971; Swift 1975a; Sexton et al. 1992; Baldwin et al. 2006; Denny et al. 2013). The tectonically stable, broad, low-gradient continental shelf is an overall low-accommodation setting. Accommodation, as used here, is defined as the space in which sediment can accumulate (Jervey 1988), which in the marine environment is commonly defined as the space between storm-weather wave base and seafloor (Catuneanu 2006). The across-shelf migration of shoreline and associated coastal environments, in response to changes in relative sea level within this low-accommodation setting, has resulted in a complex offshore stratigraphy. Previous studies related to the offshore stratigraphy of the Santee Delta region include a narrow, shore-parallel zone along Long Bay, a large coastal embayment to the north of Winyah Bay

(Baldwin et al. 2006; Schwab et al. 2009; Denny et al. 2013), and local studies based primarily on bathymetric data, sparse core data, or surficial grain-size analysis (Hoyt and Henry 1971; Swift 1975a; Sexton et al. 1992; Hayes 1994). The shallow stratigraphy documented by these studies consists of extensive sandy shoals attributed to Holocene deltaic, barrier island, and tidal delta deposition (Hoyt and Henry 1971; Swift 1975a; Sexton et al. 1992; Hayes 1994), consolidated sediments and outcropping sedimentary rock of various geologic age (Schwab et al. 2009), and intermittent exposures of Pleistocene paleochannels (Baldwin et al. 2006; Schwab et al. 2009). This study is the first attempt to integrate modern, high-resolution data with existing data over an area of approximately 8,000 km² to understand the stratigraphy, and geological evolution of this region.

MATERIALS AND METHODS

Newly-acquired, high-resolution inshore and offshore seismo-acoustic and sediment core data were integrated with existing offshore seismo-acoustic and onshore borehole data to produce a regional dataset from which the Quaternary depositional history of the lower coastal plain and continental shelf could be interpreted.

Bathymetric Data

Bathymetric data were used to define the surface morphology of the stratigraphic units that are exposed at the modern seafloor. Regional bathymetric data were compiled from various sources found in the National Oceanic and Atmospheric Administration's (NOAA) National Geophysical Data Center (NGDC) and combined into the Coastal Relief Model (CRM) maximum vertical resolution of 1 m with a grid size of 90 m.

Seismo-acoustic Data

Approximately 1,200 km of seismo-acoustic data were used to map and interpret the subsurface stratigraphy of the Santee River and adjacent continental shelf (Fig. 2.1b). These data include nearly 800 km of data acquired between 2016 and 2019. Existing offshore seismo-acoustic profiles were acquired during several previous research cruises by faculty of Coastal Carolina University working aboard the National Oceanic and Atmospheric Administration (NOAA) R/V Nancy Foster in 2004, 2005, and 2015. Additionally, as part of the Atlantic Sand Assessment Project (ASAP) funded by the Bureau of Ocean Energy Management (BOEM) to identify sand resources along on continental shelf of the Atlantic coast of the eastern United States, an extensive data set was acquired in 2015 including seismo-acoustic lines in key parts of the study area and a dense grid of data within the Folly-Kiawah area (Fig. 2.1b).

Seismo-acoustic data acquisition was performed with both high-frequency Chirp systems and a lower frequency Bubble Gun system. Chirp sub-bottom profiling systems included Edgetech's 0512i (500 –12,000 Hz), 3200 (500-24,000 Hz), and 424 (4,000–24,000 Hz) models. The Hegg Marine Solutions HMS-620 Bubble Gun was also deployed and operates at a bandwidth of 70-1500 Hz. These tools provide for decimeter to meter vertical resolution and penetration of up to 80 m in the resulting processed data.

Seismic facies— Seismo-acoustic data were interpreted using IHS Kingdom software. Key stratigraphic surfaces were defined and mapped. Seismic facies were then described using a methodology similar to that proposed by Mitchum et al. (1977) and were defined based the geometry, amplitude, frequency, continuity, and terminations of internal seismic reflectors (Fig. 2.2). External characteristics including cross-sectional geometry and bounding surface morphology were also used to describe and interpret stratigraphic units. Seismic facies (SF) were

combined with sediment-core data where possible (Table 2.1). Discrete sedimentary successions consisting of one or more SF are referred to here as stratigraphic units.

A range of terms have been used in the literature to describe channel-form deposits within the sedimentary record: paleochannel, paleochannel fill, paleovalley, paleochannel network or complex, and incised valley are the most common (see discussion in Blum et al. 2013). For the purposes of this study, the term channel refers to a modern, active, or recently abandoned, but still unfilled, geomorphic feature. Paleochannels are subsurface geologic features consisting of a basal erosional surface of an ancient, abandoned channel as well as the sedimentary fill contained therein (Fig. 2.2b). While paleochannel fill reflects local depositional conditions, paleovalley architecture, primarily paleochannel stacking patterns, reflect regional controls on accommodation (Catuneanu 2006; Gibling 2006; Holbrook et al. 2006). The paleochannel stacking pattern within a paleovalley can be aggradational, degradational, or laterally offset, reflecting both allogenic controls, such as RSL-driven accommodation, and autogenic controls related to localized incision, avulsion, or reactivation (Ashley and Sheridan 1994; Holbrook and Schumm 1999; Gibling 2006; Catuneanu 2006; Blum et al. 2013).

Alluvial valleys form as a result of channel incision in response to fluvial discharge, localized faulting, regional tectonic uplift, or base level lowering (Schumm and Ethridge 1994; Holbrook and Schumm 1999; Charleton 2008). Incised valleys, as defined by Dalrymple et al. (1994), are fluvially-eroded features that are larger than a single channel. Here the term incised valley refers to the valley of a modern river, the subsurface erosional base or valley floor, and the incised valley fill. Paleovalley, as used here, refers to a relict subsurface feature consisting of a succession of amalgamated paleochannels with sedimentary fill consisting of various fluvial, estuarine floodplain, and marine deposits.

Bounding surfaces— The geometry, morphology, and amplitude of prominent concordant and discordant seismic reflectors were used to delineate a hierarchy of bounding surfaces (Table 2.2). The identification and description of the significance and distribution of these stratigraphic surfaces is key to distinguishing genetically-related stratigraphic units in the overall stratigraphic record and to establishing a robust stratigraphic framework.

In marine systems, stratigraphic surfaces are commonly defined by applying the established concepts of sequence stratigraphy, where they are related to changes in shoreline trajectory and base level (Mitchum et al. 1977; Catuneanu 2006; Catuneanu et al. 2010; Catuneanu et al. 2011); or of allostratigraphy, where the focus is on basin-wide stratal discontinuities (North American Stratigraphic Code 2005; Catuneanu 2006). In contrast to these methodologies, hierarchical bounding surface schemes are fundamentally descriptive, with lower-order surfaces (1st – 4th order) being of limited spatial extent and largely formed by autogenic processes such as channel avulsions or tidal-inlet dynamics (Kim et al. 2014; Hajek and Straub 2017). Higher-order surfaces (5th and 6th order) are regionally-extensive and formed primarily by allogenic processes such as changes in relative sea level, climate, or tectonics (Allen 1983; Miall 1985, 1988; Collinson 1996). This approach has been extensively applied to studies of non-marine systems (Allen 1983; Miall 1985; Kocurek 1988) but rarely to marine systems (Parsons et al. 2003, Miall 2010). This methodology has the distinct advantage of capturing the details observable in modern, high-resolution, seismo-acoustic data (Table 2.2b). We follow a slightly modified version of the model proposed by Miall (2010) which integrates 4th -6th order surfaces, sequence stratigraphic surfaces and allostratigraphic surfaces for shallow-marine systems.

Core Data

Forty-six sediment cores ranging in length from 1.5 to 6 m were recovered from the islands and channels of the Santee River and delta (Long and Hanebuth 2017 and this study) (Fig. 2.1). These inshore and onshore cores helped to characterize the Holocene deposits within the modern Santee Delta. Within the study area offshore, three BOEM vibracores were recovered at the intersections of seismo-acoustic profiles (Fig. 2.1). In addition to the offshore cores within the main study area, 10 BOEM cores from offshore of Folly and Kiawah beaches (Fig. 2.1) were used to inform stratigraphic interpretations for the region.

Sediment cores were split, and core halves were described at sub-centimeter resolution. Characteristics including sediment color and composition; physical, biological, and diagenetic structures; grain size, rounding, and sorting; bed thicknesses and bed contacts were documented and captured in graphic logs (Fig. 2.3). Offshore cores were sampled for grain-size analysis, and scanned for elemental composition (XRF), bulk density; magnetic susceptibility; and high-resolution imagery (Long 2018).

Thirty-six samples were taken from seven offshore cores for dating (Table 2.3). Twenty-eight AMS-¹⁴C samples were analyzed at the University of Georgia Center for Applied Isotope Studies in Athens, Georgia, USA (Alexander, personal communication 2019). The raw ¹⁴C results were calibrated using Calib13 software version 5.0 using the Marine13 calibration set, and the age ranges reported in calibrated years before present (cal ka BP) and correspond to the 2σ error. Eight Amino Acid Racemization (AAR) samples were analyzed at Northern Arizona University and interpreted as part of the BOEM regional assessment project (Wehmiller et al. 2019). AMS-¹⁴C and AAR results are presented in Table 2.3.

Paleontological and micropaleontological analyses were completed on foraminifera, bivalve, and gastropod shells from several inshore cores as well as the SC-VC19 core (Hawkes,

personal communication 2016; Long 2018; Harding, personal communication 2018; Kelley, personal communication 2018). These analyses, when coupled with sedimentological data, helped to constrain paleoenvironmental interpretations.

Borehole Data

Data from approximately 400 onshore boreholes were reviewed and incorporated into this study to identify both the lithology of the pre-Quaternary section as well as the morphology of the regional unconformity that separates it from the overlying Quaternary section. Borehole descriptions were made by the United States Geological Survey (USGS) (Weems and Lemon 1985; Weems et al. 1985, 1987a, 1987b, 1987c; Weems and Lewis 2019), the South Carolina Geological Survey (SCGS) (Appendix 1). Borehole descriptions include lithologic descriptions and delineation of stratigraphic units (Doar 2014). These descriptions are of lower vertical resolution than vibrocore descriptions, but they are up to 30 m long, providing the deep stratigraphic control necessary to map the Quaternary section onshore.

RESULTS

The description and interpretation of stratigraphic units is based on their characterization in terms constituent seismic facies, internal and external bounding surfaces, core-based and borehole lithofacies, as well as their spatial distributions. Seismic facies (SF) are combined with core data where possible to develop interpretations of depositional environments and ages of stratigraphic units (Table 2.1).

Seismic Facies (SF)

We have defined 5 primary SF in the subsurface of the lower coastal plain and continental shelf within the study area (Table 2.1). SF comprise stratigraphic units, which represent discrete

lithosomes, deposited within the same depositional environment or coevally across associated environments. Two of the five SF, the progradational (PG) and paleochannel (CH), are subdivided further based on internal geometries or external morphologies.

Pre-Quaternary seismic facies (SF PQ)

Description— Seismo-acoustic data offshore indicate that the top of the pre-Quaternary is marked by a strongly reflective, commonly channelized, highly rugose bounding surface. Internal seismic reflectors, where visible, exhibit a uniform, locally folded and faulted, southeasterly dipping attitude (Hanebuth and Long 2020). Offshore, sediment core SC-VC24 recovered 1.96 m of fine-grained, indurated, calcareous sand at an elevation of approximately 16 m mbsl (Fig. 2.3). The top of this unit in this core is coincident with the high amplitude, irregular seismic reflector that marks the top of the PQ unit.

Onshore, the Eocene-age Santee Limestone defines the southern margin of the Santee River incised valley and crops out as both massive and cross-bedded, coarse-grained, phosphatic, fossiliferous grainstone. These outcrops continue along the southern banks of the upper Santee and South Santee Rivers to within 18 km of the coast. Borehole descriptions from both the USGS and the SCGS indicate that Eocene carbonate-rich and Paleocene siliciclastic units also underlie Quaternary sediment across the coastal plain.

Closer to the modern coast, the base of the Santee River incised valley is marked by the top of the marls of the Oligocene Cooper Group and the Santee Limestone (Payne 1970; Colquhoun et al. 1972; Eckard et al. 1986). Boreholes onshore near Bulls Bay indicate that the Miocene Marks Head Formation, Oligocene Ashley Formation, and Eocene Santee Limestone unconformably underlie Quaternary sediment at elevations ranging from 8-22 mbsl (Weems and Lewis 1997; Weems et al. 2014).

Interpretation— Beneath the coastal plain and inner shelf of South Carolina, the siliciclastic and carbonate sediments and rocks upon which Quaternary sediments lie range in age from Cretaceous to Pliocene (Hathaway et al. 1976; Popenoe 1985; Popenoe et al. 1987; Colquhoun 1995; Weems and Lewis 2002; Baldwin 2006; Schwab et al. 2009; Thielier et al. 2014).

Offshore, the contact between Quaternary deposits and pre-Quaternary rocks is associated with a prominent, high-amplitude reflector in both shallow, high-resolution seismo-acoustic and deeper seismic data. In deeper seismic profiles, the top of the Eocene Santee Limestone dips uniformly to the SSE at an angle of $\sim 0.15^\circ$. The down-dip extent of this surface within our dataset lies at a depth of 65 mbsl offshore of Bulls Island and rises to just below the seafloor offshore of the northern end of Cape Romain. In places, this unit crops out along the seafloor forming isolated patches of hardbottom (Fig. 2.4a). Offshore of Bulls Bay, the upper surface of this unit contains numerous, small-offset faults ($< 5\text{m}$) with spacing ranging from 100-500 m.

Progradational Facies

Two different types of progradational facies occur within the subsurface of the coastal plain and inner shelf. These are primarily distinguished based on the geometry and amplitude of their internal, seaward-dipping seismic reflectors. Progradational facies form in response to the seaward migration of coastal lithosomes resulting from the balance between changes in RSL, sediment supply, shoreface accretion, and from offshore-directed shelf currents (Davis 1994; Snedden et al. 2011; Patruno et al. 2015; Pendleton et al. 2017; Plink-Björklund 2019). These processes produce parallel planar-tabular as well as sigmoidal tangential clinofolds that bound thin (decimeter) clinofolds (Patruno and Helland-Hansen 2018; Plink-Björklund 2019).

Parallel-oblique progradational seismic facies (SF PGp)

Description— SF PGp is defined by planar, parallel-oblique, low to moderate -amplitude, moderate-frequency, high-continuity, seismic reflectors. Individual units of this facies are up to 4 m thick, show little internal variability and often grade laterally into thin, internally transparent units with undulatory upper surfaces (Fig. 2.4). Their upper bounding surface is always coincident with the seafloor. Externally, PGp units commonly exhibit an asymmetrical ridge-and-swale cross-sectional morphology, with a steeply-dipping seaward margin and a low-angle landward-facing margin (Fig. 2.4). In planview, these elements form cusplate shoals that extend up to 25 km offshore of the Santee Delta, Cape Romain, and Bulls Bay (Fig. 2.4). Offshore of Cape Romain, Core SC-VC24 penetrated well-defined examples of this facies and recovered 1.5 m of coarse- to very coarse-grained shelly sand and medium to fine-grained sand (Fig. 2.3). Stratigraphic units containing this facies were also observed inshore along the southern margin of Winyah Bay adjacent to Cat Island (Fig. 2.4). Offshore of Cape Romain, calibrated AMS-¹⁴C dates from Core SC-VC24 indicate that a stratigraphic unit consisting of PGp SF was deposited between 8.4 ka and modern times (Fig. 2.3 and 2.4).

Interpretation— Stratigraphic units of this SF were deposited within two distinct depositional environments; shelf sand ridges and wave-dominated delta fronts. Offshore PGp units and associated shoals were interpreted by Swift (1975a) as shoal retreat massifs, shoreface deposits that have been reworked during the Holocene transgression. Similarly, Sexton et al. (1992) and Hayes (1994) interpreted these features as deltaic lobes of the Santee/Pee Dee system deposited during hiatuses in the Holocene transgression. The internal architecture and cross-sectional geometry of offshore PGp units is nearly identical to Holocene shelf sand ridge systems previously recognized along the inner shelf of the US east coast (Fig. 2.4) (Swift 1975a; Swift et al. 1984; Goff 2009; Snedden et al. 2011; Pendleton et al. 2017) as well other locations around the world

(Snedden and Dalrymple 1999; Bassetti et al. 2006; Suter 2006; Snedden et al. 2011; Durán et al. 2018). Snedden et al. (2011) proposed a mechanism for the deposition of sand ridges offshore of New Jersey in which the initial sediment is derived from coastal lithosomes, these sediment bodies become detached from the associated shoreline and migrate seaward under storm-related currents. This process requires what Snedden and Dalrymple (1999) referred to as a ridge nucleus, which could have formed by sandy coastal deposits such as tidal deltas, nearshore bars, relict barrier deposits, or deltaic mouth-bars.

While the shoal complex offshore of Cape Romain and the Santee Delta are similar internally to these features, their planform morphology is quite different. Though most other known examples of shelf sand ridges are linear and oriented oblique to the shoreline (Snedden and Dalrymple 1999; Snedden et al. 2011; Warner et al. 2014; Pendleton et al. 2017), the examples in this study are arcuate or cusped along the inner shelf and become progressively more linear further offshore. This trend may indicate that near-shore ridges maintain their inherited morphology throughout early stages of development but transition to a more linear morphology during continued transgression and offshore migration. The prominent, seaward-dipping, internal seismic reflectors within this SF are 3rd order bounding surfaces (Fig. 2.4). Snedden et al. (2011) interpreted similar surfaces as defining periods of storm-driven accretion during the late Holocene.

Inshore, along the outer southern margin of Winyah Bay, this facies occurs adjacent to a Pleistocene beach ridge complex on Cat Island (Fig. 2.1c). Stratigraphic units defined by PGp SF at this location are interpreted as extensions of the Cat Island beach ridge/shoreface complex, and therefore document the subsurface architecture of a Pleistocene, wave-dominated shoreface system (Fig. 2.4). Beach-ridge systems are ubiquitous in delta plains and delta fronts of modern wave-dominated deltas (Bhattacharya and Giosan 2013; Ainsworth et al. 2019). Shen (2017) used

optically-stimulated luminescence (OSL) and ground-penetrating radar (GPR) to show that the onshore portion of this unit was deposited between 80 and 68 ka, i.e. during a cold stadial period (Marine Isotope Stage 4).

Tangential-oblique progradational seismic facies (SF PGt)

Description— Seismic facies PGt is characterized by tangential-oblique, moderate to high-amplitude, moderate-continuity, high-frequency seismic reflectors (Fig. 2.5). In contrast to PGp SF that exhibit continuous, nearly uniformly-dipping foresets, stratigraphic elements defined by PGt facies are commonly organized into subordinate packages bound by low-angle reactivation surfaces (Fig. 2.5). Within these packages, foreset dips tend to decrease in a seaward direction and in some instances transition into horizontal to sub-horizontal seismic reflectors.

The upper bounding surfaces are commonly rugose, are incised by small (2-3 m thick) paleochannels, and lack preserved topsets suggesting that these units have been exposed to subaerial erosion (Figs. 2.4b and 2.5). Externally, these units tend to be sheet-like or wedge-shaped, exhibiting variable thickness resulting from erosion or lapout. Stratigraphic units of PGt SF are always top-truncated, making an estimation of original thickness impossible. Maximum thickness of stratigraphic units defined by PGt SF is approximately 8 m, though most examples are less than 5 m. Based on available data, PGt units extend discontinuously from the nearshore to at least 50 km offshore (Fig. 2.5c).

No sediment cores recovered material from stratigraphic units of this SF, therefore the ages of these units are loosely constrained. Core SC-VC22 recovered 1.5 m of thin to thickly interbedded quartzose sand and mud (Fig. 2.3) from a laterally equivalent unit offshore of Bulls Bay (Fig. 2.5). At this location, the age of this unit is constrained by radiocarbon dating to between 42 and 34 cal ka BP, i.e. the later Marine Isotope Stage 3 right before the onset of the Last Glacial

Maximum (Fig. 2.3). Just to the north, off of Cape Romain, PGt SF comprise a stratigraphic unit that is overlain by Holocene shelf deposits and cross-cut by a broad, shallow paleochannel that was filled between 46 and 35 cal ka BP (Figs. 2.3 and 2.4).

Interpretation—The variability in progradation direction, as indicated by the development of 4th order bounding surfaces, suggest temporal and spatial variability in sediment supply during deposition. Small paleochannels that mark the upper boundaries of these units were likely formed as relatively shallow distributary channels that filled following avulsions. These characteristics differ markedly from PGp SF and are consistent with deposition along fluvially-dominated deltaic shorelines where sediment is largely derived from a point source via distributary channels along laterally variable, often lobate delta fronts and commonly modified by waves and tides (Fielding et al. 2005; Willis 2005; Olariu and Bhattacharya 2006; Ainsworth et al. 2016, Van Yperen et al. 2019).

Within stratigraphic units consisting of this SF, 3rd order bounding surfaces define clinofolds and separate individual tangential clinothem while 4th order surfaces bound packages of these clinofolds (Fig. 2.5). These packages are likely the result of autogenic changes within the deltaic system, such as distributary avulsions, and represent distinct deltaic lobes (Fig. 2.5). Fifth-order bounding surfaces define the bases of small (<3 m) paleochannels (Figs. 4 and 5) which were likely formed by shallow distributary channels.

Locally, laterally-continuous PGt stratigraphic units indicate up to 10 km of continuous, though punctuated, progradation (Fig. 2.5). The seaward extent of these units suggests that they formed as regressive deltaic deposits possibly in response to a significant fall in RSL, although in low-accommodation settings such as this, significant progradation can also occur irrespective of significant changes in RSL (Field and Trincardi 1991; Zecchin 2007). Progradation of coastal

lithosomes is ultimately tied to the balance between the rate of accommodation development and the rate of sediment supply (Muto and Steel 1997; Zecchin 2007). Low-accommodation may also influence the lateral extent of delta front deposits and lead to amalgamation of delta front and distributary channel deposits (Van Yperen et al. 2019). The heterolithic interval adjacent to this SF from Core SC-VC22 occurs within a channelized topset section of a PGt unit off of Cape Romain and may indicate tidal influence within a shallow delta-plain embayment (Fig. 2.3a).

In a thorough summary of regressive deposits on continental shelves, Field and Trincardi (1991) noted that regressive deposits on low-accommodation shelves, such as the study area, are rarely preserved landward of the outer shelf due to effective reworking during subsequent transgressions. This is in contrast to shelf margin or tectonically active areas, where increased accommodation facilitates the preservation of thicker regressive deposits (Matteucci and Hine 1987; Field and Trincardi 1991; Harris et al. 2013).

Horizontally-stratified seismic facies (SF HS)

Description— Seismic Facies HS is defined by high to moderate-amplitude, high continuity, moderate to low-frequency, horizontal to sub-horizontal seismic reflectors (Fig. 2.2). The external bounding surfaces and cross-sectional geometries of HS stratigraphic units are both highly variable. This SF comprises unique stratigraphic units as well as lateral equivalents transitioning into other seismic facies such as PG and CH facies (Figs. 2.4b and 2.4c). Core SC-VC22 recovered almost 3 m of mud-rich, heterolithic sediment from the upper part of a 4-5 m thick HS unit offshore of Bulls Bay (Figs. 2.3 and 2.4) indicating that this unit was deposited under low-energy, tidally-influenced conditions.

Interpretation—Stratigraphic units defined by HS SF were deposited within a range of depositional environments within which low to variable-energy conditions prevailed including prodelta, backbarrier, and open shelf settings.

Directly offshore of the Santee Delta this SF is associated with PGt deposits where it was deposited as bottomsets associated with PGt clinoforms (Fig. 2.4b). These deposits are the least laterally extensive of the HS units based upon the current dataset.

In Winyah Bay, this SF underlies, a unit defined by PGp SF (Fig. 2.4c). Although no sediment cores were taken from the Winyah Bay location, Shen (2017) recovered mud-rich, backbarrier deposits beneath a 5-m thick unit of progradational (PGp) shoreface deposits that were dated to the last interglacial period (Marine Isotope Stage-5a) from a location a few km north of Winyah Bay (Fig. 2.1b). This configuration is similar to that of the PGp SF from the southern margin of Winyah Bay (Fig. 2.4c). Offshore of Cape Romain a 5- to 6-m thick unit of backbarrier sediment was deposited between 49.9 and 44.9 ka (Fig. 2.3), although these ages are near the detection limits for AMS ^{14}C dating. Subsurface backbarrier deposits are common across the US Atlantic shelf where they are erosional remnants of backstepping barrier island systems that formed in response to the Holocene transgression (Swift 1975b).

Further to the south, in the Folly-Kiawah area, several cores recovered sediment from this facies. Cores SC-VC15 and SC-VC18 recovered indurated, mud-rich, heavily bioturbated, heterolithic sediment containing abundant marine bivalve and gastropod shells (Fig. 2.1) (Long 2018). We interpret these units as lower shoreface/inner-shelf deposits. This unit lies beneath a thick Holocene shoal complex.

Indistinct seismic facies (SF ID)

Description—This facies is defined by the lack of internal seismic reflection. Elements of this facies are typically thin (<3 m), sheet-like and occur most commonly as the uppermost part of paleo-incision fill successions. In this setting they occur as extensive, irregular sheets or lateral equivalents of PGp facies offshore. Several cores from the Folly-Kiawah area have sampled this facies and reveal them to be composed almost exclusively of well-sorted, medium- to coarse-grained sand (Long 2018). Grain size ranges from fine to very coarse sand and composition can be shelly, phosphoritic, or quartz-rich.

Interpretation— The internal stratigraphic architecture, or lack thereof, is non-diagnostic. However, the lack of internal structure is likely a function of the largely homogenous, sand-rich composition of stratigraphic units that comprise this SF. The broad, sheet-like geometries, stratigraphic positions, and composition suggest that elements that comprise these SF were emplaced by the reworking of shoreface deposits by waves and tides or as offshore shoal complexes forming a discontinuous, autochthonous, transgressive sand sheet (Swift and Thorne 1991; Swift et al. 1991; Zecchin et al. 2019). Many of these units form extensive sandy shoals along the inner shelf and, in places, are laterally equivalent to elements of PGp facies. Several cores from both the primary study area as well as the Folly-Kiawah area have penetrated this facies and indicate sand-rich successions of diverse composition and grain size, commonly exhibiting basal, coarse-grained, shelly lags (Long 2018).

Paleo-incisions

Paleo-incisions are defined based on their fill architecture as well as the substrate into which they are eroded. Both basement-incising paleo-incisions and minor paleochannels (those that do not incise into basement) are common across the offshore portion of the study area (Fig. 2.10a). Larger paleovalleys are always basement-incising (Fig. 2.6 and 2.7) while minor paleo-

incisions can either be entirely contained within the Quaternary section or have a channel floor defined by PQ basement (Long 2018). Minor paleochannels may not be directly related to base level changes but can be attributed to autogenic fluvial or estuarine channel hydrodynamics. Minor paleochannels are common along the upper surface of PGt units (distributary channels) (Fig. 2.4 and 2.5) as well as within upper sections of paleovalleys (Figs. 2.6 and 2.7).

Paleochannel seismic facies (SF CH)

Five paleo-channel SF are defined here described based the geometry of their internal reflectors. Paleochannel fill patterns and the SF which they define are concentric (CHc), horizontal (CHh), asymmetric (CHa), chaotic (CHk), and transparent (CHt) (Table 2.1, Fig. 2.2).

Description— Concentrically-filled paleochannels (CHc) are characterized by concave-up, high to moderate-frequency, continuous, high-amplitude seismic reflectors arranged in a vertically concentric configuration. Horizontally-filled paleochannels (CHh) are characterized by horizontal to sub-horizontal, high to moderate frequency, continuous, moderate-amplitude seismic reflectors. CHc and CHh are the most well-constrained by core data and are the most common of the observed paleochannel SF within the study area. Cores SC-VC19 and SC-VC21 both penetrated 5-6 m-thick paleochannels dominated by these SFs and reveal mud- and organic-rich, heterolithic sedimentary successions deposited in low-energy, tidally-influenced, backbarrier settings (Long 2018). Cores SC-VC14 and SC-VC24 penetrated two separate CHc and Chh paleochannels and recovered 2-3 m of mud and sandy mud with thinly-bedded sands and shelly sands (Long 2018). Asymmetrically-filled paleochannels (CHa) are characterized by inclined, moderate-amplitude, continuous, moderate to high-frequency seismic reflectors. A single core from the Folly-Kiawah area (SC-VC07) penetrated the margin of a small paleochannel containing this facies and recovered 2 m of sand-rich, heterolithic sediment (Long 2018). While this

succession contains a significant amount of mud, it is sandier than the CHc or CHh facies. Chaotically-filled paleochannels (CHk) are characterized by irregular, low-amplitude, discontinuous, low to moderate-frequency seismic reflectors. Transparently-filled paleochannels (CHt) are characterized by the lack of prominent internal seismic reflection and have been observed elsewhere to be either sand- or mud-rich (Long 2018).

Interpretation— Mixed-lithology asymmetric paleochannel fill (CHa) is indicative of deposition via lateral or downstream accretion of large bar forms, spits, or bayhead deltas (Mallinson et al. 2010; Alqahtani et al. 2015; Durkin et al. 2015; Ashoff et al. 2018). Several other examples of CHa units occur in the subsurface including an excellent example of laterally accreting point bar architecture in the vicinity of SC-VC24 offshore of Cape Romain where it cross-cuts a PGt element, indicating the presence of a sinuous fluvial/estuarine channel (Long 2018).

Chaotic (CHk) and transparent (CHt) paleochannel fill comprise the high-energy/sand-rich CH SF units. These represent sediments deposited in relatively high energy or variable energy settings as channel-floor bars and large bedforms (Mitchum et al. 1977; Mellet et al. 2013). No cores were recovered from these SF within the study area and these types of paleochannels are rare. Transparent paleochannel SF (CHt) are also rare and offer little information as to their depositional origin. The lack of internal seismic reflection suggests relatively homogenous sedimentary fill, which is either sand- or mud-rich. There are two prominent examples of this type of paleochannel within the main study area. These are basement-incising CHt SF paleochannels offshore of North Inlet and offshore between the South Santee River and Cape Romain (Fig. 2.10a), both of these trend to the ESE.

Incised valleys and paleovalleys

The Santee River system has occupied at least three distinct alluvial valleys during the Quaternary (Colquhoun et al. 1972; Weems et al. 1994, 1997, 2014). Onshore, the base of the modern Santee River Incised Valley is approximately 20 mbsl and is carved into underlying Eocene carbonate rocks as evidenced by existing borehole data (Payne 1970; Colquhoun et al. 1972; Eckard et al. 1986) as well as seismo-acoustic profiles and sediment samples acquired during the course of this study (Figs. 2.6 and 2.9). Sediment cores recovered from the modern Santee delta plain (Fig. 2.1) were typically limited to a depth of 5-6 mbsl where they encountered a thick freshwater peat layer that was deposited between 6-5 cal ka BP based on AMS-¹⁴C dating (Long and Hanebuth 2017). Above this laterally-persistent peat layer, heterolithic, tidally-influenced sediments were deposited within estuarine channels and floodplains beginning around 3.5 cal ka BP, based on sedimentological, micropaleontological, and AMS-¹⁴C data (Long and Hanebuth 2017).

Offshore, seismo-acoustic data indicate that the base of the Santee River Paleovalley ranges from 24 mbsl deep near shore to 30 mbsl further offshore (Figs. 2.6 and 2.9). Five km offshore, the Santee River Paleovalley incises down to 24 mbsl, into the Eocene Santee Limestone (Fig. 2.6). At this location, the Santee Paleovalley is 8 km wide, with a valley-floor morphology that is influenced by a small anticline with a vertical relief of 8 m that originates from within the pre-Quaternary section (Hanebuth and Long 2020). Twenty-five km offshore, this feature is clearly imaged (Figs. 2.6 and 2.9) and contains a fill succession consisting of a northern and a southern paleovalley, each of them incising down to approximately 30 mbsl and separated by a wide interfluvial containing high-relief erosional remnants of PQ units (Fig. 2.6).

Using existing borehole data, we have mapped the Bulls Bay Paleovalley in detail further inland to a point near Jamestown, SC where it diverges from the modern incised valley of the Santee River (Figs. 2.1 and 2.10a). In this area the Bulls Bay Paleovalley fill contains abundant feldspathic

sands, gravelly sands, and rock fragments (Fig. 2.7), which makes it texturally and mineralogically immature. Several boreholes immediately onshore of Bulls Bay contain up to 15 m of fluvial gravels and gravelly sands overlain by mud-rich estuarine deposits (BI96-4 and AW96-8; Fig. 2.1) (Weems and Lewis 1997).

The Bulls Bay Paleovalley can be traced offshore where it, much like the Santee River Paleovalley, splits into two main paleovalleys and several smaller paleochannels (Figs. 2.7 and 2.10). The paleovalleys are overlain by broad, structureless sheets, likely deposited as a transgressive sand sheets (SF ID) during the Holocene. The Bulls Bay Paleovalleys also have significant secondary paleoincisions indicating that they pre-date the LGM (Fig. 2.8).

Onshore, the Bulls Bay Paleovalley and Santee Incised Valley systems diverge from each other near the Oceda Fault Zone, as mapped by the SCGS (Clendenin in press), suggesting the possibility that the avulsion of the Santee River was fault-related, responding to locally differentiated vertical motion which led to a change in local accommodation. Alternatively, or perhaps additionally, Colquhoun et al. (1972) proposed that avulsion occurred due to autogenic processes related to the accumulation of deltaic sediment along the Bethera Scarp (Fig. 2.8).

The third, and oldest, valley of the Santee River has been mapped onshore from borehole data near Harleyville, SC, more than 60 km to the southwest of Jamestown (Weems et al. 1994, 2014). While we have yet to constrain the trend of this paleovalley in as much detail as we have the Bulls Bay Paleovalley, Weems et al. (1994, 2014), proposed that it underlies Four Hole Swamp in southern Calhoun County, SC and has been re-occupied by the modern Edisto River, a trend that would intersect the modern coastline nearly 130 km south of the Holocene Santee Delta. Borehole descriptions by Weems et al. (1987, 1997) describe paleovalley fill that is similar to that documented for the Bulls Bay Paleovalley and a valley-floor elevation that ranges from 11 to 23

mbsl. The lithology of the paleovalley-filling Waccamaw Formation is dominated by immature, coarse-grained, feldspathic sand and gravel (Weems et al. 1987, 2014). The Four Hole Paleovalley has not yet been identified offshore due to data limitations.

Bounding Surfaces

We define six orders of bounding surfaces, conformable and erosional as well as local and regional; these are summarized Table 2.2. Where possible, these surfaces adhere to those formalized by Miall (1985, 1988, 2010). First and 2nd order surfaces are recognizable only in sediment cores, are not resolvable in our seismo-acoustic data and are therefore not components of our stratigraphic framework. Third-order surfaces define the internal architecture of genetically-related stratigraphic units (Table 2.2, Figs. 2.4 and 2.5). Examples of 3rd order surfaces are the seaward-dipping reflectors of PGp and PGt SF within progradational stratigraphic units (Figs. 2.4 and 2.5) as well as the aggradational surfaces within paleochannel-fill successions.

Fourth-order surfaces separate stratigraphic units of similar accretionary trends and mark diastems or minor breaks in deposition. These surfaces are analogous to reactivation surfaces and can exhibit localized erosion. Fourth-order surfaces are most common within stratigraphic units consisting of PGt SF (Figs. 2.4 and 2.5) where they likely represent relatively short periods of non-deposition due to localized changes sediment supply related to avulsion events within deltaic distributary channels (Ainsworth et al. 2019).

Fifth-order surfaces define significant, local, erosion, commonly forming the basal surface of individual paleochannels. Sixth-order surfaces are rugose, high-amplitude seismic reflectors that mark regional erosional surfaces. In sequence stratigraphic terminology, 6th order surfaces are equivalent to transgressive ravinement surfaces and sequence boundaries (Catuneanu 2006; Miall 2010; Zecchin et al. 2019). More specifically, 6th order surfaces formed in response to high-

frequency glacio-eustatic changes (Fig. 2.8) and bound genetically-related stratigraphic units (Fig. 2.9). Onshore, Colquhoun et al. (1991) and Doar and Willoughby (2008) defined similar, regional erosional bounding surfaces that they used to define the alloformations that define the boundaries of late Pleistocene scarp and terrace morphostratigraphic units (Figs. 2.1 and 2.8).

DISCUSSION

Because of the discontinuous nature of the stratigraphic record and relative paucity of age-control, we discuss the temporal and spatial distribution of stratigraphic units as it pertains to the history of relative sea-level change. Figure 2.10 summarizes the temporal evolution of this region, and Figure 2.8 relates deposition of key stratigraphic features defined here to the history of relative sea level change during the late Quaternary.

Lowstand Systems

Regional lowstand deposition, as it pertains to the relatively shallow continental shelf within the study area, occurred when RSL was at or below the shelf margin which, within the study area, lies at a present water depth of approximately 60 m (Fig. 2.1). Therefore, lowstand conditions in this setting were not limited to glacial maxima but rather would occur whenever RSL exceeds the depth of the regional shelf margin which has happened during numerous stadial and glacial Marine Isotope Stages throughout the Quaternary (Fig. 2.8). The relationship between marine deposits and their present elevation is further complicated by regional post- and syn-depositional uplift (Doar 2014; Doar and Kendall 2014). These two factors make it difficult to directly relate depositional trends and stratigraphic units and their modern absolute elevation to global, proxy-based sea-level reconstructions (Fig. 2.8).

Paleo-incisions—Lowstand elements within the study area are limited to a complex network of paleo-incisions (Fig. 2.10a). The Santee River has occupied at least three prominent

paleovalleys throughout the Quaternary (Colquhoun et al. 1972; Weems et al. 1994, 2014). These paleovalley systems resulted from incision into indurated or lithified underlying pre-Quaternary sedimentary basement with depth of incision across the entire study area, both onshore and offshore, ranging from 25 to 30 mbsl (Figs. 2.6, 2.7, and 2.9).

Onshore, the paleovalleys of the Santee River define a younging-to-the-north trend. The Four Hole Paleovalley system defines the southern-most paleovalley system and was active from the late Pliocene to the early Pleistocene (Weems et al. 1994, 1997). Following one or a series of avulsions, the Bulls Bay Paleovalley system was likely active until approximately 200 ka, although the timing of development of the initial incision is uncertain (Colquhoun et al. 1972; Weems et al. 1997, 2014; Doar 2014). Both the Four Hole Paleovalley and Bulls Bay Paleovalley systems were eventually abandoned due to northerly avulsions associated with RSL highstands at approximately 1.4 Ma and 200 ka, respectively (Colquhoun et al. 1972; Weems et al. 1994) (Fig. 2.8). The latter, as previously described, may have been influenced by local, fault-related accommodation change and resulted in the development of the modern incised valley of the Santee River. Remarkably, this stepwise northern migration trend of the Santee River throughout the Quaternary is the opposite of that proposed by Baldwin et al. (2006) for the Pee Dee River. The consequence of these trends is that the modern configuration, where these two major river systems have nearly converged and enter the Atlantic Ocean within only a few kilometers of one another, undoubtedly having increased the sediment supply to this particular area since the late Pleistocene.

Compared to the relatively simple paleovalley geometries mapped from onshore borehole data, the high-resolution seismic offshore data set offshore allows us to better understand the complex nature of these systems. The Bulls Bay Paleovalley and Santee Incised Valley can be projected offshore, and each valley consists of two narrower paleovalleys containing multiple

paleochannels and showing evidence of recent re-channelization (Fig. 2.6 and 2.7). The lack of age control in any part of the offshore segments of these systems prevents establishing a more specific stratigraphic or temporal relationships between component paleovalleys.

Models proposed for incised valley depositional systems include the preservation of a coarse-grained fluvial lowstand systems tract within the basal part of the valley-fill which is overlain by finer-grained estuarine deposits (Dalrymple et al. 1992; Ashley and Sheridan 1994). While onshore paleovalleys within our study area certainly contain a basal, fluvial component (Fig. 2.7) (Eckard 1986), most examples imaged by high-resolution seismic data offshore do not appear to exhibit this partitioning (Figs. 2.6 and 2.7). Rather seismic facies analysis suggests that most paleochannels are filled by CHc or CHh units which, based upon limited core control, tend to be dominated by mud-rich and tidally-influenced deposits (Figs. 2.3, 2.4, 2.5, 2.6, 2.7, and 2.9).

Shelf margin systems—In addition to the paleo-incisions documented here, shelf-margin (60 mbsl) lowstand systems have been reported from adjacent areas. Matteucci and Hine (1987) defined a thick, shelf-edge deltaic system associated with Cape Fear offshore of North Carolina that extends from approximately 50 to 200 m water depth. They interpreted multiple periods of shelf-edge deposition, with the youngest deposits being of Quaternary age (Matteucci and Hine 1987). To the south of our study area, Harris et al. (2013) identified a progradational internal architecture associated with a shelf-edge protuberance in 50-60 m water depth. They termed this feature the Geneva Delta and concluded that it was active in two primary phases during periods of RSL lowstands within MIS 3, between 60 and 25 cal ka BP (Harris et al. 2013). While we lack data to verify the existence of similar features in our study area, it would be reasonable to infer that the paleovalleys we have identified would have fed shelf-margin coastal systems at various periods throughout the Quaternary. Given the relatively shallow depth of the continental shelf in

this region (Fig. 2.1), the deposition of shelf-margin systems was likely not limited to major, glacioeustatic lowstands (Fig. 2.8). Rather, shelf-margin depositional systems may have been deposited whenever RSL reached the regional shelf margin which occurred numerous times throughout the Quaternary (Shackleton 1987; Lisiecki and Raymo 2005) (Fig. 2.8).

Transgressive Systems

Paleochannel fills—While paleochannels are initially formed during falling and lowstand stages of RSL, the sedimentary successions preserved within these features are predominantly deposited under conditions of rising RSL, as evidenced by core lithofacies and seismic facies analyses (Figs. 2.3, 2.6, 2.7, and 2.9). As discussed above, CHc and CHh SFs are the most common type of paleochannel fill architectures. AMS-¹⁴C dating from a CHa element offshore of Cape Romain indicate that mud-rich, estuarine fill was deposited during the late Pleistocene prior to 40 cal ka BP (Figs. 2.4 and 2.6).

Sand sheets and shoals—Laterally extensive, sheet-like stratigraphic units consisting of ID SFs are ubiquitous within the study area. They commonly form the uppermost portion of paleochannel and paleovalley successions. Both the Bulls Bay Paleovalley (Figs. 2.7 and 2.9) and the Santee Paleovalley are capped by these sand sheets (Figs. 2.6 and 2.9). In this setting, these elements were likely deposited as late-stage transgressive sand sheets by erosion of coastal lithosomes related to wave ravinement (Swift 1975b; Thorne and Swift 1991; Cattaneo and Steel 2003). In several locations, these units overlie one another and are separated by regional, sometimes channelized, 6th order bounding surfaces that represent composite transgressive ravinement surfaces and sequence boundaries. The ID units that overlie the Bulls Bay Paleovalley shown in Figure 2.6b clearly illustrates this configuration.

Sand ridges—The internal architecture, lithology, and age of offshore sand-ridge units composed of PGp SFs is consistent with the model proposed by Snedden et al. (2011). A well-imaged example of one of these elements in 10-15 m water depth can be seen in Figure 2.6. PGp samples from the SC-VC24 core yield a mid- to late-Holocene age, indicating that it has been actively prograding during this time. While sediment may have been derived from a shoreface system, these features were ultimately shaped by storm-related shelf currents following submergence during the Holocene transgression and therefore are genetically classified as transgressive.

Backbarrier deposits—A stratigraphic unit consisting primarily of HS SF with minor channelization at its base occurs off of Cape Romain (Fig. 2.5). Core SC-VC22 (Fig. 2.3) recovered 3 m of mud-rich, tidally-influenced, heterolithic estuarine deposits from this unit. The upper meter of this succession was deposited during late Pleistocene between 41 and 44 cal ka BP based on AAR and calibrated AMS-¹⁴C data (Long 2018; Alexander, personal communication 2019; Wehmiller et al. 2019) as backbarrier deposits likely associated with the Mt. Pleasant barrier system (Figs. 2.1, 2.8, and 2.10).

Inshore, within the modern Santee delta plain, we recovered 110 m of sediment from 46 sediment cores deposited over the past 6 ka in similar environments as indicated by calibrated AMS-¹⁴C samples, microfossil and lithofacies assemblages (Long and Hanebuth 2017). Previous studies have recovered similar deposits of similar age from the Santee Delta (Payne 1970; Mullins 1973; Stephens et al. 1976; Eckard et al. 1986) and Cape Romain (Hayes 1994). The base of this interval is marked by a 2-3 m thick peat deposited between 10 to 5.5 ka (Hayes 1994; Long and Hanebuth 2017) and extends several kilometers offshore (Sexton et al. 1992) (Fig. 2.10).

Regressive Systems

PGt and PGp SF comprise regressive stratigraphic units deposited throughout the Quaternary under a range of depositional regimes. The preservation of Quaternary regressive deposits within the stratigraphic record across low-gradient continental shelves is rare (Field and Trincardi 1991). Stacked PGt units offshore of the Santee River likely attest to its proximity as a significant sediment source (Figs. 2.5 and 2.9), depositing more sediment than can be eroded and reworked during subsequent transgressive phases. The rate of RSL rise also influences the preservation potential of regressive deposits across the continental shelf (Cattaneo and Steel 2003; Zecchin et al. 2019). A rapid rise in RSL can lead to incomplete reworking of regressive units deposited during previous sea-level cycles (Catuneanu and Zecchin 2013).

Wave-dominated regressive units— A well-developed, deflected beach-ridge system, which Shen (2017) dated to 60-80 ka, is located adjacent to the modern Santee delta plain inland of Cat Island (Fig. 2.1c). It preserves discontinuity-bounded sets of beach-ridges that define a wave-dominated, cusped morphology. Although the landward extent of this beach-ridge complex is obscured by agricultural land usage, it records a minimum of 13 km of spatially-contiguous progradational beach ridges. This same beach-ridge complex continues northeast to the southern edge of Winyah Bay, where it curves towards this body of water (Fig. 2.5). Seismo-acoustic data collected from Winyah Bay, along the northern margin of Cat Island, reveal that the internal architecture of this beach ridge system consists of a PGp SF with internal, progradational surfaces that downlap the backbarrier deposits of an HS SF at a depth of 4.5 mbsl. This configuration suggests that the Pee Dee River had reached its approximate modern location during the same time period as it truncated the Cat Island beach ridges (Fig. 2.10e). This interpretation is consistent with the timing of the southerly migration of the Pee Dee River as proposed by Baldwin et al. (2006). On the southern side of the Santee Delta, equivalent beach-ridge systems are not as well developed,

suggesting a degree of asymmetry in beach ridge development, likely a result of the southerly-directed longshore current, a pattern that has been noted in many modern wave-dominated deltas (Fig. 2.10e) (Bhattacharya and Giosan 2003; Giosan et al. 2005, Ainsworth et al. 2019).

This deltaic system, which we refer to as the Awendaw Delta, is associated with the Awendaw scarp on Cat Island (Figs. 2.1, 2.8, and 2.10). On the basis of age estimates of the scarp (Doar 2014) and of the beach-ridge system (Shen 2017), the beach-ridge systems were deposited as part of a wave-dominated delta front during an intermediate MIS-3 RSL highstand (Figs. 2.8 and 2.10) (Doar 2014; Shen 2017). The deflection of beach-ridge systems adjacent to distributary channels is a result of the construction of progradational beach-ridges and mouth-bars at the coast through the littoral transport of fluvially-derived sediment, which is a common feature on wave-dominated deltas (Bhattacharya and Giosan 2003; Reading and Collinson 2006; Nanson et al. 2013; Ainsworth et al. 2019). Modern deltas of the Tiber (Italy), Sao Francisco (Brazil), Sao Pablo/Grijalva (Mexico), Elwha (USA) and Doce (Brazil) Rivers are all good examples of this geomorphic relationship (Psuty 1967; Hampson and Howell 2005; Milli et al. 2013; Zurbuchen et al. 2020). Smith et al. (2011) also provide an excellent example of this fluvial channel-beach ridge relationship in the wave-dominated lacustrine delta of the William River in Lake Athabasca, Canada.

Fluvially-dominated regressive units— The internal architecture of PGt-dominated stratigraphic units include a high degree of variability in clinothem foreset dip, abundance of 4th order surfaces, and numerous small paleochannels along the upper bounding surfaces are key differences when compared to the wave-dominated units (PGp) described above. They suggest spatial variability with regard to sediment supply, an increased abundance of distributary channels, and a stronger fluvial influence during deposition (Figs. 2.4 and 2.5). This fluvial influence

resulted in the deposition of a river-dominated delta where mouth-bars, fed by distributary channels, deposit discrete lobes with complex and highly variable stacking patterns (Field and Trincardi 1991; Olariu and Bhattacharya 2006) (Fig. 2.10). Architectural variability within PGt stratigraphic units can be significantly influenced by autogenic processes including fluvial discharge, distributary avulsion, and gravitational slumping of mouth-bar deposits along a delta front (Lee et al. 2007; Bhattacharya and MacEachern 2009; Plink-Björklund 2019). Fielding et al. (2005) provide an excellent example of the lateral variability developed in Holocene mouth-bar deposits of the Burdekin River in Australia, including the development of we define as 4th order bounding surfaces (their Fig. 2.7), as constrained by high-resolution GPR data.

Considering the stratigraphic complexity, post-depositional modifications, and paucity of age control in this area, it is difficult to constrain the age of these deposits. Offshore of Cape Romain, a unit of this SF is overlain by a mid-Holocene aged sand ridge system and cross-cut by a late Pleistocene paleochannel filled by backbarrier sediments deposited before 46 ka (Figs. 2.3 and 2.4a). To the south, offshore of Bulls Bay, a unit of this facies overlies backbarrier deposits that deposited prior to 40 ka (Fig. 2.5) and underlies a Holocene-aged sandy deposit. In this location, the PGt element overlies several large paleochannels and is itself incised by numerous smaller, younger paleochannels (Figs. 2.4 and 2.5).

In summary, fluvial-dominated deltaic deposits of the Santee River preserved on the continental shelf within the study area were deposited during multiple regressive phases including prior to 46 ka, after 42 ka but prior to 34 ka, and before 8 ka (Fig. 2.10). At other times, wave-dominated deltaic morphologies were dominant (Figs. 2.8 and 2.10). It is unclear as to exactly why these different phases occurred. River-dominated phases were likely associated with periods of increased fluvial sediment supply or dampening of the nearshore wave climate or vice versa. The

mechanism behind such forcings may include long-term climatic variability, regional or local structural deformation, or changes in nearshore oceanographic processes. Whatever the cause, this topic merits future study.

Conclusions

- 1) Thin, laterally-discontinuous Quaternary stratigraphic units, deposited during multiple glacio-eustatic cycles within fluvial, estuarine, paralic, and shelfal settings, are distributed across the modern continental shelf in the region offshore of the Santee Delta of central South Carolina. These units are correlative to RSL highstand deposits that have previously been documented extensively onshore.
- 2) The low-accommodation setting of the continental shelf influences the stratigraphic record in several key ways: a) The distance and rate of coastal lithosome progradation in response to sediment supply and glacio-eustasy; b) restriction of thick, mud-rich, transgressive deposits to paleochannels; c) widespread, thin transgressive sand sheets; and d) extensive erosion associated with composite subaerial and transgressive erosion.
- 3) Progradational, regressive stratigraphic elements deposited by mixed-process deltas, fed largely by the Santee River, record several episodes of across-shelf shoreline migration during the Quaternary. Such features have not been previously documented along the inner to middle shelf of the US Atlantic margin and may be preserved here because of locally higher sedimentation rates associated with the proximity to the Santee and possibly Pee Dee Rivers.
- 4) Sandy inner-shelf deposits, previously interpreted as shoal-retreat massifs or delta-front deposits, share strong similarities with shelf sand ridges that have been documented elsewhere along the US Atlantic continental shelf. The surface morphology of these sand ridge systems is cusate, in clear contrast to the numerous, linear sand ridge systems found elsewhere, and

their internal architecture indicates that they have been actively prograding throughout the late Holocene.

- 5) Both regional, Piedmont-draining fluvial systems and smaller coastal-plain rivers have produced a complex network of paleoincisions in this region throughout the Quaternary.
- 6) Three major shifts in the location of the Santee River incised valley have occurred during the Quaternary, at least one of these may have been influenced by fault-related changes in accommodation. A northerly migration of the Santee River throughout the Quaternary is defined by these three paleovalleys of the Santee River that young to the north.
- 7) The use of a hierarchical bounding surface scheme in this setting is preferable to the more common sequence stratigraphic or allostratigraphic nomenclature for several reasons: a) major erosional bounding surfaces (6th order), which are equivalent to sequence boundaries or transgressive surfaces of erosion, commonly become amalgamated, making it impossible to map individual surfaces; b) lower order (3-4th order) surfaces capture the internal variability associated with higher-frequency, autogenic processes which is key to the genetic interpretation of stratigraphic elements when detailed sedimentological data is not available; and c) the complex stratal architecture in this region is the result of multiple glacioeustatic cycles in a low-accommodation setting and consists of laterally-offset, sometimes disconnected, stratigraphic units lacking the stacking patterns required to establish a sequence stratigraphic framework.

Figure 2.1. a) Study location, and primary regional geomorphic features (LeGrand 1961; Popenoe et al. 1987). Santee River watershed outline from USGS North American Atlas Basin Watersheds (<https://www.sciencebase.gov/catalog/item/4fb697b2e4b03ad19d64b47f>). b) Study area and data centered on the Santee River Delta. Shelf-margin scarps from Matteucci and Hine (1987). Onshore Pleistocene scarps from Doar (2014) and Doar and Kendall (2014), bathymetry from NGDC CRF (<https://www.ncei.noaa.gov/metadata/geoportal/rest/metadata/item/gov.noaa.ngdc.mgg.dem:305/html>) c) Geomorphic features of the Santee Delta. Beach ridges mapped from aerial photographs. d) Bathymetric profile across the continental shelf directly offshore of the Santee River derived from NOAA NGDC CRF.

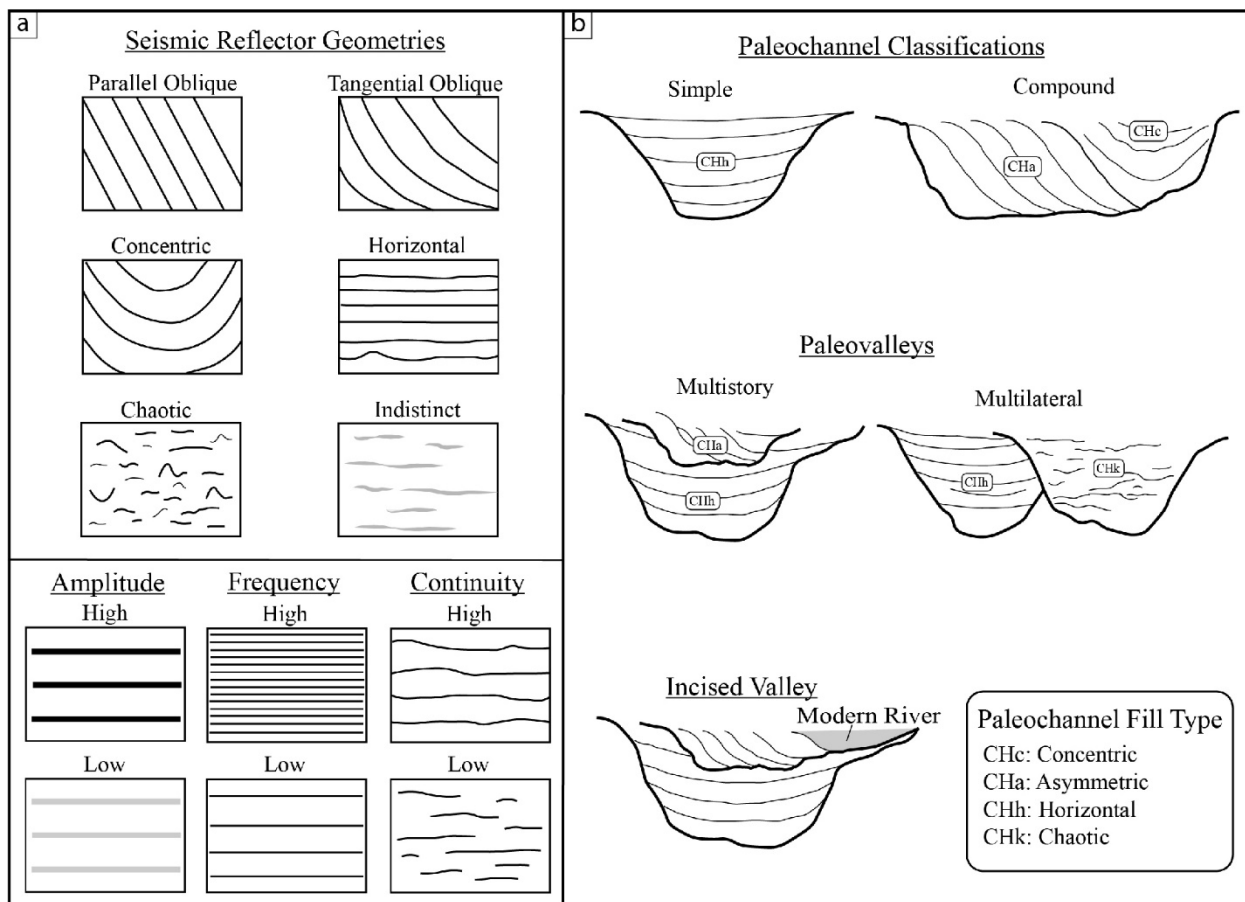


Figure 2.2. Classification and terminology of seismic reflector geometries used in this study. **a)** Characteristics of seismic reflectors. Adapted from Mitchum et al. (1977) and Mellet et al. (2013).
b) Paleo-incision classification used in this study.

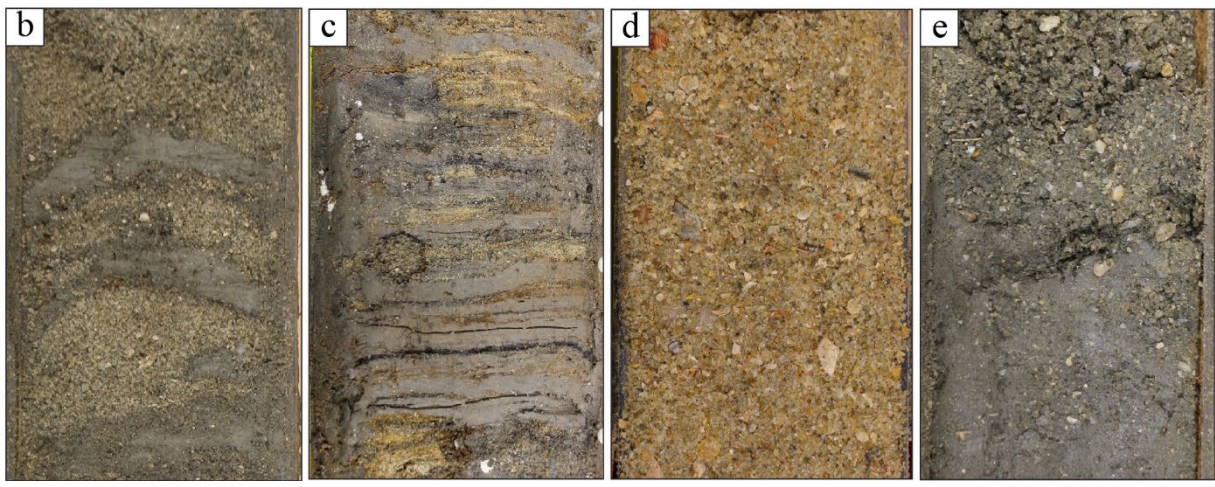
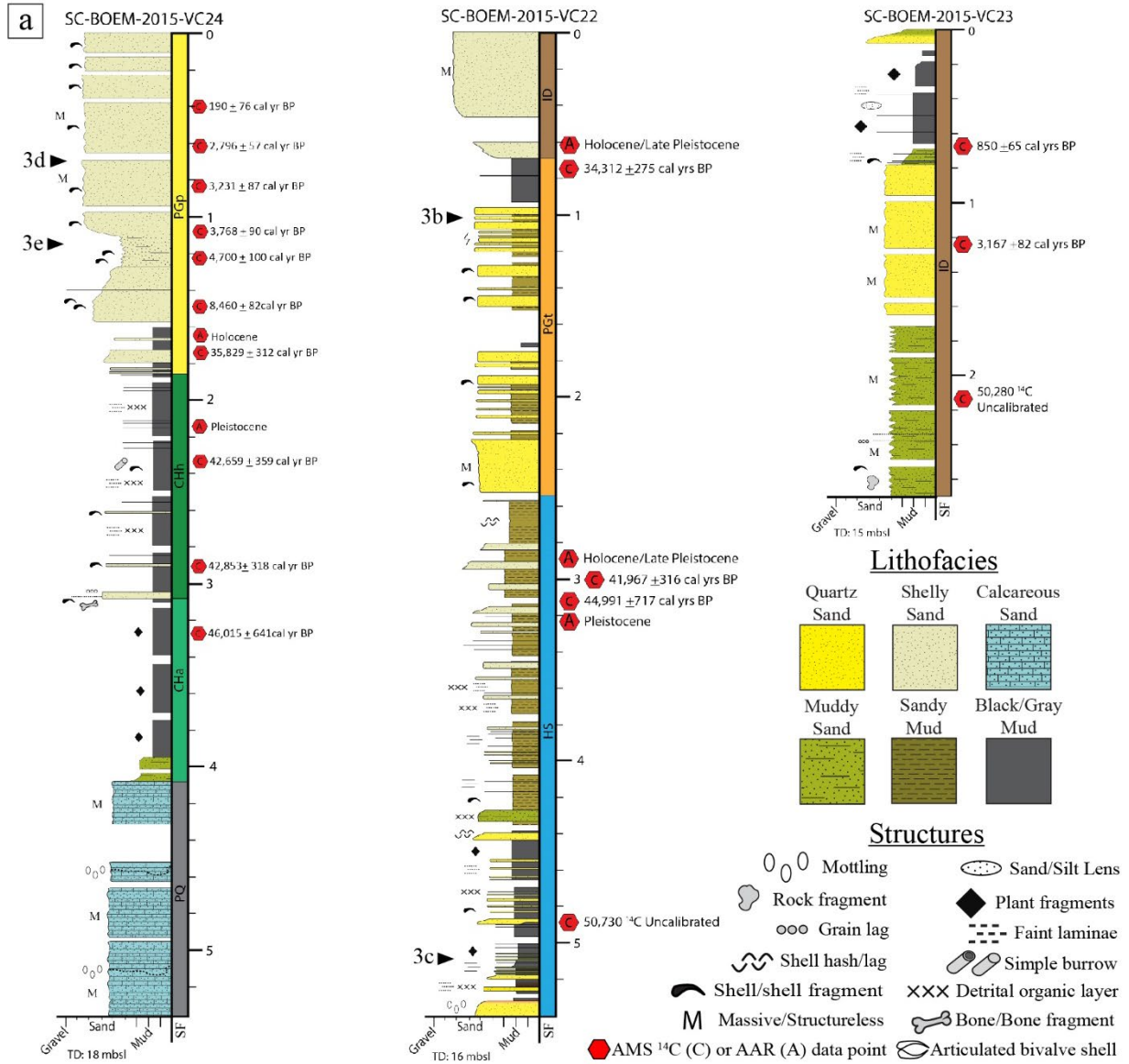


Figure 2.3. Key sediment cores from offshore of Cape Romain and Bulls Bay (see Fig. 2.1b for locations). **a)** Graphic logs of sediment cores. See Table 1 for seismic facies (SF) codes. **b)** Interbedded fine-grained sand and mud of PGt SF. **c)** Interlaminated fine-grained sand, brown mud, and dark gray/black organic detritus from HS SF. **d)** Coarse-grained, shelly sand of PGp SF. **e)** Upwards-coarsening interval defined by sandy, shelly, mud and muddy, shelly sand from PGp SF. Core photograph locations are indicated to the left of core logs in Figure 2.3a.

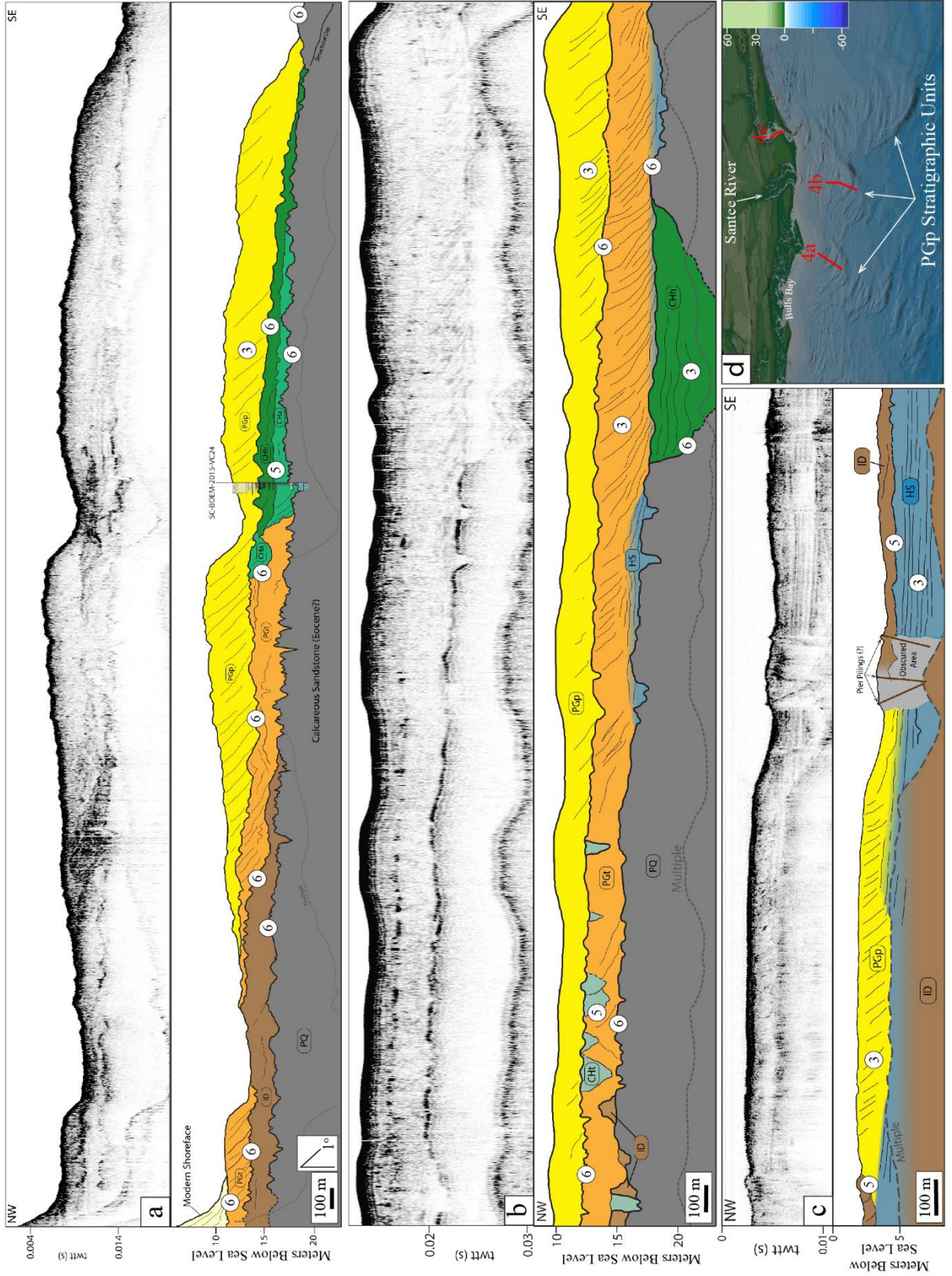


Figure 2.4. Seismo-acoustic profiles and interpretive geoseismic profiles of parallel-oblique progradational seismic facies (SF PGp). See Table 2.1 for SF colors and codes. **a)** Shore-normal profile offshore of Cape Romain. Well-defined PGp SF comprise several large sand ridges that unconformably overlie a stratigraphic unit defined by PGt SF, a large paleochannel, and pre-Quaternary rocks (PQ SF). Core lithofacies, AMS-¹⁴C dates, and AAR age estimates indicate that the sand ridge formed during the late Holocene (8.5 to 0.9 cal ka BP) mud-rich, backbarrier deposits filled the paleochannel during the late Pleistocene, before 35 cal ka BP (Fig. 2.3). **b)** Stacked stratigraphic units defined by PGt (lower) and PGp (upper) SF unconformably overlie pre-Quaternary rocks (PQ SF). A large, horizontally-filled (CHh SF) paleochannel incises the PQ unit to a depth greater than 25 mbsl. Note the numerous small paleochannels along the upper surface of the PGt unit as well as the HS SF that defines the toesets and bottomsets of the PGt clinofolds. **c)** Inshore profile along the southern margin of Winyah Bay showing a PGp unit that is correlative to well-developed beach ridge systems onshore (Fig. 2.1). This unit overlies a thick HS unit with an ambiguous contact between the two. Onshore of this location, Shen (2017) recovered mud-rich, backbarrier deposits beneath beach ridge sands in core (Fig. 2.1). **d)** Location map for profiles shown in Figure 2.3. Bathymetry highlights offshore sand ridges such as the one shown in Figure 2.4a. Profile locations are also shown in Figure 1. See Fig. 2.3 for SC-VC24 core log.

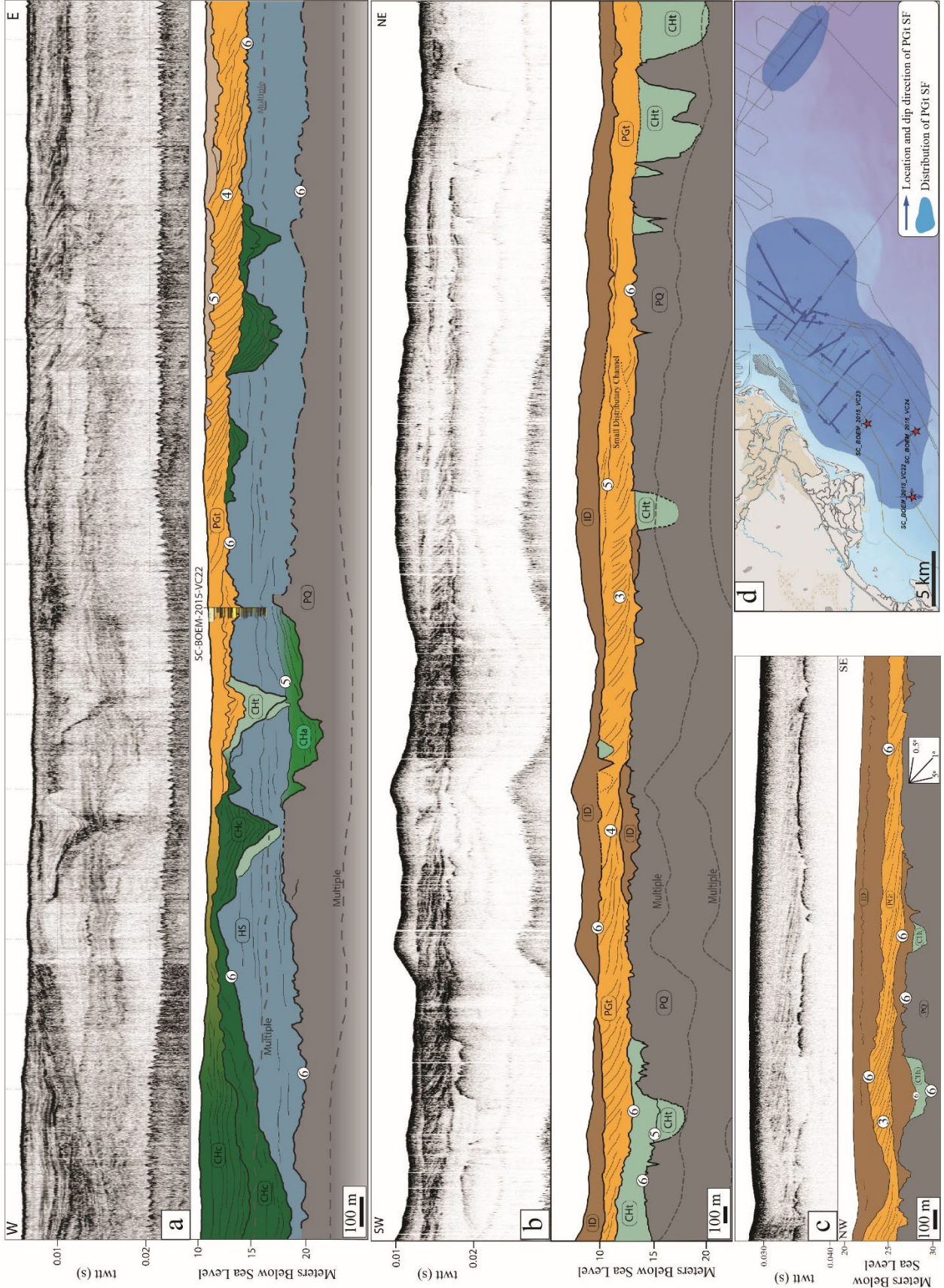


Figure 2.5. Seismo-acoustic profiles and interpretive geoseismic profiles of PGt SF and stratigraphic units. **a)** Stratigraphic unit containing PGt and CHc SF overlying a relatively thick unit composed primarily of HS SF. The CHc SF of the uppermost element defines the northern margin of the Bulls Bay Paleovalley. See Figure 3 for SC-VC22 description. **b)** A stratigraphic unit defined exclusively by the PGt SF contains numerous small paleochannels (paleo-distributaries) marked by 5th order bounding surfaces and a prominent 4th order bounding surface. **c)** A PGt stratigraphic unit overlying the regional unconformity (6th order surface) above the PQ section approximately 50 km offshore. **d)** Mapped distribution and dip direction PGt SF stratigraphic units. See Figure 1 for profile locations and Table 1 for SF colors and codes.

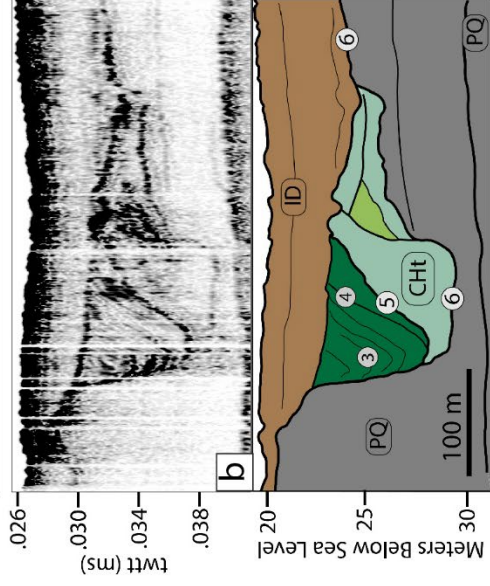
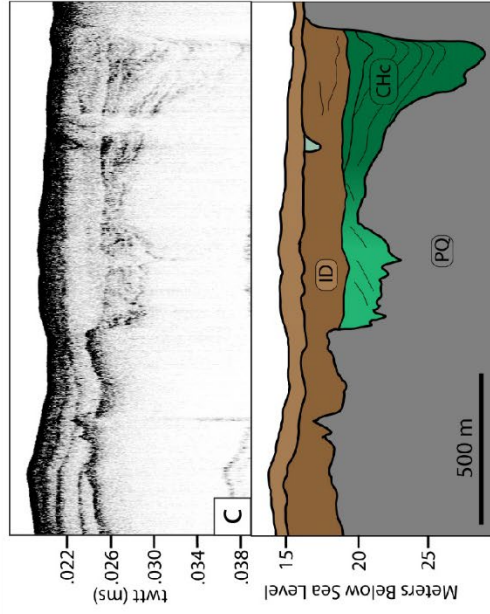
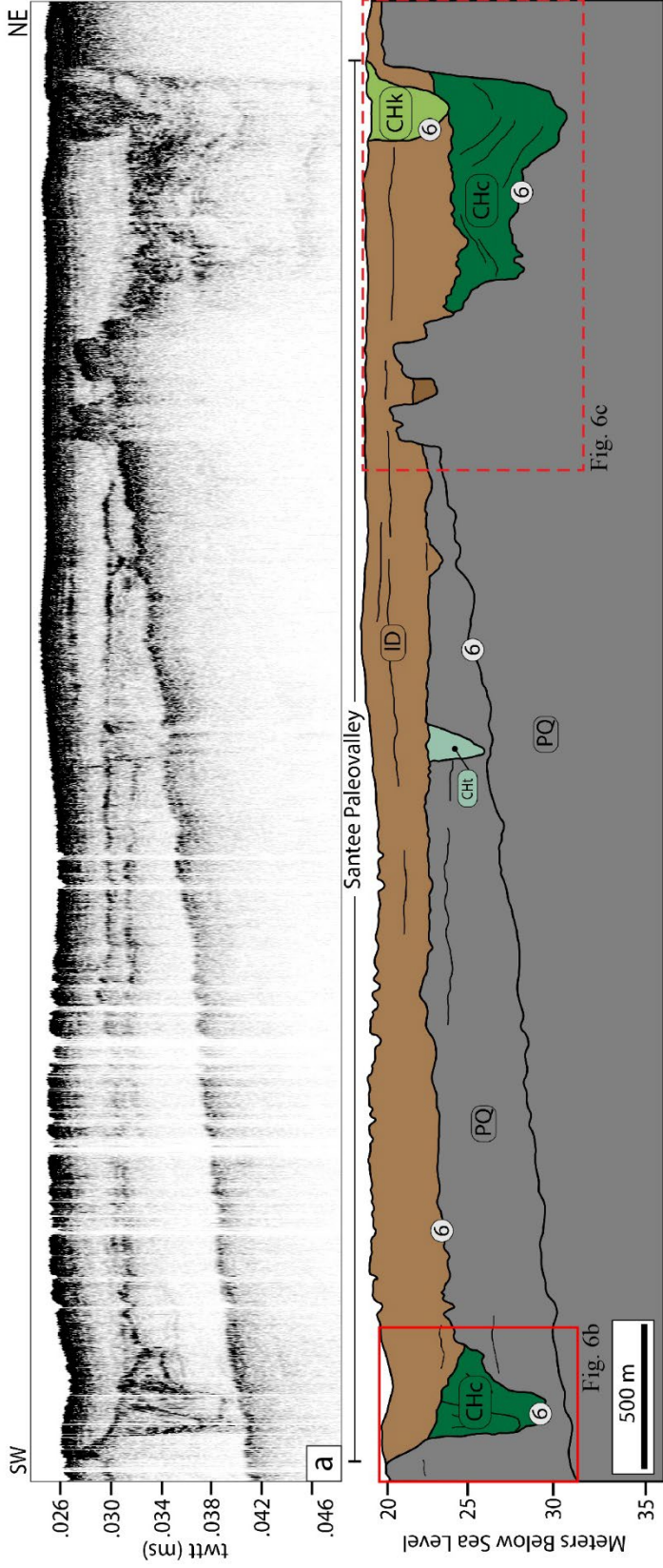


Figure 2.6. a) Seismo-acoustic profile and geoseismic interpretation of the Santee River Paleovalley offshore. The northern and southern margins of the paleovalley are defined by deeply incised paleovalleys. **b)** Detailed stratigraphic architecture of southern paleovalley of the Santee River Paleovalley. Note change in scale from Fig. 7a. **c)** Detailed stratigraphic architecture of the northern paleochannel of the Santee River Paleovalley offshore. This profile comes from an offset, parallel line a few hundred meters west of the profile in 7a. See Fig. 2.1 for location of profiles.

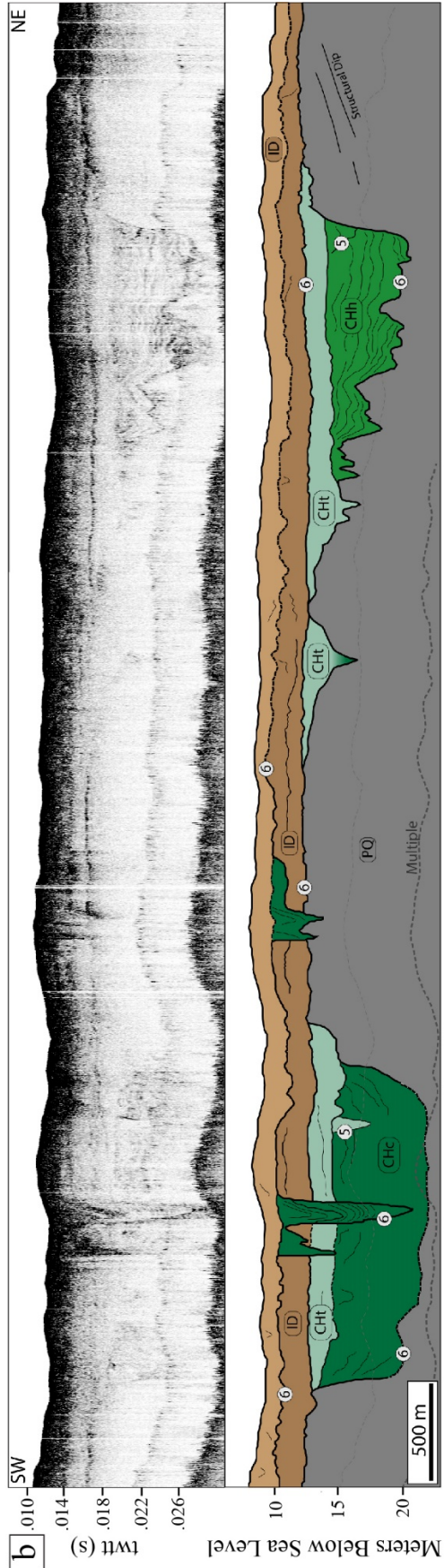
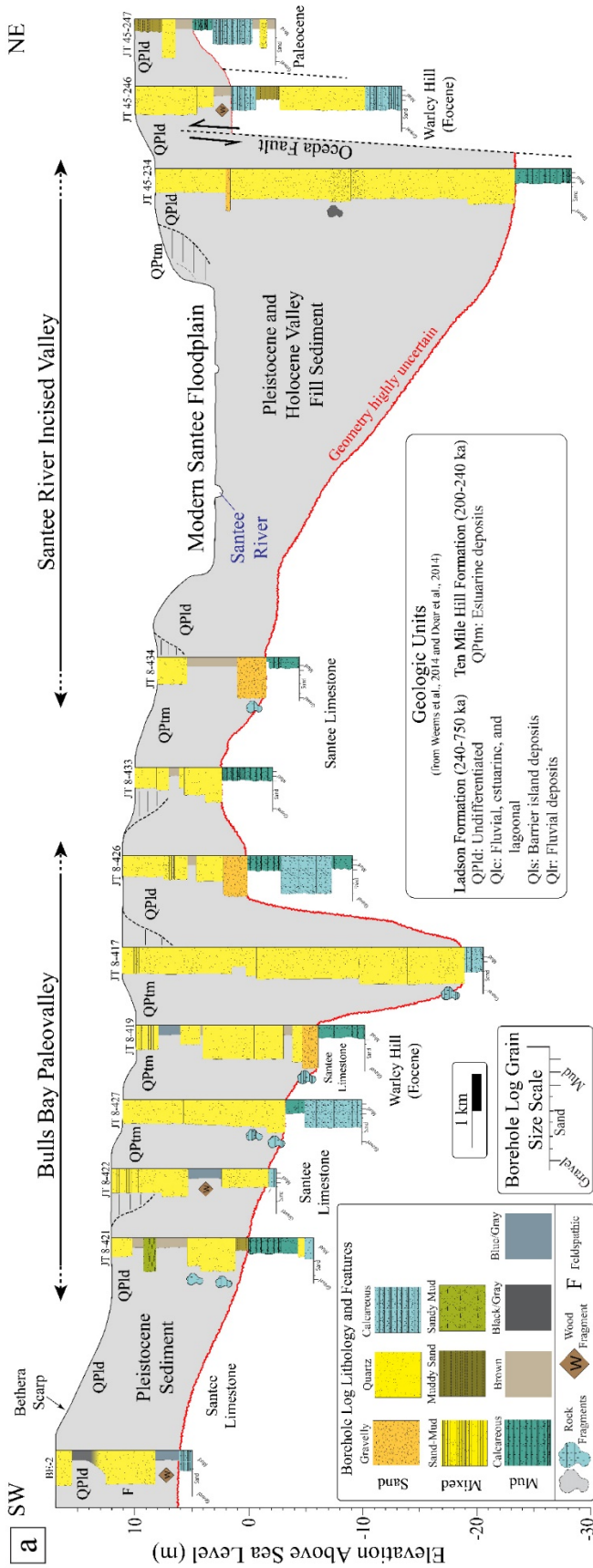


Figure 2.7. a) Structural cross section constructed from onshore borehole descriptions from the USGS and SCGS (Appendix. 1). Location of profile is a few km SE of the confluence of the Bulls Bay Paleovalley and the Santee River Incised Valley. **b)** Seismo-acoustic profile and geoseismic interpretation of the Bulls Bay Paleovalley offshore of Bulls Bay. Note two prominent stages of incision separated by a laterally-extensive ID stratigraphic unit interpreted as a transgressive sand sheet. CHc and CHh seismic facies suggest that both of the larger paleochannels are filled by predominantly fine-grained, mud-rich sediment. See Figure 1 for locations of both profiles.

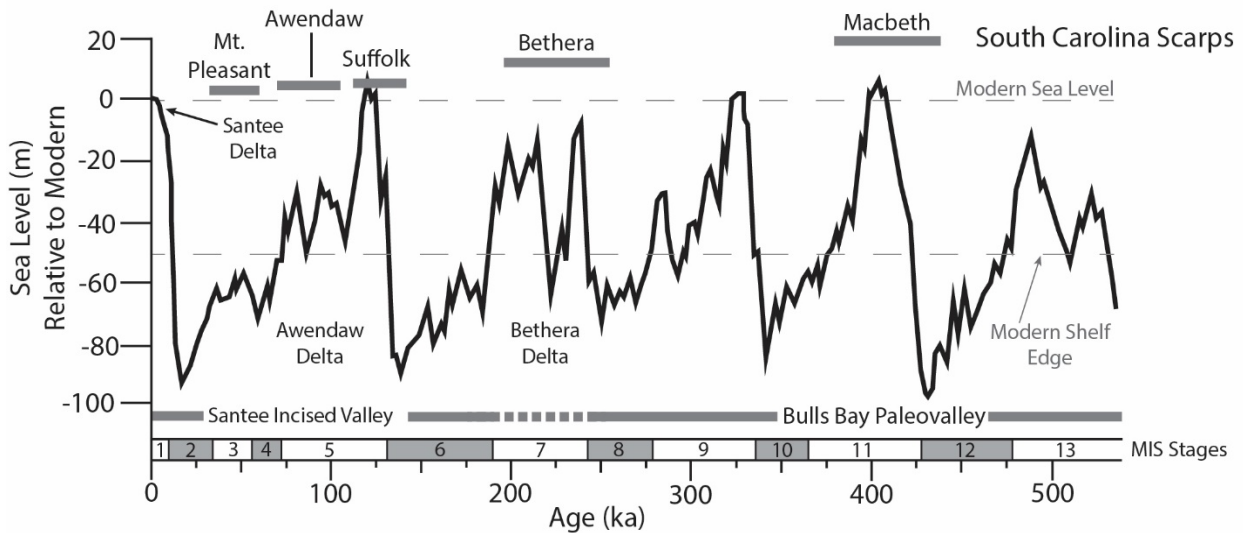


Figure 2.8. Late Quaternary sea-level curve (modified from Shackleton 1987; Lisiecki and Raymo 2005; Doar 2014, and Railsback et al. 2015). Elevation of South Carolina scarps (Doar 2014) shown by gray bars and captures the difference between the glacioeustatic highstand elevations and regional uplift. Periods of activity of the two most recent incised valleys of the Santee River (Santee Incised Valley and Bulls Bay Paleovalley) are indicated by the gray lines below the sea level curve. Timing of highstand deltaic deposition is also indicated. Shelf edge depth (middle dashed line) is the approximate depth of the modern shelf edge offshore of the study area.

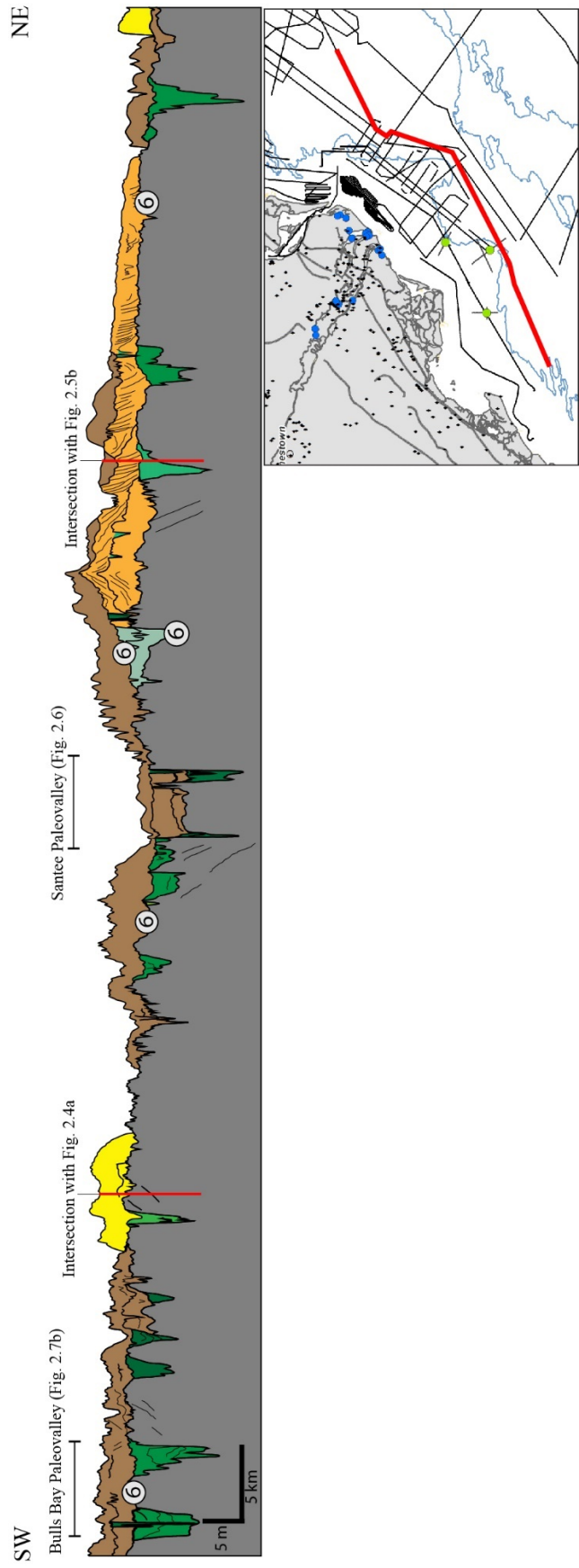
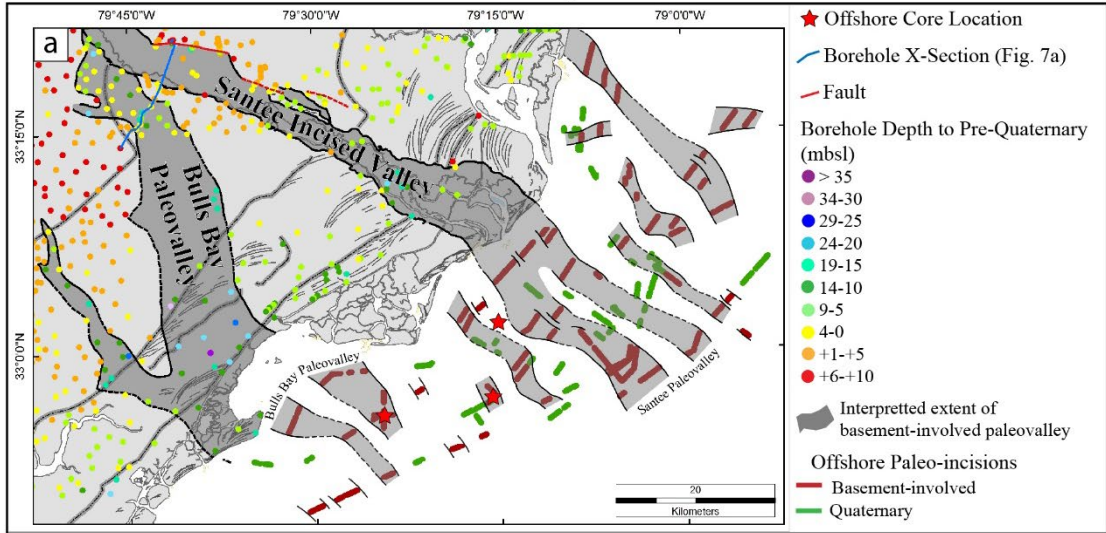
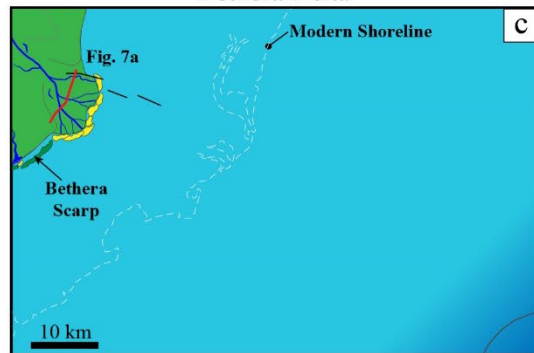
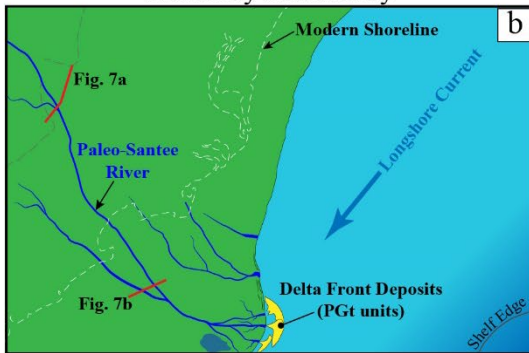


Figure 2.9. Shore-parallel regional geoseismic line based on high resolution Chirp data showing the thickness of Quaternary stratigraphic units in the offshore part of the study area. Note the relatively thick accumulations of delta-front clinoform units (PGt facies) immediately offshore of the Santee Delta and the composite 6th order bounding surfaces that extend across the area.



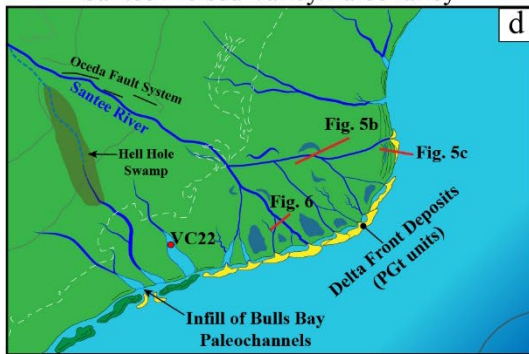
Bulls Bay Paleovalley

Bethera Delta



Santee Incised Valley/Paleovalley

Awendaw Delta



Mid-Holocene

Pre-dam Santee Delta (1775 C.E.)

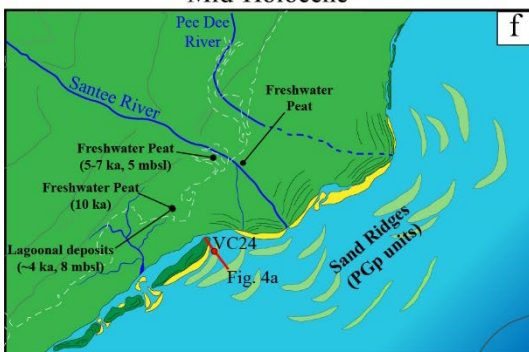


Figure 2.10. a). Map of paleo-incisions across the lower coastal plain and inner continental shelf within the study area. Basement-involved paleo-incisions (red lines) erode into pre-Quaternary basement while Quaternary paleo-incisions (green lines) are limited to the Quaternary section. This distinction is likely the result of differences in the mechanisms that drive incision with basement-involved systems controlled by allogenic mechanisms (i.e. changes in RSL) and Quaternary systems controlled by autogenic mechanisms (i.e. channel avulsions or local hydrodynamics). Gray areas are approximations of paleovalley widths and locations based on available borehole and seismo-acoustic data. The location of the central portion of the Bulls Bay Paleovalley onshore was initially mapped by Colquhoun et al. (1972) while the location of this feature onshore near Bulls Bay was mapped by Weems et al. (2014). Additional mapping completed as part of this study connects the Bulls Bay Paleovalley to the Santee Incised Valley near Jamestown, SC. The location of the Oceda Fault system is adapted from Clendenin (in press) and delineated by numerous boreholes drilled by the SCGS. Borehole cross section indicated by blue line is shown in Figure 2.7a. Onshore Pre-Quaternary depths mapped from borehole descriptions from the USGS and SCGS. **b-g)** Paleogeographic reconstructions showing the proposed evolution of the study area during the late Quaternary. **b)** Deposition of the Santee delta while the Bulls Bay Paleovalley was active. **c)** Deposition of the Santee delta during the RSL highstand associated with the Bethera Scarp. This feature was mapped by Colquhoun et al (1972). **d)** Deposition of fluvial-dominated deltaic deposits of the Santee delta during a regressive RSL phase following the avulsion of the Santee River from the Bulls Bay Paleovalley into the Santee Incised Valley. The abandoned Bulls Bay system onshore is expressed by topographic lows which, today, are still evident and occupied by Hell Hole Swamp. **e)** Deposition of a wave-dominated phase of the Santee Delta during Marine Isotope Stages 5/4. Ages of cusped beach ridge systems

from Shen et al. (2017). **f)** Deposition of the Santee-Pee Dee deltaic complex during the late Holocene. Transgressed coastal lithosomes (shown here as delta front or barrier island deposits) migrate offshore where they begin to prograde under the influence of storm-driven, offshore-directed circulation. Onshore, freshwater peats and lagoonal deposits are common during the period from 10 – 4 cal ka BP (Hayes 1994; Sexton et al. 1996; Long and Hanebuth 2017). **g)** Study area as mapped by Cook (1775). The modern shoreline appears similar to what it did 245 yrs ago, prior to the anthropogenic changes to the system.

Seismic Facies (SF)		Cross-sectional Geometry		Interpretation
Primary	Secondary	Internal	External	
Progradational Facies	Parallel (p)	High to moderate amplitude, parallel oblique, uniform, steep, seaward-dipping reflectors. Dip angles range from ~1-3°.	Wedge-shaped, asymmetrical with steeply-dipping seaward margin parallel to foreset dip. Up to 5 m thick	Prograding, wave-dominated clinoforms and Holocene shelf sand ridge deposits
	Tangential (t)	High to moderate amplitude, oblique to sigmoidal, non-uniform seaward-dipping reflectors. Common reactivation surfaces and bottomset development. Dip angle is highly variable but typically < 1°	Sheet or wedge with erosional and/or channelized upper surface. Up to ~9 m thick.	Prograding, Pleistocene, fluvially-dominated, deltaic deposits
Paleochannel Facies	Concentric (c)	High to moderate amplitude, aggradational, concentric reflectors	Lensoidal bodies with a concave-up erosional lower boundary and typically a flat-lying upper boundary. Thickness can exceed 10 meters. Commonly between 3-5 m thick but can exceed 10 m.	Mud-rich, aggradational channel fill. Commonly tidally-influenced estuarine deposits.
	Horizontal (h)	High to moderate amplitude, horizontal to sub-horizontal reflectors		
	Asymmetric (a)	High to moderate amplitude, uniformly-dipping reflectors		
	Chaotic (k)	Disorganized, moderate amplitude, discontinuous reflectors		
	Transparent (t)	Low amplitude homogeneous fill		
Horizontally Stratified Facies	HS	High to moderate amplitude, high to moderate frequency, horizontal to sub-horizontal reflectors	Highly irregular with erosional upper surface	Fine-grained, back-barrier, shelf deposits, or deltaic bottomsets associated with PG SSF
	ID	Transparent to chaotic	Sheet, sheet drape, wedge, or bank	Transgressive sand sheets and other deposits
Pre-Quaternary Basement	PQ	Variable. Transparent to high amplitude horizontal to gently dipping reflectors	Highly irregular, erosional upper surface. Base is unresolvable	Cretaceous through Pliocene consolidated to lithified sediment of variable lithology.

Table/Figure 2.2. a) Bounding surface classification and descriptions. Where possible, bounding surface order is consistent with the classification developed for fluvial systems formalized by Miall (1985, 1988). First and 2nd order surfaces are below the resolution of seismo-acoustic data and are therefore not incorporated into this study. Modified from Collinson (2006). **b)** Relationship of bounding surface scheme to sequence stratigraphic and allostratigraphic surfaces based on Catuneanu (2006). Lower figure is a schematic showing idealized relationships between bounding surfaces and stratigraphic architecture. Modified from Miall (2010).

Study Area	Core Name	Method	Surface Elevation (mbsl)	Sample Core Depth (m)	Sample Elevation (mbsl)	14C Age (BP)	Lab Error	Median Cal BP/Age	2 σ Δ Cal	Material
Folly-Kiawah	VC07*	AMS ¹⁴ C	13.72	0.82	14.54	34,220	110	38,308	349	shell
Folly-Kiawah	VC07*	AMS ¹⁴ C	13.72	1.95	15.67	21,560	50	25,486	266	shell
Folly-Kiawah	VC14*	AMS ¹⁴ C	13.66	1.92	15.58	2,020	20	1,604	84	shell
Folly-Kiawah	VC14*	AMS ¹⁴ C	13.66	3.14	16.80	38,170	160	31,531	346	shell
Folly-Kiawah	VC15*	AMS ¹⁴ C	8.87	0.67	9.54	4,270	20	4,383	93	shell
Folly-Kiawah	VC15*	AMS ¹⁴ C	8.87	1.84	10.72	35,700	140	40,311	444	shell
Folly-Kiawah	VC15*	AAR	8.87	1.84	10.72	Pleistocene			shell	
Folly-Kiawah	VC15*	AMS ¹⁴ C	8.87	3.05	11.92	4,660	25	4,888	71	shell
Folly-Kiawah	VC15*	AAR	8.87	3.05	11.92	Holocene/Late Pleistocene			shell	
Folly-Kiawah	VC18*	AMS ¹⁴ C	13.05	0.66	13.70	3,710	20	3,627	72	shell
Folly-Kiawah	VC18*	AMS ¹⁴ C	13.05	1.26	14.31	34,400	110	38,519	264	shell
Folly-Kiawah	VC18*	AMS ¹⁴ C	13.05	1.62	14.66	43,690	300	46,478	728	shell
Folly-Kiawah	VC19*	AMS ¹⁴ C	13.81	2.10	15.91	7,420	25	7,883	66	shell

Folly-Kiawah	VC19*	AMS ¹⁴ C	13.81	5.23	19.04	37,070	160	41,294	388	shell
Folly-Kiawah	VC19*	AMS ¹⁴ C	13.81	5.23	19.04	23,580	50	27,461	164	shell
Folly-Kiawah	VC19*	AMS ¹⁴ C	13.81	5.28	19.09	16,610	40	20,037	174	shell
Folly-Kiawah	VC21	AMS ¹⁴ C	12.74	0.97	13.71	7,170	25	7,634	64	shell
Folly-Kiawah	VC21	AAR	12.74	0.97	13.71	Holocene				shell
Folly-Kiawah	VC21	AMS ¹⁴ C	12.74	1.65	14.39	3,960	20	3,961	94	shell
Folly-Kiawah	VC21	AMS ¹⁴ C	12.74	3.14	15.88	7,860	25	8,328	66	shell
Cape Romain	VC24	AMS ¹⁴ C	12.01	0.40	12.41	550	20	190	76	shell
Cape Romain	VC24	AMS ¹⁴ C	12.01	0.62	12.63	3,030	20	2,796	57	shell
Cape Romain	VC24	AMS ¹⁴ C	12.01	0.87	12.88	3,360	20	3,231	87	shell
Cape Romain	VC24	AMS ¹⁴ C	12.01	0.96	12.97	31,890	100	35,350	330	shell
Cape Romain	VC24	AMS ¹⁴ C	12.01	1.07	13.09	3,820	25	3,768	90	shell
Cape Romain	VC24	AAR	12.01	1.07	13.09	Holocene				shell
Cape Romain	VC24	AMS ¹⁴ C	12.01	1.23	13.24	4,500	25	4,700	104	shell
Cape Romain	VC24	AAR	12.01	1.23	13.24	Holocene				shell
Cape Romain	VC24	AMS ¹⁴ C	12.01	1.44	13.45	8,010	30	8,460	82	shell
Cape Romain	VC24	AAR	12.01	1.44	13.45	Holocene				shell
Cape Romain	VC24	AMS ¹⁴ C	12.01	1.74	13.76	32,320	100	35,829	312	shell
Cape Romain	VC24	AAR	12.01	1.74	13.76	Pleistocene				shell
Cape Romain	VC24	AMS ¹⁴ C	12.01	2.35	14.36	39,100	230	42,659	359	shell
Cape Romain	VC24	AAR	12.01	2.35	14.36	Pleistocene				shell
Cape Romain	VC24	AMS ¹⁴ C	12.01	2.89	14.90	39,410	180	42,853	318	shell
Cape Romain	VC24	AMS ¹⁴ C	12.01	3.34	15.36	43,200	300	46,015	641	shell

Table 2.3. AMS-14C and AAR ages from offshore cores. AAR age estimates are from Wehmiller et al. (2019) and AMS-14C ages are from Dr. Clark Alexander (personal communication 2019). Cores with * are from Long (2018), locations shown in Figure 2.1.

Chapter 3

Depositional Environments Preserved within Quaternary Paleochannel Systems Offshore of the Georgia Bight, Southeastern U.S.A.

ABSTRACT

Paleochannels are common subsurface geologic features along inner continental shelves and coastal plains. Their sedimentary fillings are important archives of ancient depositional environments, influence shelf hydrodynamics, control submarine groundwater discharge, and affect the distribution of marine habitat. This study across a 450 km portion of the inner continental shelf of the southeast United States adds to the understanding of the timing of paleochannel development, the paleo-environments in which they formed, and the mechanisms that drove their formation. Integrated analysis of 714 km of high-resolution seismo-acoustic reflection data and 12 sediment cores ranging in total length from 4.91 – 5.78 m reveals that: (i) most paleochannels documented here formed in backbarrier environments (estuarine or lagoonal) and were subsequently infilled during transgression or following avulsion, preserving mud-rich, tidally-influenced deposits; (ii) the preservation of non-marine deposits is rare; (iii) paleochannels are either solitary or amalgamated to form paleovalleys within which they are arranged in multistory (vertically-stacked) or multilateral (horizontally-offset) configuration, a product of local hydrodynamic conditions, glacioeustatic cycles, and regional tectonics; and (iv) a general southerly increase in the overall degree of channelization is observed across the Georgia Bight, a function of both long-term accommodation and the underlying stratigraphy. The composition and spatiotemporal distribution of paleochannel systems has implications for offshore mineral and

resource exploration, understanding the long-term evolution of complex coastal systems, as well as to Quaternary sea level studies.

INTRODUCTION

Natural channels are modern geomorphological features that transport water and sediment and are found within fluvial, estuarine, lagoonal, and deltaic environments. In marginal marine settings they range in scale from meter-scale tidal creeks to major, 100's of meters wide distributary and estuarine channels. These systems transport muddy, sandy, and even gravelly sediment under the influence of rivers, tides, and waves. Paleochannels and paleovalleys, as used here, are subsurface geologic features consisting of a basal, concave erosional surface and the sedimentary fill contained therein, and are remnants of ancient channel systems. These sedimentary successions serve as important archives of ancient depositional environments, influence shelfal hydrodynamics, control submarine groundwater discharge, and influence the distribution of marine habitat (Green, 2009; Gonzalez-Villaneuva et al., 2015; Smoak, 2016; Roach, 2017). The records of successive paleoenvironmental conditions preserved within paleochannels is of particular significance along low-accommodation passive margins such as the US Atlantic margin where area-wide transgressive and regressive erosion associated with high frequency Quaternary glacioeustatic cycles often leave a highly fragmentary sedimentary record which is typically overprinted by transgressive processes as well (Swift, 1975; Field, 1980; Swift et al., 1984; Snedden and Dalrymple, 1999; Suter, 2006; Snedden et al., 2011; Pendleton et al., 2017).

Paleochannels are common features across the modern coastal plain and continental shelf of the eastern United States (Colquhoun et al. 1972; Toscano et al. 1989; Weems et al. 1994; Nordfjord et al. 2005; Baldwin et al., 2006; Harris et al. 2005; Luciano and Harris 2013; Long and

Hill 2016; Smoak 2016; Childers et al. 2019; Long and Hanebuth 2020). While previous studies provide valuable insight into the distribution of paleochannel and paleovalley systems, few provide the detailed facies and architectural analysis, based on sediment cores, which is required to document the variability of depositional processes and products as a result from regional paleoenvironmental changes. The primary goal of this study is to define the depositional facies, seismic facies, and planform morphologies of paleochannel and paleovalley systems preserved along the inner continental shelf, within 25 km of the coast, of South Carolina and Georgia. In order to better understand the regional distribution of we also document the spatial and temporal distribution of these features from the northern border of South Carolina to the southern border of Georgia (Fig. 3.1).

Sediments preserved within paleochannels are the product of ancient environmental conditions and depositional processes that changed in response to coastal dynamics, climate, and sea level fluctuations. The record of these responses provides valuable insight into how coastal systems have changed and serve as the foundation for predictions of future change.

Regional Setting

The Georgia Bight is an arcuate section of the US southeastern Atlantic coastline stretching from North Carolina to Florida that contains a range of coastal morphologies from simple extended strandplains to complex barrier island chains, one delta, and several estuaries (Hayes 1991; Sexton et al. 1992; Hayes 1994). The central part of the Bight experiences microtidal conditions and mean significant wave heights that ranges from 0.5 to 1 m (Nummedal and Fischer 1978; Hayes 1994), however both tidal range and wave height vary across the study area. Between the northern study area and the southern study area tidal range increases from 1.8 to 2.5 m and wave height decreases from 2.5 to 1.2 m (Hayes and FitzGerald 2013). Surface water circulation and sediment transport

along the inner shelf vary seasonally in response to storm systems (i.e. atmospheric fronts and low-pressure systems) as well as to local coastal morphodynamic processes; however, net sediment transport is directed to the southwest (Warner et al. 2012; Kana et al., 2013), a pattern that has persisted since at least the late Oligocene (Weems et al. 1994; Colquhoun 1995).

The coastal plain of the southeastern United States consists of Pliocene through Holocene barrier island complexes, piedmont-draining and coastal plain rivers, freshwater swamps, estuaries, tidal inlets, and salt marshes (Weems et al. 2014). Pleistocene barrier island and backbarrier deposits define a scarp-and-terrace morphology that documents the location of successive Quaternary sea level highstands across the coastal plain (Cooke 1936; Colquhoun et al. 1991; Doar and Kendall 2014). These ancient barrier systems extend from an elevation of ca. 45 m on the innermost coastal plain and decrease in elevation and age towards the modern coast where they commonly form the cores of Holocene barrier islands (Cooke 1936; MacNeil 1949; Hayes 1994; Weems et al. 1994; Harris et al. 2005; Doar 2014).

Basement structures as well as the antecedent stratigraphic framework that underlies the lower coastal plain have influenced coastal morphology throughout the Quaternary (Hayes, 1994; Riggs et al., 1995; Harris et al., 2005). The Georgia Bight is bound by the Cape Fear Arch to the north, the Ocala Uplift to the south, and includes the Georgia Rift/Southeast Georgia Embayment (LeGrand 1961; Heller et al. 1982; Hayes 1994). Hayes (1991, 1994) divided the coast of the Bight into six structurally influenced morphological compartments. Between these compartments variations in sediment supply, tidal range, significant wave height, and accommodation influence the distribution and geometry of barrier islands, width of backbarrier environments, as well as the number and spacing of tidal inlets (Fig. 3.1).

While paleochannel systems are common in the subsurface offshore of the Georgia Bight, they have rarely been the focus of detailed study and their regional distribution is poorly understood. Local studies have focused on the location, general morphology, and simple lithology of paleochannels beneath the lower coastal plain and inner shelf offshore of northern and central South Carolina (Harris et al. 2005; Baldwin et al. 2006; Luciano 2010; Harris et al. 2013; Weems et al. 2014; Smoak 2016), but none have focused on the detailed documentation and interpretation of depositional facies and stratigraphic architecture within these features.

METHODS

The primary dataset used in this study was acquired by a private company (APTIM Federal Services, LLC) under contract from the United States Bureau of Ocean Energy Management (BOEM) in 2015 as part of the Atlantic Sand Assessment Project (ASAP). The goal of ASAP was to evaluate the distribution of potential sand resources within federal waters (> 3 nm from shore) along the Atlantic coast of the southeastern US. Vibracores and high-resolution seismic reflection (Chirp) data were collected within eight study areas spanning 450 km of the inner continental shelf from the North Carolina-South Carolina border in the north to the Georgia-Florida border in the south (Fig. 3.1). The volume of data varies across the individual study areas, but most include a grid of Chirp profiles with vibracores collected along these profiles.

Sediment Cores

Vibracoring was accomplished using a pneumatic coring system configured to collect 6 m long, sediment cores. A total of 19 cores were recovered from offshore of South Carolina and eight from Georgia. Of these cores, seven from South Carolina and five from Georgia penetrated buried paleochannel infills (Fig. 3.1). Paleochannel cores range in length from 4.91-5.79 m with an

average recovery of 5.40 m. Sediment cores were split and visually described at sub-centimeter resolution. Characteristics including sediment color and composition; physical, biological, and diagenetic structures; grain size, rounding, and sorting; bed thicknesses and bed contacts were documented and captured in graphic logs. Lithologies are similar to those proposed by Flemming (2000) and include gravelly sand, sand, shelly sand, muddy sand, sandy mud, and mud with mud consisting of both clay- and silt-sized particles. Additionally, detrital organic (plant) material is a common constituent in most of the fine-grained lithologies. Sedimentary facies incorporate lithology, sedimentary structures, as well as trace and body fossils and are interpreted as the product of specific depositional processes (Fig. 3.2). Facies associations are grouped based on interpreted environments of deposition and the vertical facies successions (Fig. 3.3).

AMS-¹⁴C and Amino Acid Racemization (AAR) age analyses (Tab. 1) were completed as part of the BOEM regional consortium (Luciano et al., 2019). Carbonate samples for AMS-¹⁴C samples were analyzed at the University of Georgia Center for Applied Isotope Studies in Athens, GA. The raw ¹⁴C data were calibrated using Calib13 software version 5.0 with the Marine13 calibration set, and the age ranges are reported in calibrated years before present (cal ka BP) and correspond to the 2σ error. Amino Acid Racemization (AAR) samples were analyzed at Northern Arizona University's Amino Acid Geochronology Lab and interpreted as part of the BOEM regional assessment project (Luciano et al., 2019). AMS-¹⁴C and AAR data used in this study are presented in Table 3.1.

Seismo-Acoustic Data

High-resolution (Chirp) data were acquired using an EdgeTech 3200 subbottom profiler combined with an EdgeTech 0512i towfish resulting in seismic-reflection data with a bandwidth of 0.5 - 12 kHz and a corresponding vertical resolution of 0.06 – 0.10 m (Aptim 2017). A total of

511 km of Chirp data were acquired offshore of South Carolina and 203 km offshore of Georgia. The amount of data collected varies from one study area to the next (Fig. 3.1) and ranges from 5 - 196 km² in total area with shore-normal line spacing of 0.8 - 2.2 km and shore-parallel spacing of 0.4 - 4 km. The Kiawah Island location has the most comprehensive coverage with spacing of 800 m and 2 km for shore-normal and shore-parallel lines, respectively (Fig. 3.1b).

Interpretation of Chirp data consists of two components; seismic facies analysis and the analysis of stratigraphic architecture. Seismic facies within paleochannels were described using a methodology similar to that proposed by Mitchum et al. (1977) and were defined based on the geometry, amplitude, frequency, continuity, and terminations of internal seismic reflectors. Stratigraphic architecture refers to the vertical and lateral relationships between contiguous paleochannels that collectively define paleovalleys. Where data are closely spaced, paleochannel seismic facies as well as the stratigraphic architecture of paleovalleys were used to trace the planform morphology of these systems. Once correlated, the plan form morphology of specific paleochannels and paleovalleys was mapped.

Finally, in an effort to better understand the regional distribution of paleochannels we combined BOEM Chirp data from the main study areas with existing, unpublished data from surrounding areas to quantify the spatial distribution and key characteristics of paleochannels along the inner shelf of the Georgia Bight. Existing offshore seismo-acoustic profiles were acquired during several previous research cruises by faculty of Coastal Carolina University (CCU) working aboard the National Oceanic and Atmospheric Administration (NOAA) R/V Nancy Foster in 2004, 2005, and 2015. A dense grid of data was also newly acquired between 2016 and 2017 for this study under an agreement with the South Carolina Geological Survey (SCGS).

We define seismic facies and key morphometric parameters including preserved thickness, apparent width, depth of incision, and cross-sectional morphology of paleochannels and paleovalleys (Table 3.2).

RESULTS AND INTERPRETATIONS

The sedimentary facies present within cored paleochannels were deposited in low- to high-energy, tidally-influenced, intertidal and subtidal backbarrier, and fluvial environments. Integration of these facies with seismic facies links depositional processes and products to the stratigraphic architecture preserved within paleochannels.

Sedimentary Facies and Facies Associations

We have identified ten sedimentary facies from sediment cores that comprise two facies associations. Sedimentary facies, as presented here, are the products of depositional processes and reflect changes in environmental conditions on relatively short time scales. Facies associations are interpreted to represent genetically-related depositional processes that operate within specific depositional settings.

Sedimentary Facies

The majority (95 %) of sedimentary facies recovered from sediment cores taken from paleochannels of the Georgia Bight show strong indication of having been deposited under the influence of tides. Of these tidally-influenced deposits, most are fine-grained and mud-rich, a function of generally low-energy conditions.

Description (Facies 1, Laminated Mud) — F1 consists of massive to weakly laminated dark gray, organic-rich mud with rare, isolated sand grains (Fig. 3.2a). The degree of bioturbation

is low in the form of simple, typically sand-filled, burrows. Numerous specimens of Eastern Mud Snails (*Tritia obsoleta*) and articulated specimens of Dwarf Surf Clams (*Mulinia lateralis*) were recovered from this facies within Core SC-19 (Fig. 3.5d). F1 comprises 19 % (6.85 m) of the paleochannel deposits recovered by in the study area (Table 3.2).

Interpretation (Facies 1) — F1 was deposited along low-energy, muddy tidal flats or bioturbated, subtidal estuarine channels. The shells of organisms recovered from this facies in Core SC-19 support an intertidal origin in that both species inhabit benthic zones with mud-rich substrates and are commonly found along modern upper tidal flats within this region (Walker and Tenore, 1984; E. Burge, J. Harding, and P. Kelley, personal communications, 2019; Global Invasive Species Database, <http://www.issg.org/database>). Some F1 deposits may be muddy subtidal deposits associated with zones of high turbidity and suspension sedimentation, a common component of estuarine systems within the Georgia Bight and elsewhere around the world (Howard and Frey, 1973; Dalrymple et al., 1992; Dalrymple et al., 2012).

Description (Facies 2, Laminated Mud and Organics) — F2 consists of massive brown or dark gray mud cyclically interlayering with black, fine-grained organic detritus (Fig. 3.2b). Individual mud layers are less than 1 cm thick. Organic layers are much thinner and exhibit a gradational contact with the underlying mud layer and a sharp contact with the overlying mud layer. Thick accumulations of F2 occur in several cores including Core GA-11 where it comprises the lower 4 m (Fig. 3.5a). F2 comprises 22 % (7.90 m) of the cored paleochannel deposits (Table 3.2).

Interpretation (Facies 2) — Similar to F1, F2 was deposited along low-energy intertidal tidal flats or sheltered subtidal channels. The rhythmic interlamination of mud and organic material reflects variability in tidal energy.

Description (Facies 3, Layered Sand and Mud) — F3 is characterized by interlayered mud and sand and is subdivided into Facies 3a (F3a) and Facies 3b (F3b), based upon the nature of the interlayering. Mud and sand layers within F3a are typically thin (< 1 cm) and repeat in a cyclical manner, with cycles exhibiting organized vertical trends that either coarsen or fine upwards (Figs. 3.2c and 3.2d). Individual mud layers can be massive or contain faint sand laminae, and laminae of organic detritus are common. Individual sand layers commonly contain thin (< 1 mm), discontinuous mud laminae. Sand and mud layers can also be organized into coarsening-upwards trends are defined by an upwards increase in both thickness and abundance of very fine- to fine-grained sand layers. Bioturbation is typically sparse to absent with the most common type being simple lined or unlined sand-filled burrows. F3a comprises 19 % (6.60 m) of the recovered paleochannel deposits (Table 2).

F3b consists of massive to faintly laminated mud interlayering with fine- to medium-grained, well-sorted sand that are massive, horizontally- or ripple-laminated. Laminae in sand layers are defined by thin (< 2 mm) mud drapes. Bed thicknesses range from less than 1 to 10 cm. Contacts between mud and sand layers are sharp (Fig. 3.2e), although often distorted due to the coring process. Small shell fragments (1 – 3 mm) can be locally abundant within coarser-grained sand layers. F3b comprises 11 % (4.05 m) of cored paleochannel deposits (Table 3.2).

Interpretation (Facies 3a) — F3a is interpreted as rhythmic bedding deposited on mixed-energy intertidal flats or channels, common features of estuarine or lagoonal environments where depositional energy is highly variable and largely attributed to tides (Allen, 1970; Howard and Frey, 1973; Reinick and Singh, 1980; Reading and Collinson, 2006). Vertical trends of thickening and thinning of mud or sand layers within F3a may be related to spring-neap or annual/seasonal discharge variability (Tessier 1998, Dalrymple et al. 2012; Friedrichs 2012).

Interpretation (Facies 3b) — The interlayering of sharp based sand and mud layers, irregular layer thickness, thickness of massive mud layers, and general lack of bioturbation suggest deposition in a tidally influenced, subtidal to lower intertidal environment (Allen 1970; Reineck and Singh 1980). Although generally lacking a pronounced cyclicity, interlayering within some intervals of F3b do appear rhythmic and may have been deposited within mixed energy tidal flats. Well-sorted fine- to medium-grained sand interbedded with mud drapes or thicker mud deposits associated with fluid muds are common features of estuarine channels and reflect deposition by sandy bedforms (Kapsimalis et al. 2004; Desjardins et al. 2012; Chaumillion et al. 2013; Zhang et al. 2018).

Description (Facies 4, Massive Muddy Sand) — F4 consists of massive, very fine- to fine-grained muddy sand and sandy mud (Fig. 3.2f). The upper and lower contacts of this facies are typically sharp and irregular. In Core SC-19, F4 occurs as coarsening-upwards packages that are 10 - 15 cm thick and defined by muds and sandy muds near their bases and muddy sands near their tops (Fig. 3.5b). F4 comprises 11 % (3.70 m) of paleochannel deposits across the study area (Table 3.2).

Interpretation (Facies 4) — F4 is interpreted as heavily bioturbated, subtidal heterolithic deposits. Although poorly-sorted overall, smaller areas of concentrated well-sorted sand or mud suggest that the original fabric of these facies were likely interbedded sands and muds and that the disorganized nature of these beds is a product of intense bioturbation (Fig. 3.2f). Deposits in brackish water environments commonly contain trace fossil assemblages that are of low species diversity and overall intensity of bioturbation that increases in both diversity and intensity with proximity to normal marine waters (Howard and Frey 1973; Reinick and Singh 1980; Dalrymple et al. 2012; Desjardins et al. 2012). This episodic increase in bioturbation within a backbarrier

setting may be the result of short-term or seasonal changes in conditions such as salinity, oxygen content, nutrient levels, or circulation. These changes may be driven by freshwater discharge, storm events, or changes in estuary mouth morphology (Cooper, 1993; Holbrook, 2001; Hughes, 2012).

Description (Facies 5, Fine-grained Shelly Muddy Sand) — F5 contains massive, fine- to medium-grained, moderately sorted, sand, and shelly sand beds that exhibit sharp upper and lower contacts with the adjacent, typically mud-rich units of F1, F2, and F3 (Figs. 3.2g and 3.5). In Cores GA-09 and SC-04 abundance and thickness of F5 beds increase notably (Fig. 5). F5 comprises 3 % (1.06 m) of the cored paleochannel deposits (Table 3.2).

Interpretation (Facies 5) — We interpret F5 to represent storm-related event beds deposited within overall low-energy backbarrier settings. The lack of internal sedimentary structures, coarse grain size, and sufficient particle sorting suggest high-energy transport with minimal hydraulic sorting during bulk transport and rapid deposition by strong currents while the abundance of shell fragments suggests a marine influence (Blatt et al., 1972).

Description (Facies 6, Coarse-grained Shelly Muddy Sand) — F6 consists of massive, very poorly sorted, fine- to coarse-grained, shelly muddy sand (Figs. 3.2 and 3.5). The thickest occurrence of F6 is within Core GA-11 where the base is defined by a coarse shelly lag and marks the base of a paleochannel (Fig. 3.5a). F6 comprises 2 % (0.80 m) of the investigated paleochannel deposits (Table 3.2).

Interpretation (Facies 6) — Although coarser-grained than F5, the mode of emplacement for F6 is similar. The decrease in sorting and increase in grain size of F6 relative to F5 suggests

storm-driven deposition in a more proximal setting with proximal referring either to channel access or marine source.

Description (Facies 7, Shelly Sand) — This facies is composed of well-sorted, fine- to coarse-grained sand with shell fragments and isolated gravelly or shelly layers. Individual beds are 5 to 30 cm thick and may be capped by thin mud drapes. Internally, this facies is massive or shows faint horizontal lamination with isolated mud lenses (Fig. 3.2i). The thickest deposit of F7 occurs in Core GA-05 where it forms the upper part of a marginal paleochannel fill succession. F7 comprises 4% (1.35 m) of paleochannel deposits within cores from the study area (Table 3.2).

Interpretation (Facies 7) — We interpret F7 as the deposits of flood-tidal deltas or inlet shoal complexes. Grain size, sorting, and development of upper flow regime structures indicate deposition under high-energy currents while mud drapes form during slack tides or in sheltered portions of the system. Submarine flood- and ebb- tidal deltas are a significant component of the Georgia Bight barrier system, accounting for nearly 80% of Holocene sand deposits (Hayes and Sexton 1996).

Description (Facies 8, Cross-bedded Sand) — F8 consists of very well sorted, medium-grained, cross-bedded sand with isolated thin mud drapes (Fig. 3.2). Individual beds are 5 - 10 cm thick with 1 - 2 cm thick muddy interbeds. Volumetrically, F8 is the least significant of the facies defined here comprising only 1% (0.20 m) of paleochannel deposits recovered (Table 3.2).

Interpretation (Facies 8) — We interpret F8 as bedload deposits resulting from the migration of subaqueous dunes along the floor of tidally-influenced channels. Mud drapes were deposited during periods of slack tides on the lee side of dunes.

Description (Facies 9, Gravelly Shelly Sand) — F9 consists of massive, medium- to very coarse-grained, gravelly, shelly sand. All shells are fragmented and up to 5 mm with quartz grains up 0.5 cm in diameter comprise the gravelly intervals. F9 occurs only in Core GA-05 where it is 1 m thick and forms the basal unit of the paleochannel fill. F9 thus contributes to 2 % (0.85 m) of the sampled paleochannel deposits (Table 3.2).

Interpretation (Facies 9) — Coarse grain size, shell content, and stratigraphic position of F9 suggests deposition within the basal section of a tidal channel under consistently high-energy conditions. The lack of fine-grained, slack-water deposits may indicate that these facies were deposited in tidal inlet channels.

Description (Facies 10, Gravelly Sand) — F10 is made of gravelly, coarse-grained, heavily oxidized sand intercalated by thin beds of horizontally or ripple-laminated muddy sands. F10 sand is compositionally and texturally less mature than sand found in any other facies. Sands and gravels are subrounded to subangular and contain lithic fragments and feldspathic grains. F10 is found only within the basal section of Core GA-07 and comprises 5% (1.90 m) of paleochannel deposits in the study area (Table 3.2).

Interpretation (Facies 10) — The coarse grain size, composition, texture, thorough oxidation, and lack of shelly material of F10 suggests deposition as bedload, possibly within a fluvial channel. Thin mud drapes suggest intermittent slack water conditions potentially related tidal influence though the presence of ripple lamination within mud-rich layers suggests some deposition by traction rather than exclusively suspension. F10 is the only non-marine facies recovered from the BOEM cores. Core GA-07 is seaward of the Altamaha River in the St. Simons Island area (Fig. 3.1). Howard and Frey (1973) noted that the Altamaha system has coarse sand

deposits throughout its length compared to other systems where this caliber of sediment is typically restricted to fluvial regions or areas adjacent to coarse-grained Pleistocene outcrops.

Facies Associations

F1-F6 comprise Facies Association 1 (FA1) which consists of low- or mixed-energy, tidally influenced, backbarrier deposits of intertidal flats, event (storm) beds, mud-rich and heterolithic channel environments (Fig. 3.3). The most abundant facies within this association are F1, F2 and F3. Collectively, these three facies comprise 71% of all paleochannel fills recovered in sediment cores from all of the study areas.

Facies Association 2 (FA2) consists of the predominantly sand-rich F6-F9 (Fig. 3.3) deposited under high-energy conditions within subtidal environments including channel-floors, flood-tidal deltas, and tidal inlets (Fig. 3.3). Where this facies association occurs it commonly consists of fining-upwards facies successions (Fig. 3.5a). For example, in Core GA-05, a vertical facies succession of F9, F8, F7, and F6 is consistent with the models proposed for tidal inlet fill (Moslow and Tye 1985; Fenies and Faugères 1998). FA2 accounts for a relatively minor part of sediment cores (10 %) but is significant in terms of constraining depositional environments associated with several paleochannel types.

Geochronology

Ages of paleochannel fill deposits are informed by 14 AMS-¹⁴C dates and 3 AAR age estimates from paleochannel deposits along Georgia and South Carolina from 7 cores in 4 study areas (Fig. 3.5 and Table 3.1). In addition to these intra-channel data, 15 AMS-¹⁴C dates and 5 AAR age estimates from extra-channel deposits are included and help to constrain the relative ages of paleochannels (Table 3.1). These extra-channel units are tabular, laterally-extensive marine or

backbarrier deposits that overlie, underlie, or are truncated by paleochannels (Fig. 3.5). AAR age estimates are based on comparisons of amino acid D/L values in samples of *Mulinia* shells from both offshore cores (with ^{14}C ages) and adjacent GA and SC onshore late Pleistocene marginal marine units, the latter of last interglacial age (MIS 5) based on U-series geochronology (Wehmiller et al., 2004; Wehmiller et al. 2019).

Paleochannels within the study area were filled during at least three phases. These phases occurred during the mid-Holocene (4 – 8 cal kyr BP), late Pleistocene (42 - 47 cal kyr BP), and prior to the late Pleistocene (> 47 cal kyr BP). The oldest phase (> 47 cal kyr BP) is the most poorly constrained, a function of both the paucity and limitations of the data. Several instances of apparent age mixing occur within the sandier extra-channel units where significantly older samples overlie younger ones, likely a product of transgressive reworking. This can be seen within upper units of SC-07, SC-21, and SC-22 (Fig. 3.5), suggesting that in these successions, AMS- ^{14}C ages do not represent a minimum age for these units. In contrast to these apparently mixed successions, intra-channel successions with that contain several samples exhibit younging-upwards successions such as seen in SC-14, SC-21, SC-22, and SC-24 (Fig. 3.5). Mid-Holocene age paleochannels are preserved off the coasts of St. Simons Island, GA, and Kiawah Island, SC. Late Pleistocene-aged paleochannel systems are found offshore of Ossabaw Island, GA, and Cape Romain, SC.

Seismic Facies and Stratigraphy of Paleochannels

Paleochannels and paleovalleys incise into underlying Eocene, Oligocene, Miocene, and Pleistocene stratigraphic units (Figs. 3.6, 3.7 and 3.8) (Popenoe et al. 1987; Harris et al. 2005; Weems et al. 2014). Seismic facies found within paleochannels, when combined with sedimentological and geochronological data from sediment cores, provide valuable information about timing, depositional processes, and mechanisms associated with the incision and filling of

these features. The stratigraphic architecture of paleovalleys, and the paleochannel systems which comprise them, can be controlled by autogenic (i.e. lateral migration, avulsion) or allogenic forcing (i.e. relative sea level, climate, sediment supply) (Dalrymple et al. 1992; Hughes 2012).

Seismic Facies

Five paleochannel seismic facies are defined here based the nature of their internal seismic reflectors. Paleochannel fill patterns and the seismic facies which they define are concentric (CHc), horizontal (CHh), asymmetric (CHa), chaotic (CHk), and transparent (CHt) (Fig. 3.4).

Concentrically filled paleochannels (CHc) are characterized by aggradational, concave, high to moderate-frequency, continuous, high-amplitude seismic reflectors. Horizontally filled paleochannels (CHh) are characterized by aggradational, horizontal to sub-horizontal, high to moderate frequency, continuous, moderate-amplitude seismic reflectors (Fig. 3.4). CHc and CHh are discussed together here due to their similarities in seismic character. The geometry and character of these seismic facies indicate filling via vertical aggradation in laterally stable channels. Most paleochannel cores penetrated one of these two seismic facies and they are the most common of the observed paleochannel seismic facies types across the study area. Five cores from five of the study areas in both Georgia and South Carolina recovered thinly layered, mud-rich sediments of FA1 from CHc and CHh paleochannels (Fig. 3.5). CHc paleochannels comprise 47 % and CHh paleochannels comprise 6 % of the paleochannels encountered across all study areas (Table 3.2).

Transparently filled paleochannels (CHt) are characterized by the lack of prominent internal seismic reflection (Fig. 3.4). While this lack of seismic reflectivity limits the use of seismic reflection data for the interpretation of paleochannel depositional processes and architecture,

sediment cores reveal significant variability within CHt paleochannels (Fig. 3.5). Five cores from three study areas in Georgia and South Carolina reveal this seismic facies and indicate compositions ranging from the mud-rich F2 deposits of Core GA-11 to the exclusively sand and gravel-rich F10 deposits of Core GA-07 (Fig. 3.5). In the Kiawah Island study area, heterolithic F3, F4, F6, and F7 deposits from Cores SC-07 and SC-14 comprise the sediment fill of two stacked, but CHt paleochannels which are separated by a thin, laterally-continuous sand sheet (Fig. 3.5). CHt paleochannels comprise 35 % of all paleochannels encountered across all study areas (Table 3.2).

Asymmetrically filled paleochannels (CHa) are characterized by inclined, moderate-amplitude, continuous, moderate to high-frequency seismic reflectors that onlap paleochannel margins and downlap paleochannel floors. Two distinct types of this seismic facies occur within paleochannels, bilateral and laterally-accreting. Bilateral CHa are defined by concave seismic reflectors that downlap the paleochannel floor. They commonly form along the margins of CHc paleochannels where they constitute a small fraction of the overall paleochannel fill (Fig. 3.7b). Laterally-accreting CHa seismic facies are less common. This facies is defined by sigmoidal seismic reflectors that form the bulk of the paleochannel fill in which they occur (Fig. 3.4a). Three cores from the Kiawah Island and Cape Romain areas recovered mud-rich to heterolithic sediments of F1 and F3 from bilateral CHa facies (Figs. 3.5 and 3.7). The similarity in paleochannel fill and association with CHc suggests that this seismic facies represents the early infill stage of paleochannels under low-energy conditions. Although none of the cores from this study penetrated laterally accreting CHa paleochannels, this channel type has been observed from Chirp data within the study area (Figs. 3.4 and 3.7). Similar facies have been documented from fluvial, estuarine, and backbarrier environments where they represent the deposits of point bars that formed along

the margins of sinuous estuarine channels or tidal inlets due to lateral migration (Dalrymple et al. 1992; Dalrymple et al. 2012; Hughes, 2012; Fitzgerald and Miner 2013). CHa paleochannels comprise 4 % of all paleochannels encountered across all study areas (Table 3.2).

Chaotically filled paleochannels (CHk) are characterized by irregular, low-amplitude, discontinuous, low to moderate-frequency seismic reflectors (Fig. 3.4). Cores GA-05 and GA-11 from the St. Simons Island and Ossabaw Island study areas, respectively, indicate that CHk paleochannel fill consists of sand-rich FA2 deposits (Figs. 3.3, 3.4 and 3.5). CHk intervals define the basal fill succession within paleochannels at these two locations. The composition and stratigraphic position of CHk facies suggest that they represent high-energy, basal channel fill deposits (Fig. 3.4 and 3.5). CHk comprise 8 % of all paleochannels encountered across all study areas (Table 3.2).

Stratigraphic Architecture

Paleochannels within the study area occur either in isolation or as components of a paleovalley with the latter case being more common in all study areas (Figs. 3.6, 3.7, and 3.8). Individual paleochannels can be described as either simple, containing one type of continuous seismic facies, or compound, containing more than one type of genetically related seismic facies (Fig. 3.4b). An excellent example of a compound paleochannel is shown in Figure 3.5a. Here, a CHa transitions laterally into a CHc without a significant erosional surface between the two, suggesting that the two facies represent changing depositional conditions during channel infill.

Paleovalley architecture is defined based on the stacking patterns exhibited by their constituent paleochannels (Fig. 3.4b). Multistory paleovalleys commonly show an upward decrease in paleochannel size resulting in a nested configuration. Figures 3.6 and 3.8 illustrate two

examples of this type of architecture from the Kiawah and Cumberland Island study areas. Paleochannels within multilateral paleovalleys are offset laterally relative to one another and show minimal or no vertical translation (Fig. 3.4b). Specific paleovalleys referred to herein are named based upon sediment cores which penetrate them (e.g. SC-21 Paleovalley).

In places, particularly offshore of Georgia, the upper bounding surfaces of paleochannels and paleovalleys are defined by extensive erosional surfaces that occur at different stratigraphic levels (Fig. 3.8). This situation differs from the South Carolina study areas where they typically share a common surface (Fig. 3.7), which seems to be associated with a regional transgressive surface. This difference between a southern and a northern province likely reflects an overall decrease in accommodation resulting in the amalgamation of transgressive erosional surfaces.

Morphology and Geographic Distribution of Paleochannels

Knighton (1998) defined the three primary components of channel morphology as perpendicular cross-section (vertical plane perpendicular to channel axis), longitudinal cross-section (vertical plane parallel or oblique to channel axis), and plan form (horizontal plane). Each of these components offers insights into the depositional and erosional processes responsible for paleochannel development and infill. Making the distinction between cross-sectional and longitudinal sections can be difficult and is strongly dependent upon the distribution and density of data lines; with widely spaced or sparse datasets, determining these components can be a significant problem. Figure 3.7 provides an example of the effect that data distribution and orientation can have on defining this parameter. Here, intersecting chirp profiles show a shore-oblique paleovalley with an apparent width that ranges from 2,600 to 627 m. In these situations, it is the narrowest width that most closely approximates the true width and the corresponding cross-sectional morphology. Due to this type of limitation, we here do not distinguish between

perpendicular and longitudinal cross-section morphology, rather we refer only to apparent width or cross-sectional morphology unless otherwise specified.

The thickness of preserved paleochannels ranges from 1-18 m with an average value of 4.7 m (Table 3.2). The thickest preserved paleochannel is found in the Ossabaw Island area. This feature fill is characterized as a CHt seismic facies and has a rugose basal erosional surface that extends below the maximum penetration depth of our data; therefore, the recorded depth is a minimum value for this feature. The Cape Romain/Santee, Kiawah Island, and Cumberland Island areas all contain paleochannels with a maximum preserved thickness around 11 m, while paleochannels in the North Myrtle Beach, St. Catherine's, and St. Simons areas have an average preserved paleochannel thickness of 5-6 m (Table 3.2).

General descriptions of perpendicular cross-sectional morphology include u-shaped or roughly tabular forms and can have either smooth or rugose basal bounding surfaces (Fig. 3.4). CHc and CHh typically exhibit u-shaped morphologies with smooth basal surfaces (Figs. 3.4, 3.6, 3.7, and 3.8). Laterally-accreting CHa paleochannels commonly form tabular bodies, a function of the lateral migration of the channel with little to no vertical aggradation. The morphology of oblique or longitudinal cross-sections show a higher degree of morphological variability than perpendicular cross-sections (Fig. 3.7). This difference is illustrated by the youngest CHc paleochannel contained within the SC-21 paleovalley shown in Figure 3.7 (Line 027). Paleochannel thickness in the SE corner of this system ranges from 1 to 7 m over a distance of a few hundred meters.

Cross-sectional morphology can be locally complex. An example of this variability can be seen in the Kiawah Island area where several channel floor "mounds" can be seen at the base of a CHa/CHc paleochannel within the SC-21 paleovalley. These mounds may represent either

erosional remnants of older paleochannel fill, or depositional features such as channel-margin slump blocks or small bars or large bedforms (Fig. 3.7b).

Accurate mapping of the planform morphology of paleochannels and paleovalleys requires a dense of seismic data such as those available in the Kiawah Island and North Myrtle Beach areas. Correlative paleochannels and paleovalleys are defined based on stratigraphic architecture and the distribution of seismic facies (Fig. 3.7). Offshore of Kiawah Island, paleochannels most commonly occur as components of three mappable paleovalleys rather than in isolation. Core SC-21 penetrates a CHa/CHc paleochannel within a prominent paleovalley, referred to as the SC-21 paleovalley. At least four generations of paleochannels comprise this feature which trends NW-SE across the area and appears to be connected to several, smaller tributary systems (Fig. 3.7c). A second paleovalley to the SW of the SC-21 paleovalley trends parallel to its northern neighbor and is penetrated by Core SC-19 (Fig. 3.7c). The SC-19 paleovalley is composed of CHa, CHc, CHt, and minor CHk paleochannels, the cross-cutting relationships and stacking patterns of these paleochannels and paleovalleys define at least four successive phases of incision and infill. It is the youngest of these paleochannels that is intersected by Core SC-19 and shown in Figure 3.6. Two hundred-fifty kilometers to the south, offshore of Cumberland Island, GA. Chirp profiles define the GA-03 paleovalley (Fig. 3.8). Here, nested CHc paleochannels comprise the youngest of several paleovalleys which trend roughly normal to the modern coastline.

Three hundred forty-seven paleochannels and paleovalleys were documented from 1,089 km of seismic data from all eight study areas. Key morphometric parameters including are summarized in Table 3.2. Seismic imaging of paleochannels in the subsurface is dependent upon the distribution of data. We characterize the distribution of data using two parameters, the total

amount of data (line length) and total area covered. The total amount of data acquired varies considerably between study areas and ranges from 7 – 314 km. The total area covered also ranges from 5 – 914 km² (Table 3.2). To account for the differences in the amount and distribution of data, we consider the total number of paleochannels observed relative to the total length of Chirp profiles, a parameter we refer to as the channel density which has units of number of paleochannels per kilometer (n/km). Paleochannel density is an estimate of how many paleochannels are encountered per km of Chirp data and ranges from 0.07 n/km in the North Myrtle Beach Area to 0.76 n/km in Ossabaw Island with an average value of 0.44 n/km (Fig. 3.9). Since this estimate does not account for the width of individual paleochannels or paleovalleys, other morphometric parameters presented in Table 3.2 are used in combination with paleochannel density to fully characterize the spatial distribution of these features.

DISCUSSION

Origin of Paleochannels

Combining the distribution of paleochannels and paleovalleys found along the inner shelf encountered along the Georgia Bight with core-calibrated sedimentary facies suggests that more than half (52 %) of paleochannels are filled by fine-grained, mud-rich, heterolithic, tidally-influenced backbarrier deposits. These channels formed in estuarine and lagoonal environments similar to those found along the modern coast within the study area during several periods throughout the Quaternary.

Tidal channels of modern backbarrier systems of the Georgia Bight provide strong modern analogues for the planform and cross-sectional morphology of paleochannel systems preserved in the subsurface along the inner shelf. The tidal creeks and estuarine channels associated with St.

Catherines Sound along the northern coast of Georgia are a good example. This system consists of a tidal inlet (St. Catherines Sound) that is approximately 2.5 km wide with a maximum depth of 13 m. The Medway River, the largest of the tidal rivers, trends roughly perpendicular to the coast and has a maximum width of 1.8 km and a maximum depth of approximately 10 m. Additionally, numerous smaller tidal channels dissect the backbarrier marshes and exhibit planform morphologies ranging from highly sinuous to nearly straight and are oriented parallel, oblique, and perpendicular to the coast. Within these smaller rivers, maximum channel depths range from 4 – 7 m with an average depth of 6 m and channel widths range from 350 – 700 m. Channel cross-sections are commonly symmetrical but become asymmetrical due to the presence of point or mid-channel bars. These dimensions are comparable to the paleochannel systems shown in Figures 3.6, 3.7, and 3.8. When compared to paleochannel systems, the dimensions and orientations of these modern channels support the interpretation that the most common types of paleochannels encountered in this study formed in similar backbarrier environment.

Origin of Paleovalleys

Paleovalley architecture is a result of both allogenic (driven by extra-basinal processes) and autogenic (driven by intra-basinal processes) mechanisms. The stratigraphic architecture of paleovalleys can be closely linked to changes in accommodation (Catuneanu 2006; Gibling 2006). The Stono and North Edisto Rivers near the Kiawah Island study area have occupied roughly the same location during several different sea level cycles throughout the Quaternary (Harris et al. 2005; Weems et al. 2014). This type of re-occupation generates paleovalleys containing paleochannels that formed during successive glacioeustatic cycles. In backbarrier settings, antecedent topography associated with ancestral backbarrier channel systems may play a role in the location of subsequent tidal drainage systems.

Core SC-19 penetrated nested CHc paleochannels within a multistory paleovalley (Fig. 3.6). Three *in-situ* samples of two common tidal flat mollusk species yielded calibrated AMS-¹⁴C dates (8, 20, 27, and 41 cal kyr BP) that indicate the underlying paleochannel pre-dates the Holocene transgression and was deposited during a previous sea level cycle while the youngest paleochannel filled at around 8 cal ka BP (Fig. 3.6). The paleochannels penetrated by Core GA-11 offer another example of diachronous, co-located paleochannels. The base of this core recovered 20 cm of well-indurated F1 deposits from a lower paleochannel which is separated from an overlying, younger paleochannel by a 60 cm thick marine sand sheet (Fig. 3.5a). Paired AAR and AMS-¹⁴C data suggest that this lower channel pre-dates 30 ka BP. The large CHc paleovalley penetrated with Core GA-03 lacks age-control but is a good example of diachronous paleovalley stacking (Fig. 3.8). Here, at least two distinct paleovalleys and one distinct paleochannel record three periods of development and a minimum of six periods of renewed channel incision. The upper surface of each paleovalley is defined by a separate, regionally extensive, horizontal erosional surface. The nature of these surfaces suggests that they are transgressive erosional surfaces and are likely a result of at least three glacioeustatic sea level cycles.

Paleovalley formation resulting from renewed incision due to autogenic processes can result in similar paleovalley architecture as those that form in response to allogenic processes. Channel avulsion, re-occupation, and headward erosion are common processes in tidal channel systems and result in changes to discharge leading to either incision or infilling (Zeff 1988; Holbrook 2001; Hughes 2012). These changes in channel hydrodynamics strongly influence paleochannel morphology and can result in complex paleovalley architectures. The SC-21 paleovalley in the Kiawah Island study area provides an excellent example of multistory paleovalley formation that is the result of autogenic processes (Fig. 3.7). It contains three primary

CHc/CHa and CHc paleochannels that share a common basal surface which is associated with a specific stratigraphic horizon within the underlying pre-Quaternary section. Core SC-21 penetrates the margin of a CHc/CHa paleochannel that filled between 8 and 4 cal kyr BP during the Holocene transgression. This paleochannel is in turn incised into by a younger CHc paleochannel. Since both paleochannels are of Holocene age formation was almost certainly driven by renewed incision within the system related to changes in hydrodynamic conditions.

The distinction between paleovalleys that develop as a result of re-occupation of backbarrier channel systems (i.e. allogenic) from those that develop due to periods of renewed channel incision as a result of changing hydrodynamic conditions (i.e. autogenic) is not straight forward. Due to the relatively limited range in depositional and seismic facies, dating of individual paleochannels within the paleovalley may be the only reliable means of making this distinction.

Trends in Paleovalley Architecture

Northern study areas differ significantly from those in the southern areas in the degree of channelization and stratigraphic architecture (Fig. 3.10). Offshore, paleochannels in this area are rare, with a degree of channelization in the North Myrtle Beach area of 0.07 n/km, the lowest value found in any of the study areas (Fig. 3.9). In this area, paleochannels incise into folded and faulted Cretaceous carbonate rocks and are covered by a thin, discontinuous drape of Holocene sand (Fig. 3.10). Regional trends in paleochannel development along the inner continental shelf appear to follow those identified by Hayes (1994) for modern coastal systems. The northern-most portion of the study area coincides with Hayes compartment II which is dominated by welded barriers (68 %) and Pleistocene strandplain (20%) shorelines. He attributed this development to a high coastal plain gradient limiting the development of extensive backbarrier lagoons and estuaries. He explained these high sub-regional gradients with proximity to the Cape Fear Arch, a basement-

involved tectonic feature that has remained active throughout the Holocene (LeGrand 1961; Richards 1967; Hayes 1994; Van De Plassche et al. 2014).

While not as low as in the North Myrtle Beach area, the Cape Romain/Santee Delta area also exhibits a low degree of channelization with a value of 0.20 n/km. In this area paleochannels incise into structurally-tilted Eocene and Oligocene rocks, and flat-lying Pleistocene deposits (Fig. 3.10; Long and Hanebuth, 2020). Laterally-discontinuous Pleistocene stratigraphic units exhibit rare vertical stacking and are commonly offset laterally. Holocene sand sheets while discontinuous, are more laterally-extensive than in the North Myrtle Beach and are up to 5 m thick. In addition to the smaller paleochannels and paleovalleys present across the study area, the Piedmont-draining Santee and Pee Dee Rivers have formed incised valleys across the shelf in response to multiple sea level regressions and have been significant sediment sources in the region throughout the Quaternary (Colquhoun et al. 1972, Weems et al. 1994; Baldwin et al. 2006; Long and Hanebuth 2020).

Further to the south, offshore of southern South Carolina and Georgia, increasing tidal range, increasing sediment supplied to the coast from major Piedmont-draining rivers, and a decrease in coastal gradient associated with the underlying SE Georgia Embayment has led to well-developed modern barrier-backbarrier and large estuarine systems (Howard and Frey 1973; Hayes 1994). These conditions were likely prevalent throughout the Quaternary as evidenced by the existence of well-developed paleo-backbarrier systems preserved across the modern coastal plain. Near Kiawah Island, the maximum depth of paleochannels and paleovalleys coincides with the top of resistant stratigraphic units (Fig. 3.7) and are incised into Oligocene and Eocene rocks and thin, tabular Pleistocene sediments (Fig. 3.10; Popenoe et al. 1987; Weems and Lewis 2002; Harris et al. 2005)

Offshore of southern Georgia, in the southern-most part of the study area, the multi-tiered stratigraphic architecture of the Georgia inner shelf differs from that of South Carolina (Figs. 3.8 and 3.10). Here, multiple, sheet-like Quaternary stratigraphic units are stacked vertically and bound by extensive erosional surfaces (Fig. 3.8). Paleochannels and paleovalleys associated with these regional erosional surfaces incise into the Quaternary units and are covered by laterally-extensive Holocene sand deposits. The thickness of Quaternary sediments in this part of the study area is likely a function of long-term trends in accommodation and preservation related to the influence of both the Cape Fear Arch and the SE Georgia Embayment/South Georgia Rift. Uplift and subsidence trends in this region are associated with glacial isostatic adjustment, dynamic topography, sediment loading, and thermal subsidence, vary spatially, and have continued at least throughout the Quaternary (Heller et al., 1982; Rowley et al. 2013; Doar 2014; Rovere et al. 2014; Van de Plassche et al. 2014). Rovere et al. (2014) estimated the influence of the dynamic topography component to range from -2 to +8 m/Ma along the Georgia coast to 13 – 23 m/Ma near the northern limit of our study area.

CONCLUSIONS

- 1) Integrated sedimentological and stratigraphic analysis of paleochannels along the inner shelf of the Georgia Bight indicates that these geological features were mainly formed in backbarrier environments and preserved predominantly mud-rich, tidally-influenced deposits.
- 2) Paleochannels comprise paleovalleys that formed during the late Pleistocene and Holocene due to both allogenic and autogenic processes. Tidal channels within backbarrier systems show a tendency to form in the vicinity of pre-existing older paleochannels which were formed during previous sea level cycles. Paleovalley architecture of tidal channel systems also show that

renewed incision related to autogenic processes can result in stacked or nested paleochannels that are of approximately similar age.

- 3) The youngest generation of paleochannels from South Carolina and Georgia are of mid-Holocene age (8 – 4 kyr BP). Paleochannels and backbarrier deposits from the Cape Romain (SC) and Ossabaw Island (GA) areas likely formed between 46 and 30 cal kyr BP, possibly providing evidence of deposits associated with Marine Isotope Stage 3 along the inner shelf. Several older ages exceed the AMS-¹⁴C limit, suggesting that older generations of paleochannels also exist.
- 4) Both the density of paleochannels (degree of channelization) and the thickness of preserved Quaternary stratigraphic units within the Georgia Bight generally decrease to the north. This trend, which coincides with coastal compartments defined by Hayes (1994), suggests a relationship between regional structural trends and either the original development or the long-term preservation potential of paleochannels and paleovalleys.
- 5) In several study areas, mud-rich paleochannels are exposed on the modern seafloor, potentially influencing local morphodynamics and serving as a secondary source of fine-grained sediment.
- 6) Where data coverage permits, individual paleovalleys can be correlated based on paleochannel architecture and paleochannel associations within each paleovalley. The morphologies of these paleovalleys typically define shore-oblique to shore-parallel orientations.
- 7) The preservation of fluvial deposits within paleochannels in this region appears to be rare within our data set. Core data and stratigraphic architecture of most paleochannels show little evidence of basal fluvial successions.

FIGURES

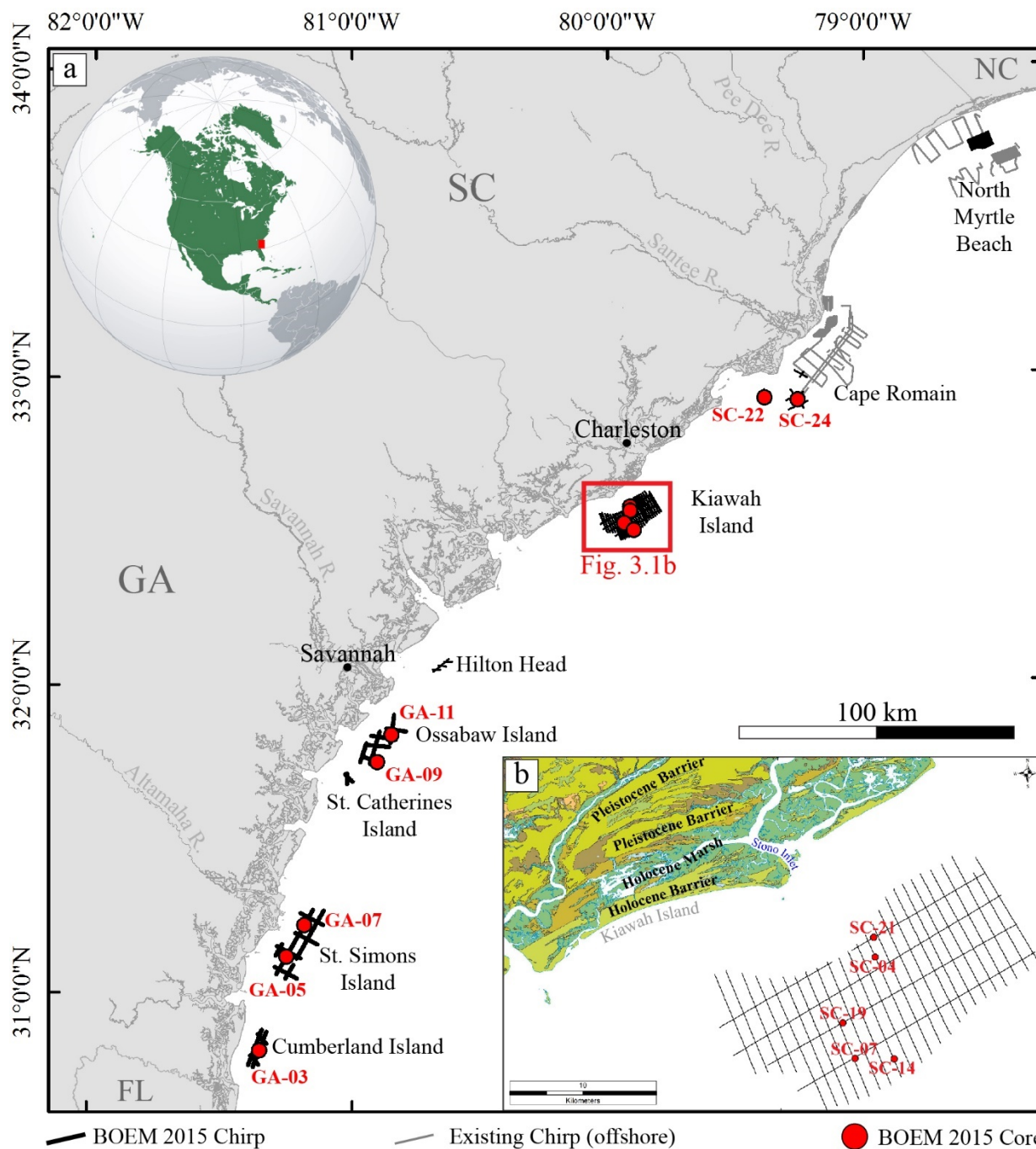


Figure 3.1. a) Coastline of the Georgia Bight with the location of the eight study areas and seismic-acoustic and sediment-core data used in this study. b) Kiawah Island study area with location of sediment cores and Chirp profiles. Onshore surface geology from Weems et al. (2014).

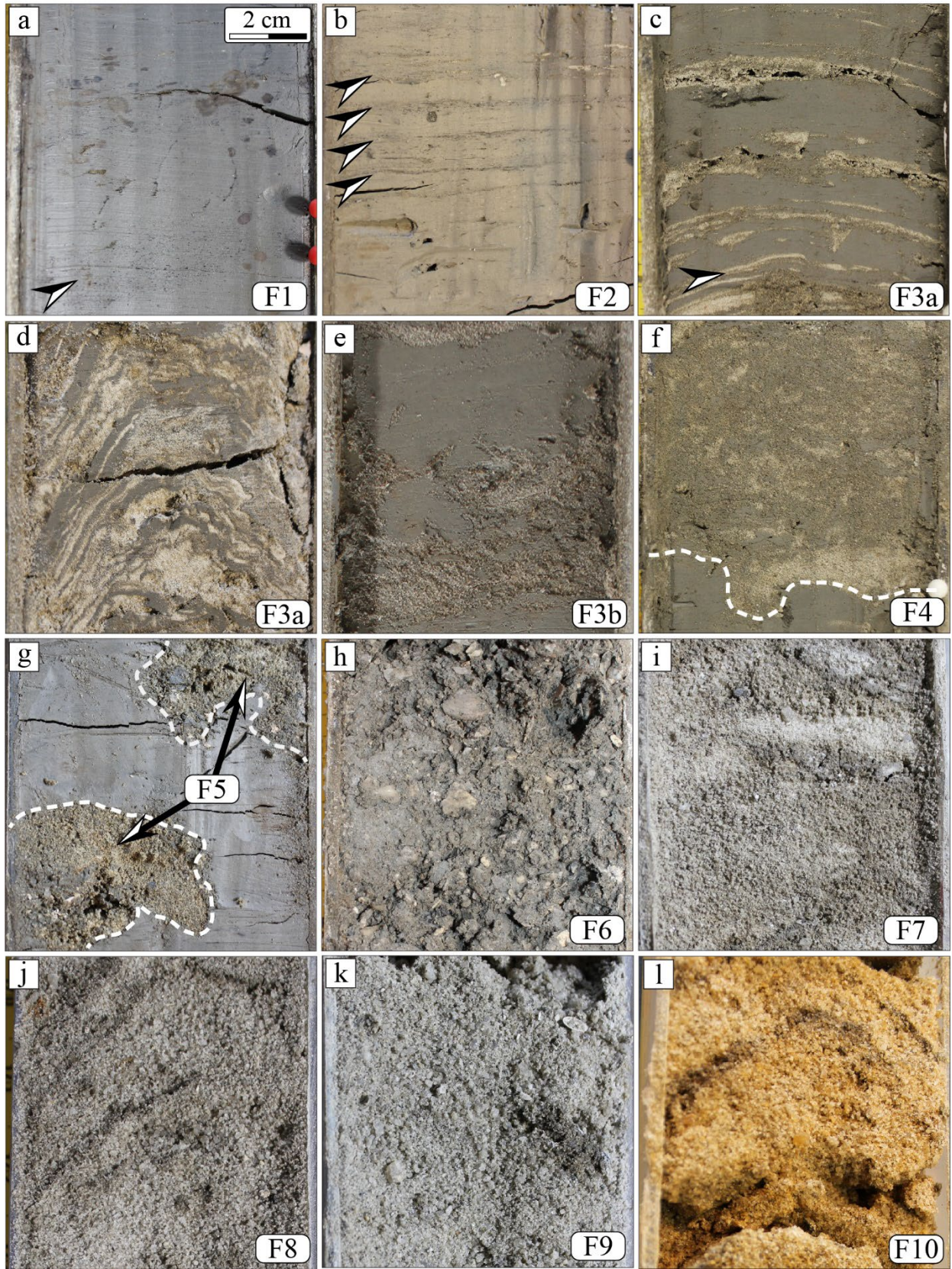


Figure 3.2. Sedimentary facies types **a)** Massive Mud (F1): Massive mud with disseminated organic detritus (white arrow). **b)** Laminated Mud and Organics (F2): interlayered mud and organic detritus. Rhythmic bedding defined by regular spacing of organic material (arrows). Layered Sand and Mud. **c)** F3a: mud-rich with regularly-spaced laminated very fine-grained sands (downward bending caused by coring). **d)** F3a: sand-rich occurrence with approximately even amounts of interlayered sand and mud. Note thin mud drapes within thin sand layers. **e)** F3b: irregularly interlayered thick muds and thin sands. **f)** Massive Muddy Sand (F4): sharp-based, intensely bioturbated heterolithic sediment. **g)** Fine-grained Shelly Muddy Sand (F5): sharp-based and sharp-topped fine to medium-grained, shelly sand bed (bed disruption caused by coring). **h)** Coarse-grained Shelly Muddy Sand (F6): massive, muddy, shelly (fragments), medium to coarse-grained sand. **i)** Shelly Sand (F7): well-sorted, medium to very coarse-grained sand. Note thin gravel layer near center of photograph. **j)** Cross-bedded Sand (F8): inclined sets of very well-sorted medium-grained sand with thin dark gray mud drapes (dip of layers exaggerated by coring-induced deformation). **k)** Gravelly Shelly Sand (F9): coarse-grained quartz sand and gravel with isolated shells and shell fragments. **l)** Gravelly Sand (F10): thoroughly oxidized, medium-grained, gravelly sand with thin brown mud drapes.

Facies (%)	Description	Interpretation	Facies Associations	Depositional Setting	Core Log Motif
F1 (19)	Massive to weakly laminated mud disseminated organic detritus	Suspension sedimentation on low-energy intertidal flats or sheltered tidal channels			
F2 (22)	Interlaminated mud and fine-grained organic detritus with isolated sand grains or thin, silty or sandy laminae				
F3 F3a (19) F3b (11)	Regularly (3a) and irregularly (3b) interlayered very well sorted, very fine- to fine-grained sand and mud	Suspension and traction sedimentation on mixed-energy intertidal flats (3a) or subtidal traction deposition of sand with tidal mud drapes or fluid mud (3b)	FA1	Backbarrier	
F4 (11)	Very poorly sorted, very fine- to fine-grained, massive muddy sand and sandy mud	Highly bioturbated heterolithic deposits			
F5 (3)	Thin beds of moderately sorted, fine- to medium-grained sand or shelly sand	Distal* storm deposits within intertidal or subtidal environments			
F6 (2)	Very poorly sorted, fine- to coarse-grained, shelly, muddy, massive sand or sandy mud	Proximal* subtidal storm deposits			
F7 (4)	Well sorted, fine- to coarse-grained sand with shells. Rare mud layers and gravel layers	Bedload deposition possibly associated with tidal delta or inlet shoals	FA2	Subtidal Channel and Inlet	
F8 (1)	Very well sorted, medium-grained, cross-bedded sand with thin mud drapes	Subaqueous dunes with mud drapes			
F9 (2)	Medium-grained to gravelly, shelly sand and fragmented shell beds	High-energy marine -influenced channel floor deposits			
F10 (5)	Oxidized, moderately-sorted, subrounded to subangular, immature medium-grained to gravelly sand with isolated thin mud layers and lenses	High-energy, non-marine, bedload deposits with minor suspension deposition	N/A	Fluvial Channel	

Figure 3.3. Summary of sedimentary facies types and facies associations identified in this study. Percentage listed beneath facies name represents the fraction that each facies comprises out of all sedimentary paleochannel fill succession deposits. Facies Associations 1 and 2 both represent sediments deposited in a backbarrier estuarine or lagoonal environment, with FA1 being generally deposited under low energy conditions and FA2 under higher energy conditions. F10 is only found in one sediment core and is the only non-marine facies. *Proximal and distal, as used here, refers to relative distance from inlet or barrier with distal being the furthest landward or upstream.

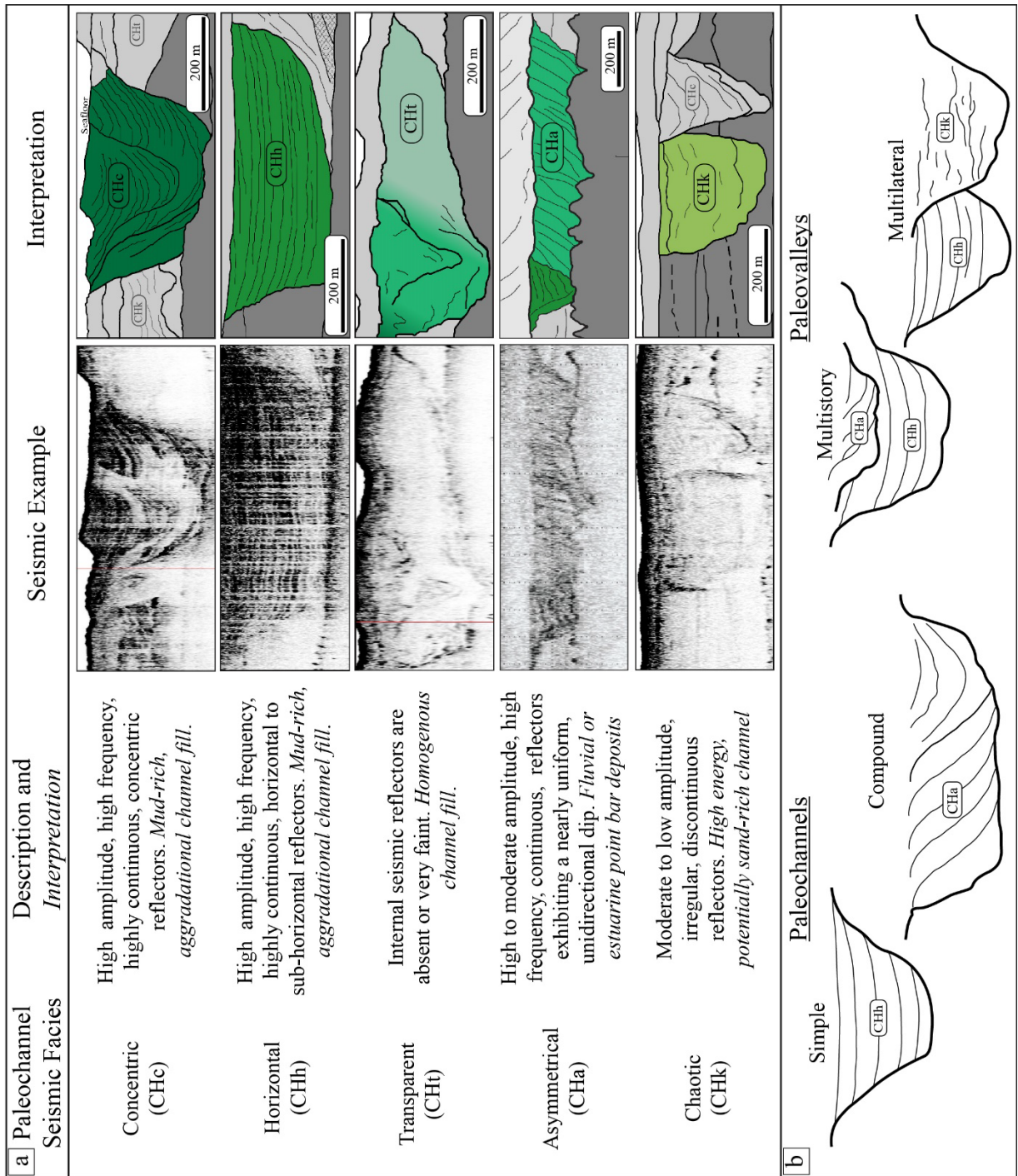
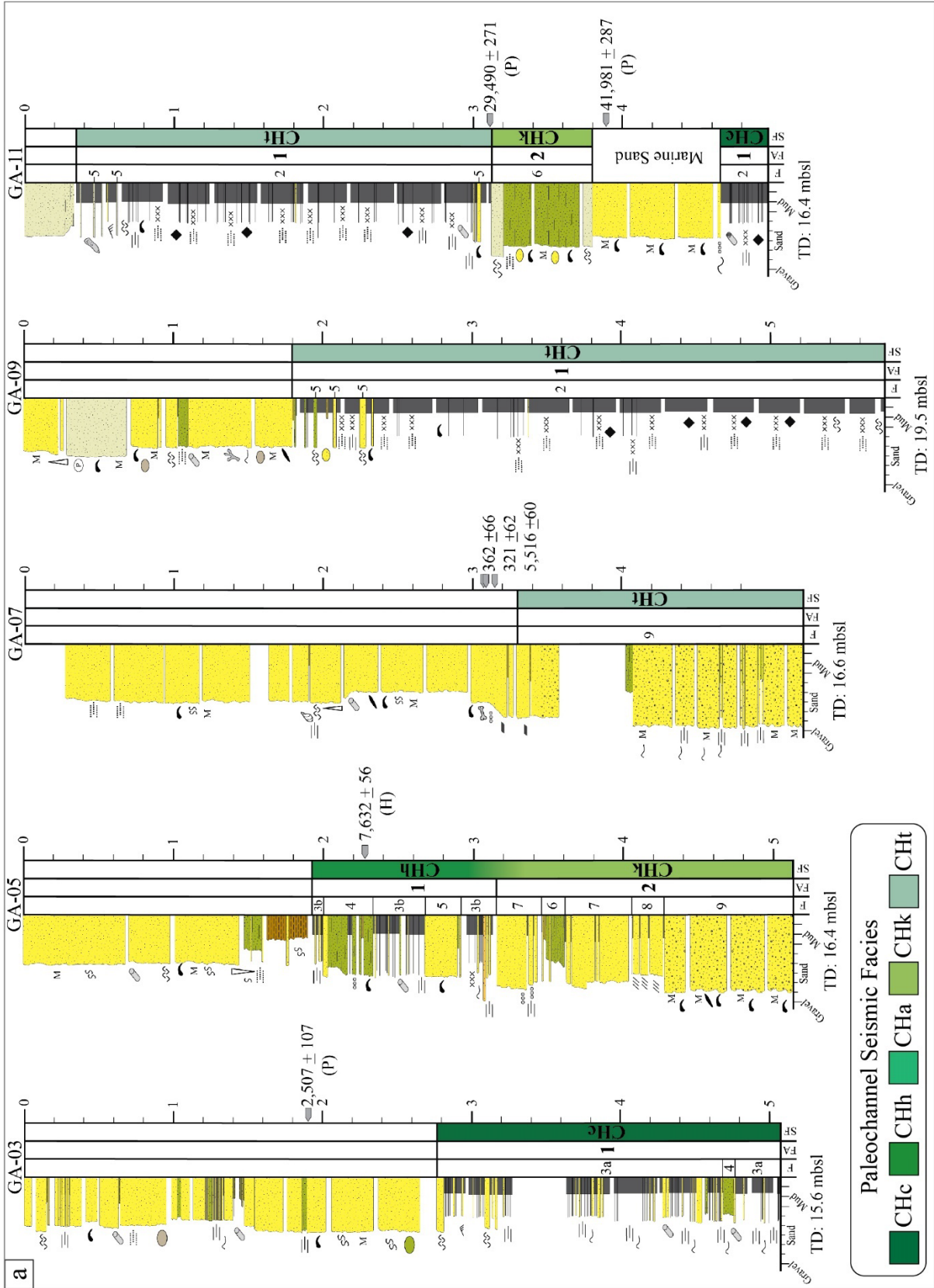
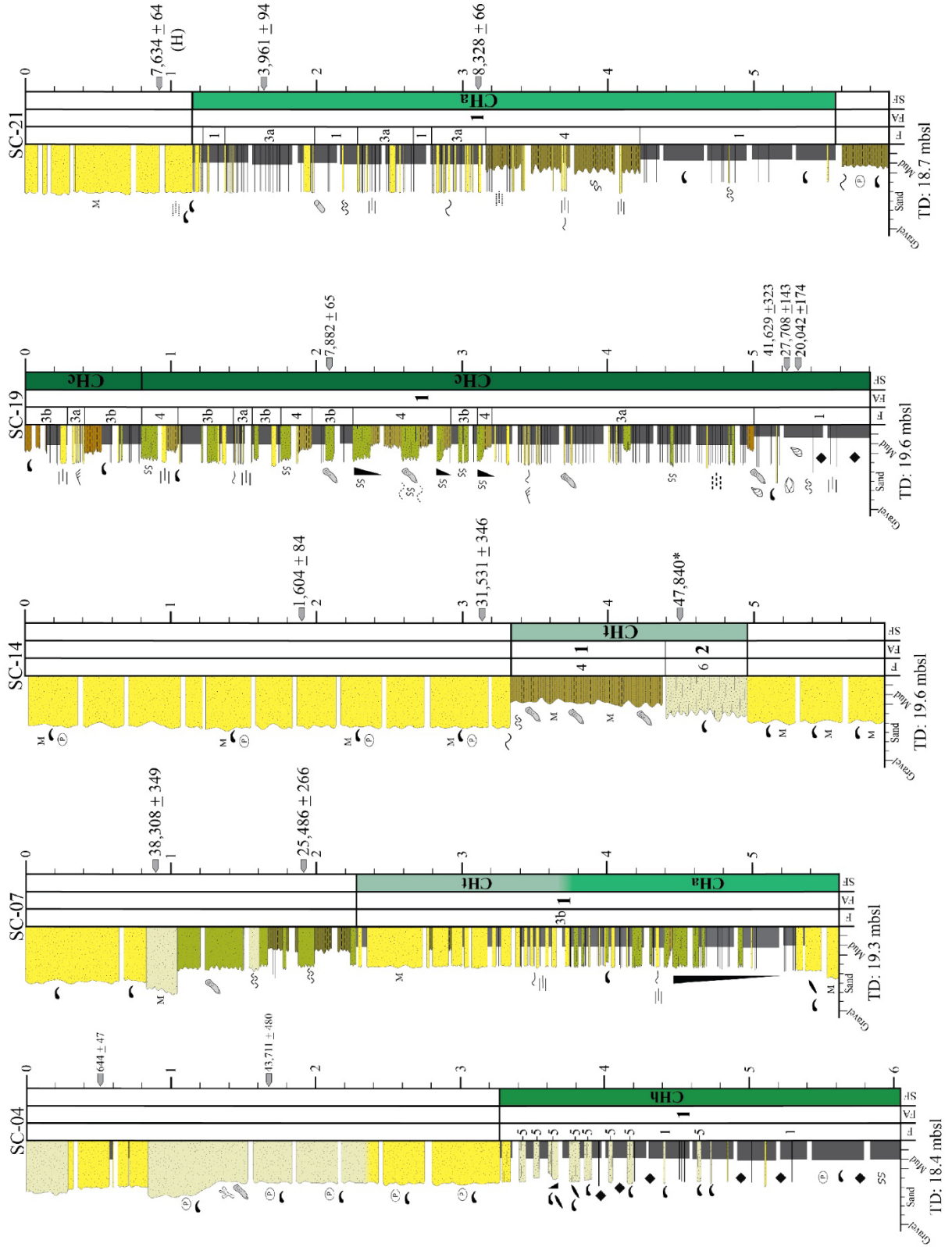


Figure 3.4. Seismic paleochannel facies classification defined in this study. **a)** Seismic facies of paleochannel fills observed across all eight study areas. **b)** Terminology used for stratigraphic architecture of paleovalleys. Multistory and multilateral terminology is based on Gibling (2006).



b



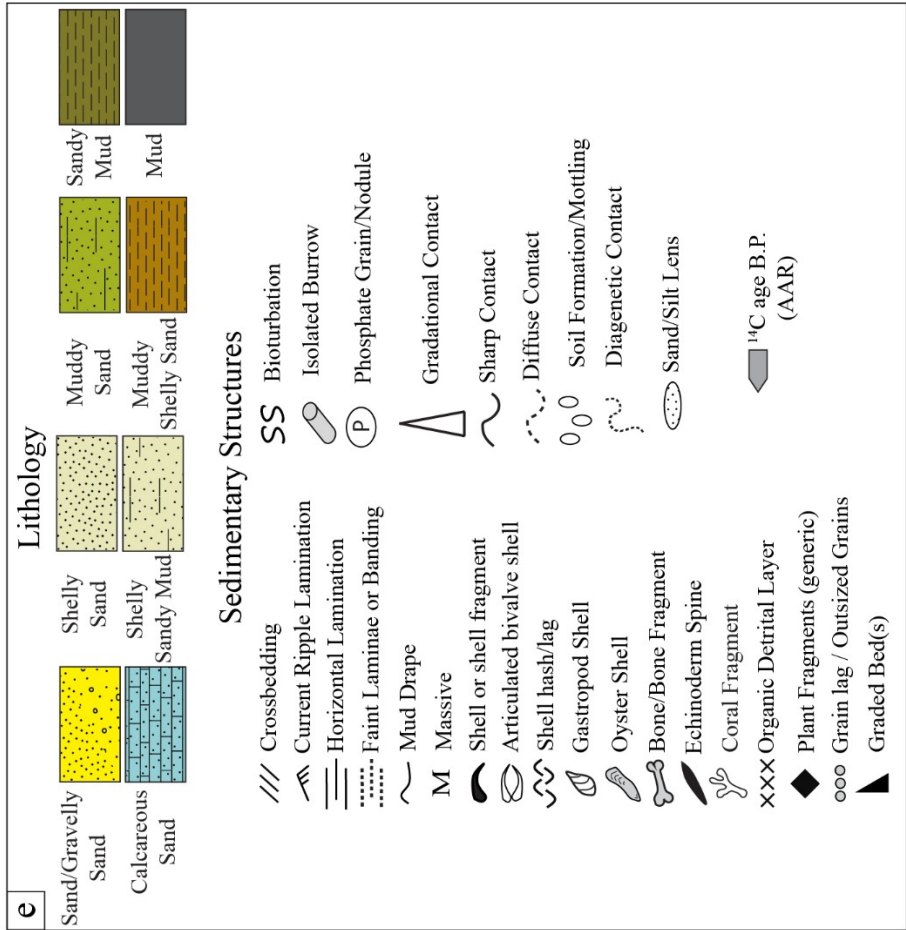
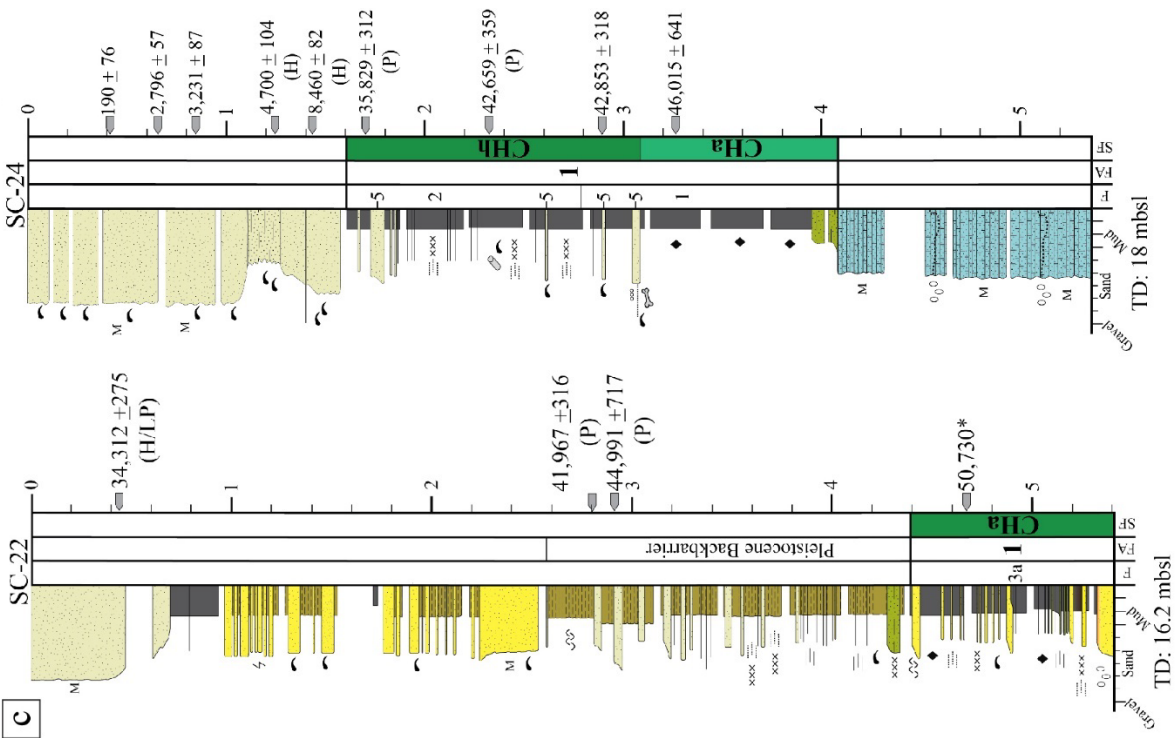


Figure 3.5. Sediment core logs from **a)** the Georgia sector, **b)** and **c)** the South Carolina sector. Dating provided as AMS-¹⁴C ages with 2σ error (cal yr BP ± yr) and AAR age estimates (in parentheses: H: Holocene, LP: Late Pleistocene, P: Pleistocene). **d)** Shells from common tidal flat species recovered from the lower F1 interval in Core SC-19. From left to right: dwarf mud snail (*Mulinia lateralis*), oyster spat, and eastern brown mud snail (*Tritia obsoleta*) **e)** Legend for colors, patterns, and symbols used to represent lithologies and sedimentary structures in the core logs. See Figure 3.1 for core locations.

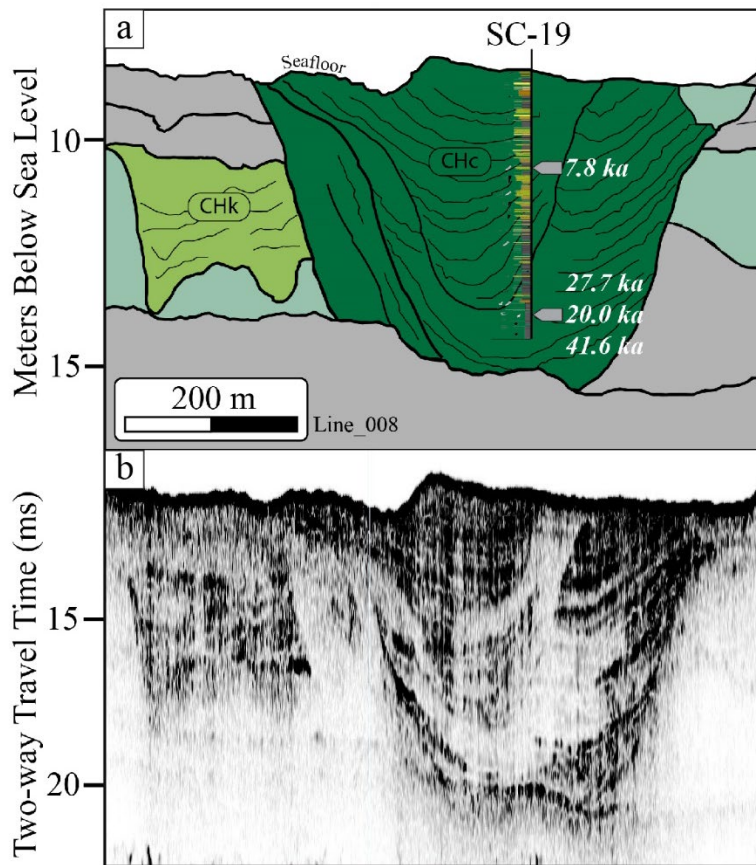


Figure 3.6. Example of an integrated seismic-core description and interpretation. **a)** Interpretation of Chirp profile in the Kiawah Island study area showing a multi-story paleovalley comprised of three distinct CHc paleochannels. Core SC-19 penetrates the two youngest paleochannels that, based on calibrated AMS-¹⁴C data, were infilled during the mid-Holocene and late Pleistocene

respectively. This paleovalley truncates an older paleovalley that consists of CHt and CHk paleochannels. **b)** Chirp profile associated with interpretation in Fig. 3.6a.

Figure 3.7. **a)** Integrated seismic-core interpretation fence diagram from the inner portion of the Kiawah Island (SC) study area. Blue line indicates the orientation of the SC-21 paleovalley. The influence of erosion-resistant strata is evidenced by the limitation on maximum depth of incision at a specific level across the Kiawah Island study area. **b)** Close-up of the margin of the SC-21 paleovalley showing the distribution of seismic facies, core lithology, and AMS-¹⁴C ages associated with the CHa paleochannel within the paleovalley. The mounds labeled here are either erosional remnants of a previously deposited paleochannel fill or bar-like depositional features associated with the channel floor. Circled numbers indicate individual successive paleochannels each representing a phase of incision and infilling. **c)** Overview map of paleochannels and paleovalleys in the Kiawah Island area. The locations of Figure 3.7a are Figure 3.6 are shown by the red lines. The planform morphology of the SC-21 and SC-19 paleovalleys (blue arrows) trend oblique to the modern coast with intermediate segments that run shore-parallel. Paleochannels recognized in previous studies (brown and green arrows) are included for comparison and to get a better overall picture of the total extent of paleochannel development in the area.

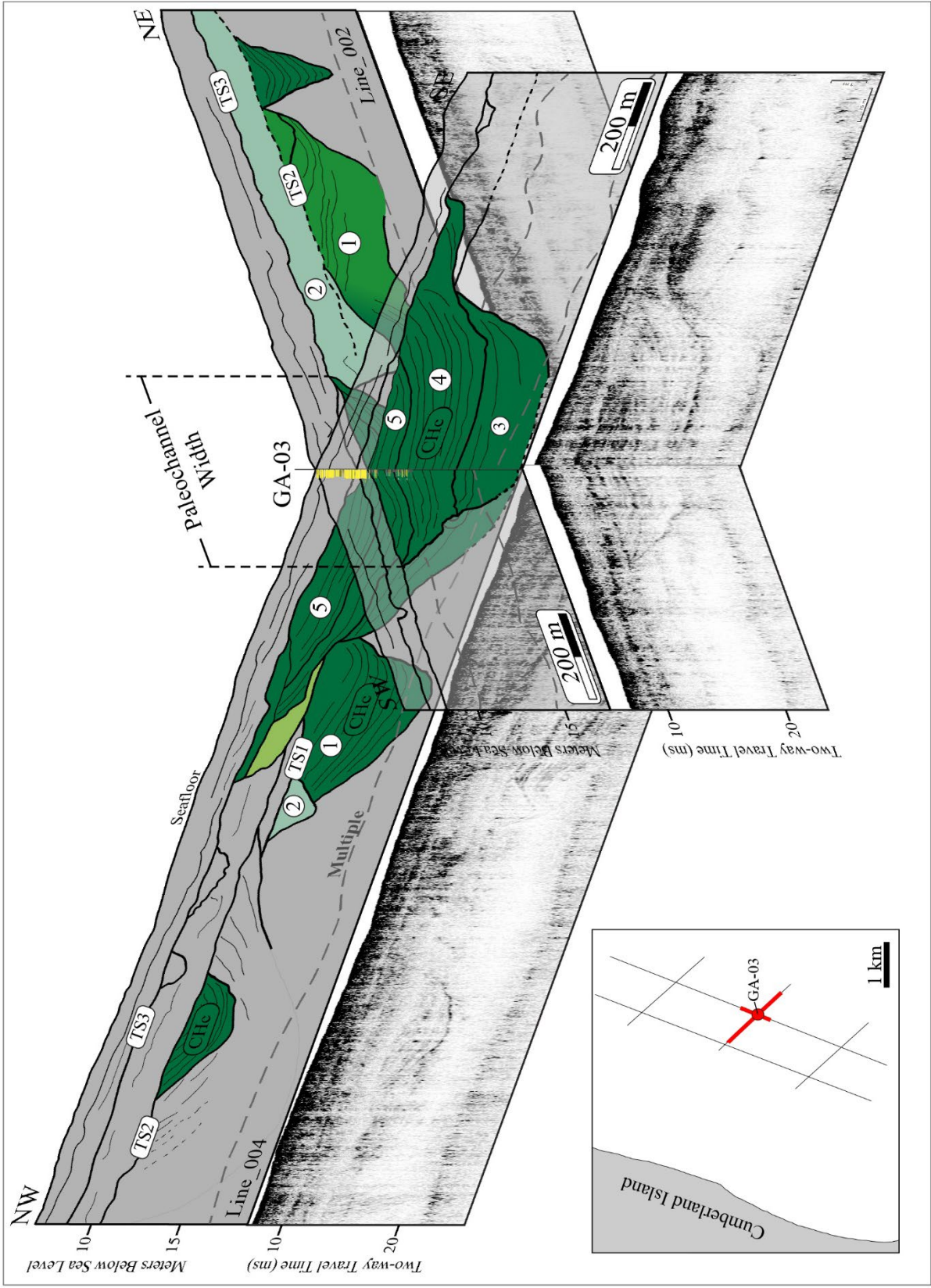


Figure 3.8. Interpretive fence diagram from the Cumberland Island (GA) study area. Two distinct paleovalleys are distinguished and exhibit at least five successive phases of paleochannel development (numbered 1-5). The tops of each paleovalley are marked by distinct erosional surfaces (TS1, TS2, and TS3) interpreted to be the result of three distinct transgressions. This configuration differs significantly from what was found in South Carolina waters where the thin Quaternary section preserves a single, composite transgressive erosional surface (Fig. 3.7). Intersecting seismic profiles and interpretations constrain the true width of the largest and youngest CHc, multistory paleovalley to 450 m.

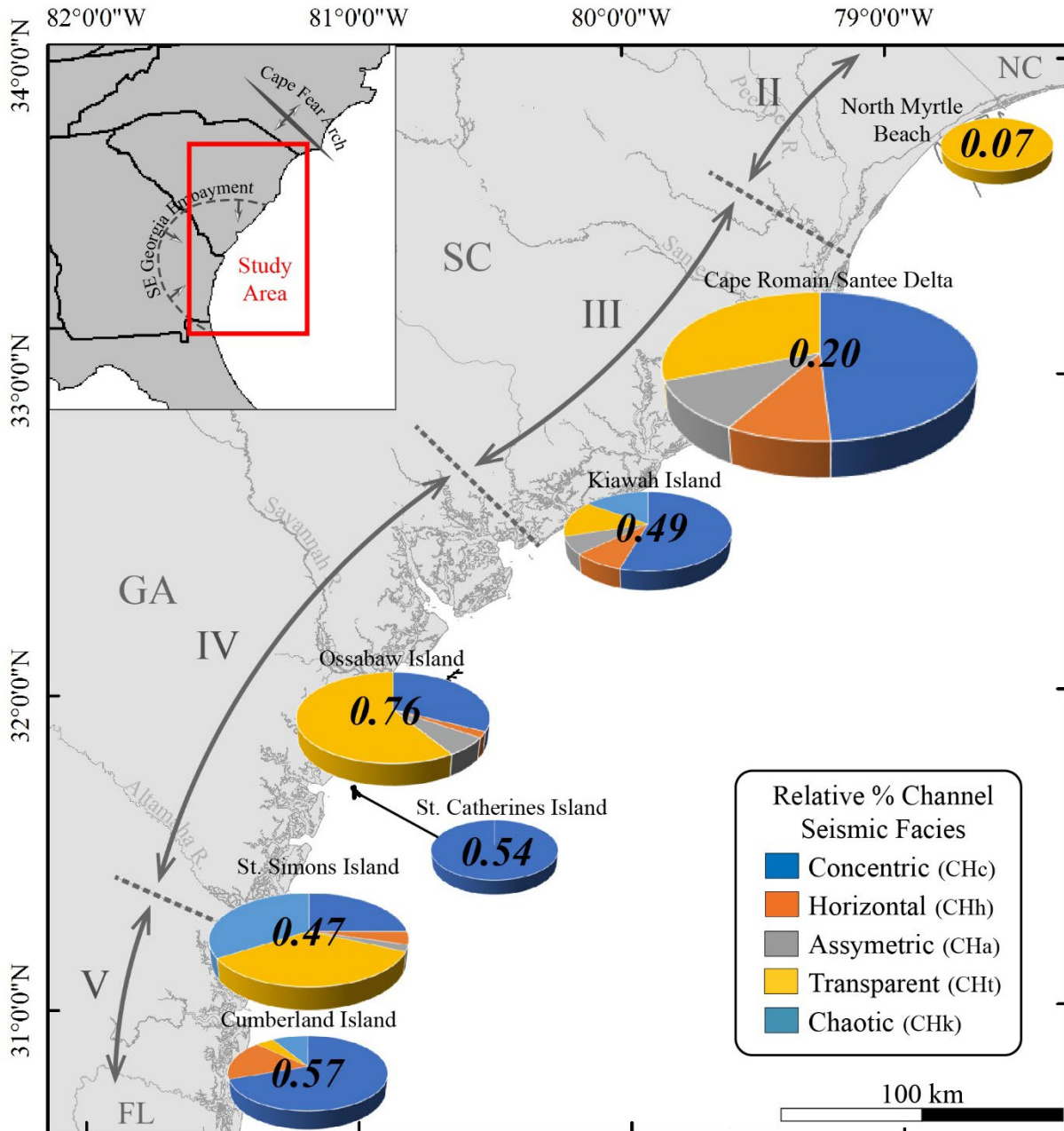


Figure 3.9. Summary of paleochannel distributions. Pie charts show the relative % of each paleochannel seismic facies found within each study area and are scaled based on the size of each study area. Labels on pies are the degree of channelization (n/km). Coastal compartments of Hayes (1994) are indicated by roman numerals. Location of regional tectonic features (Cape Fear Arch

and SE Georgia Embayment) in inset map are from LeGrand (1961) and Hayes (1994). Coastal compartments (roman numerals) are from Hayes (1994).

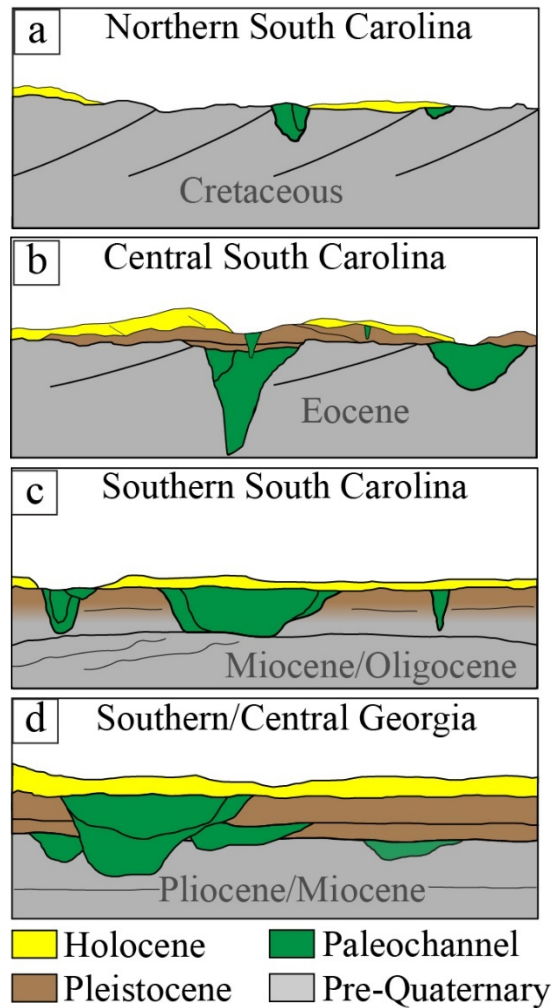


Figure 3.10. Generalized trend in paleovalley architecture from north to south. **a)** The North Myrtle Beach area contains a limited number of small, isolated paleochannels eroded into structurally-deformed Cretaceous rocks. No cores were recovered from within the paleochannels however cores from extra-channel locations are typically very short (~ 1 m), entirely sandy, often heavily oxidized, and commonly contain rock fragments (Long, 2018). **b)** The central South Carolina area includes offshore paleovalleys associated with the Santee and Pee Dee rivers. Isolated remnants of Pleistocene deposits are thin and Holocene units are discontinuous

transgressive sand sheets and sand ridges (Long and Hanebuth, 2020). **c)** In southern South Carolina paleochannel density increases relative to the northern locations with most paleochannel fill consisting of mud-rich, tidally-influenced sediment. The influence of pre-Quaternary stratigraphy is evident by the limitation of paleoincision depths in the area, a relationship also noted by Harris et al. (2005). **d)** Offshore of Georgia, stacked Quaternary paleoincisions and extra-channel tabular stratigraphic units were deposited over multiple sea level cycles, and their preservation is a function of the overall higher long-term accommodation in this area, potentially related to subsidence within the Southeast Georgia Embayment.

Study Area	Core Name	Water Depth (mbsl)	Sample Depth (m)	Intrachannel (I) or Extrachannel (E)	Raw ¹⁴ C Age (a BP)	Error (a)	Calibrated Median ¹⁴ C Age (cal a BP)	2σ Age Error
Kiawah Island	SC-04	12.3	0.55	E	1,080	20	644	47
Kiawah Island	SC-04	12.3	1.62	E	40,500	190	43,711	480
Kiawah Island	SC-07	13.7	1.95	E	21,560	50	25,486	266
Kiawah Island	SC-14	13.7	1.92	E	2,020	20	1,604	84
Kiawah Island	SC-14	13.7	3.14	E	38,170	160	31,531	346
Kiawah Island	SC-14	13.7	4.46	I	47,840	520	0	0
Kiawah Island	SC-19	13.8	2.10	I	7,420	25	7,883	66
Kiawah Island	SC-19	13.8	5.23	I	37,070	160	41,315	323
Kiawah Island	SC-19	13.8	5.23	I	23,580	50	27,708	144
Kiawah Island	SC-19	13.8	5.28	I	16,610	40	20,042	174
Kiawah Island	SC-21	12.7	0.97	E	7,170	25	7,634	64
Kiawah Island	SC-21	12.7	1.65	I	3,960	20	3,961	94
Kiawah Island	SC-21	12.7	3.14	I	7,860	25	8,328	66
Cape Romain	SC-22	10.9	0.47	E	30,710	90	34,312	275
Cape Romain	SC-22	10.9	0.47	E	AAR		Holocene / Late Pleistocene	
Cape Romain	SC-22	10.9	2.89	E	37,990	180	41,967	316
Cape Romain	SC-22	10.9	2.89	E	AAR		Pleistocene	
Cape Romain	SC-22	10.9	2.97	E	42,240	230	44,991	717
Cape Romain	SC-22	10.9	2.97	E	AAR		Pleistocene	
Cape Romain	SC-22	10.9	4.75	I	50,730	580	0	0
Cape Romain	SC-24	12.0	0.62	E	3,030	20	2,796	57
Cape Romain	SC-24	12.0	0.87	E	3,360	20	3,231	87
Cape Romain	SC-24	12.0	0.96	E	31,890	100	35,350	330
Cape Romain	SC-24	12.0	1.07	E	3,820	25	3,768	90
Cape Romain	SC-24	12.0	1.23	E	4,500	25	4,700	104
Cape Romain	SC-24	12.0	1.44	E	8,010	30	8,460	82
Cape Romain	SC-24	12.0	1.74	I	32,320	100	35,829	312
Cape Romain	SC-24	12.0	2.35	I	39,100	230	42,659	359
Cape Romain	SC-24	12.0	2.89	I	39,410	180	42,853	318
Cape Romain	SC-24	12.0	3.34	I	43,200	300	46,015	641
Cape Romain	SC-24	12.0	0.40	E	550	20	190	76
Cumberland Is	GA-03	10.4	1.93	E	2,810	20	2,572	107
Cumberland Is	GA-03	10.4	1.93	E	AAR		Pleistocene	
St. Simons Is	GA-05	10.9	2.25	I	7,160	25	7,632	56
St. Simons Is	GA-05	10.9	2.25	I	AAR		Holocene	
St. Simons Is	GA-07	11.3	3.12	E	720	20	362	66
St. Simons Is	GA-07	11.3	3.14	E	660	20	321	62
St. Simons Is	GA-07	11.3	3.17	E	5,150	25	5,516	60
Ossabow Is	GA-11	14.0	3.12	I	25,810	70	29,490	271
Ossabow Is	GA-11	14.0	3.12	I	AAR		Pleistocene	
Ossabow Is	GA-11	14.0	3.96	E	38,010	150	41,981	287
Ossabow Is	GA-11	14.0	3.96	E	AAR		Pleistocene	

Table 3.1. Radiocarbon (^{14}C) and Amino Acid Racemization (AAR) ages for paleochannel fills and adjacent intervals. AMS- ^{14}C dates were measured at the University of Georgia; AAR data were measured at Northern Arizona University.

Area	Area (km ²)	Total Line Length (km)	Total # of Paleochannels	Data Density (km/km ²)	Channel Density (n/km)	Avg Depth (mbsl)	Max Depth (mbsl)	Avg Thickness (m)	Max Thickness (m)	Avg Apparent Channel Width (m)	% CHc	% CHh	% CHa	% CHt	% CHk
North Myrtle Beach	102	283	21	2.8	0.07	16	22	3	6	173	0	0	0	100	0
Cape Romain / Santee Delta	914	274	55	0.3	0.20	18	31	5	11	620	49	9	11	31	0
Kiawah Island	227	314	154	1.4	0.49	14	24	5	12	429	55	8	7	15	15
Ossabaw Island	125	60	46	0.5	0.76	15	28	6	18	556	33	2	7	59	0
St. Catherines Island	5	7	4	1.4	0.54	10	12	4	6	1,107	100	0	0	0	0
St. Simons Island	270	93	44	0.3	0.47	12	15	3	7	344	25	5	2	34	34
Cumberland Island	78	41	23	0.5	0.57	14	20	5	11	380	70	17	0	4	9
Totals	1,443	1,089	347												
Averages	246	153	50	1.04	0.44	14	21	4	10	516	47	6	4	35	8

Table 3.2. Data distribution and key morphometrics of paleochannel systems in all study areas.

Chapter 4

Late Holocene Stratigraphy and Facies Distributions of an Anthropogenically-modified Delta Plain (Santee Delta, SC, USA)

ABSTRACT

The Santee River of South Carolina has the second largest watershed in the eastern United States and forms the largest river-fed delta along the US east coast. Anthropogenic modifications to the delta plain of the Santee, and in many coastal environments within the region, have significantly altered the natural configurations of floodplains, channels, and shorelines. This study incorporates historical data and modern state-of-the-art data and methods to evaluate the sediment distribution within the modern delta plain as well as the record of environmental change throughout the late Holocene as it is preserved within the subsurface stratigraphy. We incorporate high-resolution seismo-acoustic and bathymetric data, detailed sediment core analysis, AMS-¹⁴C radiometric dating, micropaleontological analysis, and surface sediment samples to define geomorphic zones based on dominant depositional processes related to fluvial discharge, tides, and waves. Tidal- and wave-influenced conditions were established in the delta plain by around 3 ka BP and continued into historical times, when the construction of rice fields across most of the delta plain fixed channel positions and isolated floodplains. Sediment distribution in the modern delta plain is significantly influenced by the artificial canals and embankments associated with these fields. The influence of these modifications can also be seen within the stratigraphy beneath the delta plain, recording local changes in deposition and erosion resulting from changes in circulation and sediment supply.

INTRODUCTION

Marine deltas are discrete constructional landforms that develop where a river provides sediment to a marine basin (Bhattacharya 2006; Giosan and Goodbred 2007) forming an interface between terrigenous and marine depositional systems. These environments are influenced by complex hydrodynamic processes associated with river discharge, tides, and ocean waves. Most modern river deltas are heavily populated and have been extensively modified for agriculture and navigation (Syvitski et al. 2009). They host extensive wetlands which are among the most productive ecosystems on earth, providing diverse natural habitats and protecting inland communities from the effects of large storms (Stedman and Dahl, 2008; Hoitink et al., 2020). Delta plains, the subaerial regions of a delta containing active and relict distributary channels (Reading and Collinson 2006), are low-lying coastal areas which are sensitive to subtle changes in relative sea level (RSL) (Stanley and Warne 1994). The composition and distribution of sediments within delta plains are integral components of coastal wetland ecosystems. Subsidence of these areas resulting from human activity including groundwater and hydrocarbon reservoir depletion, decreased sediment supply due to dam construction, and agricultural practices, coupled with natural sediment compaction, only serves to increase the vulnerability of modern delta plains (Syvitski et al. 2009; Anthony et al. 2014; Auerbach et al. 2015). Understanding the modern and ancient depositional systems preserved in the subsurface stratigraphy of Holocene deltas provides a history of how and when these ecosystems have changed and to what environmental factors, both intrinsic and external, may have driven these changes.

Geomorphic and Geologic Setting

Throughout the late Quaternary, fluctuations in RSL, driven mostly by glacioeustasy, have exerted a primary control on the nature and distribution of coastal depositional systems across the

coastal plain of the southeastern United States (Cooke 1936; Colquhoun 1961; Colquhoun et al. 1972; Gayes et al. 1992; Colquhoun 1995; Doar, 2014). A period of rapid global sea-level rise beginning at the end of the Pleistocene slowed approximately between 8,500 – 6,500 years ago, reaching its current level in this region approximately 5,000 years ago (Stanley and Warne 1994). This time interval of decelerating sea-level rise is coincident with the deposition of Holocene deltaic sequences around the world (Stanley and Warne 1994, 1997). Regionally, post- and syn-depositional modifications owing to dynamic topography, neotectonics, glacio-isostasy, and hydro-isostasy have influenced the coastal sedimentary record of RSL (Richards 1967; Hathaway et al. 1976; Cronin et al. 1981; Colquhoun 1995; Peltier, 1999; Weems and Lewis 2002; Baldwin et al. 2006; Moucha et al. 2008; Englehart et al. 2011; Bartholomew and Rich 2012; Rowley et al. 2013; Doar and Kendall 2014; Rovere et al. 2014). Van de Plassche et al. (2014) estimated that the rate of RSL rise over the past 4,000 years ranges from 0.72 – 0.80 mm yr⁻¹ along the coast of central South Carolina.

Global and local climatic changes during the Holocene have been both episodic and periodic, with frequencies ranging from multi-decadal through millennial (Mayewski et al. 2004; Cronin et al., 2005). Regional variations in precipitation and temperature related to larger-scale atmospheric circulation can strongly affect local coastal environments (Cronin et al., 2005; Wright et al., 2017). The temperature and salinity of coastal waterways, as well as the intensity and frequency of major storms both have control over local hydrology, precipitation and runoff, sediment supply, coastal morphodynamics, and biological productivity. Anthropogenic perturbations to the global climate over the past 150 years likely have and will continue to modify regional and local coastal environments (Molina et al, 2014).

Twenty-three kilometers from the coast the Santee River bifurcates into its two main distributaries, the North and South Santee Rivers, defining the landward limit of the Santee delta plain (Fig. 4.1). Closer to the coast, both distributaries branch again where the northernmost branch forms the broad and shallow North Santee Bay (Fig. 4.1). The distributaries of the Santee River enter the Atlantic Ocean near the central coast of South Carolina forming the only river-fed delta on the east coast of the United States (Eckard et al., 1986). Delta plain geomorphology from historical maps indicate that the modern configuration of the Santee delta distributary system appears to have been stable for at least the past 260 years (Cooke, 1773; Lewis, 1979).

The Santee River drains an area of approximately 44,000 km² (Kjerfve 1976; Hockensmith 2004) and has its headwaters in the Piedmont and Blue Ridge regions of North and South Carolina. Mean annual discharge from the Santee River is 311 m³ s⁻¹ (Torres 2017), up to 85 % of which flows through the North Santee (Fig. 4.1; Matthews and Shealy 1982). Currently, the Santee River delivers an estimated 0.81 – 0.86 Mt yr⁻¹ of suspended-sediment load to the coast (McCarney-Castle et al., 2010). The tidal range at the mouth of the river is approximately 1.16 m (Torres 2017). The distribution of fresh, brackish, and saltwater within the Santee system is a function of river discharge and ocean tides (Hockensmith 2004).

The incised valley of the modern Santee River formed during glacioeustatic lowstands during the late Pleistocene (Weems et al. 1994; Eckard et al. 1986; Long and Hanebuth 2020). Beneath the modern delta plain, the incised valley is up to 20 m deep and its infill consists of a basal succession of Pleistocene fluvial deposits overlain by Holocene delta-plain deposits (Eckard et al. 1986). Holocene delta plain deposits are bound to the north and south by Pleistocene beach ridge complexes (Fig. 4.1; Shen et al. 2017).

Anthropogenic Modifications

The human history of the Santee delta spans the last 3,400 years (Espenshade and Brockington 1989). The natural system has been manipulated and modified for protection, fishing, navigation, and agriculture and has significantly influenced the hydrologic, ecologic, and sedimentary systems on both regional and local scales. While the Santee delta is small by global standards, anthropogenic modifications made within the watershed and the delta itself may result in additional subsidence and a change in both freshwater discharge and sediment supply, rendering it increasingly vulnerable to modern RSL rise, much like many large Holocene deltas around the world (Stanley and Warne 1994; Syvitski et al. 2009).

Regional modifications — The Santee Canal, was commissioned in 1793 and completed in 1800 (<https://www.oldsanteecanalpark.org/About/index.aspx#history>). The 35-km long waterway connected the Santee River near Jamestown to the Cooper River near the town of Moncks Corner and ultimately Charleston Harbor (Fig. 4.2).

Ninety-five kilometers inland from the coast, two large dams, one each on the Santee (Wilson Dam) and Cooper Rivers (Pinopolis Dam) with a connection through a 5-km long canal, were completed in 1941, effectively re-routing 88 % of the natural water discharge from the Santee River into the Cooper River (Kjerfe, 1976). Between 1942 and 1985, an estimated 0.65 Mt yr^{-1} of sediment was deposited near the mouth of Lake Marion on the Santee River as a consequence of the new reservoir (Patterson et al., 1996). Prior to dam construction, the Santee River had a mean annual freshwater discharge of $525 \text{ m}^3 \text{ s}^{-1}$ (Kjerfe, 1976). The diversion of the discharge led to significant siltation issues in Charleston Harbor (Kjerfe, 1976). In response to this human-made issue a re-diversion canal was completed in 1985 from Lake Moultrie back into the Santee River (Fig. 4.1; Kjerfve 1976). This re-diversion restored mean annual discharge of the Santee system to $400 \text{ m}^3 \text{ s}^{-1}$ (Kjerfe et al. 1994), although more recent studies place this value closer to $311 \text{ m}^3 \text{ s}^{-1}$

(Torres 2017). McCarney-Castle et al. (2010) modeled suspended sediment flux from the Santee River prior to dam construction at 5.80 Mt yr^{-1} , a seven-fold increase relative to modern conditions (McCarney-Castle et al. 2010). Overall, reduced freshwater discharge through the Santee River has resulted in an increasing dominance of salt-tolerant plant species in the inner Santee delta plain (Kjerfe et al. 1994; Nixon 2004).

Local modifications — The record of human habitation within the Santee delta plain extends as far back as 1,400 BCE with the first known establishment of seasonal occupation by indigenous people along the shores of Minim Island (Espenshade and Brockington, 1989). This early occupation occurred soon after the establishment of brackish marshes at this site (Espenshade and Brockington, 1989). Subsequent occupations occurred from 600 – 200 BCE, and from 100 – 300 CE (Espenshade and Brockington, 1989). The earliest continuous European settlements along the Santee date to the 17th century (Lewis, 1979).

By the late 18th century approximately 120 km^2 of wetland forest in the Santee delta plain were cleared for the cultivation of rice within two decades (Fig. 4.1; Lewis, 1979). The conversion of the former cypress swamps and marshes into rice fields includes the digging of a dense canal network, construction of levees, and the installation of large wooden drainage gates. Rice field construction likely had both long-term and short-term impacts on the natural system. Short term impacts include exposure and destabilization of fluvial and estuarine floodplain soils. Significant portions of these fields are still maintained and even have been added to during recent decades for use as waterfowl hunting reserves and wildlife refuges (Lockhart 2017).

First proposed in 1808, the construction of the Atlantic Intracoastal Waterway (AIWW) was federalized in 1919 and completed by 1936 (Charles 2016). Construction of the local AIWW between the northern margin of South Island along Winyah Bay and the southern end of Murphy

Island was completed in phases with one of the earliest known section evident on maps from 1838 (Bradford, 1838). The next phase of AIWW construction, between the North and South Santee Rivers, was completed prior to 1909 (Carter, H.H., 1909). Today, this artificial canal is approximately 3 m deep and 120 m wide and connects the originally unconnected hydrological systems of Winyah Bay, North Santee Bay, North Santee River, South Santee River, and Cape Romain (Fig. 4.1). The AIWW influences salinity, currents, and material transport interactions between the North and South Santee where they intersect (Hockensmith, 2004). This artificial waterway connects the North Santee River, the South Santee River, Winyah Bay, and waterways to the south including Bulls Bay, creating a complex system influenced by tides and fluvial discharge.

A pair of jetties was completed at the entrance to Winyah Bay in 1902 (US War Dept., 1903). The North Jetty begins near the southern tip of North Island and extends 2.5 km offshore while the South Jetty begins along the coast of South Island and extends 3.4 km offshore (Fig. 4.1). Wright et al. (2017) described how the most recent of several phases of growth of the spit at the southern end of North Island as well as the accretion of sediment along the coast of South Island are results of changes in nearshore circulation caused by these jetties.

The majority of the land in the delta plain is publicly-owned and largely undeveloped. The Santee Coastal Reserve was established in 1974 on land donated to the state of South Carolina by The Nature Conservancy and occupies 97 km² along the South Santee, Murphy Island, and Cedar Island (Fig. 4.1). The Santee Delta Wildlife Management Area occupies part of the central island area near SC Route 17 and the Tom Yawkey Wildlife Preserve (established in 1976) is equivalent in size to the Santee Wildlife Management Area and occupies all of South and Cat Islands (Fig.

4.1). While historical infrastructure is maintained, new construction is limited, and no commercial development exists along this part of the South Carolina coast.

The main objectives of this research are to: 1) define and map the distribution of modern depositional facies of the Santee delta plain; 2) use these depositional facies to inform an interpretation of the Holocene stratigraphy; and 3) define the roles that anthropogenic modifications may have had on both the distribution of modern facies and the late Holocene stratigraphy.

MATERIALS AND METHODS

Bathymetric Data

Bathymetric data was incorporated into this study to define channel morphology including mapping of accretionary bedforms and bars, as well as erosional features such as large scours. These data come from two sources; a survey completed in 1935 by the Army Corps of Engineers prior to the completion of the dam system upstream, and newly-acquired high-resolution interferometric bathymetry data. The historical survey has a spatial resolution of approximately 5 m and a vertical resolution of approximately 15 cm and covers both the North and South Santee Rivers from 17 km inland to the coast including North Santee Bay and many of the larger creeks. These historical maps were georeferenced using Esri's ArcGIS and depth values were digitized and interpolated to create a 30 x 30 m bathymetric grid. Interferometric bathymetry profiles were acquired using a 3DSS-DX-450 compact dual transducer 3D sidescan sonar from Ping Digital Signal Processing Inc. This tool operates at a frequency of 450 kHz and has a beam width of 0.4°. Data were processed using Chesapeake Technology's SonarWiz7 and gridded using CUBE and Natural Neighbor algorithms at various spatial resolutions.

Geophysical Data

Between 2016 and 2017 we acquired approximately 800 km of high-resolution seismo-acoustic (Chirp) profiles from the channels and creeks within the Santee system from Jamestown to the mouths of the North and South Santee Rivers (Fig. 4.1). Subbottom data were acquired using the Edgetech 3200 sub-bottom profiling system with both the 0512i and 424 towfish providing for a total frequency range of 0.5 – 24 kHz. This instrumentation yielded a maximum subbottom vertical penetration of 10 m with a vertical resolution of 0.1 – 1 m. Chirp data sets were processed to correct for heave and to remove water column noise. Data were visualized using IHS Kingdom Suite™ and are the foundation for our interpretation of subsurface stratigraphic architecture

Sediment Data and Depositional Facies

To characterize both modern and subsurface depositional facies we utilize both surficial and subsurface sediment samples recovered from 136 grab samples, 10 shallow hand-dug trenches, 8 hand-auger cores (13 m), 11 push cores (14 m), and 25 vibracores (74 m). Of the 165 grab samples, 116 were recovered from within fluvial and estuarine channels with the remainder taken from onshore locations. Shallow trenches helped to constrain the architecture, depositional structures, and grain size distributions associated with surficial depositional features and settings including washover fan complexes, fluvial bars, estuarine shoals, and tidal flats. Sediment push and hand auger cores from 0.3 – 5.5 m in length were described at the cm-scale for sediment composition, grain size, color, physical and biogenic structures, and bed thickness and provided a comprehensive record of sedimentological and stratigraphic change.

Geochronologic Data

Twenty-five samples chosen from 11 sediment cores for AMS-¹⁴C analysis (Tab. 4.1) analysis to resolve the ages of lithofacies observed from sediment cores and Chirp data. Thirteen samples consisted of shell material while the remaining twelve were woody material. To minimize the potential of analyzing reworked or transported samples articulated bivalve specimens comprise the shelly samples while plant fragments and wood samples were taken from peat accumulations (Tab. 4.1). Analysis was completed at the Poznań Radiocarbon Laboratory in Poznań, Poland and yielded uncertainties of 30 - 45 yrs. Reported radiocarbon dates were calibrated using the CALIB Rev 5.0 by applying the IntCal13 calibration data set with ages reported here as the median calibrated age (cal yr BP) and uncertainty that corresponds to the full 2σ range. No reservoir effect was applied to the calibration of these samples as we interpret that all dated biological material had lived in the types of paleo-coastal environments with immediate atmospheric gas exchange.

Paleontological Data

Twenty samples were taken from two sediment Cores (SOU-01-V01 and CAN-01-V01) for micropaleontological analysis. The purpose of this analysis was to identify the assemblages of various microorganisms, primarily foraminifers, diatoms, and testate amoebae, whose distribution is strictly bound to specific environmental conditions. The species diversity as well as the ratio of agglutinated to calcareous microfossil tests is a function of salinity, alkalinity, carbonate saturation, and preservation potential (Leckie and Olson 2013). This information is then used to constrain environmental conditions at the time of deposition for discrete stratigraphic intervals.

RESULTS

Lithofacies and Depositional Environments

When appropriate, lithofacies from sediment cores are directly related to analogue examples in local modern depositional environments within the Santee delta plain primarily based on facies types. Despite the extensive anthropogenic modifications that are found throughout the delta plain, most subsurface lithofacies and successions of lithofacies have modern counterparts.

Lithofacies— We have defined 13 distinct lithofacies based on grain size and composition (Fig. 4.4). Five primary materials are found in all lithofacies; carbonate shell material, gravel, sand, mud (clay + silt), and organic (i.e. plant) material. Freshwater and salt marsh peat deposits (F1) are common within the study area and occur as both thin layers and thick accumulations (>1 m). Freshwater (swamp) peats consist of woody material while brackish (salt marsh) peats include significant amounts of grassy material. The preservation of organic material is an indication of oxygen-poor, geochemically reducing conditions (Reinick and Singh, 1980) which can commonly be found in poorly drained floodplain and backbarrier environments (Reinick and Singh 1980; Collinson 2006).

Mud-rich lithofacies (F2-F9) exhibit a wide range of textures and colors related to their composition and depositional conditions. Internally, these lithofacies can be massive or well laminated occurring as very thin laminae or thick beds. Color, typically imparted by iron-rich minerals, can be an indicator of how well-oxygenated an environment was at the time of deposition, with red and brown associated with oxidized iron and gray and green colors indicating reducing conditions (Reinick and Singh 1980). Black is commonly associated with the mineralization of ferrous sulfides as well as the presence of organic matter within mud-rich lithofacies (Blatt et al. 1972).

Sand-rich and gravelly lithofacies (F10-F13) range from thinly laminated very fine-grained sand to thickly-bedded gravelly sand and gravel. Sand composition varies as a function of sediment

source with fluvial sands and gravels typically being texturally and mineralogically less mature than aeolian and marine sands. Carbonate shell content is variable and may have originated in fluvial, estuarine, or marine settings, commonly increases with proximity to the coast.

Delta Plain Zones and Depositional Environments

Although the Holocene Santee delta is a recognizable geomorphic coastal feature, and its geological history records multiple phases of deltaic progradation (Long and Hanebuth, 2020), it is currently in a destructive phase due to backstepping during the Holocene transgression and generally lacks elements associated with classic deltaic deposition such as active prograding mouth bars and offshore clinothems (Mullin 1973; Eckard et al. 1986; Goodbred and Saito 2012). Rather, sediment distribution and salinity profiles found within the Santee delta plain more closely resemble those of an estuary (Payne 1970; Hockensmith 2004). The presence of deltaic distributary channels and associated freshwater discharge, results in a complex relationship between depositional facies, tidal and wave influence, and salinity within this system.

The modern distribution of lithofacies across the Santee delta plain exhibits a pronounced downstream trend. This trend is defined by three zones defined by gradational boundaries that vary both temporally and spatially in response to changes in fluvial discharge, tides, and wave energy. Upstream, a zone defined by coarse-grained sand (F12) and gravel (F13) deposits with structures indicating downstream transport. The next zone downstream channel and channel margin deposits are mud-rich and heterolithic sediments with sedimentary structures and bedforms that indicate both upstream and downstream transport reflecting the influence of both fluvial and marine processes on deposition. Farthest downstream, and most seaward, is a zone in which sand content significantly increases in response to increased wave influence. This tripartite segmentation in estuaries was first proposed by Dalrymple et al. (1992) in a generalized estuarine depositional

model using sedimentary facies as criteria for their delineation. Subsequently, these trends have been well documented from both modern and ancient estuarine and tidally-influenced deltaic systems and found to be related to variations in fluvial discharge, salinity gradients, tidal currents, and wave energy (Kapsimialis et al., 2004; Dalrymple and Choi, 2007; Goodbred and Saito, 2012; Johnson and Dashtgard, 2014; LaCroix and Dashtgard, 2014).

Fluvial-dominated zone — The most landward/upstream region of the delta plain, the fluvial-dominated zone (FDZ), begins where the Santee River bifurcates into its two main distributaries, the North and South Santee Rivers, 22 km from the coast (Fig. 4.3). The upstream limit of tidal forcing within the Santee River occurs between 16-19 km upstream from this point (Torres 2017). Therefore, tides influence deposition across the entire delta plain, but they exert a minimal influence within the FDZ making this zone analogous to upper delta plain regions of an active delta (Reading and Collison 2006). The shoreward limit of this fluvial environment is the maximum upstream limit of low-discharge, high-tide brackish water as reported by Hockensmith (2004). We subdivide the FDZ into two primary depositional environments, channels and floodplains.

Most FDZ channels exhibit low sinuosity and range in riverbed depth from a few decimeters in broad, shallow reaches to more than 10 m at tributary confluence meanders. Overall, the South Santee is considerably shallower than the North Santee, potentially a function of discharge and sediment availability. Channel deposits are typically coarse-grained (F12 and F13; Figs. 4.4 and 4.3), moderately well- to well-sorted, and are commonly texturally and compositionally immature (Fig. 4.5). Bedforms include large subaqueous dunes up to several meters in height with wavelengths that can exceed 200 m (Figs. 4.5 and 4.6). Chirp profiles through large dune bodies reveal a stratigraphy with several, truncated, low-angle bounding surfaces,

suggesting multiple phases of deposition and erosion (Fig. 4.5). Side, point, diagonal, and channel junction bars (Charleton, 2008) are common in the fluvial channels. Thin mud layers (F3) are deposited along dune foresets and within troughs between dunes and ripples during slackwater conditions (Fig. 4.5b) and can be preserved in the subsurface as mud draped cross-bedding (Fig. 4.5e). Thicker deposits, up to 1 m, of F3 accumulate on top of point bars where they are transitional into adjacent vegetated marshes.

Fluvial floodplain depositional environments comprise freshwater swamps, muddy overbanks, channel levees, and oxbow lakes. These environments are dominated by fine-grained and organic-rich lithofacies (F1, F2, F4, F5, and F12). Freshwater peat deposits (F1) are common in shallow sections of cores and trenches within the FDZ and in deeper sections of cores farther downstream. Modern fluvial floodplains in the upstream part of the FDR are heavily forested and poorly-drained, analogous to the environments in which freshwater peats were deposited. A series of sediment cores across the floodplain adjacent to the North Santee River indicate predominantly low-energy, poorly-drained conditions resulting in the deposition of muddy (F3 and F5) and organic-rich (F1) sediments (Fig. 4.7) with episodic, coarser-grained (F12) deposits likely associated with major flood events. The core closest to the main channel, SCI-01-V01, shown in Figure 4.7, penetrated a 1.5 m thick succession of interbedded sand (F12) and muddy sand (F7) that we interpret to be distal channel levee deposits. Although levee deposits are common in fluvial systems (Reinick and Singh, 1980; Charleton, 2008) in the modern Santee system they are limited to the unmodified margins of channels. A relatively thick (1.6 m) sandy interval (F12) near the middle of Core SCI-03-V01 is interpreted to be have been deposited as either a crevasse splay or minor floodplain channel (Fig. 4.7). At the inland extent of the floodplain cross-section (Fig. 4.3), Core SCI-02-V01 penetrated two freshwater peat beds. The youngest of these was deposited as

recently as 1.7 cal yr BP (\pm 127 yrs) and the oldest was deposited at 6.4 cal yr BP (\pm 86 yrs) on the basis of AMS- ^{14}C dating (Fig. 4.7; Tab. 4.1). Oxbow lakes in the modern Santee River within the study area are limited to the area near the distributary channel bifurcation point (Fig. 4.1) and are fringed by low-lying marsh grass and forested zones. Sediment cores from a partially connected oxbow lake recovered black to dark-gray organic-rich mud (F4) and abundant organic material. Modern morphological conditions in the downstream portions of the FDR have been heavily modified and are separated from the channels by artificial levees. These floodplains are covered by grass and aerially exposed for much of the year resulting in surficial sediments consisting of thoroughly oxidized, bioturbated, organic-rich mud (F2; Fig. 4.7).

Mixed-energy zone — The mixed-energy zone (MEZ) of the delta plain is the most complex and diversified of the three main regions in terms of influential processes and types of depositional facies (Fig. 4.3). Here the interaction of fluvial, tidal, and marine processes results in depositional patterns that are temporally and spatially variable (Fig. 4.8). The upstream extent of this region is defined by an increase in mud-rich and heterogeneous lithofacies (F3, F4, F6, F7, and F9), a common indicator of the fluvial-estuarine transition in modern systems and analogous to lower delta plains of a modern active delta (Dalrymple et al., 1992; Reading and Collinson, 2006; Kapsimalis et al, 2004; LaCroix and Dashtgard, 2014). Suspended sediment supplied by the river flocculates and settles upon entering brackish water, this zone of high-suspended sediment concentration is referred to as the estuarine turbidity maximum (ETM; Dalrymple et al., 2012; Jalon-Rojas et al., 2015). Clay and organic particles begin to flocculate at salinities less than 3 ppt (Reinick and Singh 1980). Therefore, we use the minimum downstream limit of freshwater defined by Hockensmith (2004) as a gradational boundary between the fluvial-dominated and mixed-energy regions (Fig. 4.3). Both the overall volume of mud and the thickness and frequency of mud

layers is greatest near the ETM and decreases in both upstream and downstream directions (Dashtgard and LaCroix 2015). The location of the ETM within an estuary varies as a function of river discharge and tides and over longer periods of time (Allen 1970; Kapsimialis et al. 2004). During high tide and low river discharge, brackish water extends upstream approximately 21 km (along-river distance) in both the North and South Santee Rivers (Hockensmith 2004). During low tides and high river discharge brackish water extends 1.6 km inshore in the North Santee Bay while the water in the South Santee is entirely fresh (Hockensmith, 2004). Density currents that develop from salinity stratification (i.e. estuarine circulation) also can influence the distribution of suspended sediment (Dalrymple et al. 2012; Flemming 2012).

The degree of stratification in estuaries is dependent upon the balance between tidal discharge and fluvial discharge, a ratio that is often controlled by the tidal range (Flemming, 2012). Microtidal estuaries tend to more stratified than meso- or macrotidal estuaries (Flemming, 2012). Salinity profiles taken along the North and South Santee Rivers presented by Payne (1970) taken during high and low fluvial discharge periods indicate that both systems are generally well-mixed with minor salinity stratification developing coincident with higher fluvial discharges; a relationship also demonstrated for the Santee by Hockensmith (2004). Kapsimalis et al. (2004) found that stratification within the Gironde Estuary of France developed under similar conditions, with high fluvial discharge leading to increased density circulation and ultimately to a higher degree of stratification.

Similar to the sub-division of the FDZ, the MEZ can most easily be divided into channel and floodplain environments. However, because of the increasing influence of tides, transitional and intertidal environments become important. Sediments within MEZ channels vary widely in terms of composition and grain size (Fig. 4.3). Channel sands within the South Santee are similar

in grain size and composition (F12 and F13) to those of the FDZ, a trend that continues nearly to the mouth of the river (Fig. 4.3). Channel sands within the North Santee River become finer and enriched in quartz between the AIWW and the mouth of North Santee Bay (Fig. 4.3). Here, channel deposits of the North Santee River consist of ebb-oriented dunes composed of moderately- to moderately-well-sorted, fine- to medium-grained sand (Fig. 4.3).

Channel deposits of the North Santee Bay are significantly different than those of the other two distributary channels. The North Santee Bay is relatively wide (1.25 km) and shallow (< 3 m). Most of the sediment samples taken from the bay are poorly- to very poorly-sorted, fine- to medium-grained muddy sand (F9), sandy mud (F7), and mud (F3 and F4; Fig. 4.8). Channel floor morphology is variable with small (< 1m), ebb-oriented dunes, but there are areas with no obvious bedform development (Fig. 4.8). Chirp profiles also show weakly reflective fluid mud layers that occur within bathymetric lows on the bay floor (Fig. 4.9a).

Diagonal, side-attached bars are common along the margins of the North and South Santee Rivers upstream of the AIWW (Fig. 4.5a). Several key features of both FDZ and MEZ channel environments are found within the Santee River including a deep (11 m) meander scour, sinuous-crested channel-floor dunes, and associated point bar bedforms (Fig. 4.6). Facies analysis and AMS-¹⁴C dating indicate that tidally-influenced channel deposition began within the North Santee Bay area by at least 1.8 cal ka BP (Figs. 4.8 and 4.9) including a period marked by a significant shift in depositional patterns within the bay after approximately 530 cal yr BP (1485 – 1587 CE) (Figs. 4.8 and 4.9). This shift is marked by an abrupt change from coarser F9 and F7 deposits to finer F6 and F4 deposits along the SW margin of the bay along Crow and Cane Islands, out to the inlet and a change from poorly-oxygenated F4 deposits to oxidized F2 and F3 deposits along the NE margin of the bay along Cat Island near the AIWW (Figs. 4.8 and 4.9).

A large, internally complex diagonal bar occupies the northwestern portion of North Santee Bay. This feature has a maximum width of 500 m, is 2-km long and has a vertical relief of approximately 2.5 m (Fig. 4.9). Chirp data shows that the formation history of this bar, referred to NSB-10, consists of three distinct depositional intervals, each separated by sharp erosional surfaces, and overlies a freshwater peat deposit (Fig. 4.9a). The deepest interval, and depositional core of the bar, consists of muddy sand (F9) and sandy mud (F7) with numerous irregularly-spaced thin, medium- to coarse-grained sand beds and shell lags that were deposited ca. 1.3 cal ka BP (\pm 60 yr) (Fig. 4.9). In the Cores NSB-10-V01 and NSB-10-V02, 1 – 1.5 m thick fining-upward packages containing thin basal gravelly-sand layers were deposited ca. 550 cal yr BP (\pm 60 yr) (Fig. 4.9). In Chirp profiles, these basal sandy layers display faint crossbedding and represent the earliest phases of bar growth. The vertical fining-upward profile is similar to those seen in modern fluvial and estuarine point bar deposits (Collinson, 2006; La Croix and Dashtgard, 2014; Ghinassi et al., 2018) and may represent a period of lateral migration of the bay as a whole prior to anthropogenic stabilization. The middle interval consists of clay- and organic-rich, strongly-laminated, dark-gray mud (F4) containing numerous, thin, medium- to coarse-grained, well-sorted sand beds with sharp upper and lower contacts (Figs. 4.8 and 4.9). The grain-size distribution, color, preservation of laminae, and lack of bioturbation suggests sedimentation from suspension in a low-energy, oxygen-poor environment subject to episodic deposition of high-energy event beds. This observation is consistent with conditions in sheltered backbarrier lagoons or estuarine channels with storm-related washover deposition. The surface of the NSB-10 bar is covered by a 1-m thick blanket of cross-bedded, slightly muddy, medium-grained sand (F12; Fig. 4.9). Seismic reflection indicates that this sand cover accretes in all directions, i.e. upstream, downstream, and laterally, likely in response to tidal currents. Detailed maps made by the Army Corps of Engineers

prior to the construction of the Wilson and Pinopolis Dams, indicate that the NSB-10 bar has maintained its current location and approximate size for at least the past 85 years.

Intertidal and upper subtidal transitional areas in the Santee delta plain MEZ consist of intertidal marshes, muddy tidal flats, and subtidal platforms. The subtidal platforms occur in low-energy regions of channel confluences and sheltered portions of channels within the study area. Along the channel margin of the North Santee River immediately downstream of the AIWW, a well-developed subtidal platform is approximately 500-m long and 150-m wide. A sediment core recovered from this feature consists of a basal well-sorted, fine- to medium-grained, quartz-rich sand layer (F12) separated from an overlying, 80-cm thick mud interval (F3 and F4) by a thin layer of coarse, woody detritus. The mud-rich section has two distinctly different compositions. The lower half is massive, brown, organic-rich mud (F3) while the upper half has well-developed, unevenly spaced dark-gray and black mud layers (F4). The contact between the two sub-facies is sharp, and the contact is likely the result of a change in local circulation from more restricted, oxygen-poor conditions to more open, well-oxygenated conditions. A sediment core through a similar feature in North Santee Bay contains a comparable upper succession (Fig. 4.8h). During spring low tide, the surface of this subtidal platform lies at approximately 10 cm water depth. Based on the fine-grained composition and location of these platforms within zones of channel flow separation, they may be analogous to counterpoint bars (Smith et al., 2009).

In several locations, both in the modern system and in the sedimentary record, the crude interlayering of dark-gray and black mud with organic detritus becomes more pronounced and regularly-spaced with layers that become thinner (< 1 cm). This specific type of mud-rich deposit consists of thinly laminated dark-gray mud and black, fine-grained (< 1 mm) organic detritus (Fig. 4.8b). This mud facies (F6) was deposited from suspension in low-energy, oxygen-poor, tidally-

influenced settings such as sheltered regions along estuarine channels. Decimeter-thick, well-sorted, medium- to coarse-grained sand beds (F12) are common within F6 found in the subsurface of the North Santee Bay (Fig. 4.8). The irregular spacing and dramatic increase in grain size relative to the fine-grained background sedimentation associated with the F6 beds, suggests that they represent event beds. Microfossil assemblages from a similar succession in Core CAN-01-V01 from Cane Island at the mouth of the North Santee Bay indicate that marine, brackish, and freshwater input into the bay fluctuated throughout deposition (Fig. 4.9). Testate amoeba including *Diffugia oblongata* indicate freshwater or brackish environments while the presence of calcareous benthic foraminifera such as *Ammonia tepida* indicate episodic marine influence.

Intertidal zones within the MEZ consist of both vegetated marshes as well as unvegetated, muddy flats with the former being by far the most common (Fig. 4.8). Muddy tidal flats are rare and extend from the intertidal marshes towards approximately the low-tide level (Fig. 4.8e). They are composed of dark-gray to black mud (F4) and fine-grained organic detritus. Intertidal vegetated marshes extend from the base of artificial embankments down to the low-tide line (Fig. 4.8f) and are found along all channel margins within the MER of the Santee delta plain. Vegetation is almost exclusively salt-tolerant grass, specifically *Spartina alterniflora* and *Juncas roemerianus* (Nixon, 2004). The substrate of these areas consists of intensely bioturbated, heavily rooted, organic-rich brown (F3) and black (F4) mud. Core SOU-01-V01 near the southeast margin of South Island, recovered approximately 4 m of continuous organic-rich F4 lithofacies with intercalated shelly sand beds (F11) near the base. The distribution of benthic foraminifera in this core indicates a marine influence associated in the basal sands. Micropaleontological data indicate that the upper mud-rich interval was, in contrast, deposited entirely in a brackish environment, much like the marshes of the modern system. Traditional mixed-energy tidal flat deposits that are rhythmically-

interlayered, unvegetated sand and mud couplet successions (Allen, 1970; Reinick and Singh, 1980), are absent within the modern MEZ but have been recovered from sediment cores (Fig. 4.8a).

Oyster reefs are common in the more shoreward areas of the MEZ delta plain (Fig. 4.3). Although the modern distribution of these features is not well-constrained, these bioherms occur along the margins of vegetated tidal flats and within the shallow channels of the North and South Santee Rivers from the downstream margin of Cane Island to approximately 1 km upstream of the AIWW (Fig. 4.3). Oyster reefs consist of live oysters that are anchored to the substrate and mounds of disarticulated oyster shells and shell fragments with a matrix of very poorly sorted sandy mud (F7), shelly sandy mud (F8), and muddy fine- to coarse-grained sand (F9). Core CAN-02-V01 penetrated an ancient oyster reef that was active $600 (\pm 65)$ cal yr BP (1414-1417 CE) (Fig. 4.9).

Because of extensive anthropogenic modifications, MEZ floodplains largely consist of low-lying regions covered by grass and separated from channels by artificial embankments (Fig. 4.3). As previously mentioned, the cypress forests that had covered the delta plain were cleared for rice cultivation in the late 18th century, replaced by numerous fields, isolated from each other and the river system by a dense network of rectilinear canals sided by 1 – 2-m high elevated, narrow embankments (Fig. 4.3). Using an average width of 4 m and an average depth of 1 m for canals, and a dry bulk density of $0.823 - 0.920$ g/cm³ measured from samples of organic-rich mud in CAN-01-V01 we estimate that the approximately 7,700 km of canals within the Santee system potentially mobilized 28 -31 Mt of predominantly fine-grained, floodplain sediment. This disturbed sediment was primarily used for the construction of embankments.

Marine-dominated zone — The upstream limit of the marine-dominated zone (MDZ) in the Santee delta coincides with the inshore reach of ocean-derived sand along the margins of

Murphy and Cedar Island and the shoals associated with flood-tide deltas of the North and South Santee inlets (Fig. 4.3). These inner environments (i.e. distal to the shore) of the MDZ contain depositional facies influenced by fluvial, tidal, and marine processes and transition seaward to those entirely controlled by marine processes (Fig. 4.3; Collinson and Reading, 2006). Subtidal environments in this region include the two main inlets of the North and South Santee Rivers as well as natural channels distributed amongst the shoal complexes of flood-tidal deltas (Fig. 4.3). The outer (i.e. most seaward) environments comprise the delta front of the Santee and ebb-tidal deltas, and include subaerial beach ridges, and smaller barrier systems (Fig. 4.3).

While tidal flats in the MEZ are almost exclusively muddy, tidal flats and intertidal regions within the MDZ tend to be heterolithic to sand-rich, reflecting an overall increase in depositional energy associated with proximity to the coast and increased wave activity. Wave-influenced tidal flats consist of interlayered fine-grained sand (F12), mud (F3 and F4) and organic material (Fig. 4.10f). The organic-rich layers consist of discrete cm-scale peat beds (F1) and laminae as well as fine (<1mm) to coarse (> 1cm) organic fragments of grass or wood. Modern wave-influenced, mixed-energy tidal flat deposits are limited to the northeastern margins of Murphy and Cedar Islands (Fig. 4.3).

The seaward margins of islands near the inlets of both rivers are covered in relatively thick (40 – 50 cm) accumulations of well-sorted, fine- to medium-grained, quartz-rich sand; the Cane Island cores (CAN-01-V01 and CAN-02-V02) are good examples of these deposits (Fig. 4.9b). These well-sorted sands within the intertidal zone of the North Santee overlie heterolithic, mixed-energy deposits suggesting that this location has experienced a general increase in depositional energy over time. This finding supports Stephens et al.'s (1976) conclusion that there has been significant incursion of marine-derived sand into the main downstream channels of the North

Santee system commensurate with the reduction in fluvial discharge resulting from the construction of upstream dams. In addition to the sandy island margins mentioned above, subtidal and intertidal shoals are found in the flood-tidal delta systems of the North and South Santee Rivers (Fig. 4.3). These flood-tidal deltas consist of submerged and emergent sandy shoals that extend up to two km upstream in both systems (Fig. 4.3). Sediment cores and Chirp profiles indicate that these shoals are up to 4 m thick and consist of well-sorted, fine- to medium-grained, horizontally- and planar-bedded, quartz-rich (F12) and shelly sand (F11; Fig. 4.10g). Seaward of the coast, ebb-tidal deltas of the Santee are well-developed (Fig. 4.3). Regionally, ebb-tidal deltas contain up to 77 % of Holocene sand found along the coasts of South Carolina and Georgia (Sexton and Hayes, 1996).

The tidal inlet of the North Santee River is approximately 10-m deep, 500-m wide and contains coarse-grained sand and large shell fragments. The inlet of the South Santee River is several meters shallower, likely a function of both lower fluvial discharge and the smaller tidal prism of the shallower and narrower South Santee River. A comparison of the modern spits at the southern ends of both South Cedar and South Islands with historical bathymetric data (Durica et al., 2019) indicates that these features have accreted approximately 300 – 500 m to the south since 1934.

Beach ridge systems are common along the modern coast of the Santee delta. Beach ridges, as defined by Otvos (2000), are relict strandplain ridges containing wave-built, swash-built and aeolian lithosomes that form in response to overall long-term coastal progradation (Taylor and Stone, 1996). Aeolian deposits are very well-sorted, fine-grained, quartz-rich sands (F12) while shoreface deposits exhibit a wider range in sorting, grain size, and composition in the study area (F11, F12, and F13). Holocene beach ridge systems record periods of shoreline progradation and

are preserved on South Island, Cedar Island, and Murphy Island. Recent beach ridge accretion is limited to the southeastern margin of South Island and the spits associated with the inlets of both rivers as well as the North Island spit of Winyah Bay (Wright et al. 2017).

In contrast to these accretionary shorelines, the seaward-facing coasts of Cedar and Murphy Islands exhibit evidence of erosion and backstepping (Fig. 4.3). These transgressive shoreline sections (Hayes and Fitzgerald, 2013) contain abundant storm-washover deposits and outcrops of late Holocene marsh ledges. (Fig. 4.10b). AMS-¹⁴C dating of woody material from the marsh terrace that crops out along the shoreface of Murphy Island indicates that it was deposited approximately within the last 170 years.

The southeastern coast of the United States is subject to seasonal hurricanes and large storms and has experienced 41 tropical cyclones making landfall in South Carolina since 1851 (National Weather Service, <https://www.weather.gov/chs/TChistory>). Several well-developed washover-fan complexes along the eastern margins of Murphy and Cedar Islands record deposition by storm surge associated with these events (Figs. 4.3 and 4.10). Lithofacies (F12) and physical structures within washover deposits are consistent with the model proposed by Schwartz (1982) and made up of proximal (i.e. seaward) areas that are dominated by horizontal stratification and distal (i.e. landward) areas that are dominated by delta foreset stratification (i.e. prograding planar tabular cross-stratification). The internal architecture of a 32-m long by 0.8-m deep trench through a washover fan complex emplaced by Hurricane Matthew in 2016 suggests early deposition of dune-derived sand occurred as laterally-offset, landward-building lobes (Fig. 4.10d) that were dissected by a 7.5 m wide runoff channel containing ebb-oriented sedimentary structures.

Geochronology

Twenty-five AMS-¹⁴C dates obtained during this study yield ages ranging from modern to 6,702 cal yr BP (Tab. 4.1). Two distinct age populations exist within our data set; 17 of the 25 ages fall between 0 and 1,846 cal yr BP, while 7 ages fall between 5.1 and 6.7 cal ka BP. A single sample with an age outside of these ranges of 3.6 cal ka BP (\pm 125 yr) was recovered from a thin peat layer within Core CDR-01-V01 taken from the margin of the North Santee River along Cedar Island (Tab. 4.1). The older of the two populations contain samples exclusively derived from freshwater peats, while the younger population contains samples measured from freshwater peats as well as articulated bivalves. This apparent 3.3 kyr gap in time separates the older freshwater floodplain deposits from younger estuarine deposits.

DISCUSSION

Pre- and Mid-Holocene Stratigraphy

The base of the incised valley of the Santee River onshore was eroded as deep as 20 meters below modern sea level (mbsl) into the underlying Eocene Santee Limestone (Payne, 1970; Eckard et al. 1986; Weems and Lewis 1997) (Figs. 4.3 and 4.12). Descriptions from boreholes drilled along the southern margin of the South Santee River indicate that the base of the incised valley rises to the south from 17 to 7 mbsl (Fig. 4.3; Weems and Lewis, 1997) over a distance of less than 2 km (Fig. 4.3). In the deeper parts of the incised valley, fill consists largely of coarse-grained fluvial sediment deposited during the falling and lowstand phases of a late Pleistocene glacioeustatic sea level (Eckard et al. 1986). At several locations along the North Santee River, Eocene basement rises to approximately 10 mbsl and defines the thalwegs of the modern fluvial channels (Fig. 4.6 and 4.12), suggesting that basement morphology may influence depth and course orientation of the modern riverine system. Upstream, above the delta plain, coarse-grained,

fossiliferous carbonates of the Santee Limestone crop out in the form of ledges 3 to 4-m high along the southern banks of the Santee River.

Peat deposits recovered from five sediment cores in both the FDZ and MEZ indicate freshwater floodplain environments were common across the present-day Santee delta plain during the mid-Holocene (Figs. 4.7, 4.9, and 4.12). It is unclear how laterally continuous these peat layers are, however, Chirp data calibrated to sediment cores indicate, that they underlie estuarine channel deposits beneath most of North Santee Bay and extend beneath the modern marsh of South Island (Figs. 4.9 and 4.12). Sexton et al. (1992) penetrated a freshwater peat deposit in a sediment core taken 2 km offshore of the North Santee inlet. This peat lies at approximately the same elevation (5 - 7 mbsl) as those recovered onshore and therefore may be time-correlative, indicating that fluvial floodplain deposition at this time extended seaward of the modern shoreline. Assuming an original depositional elevation close to sea level, the depths and ages of peat deposits sampled are in good agreement with reconstructions of sea level in the western Atlantic Ocean during this period (Toscano and MacIntyre, 2003); however, this does not account for any post-depositional elevation changes that are common in this region (Muhs et al. 2003; Englehart et al. 2011; Doar and Kendall 2014; Van DePlassche et al. 2014; Kopp et al 2015).

The vertical succession of freshwater peats beneath estuarine and marsh deposits suggests a rise in RSL sometime after 6 cal ka BP. But it is difficult to attribute the Holocene stratigraphic succession beneath the Santee delta plain to changes in RSL alone. Based on the distribution of interpreted transgressive lag deposits from Cape Romain, 15 km south of the study area, Ruby (1981) and Hayes (1994) have proposed that over the last 5,000 there have been several transgressive-regressive sea-level cycles. The most significant event flooded the Cape Romain area up to 3 km inland approximately 4,000 years ago. Gayes et al. (1992) proposed a similar sea-

level highstand for Murrells Inlet, SC, 50 km to the north of the Santee, but found no evidence of this event in the Santee Delta. Colquhoun and Brooks (1986) also proposed numerous, low-magnitude (± 1 m) sea level fluctuations over the past 6,000 years. More recent studies from North Carolina, South Carolina, and Florida have concluded that the rate of sea-level rise during the late Holocene has decreased relative to the early Holocene and that evidence is lacking for the proposed late Holocene highstands discussed above (Van De Plassche et al., 2014; Hawkes et al., 2016). This study has demonstrated the dynamic nature of fluvial and estuarine systems, and it is likely that autogenic processes, including channel avulsion and migration, have had a significant influence on the preservation of Holocene stratigraphy within the study area.

Late-Holocene Stratigraphy and Human Influence

There is a significant time gap between the youngest age of freshwater peats (5.9 cal ka BP \pm 54) and the oldest age of overlying estuarine deposits (3.6 cal ka BP \pm 125; Tab. 4.1). In Core NSB-10-V01, estuarine channel sediments deposited around 1.3 cal ka BP lie on freshwater peat deposited 5.9 cal ka BP defining a stratigraphic gap of more than 4,000 years (Fig. 4.9). Most of the cores collected in this study are from channelized environments within the delta plain (Fig. 4.1); therefore, erosion related to channel migration and incision may be the source of the time gap observed within the data set.

Sediment cores taken from the FDZ floodplain reveal late Holocene depositional environments that are significantly different from those found in the modern floodplain. Core SCI-02-V01 from the interior of the floodplain, shows evidence of minor exposure in several stratigraphic intervals below a thick peat layer that was deposited in a poorly-drained, wooded floodplain environment 1.8 cal ka BP, which is an environment quite different from the modern floodplain, which was almost completely deforested. Both the thick overbank sand in Core SCI-

03-V01 and the levee deposits in Core SCI-01-V01 provide evidence of sediment and water flux from the adjacent fluvial channel into the floodplain environment (Fig. 4.7). The artificial embankments that separate the modern floodplains from the channels significantly reduce, if not eliminate, this exchange today (Fig. 4.3). Interconnectivity of channels and floodplains in a natural system establishes a dynamic equilibrium where net subsidence and erosion is balanced by net sedimentation and maintains floodplain habitat, biodiversity, and nutrient cycling (Hupp et al., 2009). The uppermost sections of all three floodplain cores consist of brown to orange mud (F2 and F3), indicating oxidation down to a depth of 40 cm that has developed in response to man-made draining of the floodplain associated with prolonged, widespread periods of subaerial land surface exposure and, thus, soil ventilation (Fig. 4.7).

The most impactful of the anthropogenic modifications made to the lower Santee delta plain were the construction of embankments and canals associated with the development of rice plantations. These changes have influenced both the modern system and the stratigraphic record of the last few centuries. Artificial embankments stabilize channels and their banks, reduce the area of tidal flats, isolate channel environments from floodplain environments, increase the relative depth of channels, support sediment bypassing, and alter the tidal prism of the backbarrier system (Auerbach et al. 2015; Wilson et al. 2017; Bain et al. 2019; Hoitink et al. 2020). The dense, highly connected network of artificial canals can have two seemingly contrasting effects on floodplains. First, when canals are open to circulation from the surrounding channels, they can serve to increase sediment flux to the floodplain. The density of canals is higher than that of natural tidal creeks on the floodplain and their courses are straighter. Canals, therefore, have the capacity to deliver more sediment relative to a more natural configuration (Giosan et al. 2013). However, if floodplain canals are isolated from the main channels, or only connected intermittently, sediment flux to the

embanked floodplain is limited. Along the outer parts of Cedar and Cane Island in the Santee delta plain, embankments, canals, and irrigation gates are no longer maintained. Here canals drain and flood with the tides resulting in the canals acquiring a more natural morphology and show evidence of both lateral and headward erosion, processes that actively shape natural tidal creeks (Fig. 4.3; Hughes 2012). The result is a network of moderately sinuous, rectilinear channels with dendritic channel heads. These processes can potentially lead to increased erosion of the marsh platform and ultimately to an interconnected network that can alter the circulation of the delta plain system (Zeff 1988; Bain et al. 2019). Alternatively, studies from the Ghanges-Brahmaputra delta plain show that the impoundment of natural channels has led to increased sedimentation within these channels effectively reducing the regional tidal prism and focusing sedimentation into channels rather than on embanked floodplains (Wilson et al. 2017). With continued Holocene RSL rise, the frequency with which channelized marshes become flooded will likely increase which may increase both channel erosion and degree of connectivity of delta plain marshes. While the evidence of erosion and lateral migration is apparent from aerial photographs, the balance between enhanced sediment accretion and progressive headward erosion is entirely unknown but presents an interesting avenue for future research.

In addition to these long-lived changes, stratigraphic and historic records provide evidence that short-term changes also have influenced the local deltaic depositional environments. Sediment core and Chirp data from North Santee Bay indicate that the bay has been an active distributary for at least the past 1.4 cal kyr BP, depositing a range of heterolithic deposits that are comparable to these from the modern environment (Figs. 4.8 and 4.9). Sandy muds and muddy sands intercalated with discrete sand layers, oyster reefs, and organic-rich mud layers record deposition by mixed-energy, tidally-influenced bottom currents under brackish water conditions until

approximately 555 cal yr BP (1470 cal yr CE) (± 60 yr) (Fig. 4.9). In sediment cores taken along the southwestern margin of the bay, near Crow and Cane Islands (Fig. 4.3), these channel deposits are overlain by thinly-laminated, low-energy, laminated mud deposits (F6), and provide evidence of a significant shift in depositional energy (Figs. 4.9 and 4.12). Along the northeastern margin of the bay, adjacent to Cat Island, Core CAT-01-V01 shows a change from low-energy, poorly-oxygenated black, organic-rich muds to muds deposited under more oxygenated conditions (F2 and F3) (Figs. 4.8 and 4.12) at approximately the same time as the changes along the western margin of the bay occurred, after 551 cal yr BP (± 71). In the North Santee River within the MEZ, adjacent to Cedar Island (Fig. 4.3), sediment cores record a similar shift in facies. Mixed-energy estuarine channel and tidal flat deposits abruptly shift to homogeneous, low-energy suspension deposits at some point after 648 cal yr BP (1377 cal yr CE) (± 71 yr). Although the timing of this shift is poorly-constrained, it is feasible to propose that these changes mark a shift in circulation within the North Santee Bay that coincided with rice field clearing that occurred during the latter half of the 18th century. The clearing of lowland forests and construction of canals and embankments undoubtedly mobilized large volumes of fine-grained floodplain sediment. In this situation the rapid influx of sediment into the estuary would have lastingly increased its turbidity, probably developing hyperturbid conditions (Hoitink et al. 2020) resulting in increased sedimentation rates within the bay. Alternatively, changes in coastal morphology, particularly in the coastal sand spits and submarine tidal deltas at the mouths of the North and South Santee Rivers, could have potentially altered circulation within backbarrier channels and embayments, a process-response relationship that has been observed in modern wave-built estuaries (Cooper, 1993).

The most significant anthropogenic modification to the Santee MDZ is a pair of jetties at the mouth of Winyah Bay. Completed between 1890 and 1905, the jetties led to dramatic changes in sedimentation patterns and coastal geomorphology along the coast of South and North Island (Wright et al. 2017). A review of historical maps by the United States Coastal and Geodetic Survey indicates that the waters offshore of South Island remained shallow but open until about 1929, when a long, narrow barrier developed (Fig. 4.11c). Between 1929 and 1967 the area behind this barrier filled, leading to the development of estimated 8 km² of new salt marsh over the past 100 years. Prior to the construction of the Winyah Bay jetties, a small lagoon existed just to north of the future site of the Southern Jetty (Fig. 4.11a). After construction, the jetties altered local circulation leading to the deposition of ~2.5 m of mud-rich sediment within the newly established marsh and tidal flats. This succession is preserved within the SOU-05-V01 core that was recovered from the location of this paleo-lagoon. Additionally, the area adjacent to a beach ridge system that existed as the active shoreline south of the jetty filled in with intertidal marsh sediment in an incremental fashion as seen in core SOU-04-V01 (Fig. 4.11).

CONCLUSIONS

1. The modern distribution of depositional facies within the Santee delta plain display a spatial trend defined by the transition from fluvially-dominated to mixed-energy to marine-dominated facies from the upper delta plain to the coast. Though this trend is pronounced, it is spatially-variable with gradational boundaries between zones that shift in response to fluvial discharge, tidal influence, and wave action.
2. Late Holocene deposition within the Santee delta plain is marked by tidally-influenced, estuarine deposits beginning around 3.6 cal ka BP following the flooding of a freshwater-dominated floodplain and continues to modern times.

3. Anthropogenic changes to the delta plain have strongly influenced the distribution of modern depositional facies by: 1) restricting the lateral distribution of tidal flat systems and associated environments; 2) saturated, low-energy fluvial floodplains have become well-drained and are subject to widespread subaerial exposure; 3) the dense network of artificial canals that are no longer being maintained, are evolving into a more natural channel morphology and eroding upstream (headward) increasing the overall erosion of the marshes and influencing the connectivity of marsh channels; and 4) jetty construction at the beginning of the 20th century has altered coastal hydrodynamics and resulted in significant changes to the coastal system.

Localized anthropogenic changes, particularly the construction of rice field systems, have influenced the stratigraphic record. The construction of artificial levees and canals have: 1) “deepened” the river which has the potential to increase bed shear stress, and consequently erosion, during floods; 2) reduced floodplain sedimentation thus limiting the ability of the system to aggrade and keep up with modern RSL rise; 3) prevented the natural lateral migration of channels; and 4) introduced large volumes of fine-grained material during construction potentially developing hyperturbid conditions resulting in the deposition of thick, muddy subtidal platforms around the North Santee Bay.

FIGURES

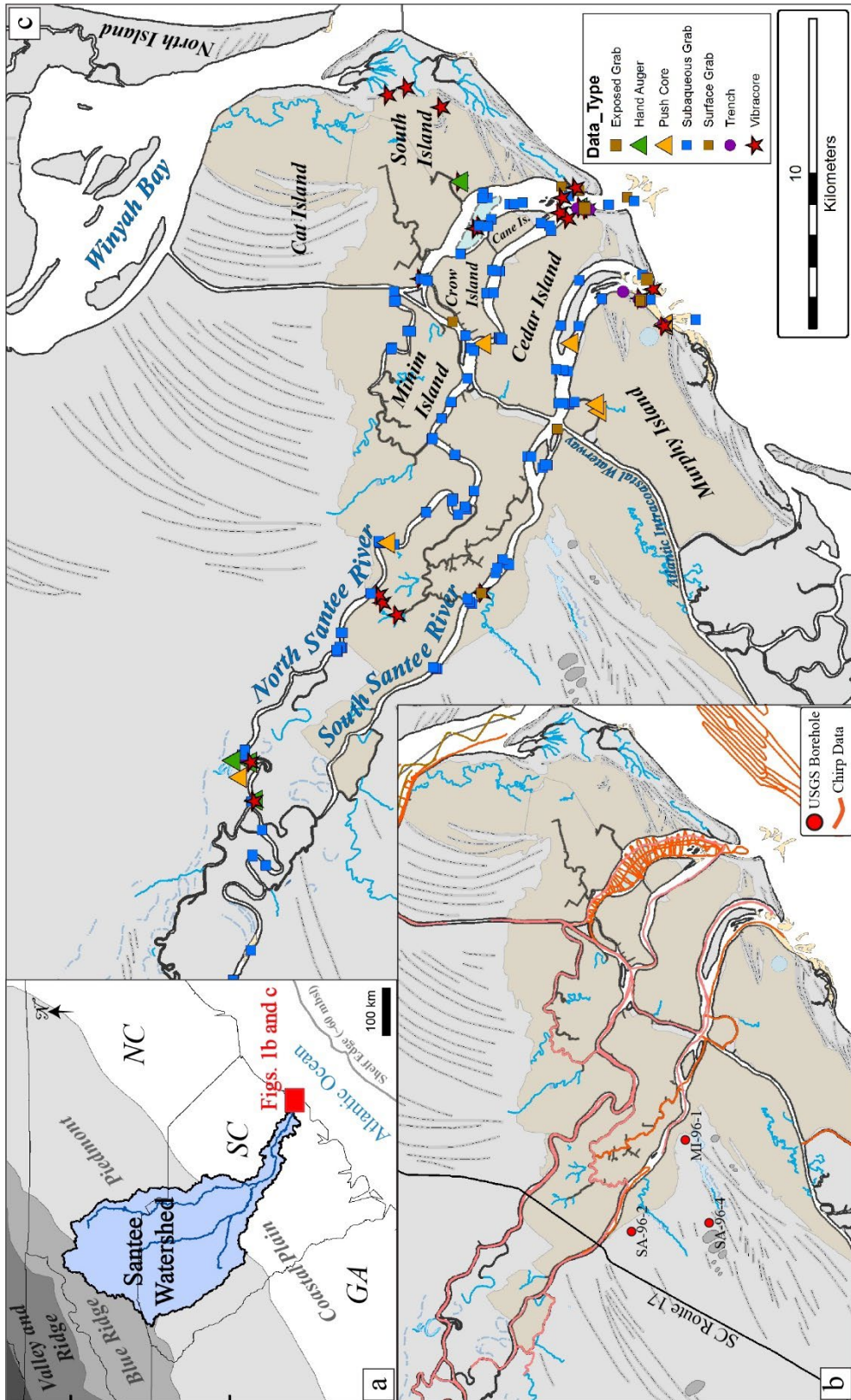


Figure 4.1. Study area. **a)** Location of study area and watershed of the Santee River relative to major geologic provinces of the United States east coast. **b)** Distribution of Chirp seismo-acoustic data acquired during this study. Red circle mark the location of key USGS boreholes. **c)** General morphology and sediment samples of the study area. Light brown areas have been modified for rice cultivation.



Figure 4.2. Bradford map entered into the Library of Congress in 1838 clearly shows the original Santee Canal as well as the Minim Canal along the SW shore of Winyah Bay. The North and South Santee rivers as well as the more seaward distributaries show nearly identical locations relative the modern setting, a configuration that is also observed on a detailed map from 1773 (Cook).

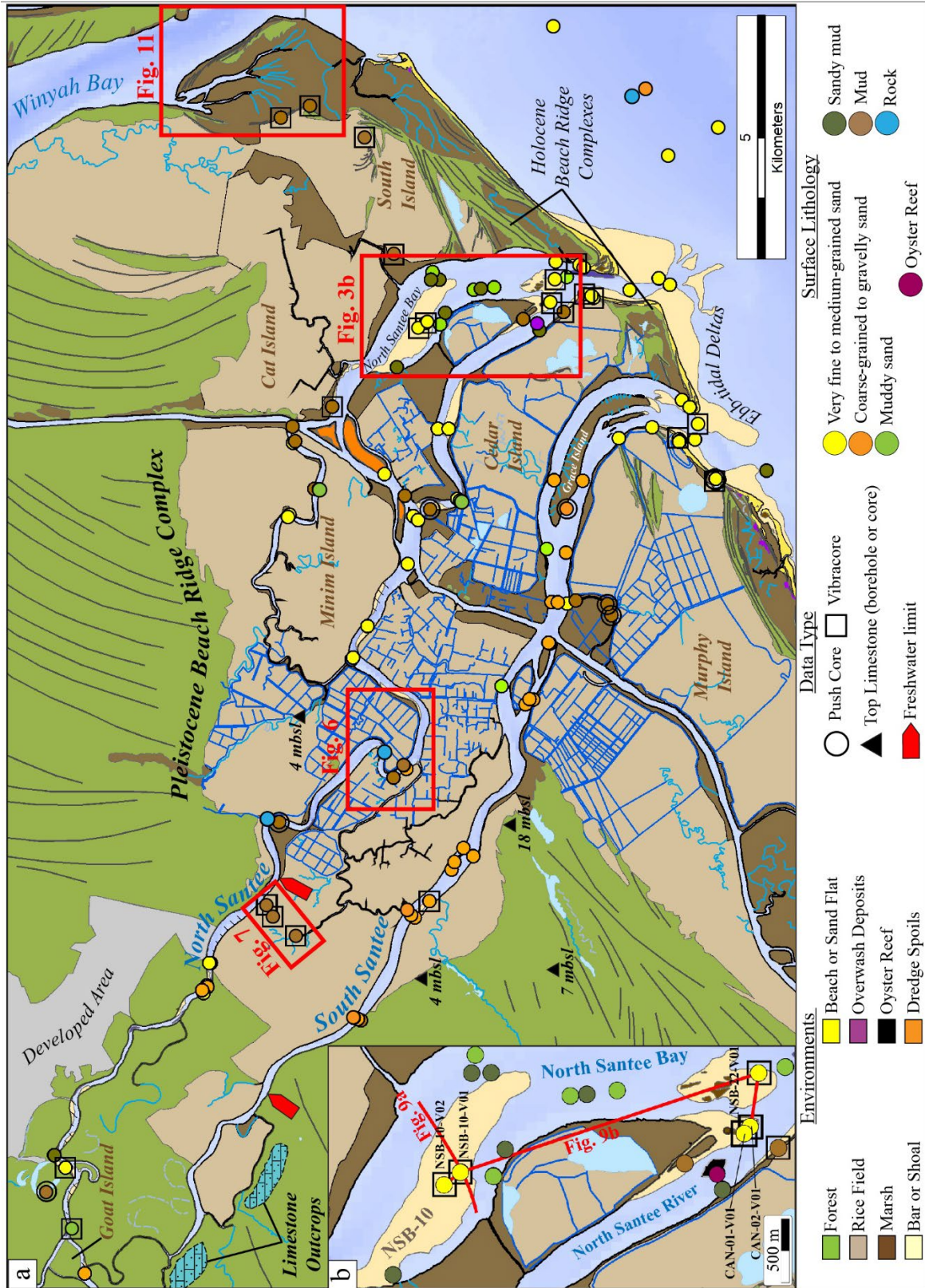


Figure 4.3. a) Morphosedimentary map of the Santee delta plain and surrounding areas showing geomorphology, generalized surficial sediment composition, and location of sediment samples recovered during the course of this study. **b)** Detail of North Santee Bay.

Lithofacies	Code	Distribution and Appearance	Symbol
Peat	F1	Freshwater swamps (woody), marshes (grassy), and commonly as detrital layers in fluvial and estuarine environments. Massive with minor amounts of sand or mud.	
Orange Mud	F2	Exposed fluvial floodplains and marshes. Massive. Commonly organic-rich.	
Brown Mud	F3	Marshes, subtidal platforms, and tidal flats. Massive. Commonly organic-rich.	
Dark Gray or Black Mud	F4	Estuarine channels, subtidal platforms, marshes, and tidal flats. Massive to thinly laminated. Organic-rich.	
Blue-Gray Mud	F5	Fluvial floodplains. Massive. Organic-rich.	
Clay-organic Laminated Mud	F6	Specific to subtidal platforms. Strongly laminated. Organic-rich. Fresh surfaces are very dark gray and quickly oxidize to bright orange.	
Sandy Mud	F7	Estuarine channels and marshes. Massive and poorly-sorted	
Shelly, Sandy Mud	F8	Estuarine channels and oyster reefs. Massive and poorly-sorted	
Muddy Sand	F9	Estuarine channels. Massive and poorly-sorted	
Muddy, Shelly Sand	F10	Estuarine channels. Massive and poorly-sorted	
Shelly Sand	F11	Shoreface, inlets, and tidal deltas within paralic environments. Massive to thinly-bedded.	
Sand	F12	Common in most environments. Massive to laminated.	
Gravel	F13	Common in fluvial channel environments, less common in estuarine channel and paralic shoreface environments. Massive to thinly-bedded	

Core Log Structures			
	Crossbedding		Gradational Contact
	Horizontal Lamination		Sharp Contact
	Faint Laminae or Banding		Soil Formation/Mottling
	Shell or shell fragment		Branch/Log
	Rip-up-clasts		Roots / Rhizoliths
			Plant Fragments (generic)
			Grassy Organic Material
			Woody Organic Material
	M Massive/Structureless		AMS- ¹⁴ C Median Age (2σ error)

Figure 4.4. Names, codes, descriptions of lithofacies, and core-log structures defined for sediment samples and sediment cores recovered in this study.

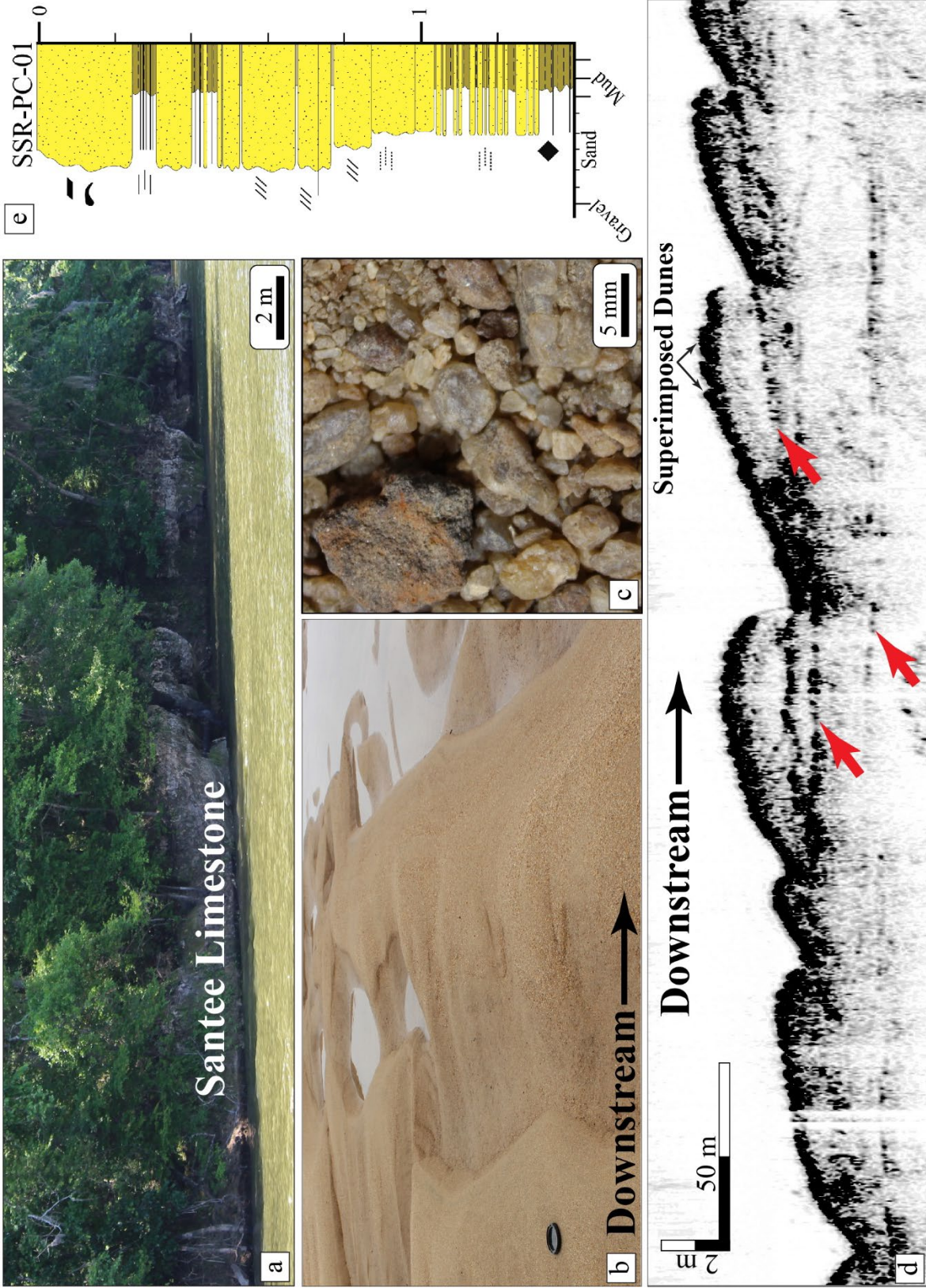


Figure 4.5. Fluvial-dominated Zone (FDZ) of the Santee delta plain. **a)** Sinuous-crested dunes along a large oblique bar in the South Santee River. **b)** Mud lenses deposited within the troughs of cusped ripples on the same bar as shown in **a**. **c)** Quartz, and lithic grains in gravel from a grab sample taken from the North Santee River (NSR-GS-09). **d)** Chirp profile from the North Santee River just downstream of the bifurcation with the South Santee showing large subaqueous dunes with superimposed smaller dunes along the stoss side. Red arrows mark internal surfaces. **e)** Graphic log of a push core taken from the South Santee River near the AIWW. Coarsening-upwards succession with punctuated thin mud drapes is the result of the migration of subaqueous dunes probably similar to those shown in 5a.

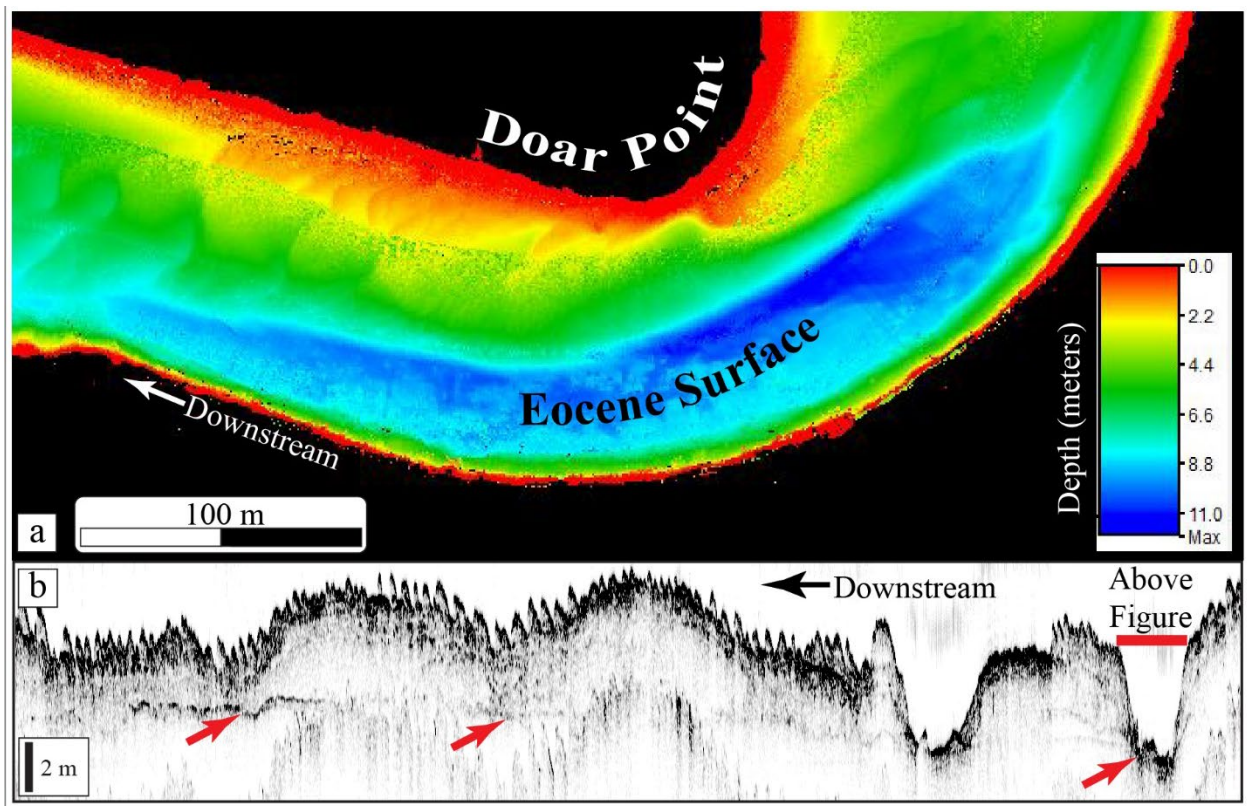


Figure 4.6. **a)** High-resolution bathymetry along a meander in the North Santee River. The inner margin downstream of Doar Point shows translation of point-bar deposits and development of 3-

Dunes across most of the channel floor. The deepest part of the channel is relatively flat and featureless. **b)** Chirp profile partially coincident with bathymetric figure above. Eocene carbonate beds (red arrows) form an erosion-resistant boundary at the floor of the modern channel in several locations along the North Santee River. In shallow parts of this profile the river bottom is covered by downstream-oriented, meter-scale dunes. See Figure 3 for location.

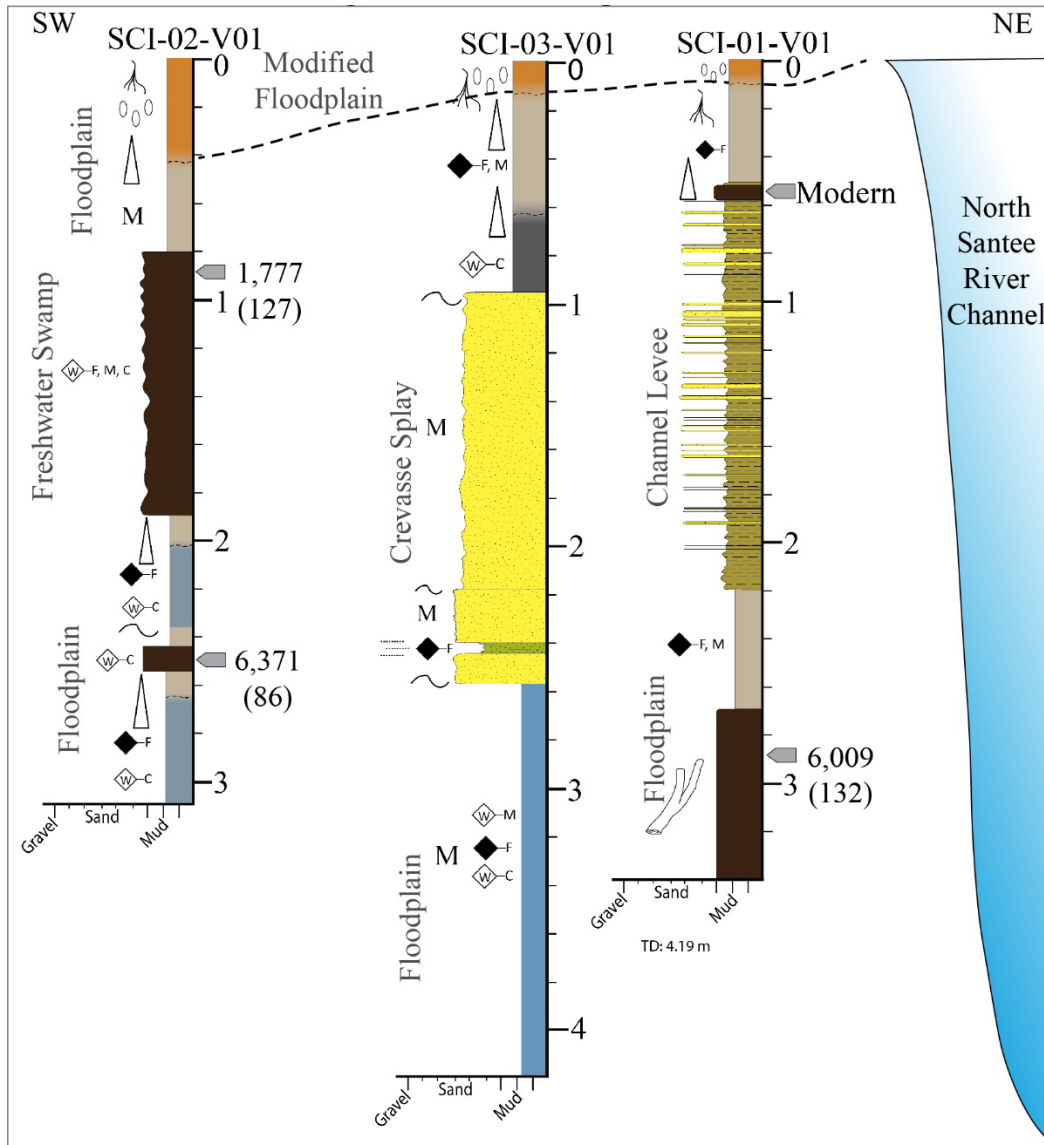


Figure 4.7. Vibracores recovered from the modern fluvial floodplain adjacent to the North Santee River near Rt 17. Calibrated AMS-¹⁴C ages combined with sedimentological evidence indicate

that this area has been a stable floodplain for at least that past ~6,000 yrs suggesting a laterally stable fluvial channel system. The presence of a strongly oxidized zone near the top of all 3 cores along with the absence of such zones below suggest that until recent times, the water table within the floodplain was high. This area lies within the part of the Santee system that were cleared for rice cultivation in the 18th century therefore the change to more well-drained floodplain conditions may be related to this anthropogenic modification. See Figure 3 for location.

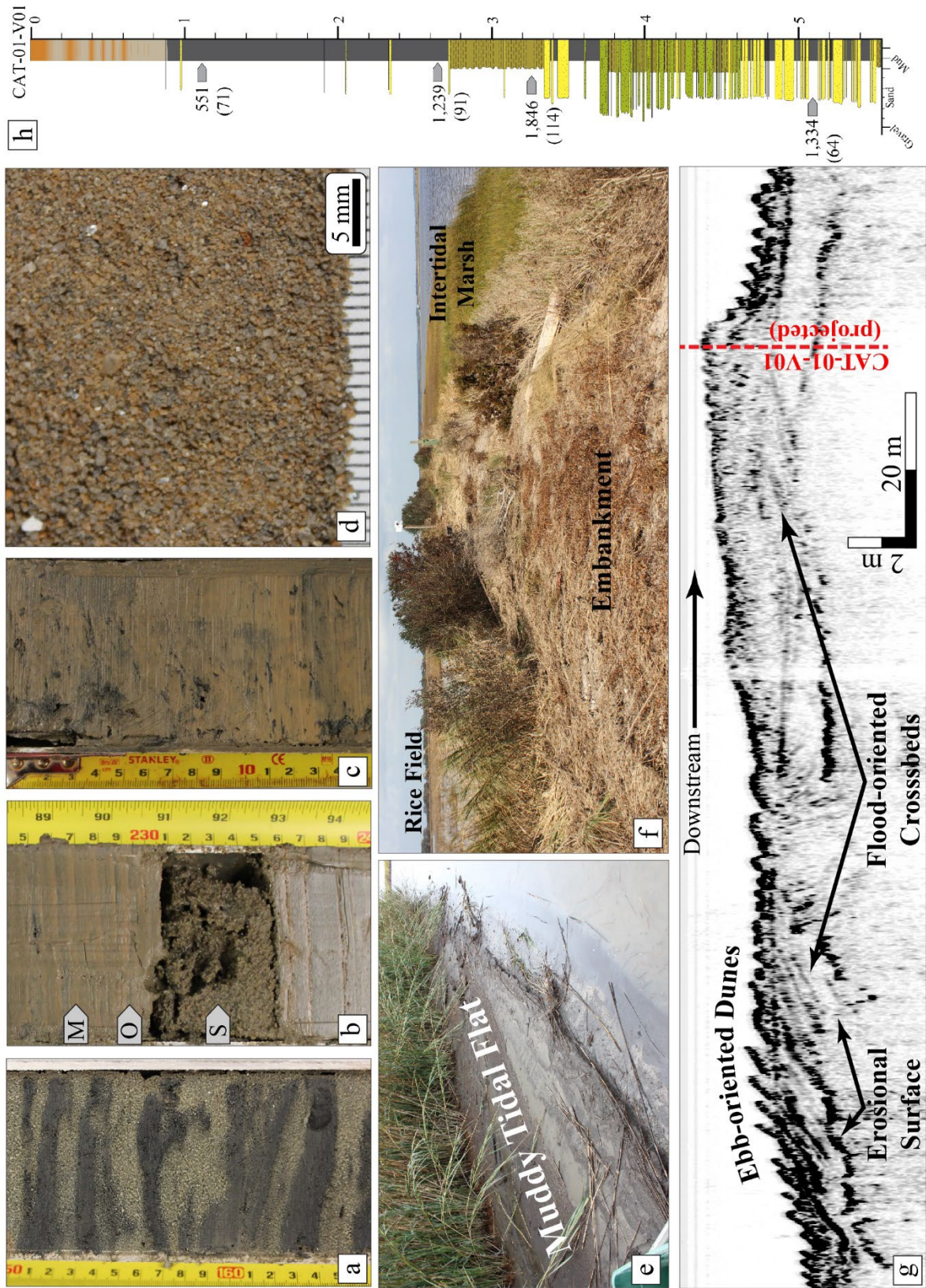


Figure 4.8. Mixed-energy Zone (MEZ) of the Santee Delta Plain. **a)** Intercalated, cm-scale mud (F4) and sand (F12) layers interpreted to have been deposited in a mixed-energy tidal flat setting. **b)** Thinly-laminated mud (M) and fine-grained organic detritus (O) of F6 with a medium-grained, well-sorted sand (F12, labeled as S) bed. Mud within F6 is very dark gray but quickly oxidizes to brownish orange upon exposure. **c)** Heavily bioturbated, organic-rich, oxidized mud (F3) that forms the substrate of intertidal marshes. **d)** Muddy sand (F9) from North Santee Bay. Dark grains are mud and brown color is due to thin mud coatings on predominantly quartz grains. **e)** Muddy tidal flat at the confluence of Minim Creek and the AIWW. Note abundant organic detritus on surface. **f)** Typical channel margin within the MEZ. A ~2-m high artificial embankment separates a rice field from the intertidal marsh and channel. **g)** Chirp profile along the NE margin of Cat Island in the North Santee Bay just downstream of the AIWW. Note multiple phases of both ebb-oriented and flood-oriented bedforms and crossbedding above a high-impedance erosional surface. **h)** Log of Core CAT-01-V01 recovered ~10 away from the Chirp profile shown in G. Upper muddy interval (0 – 270 cm) was deposited along a subtidal platform. The sharp contact between the uppermost orange and brown muds (F2 and F3) likely marks a change to more oxygen-rich conditions related to a change in circulation within North Santee Bay that occurred after 551 years ago. The lower, sand-rich intervals correspond to the complex stratigraphy shown in the Chirp profile and were likely deposited as estuarine bedforms and bars.

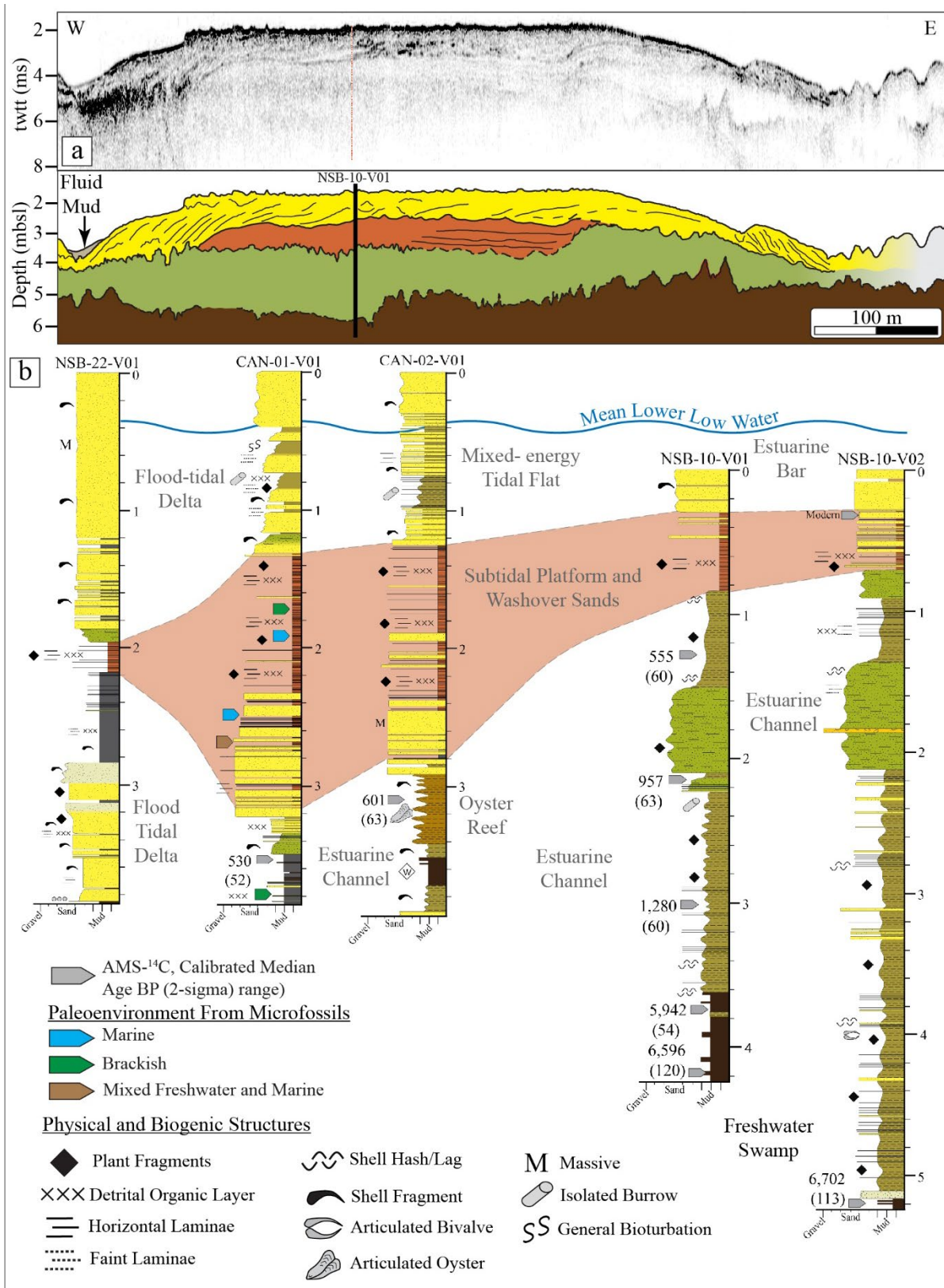


Figure 4.9. Stratigraphy of North Santee Bay. **a)** Chirp profile and interpretation across the NSB-10 bar in North Santee Bay. **b)** Logs of sediment cores recovered from the western side of North Santee Bay. See Figure 3 for location.

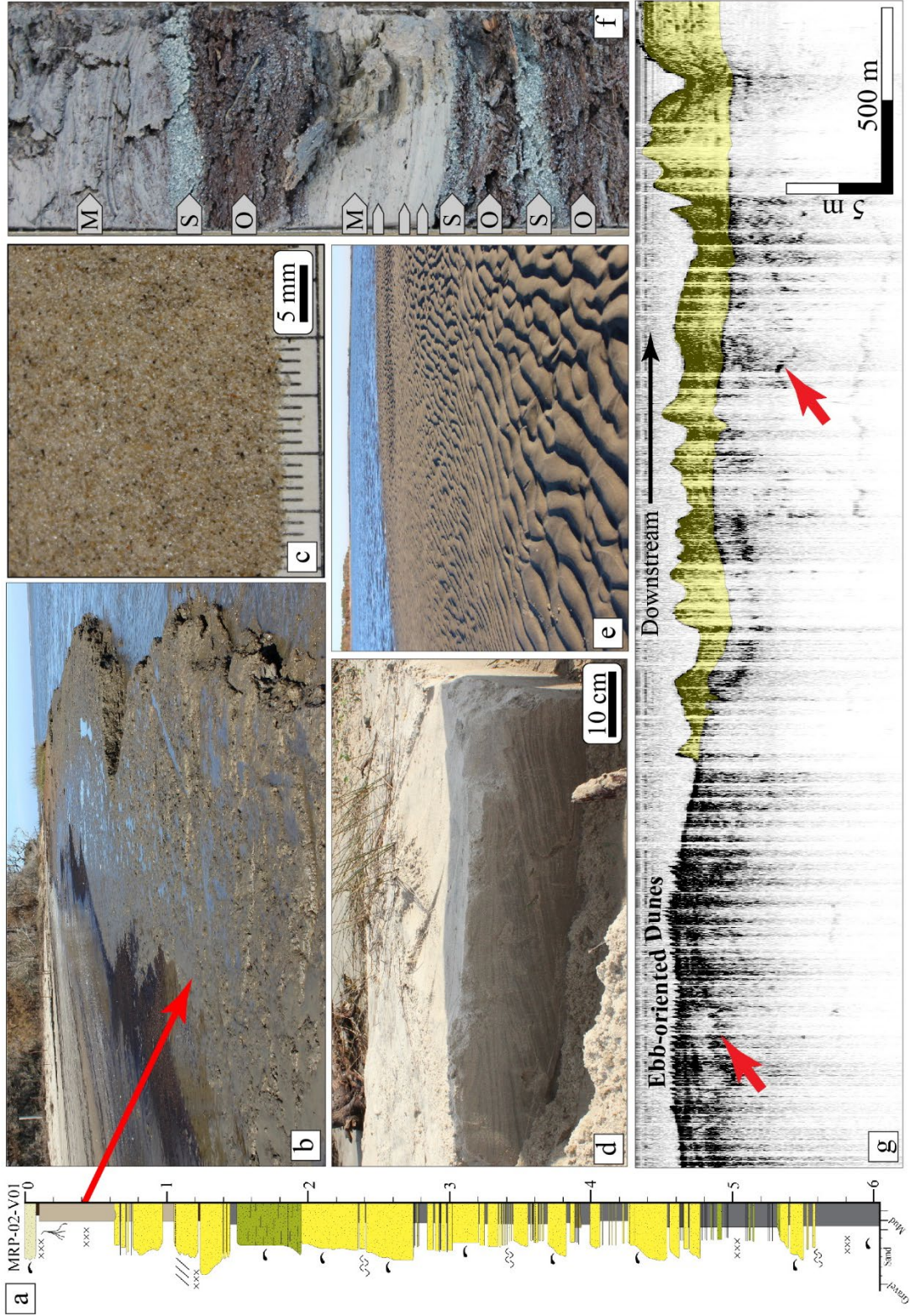


Figure 4.10. Marine-dominated Zone (MDZ) of the Santee delta. **a)** Sediment core from seaward-facing margin of Murphy Island along near the South Santee Inlet. **b)** Late Holocene marsh deposits cropping out along the seaward margin of Murphy Island. **c)** Very well-sorted, fine-grained, quartz-sand from a subaqueous grab sample in the North Santee Inlet (NSI-GS-01). **d)** Landward-dipping foresets of a washover fan complex deposited by Hurricane Matthew in 2016 along the margin of Murphy Island. **e)** Sinuous-crested ripples on the surface of a flood-tidal delta shoal near the South Santee Inlet. **f)** Bedding in a hand auger through a wave-influenced tidal flat along the shore of Murphy Island. Here the mixed-energy setting results in the deposition of mud (M) and/or organic material (O) when energy is low and sand (S) when energy is high **g)** Chirp profile along the South Santee River showing several seismic reflectors (red arrows), surface bedforms, and a portion of the flood-tidal delta shoal (yellow).

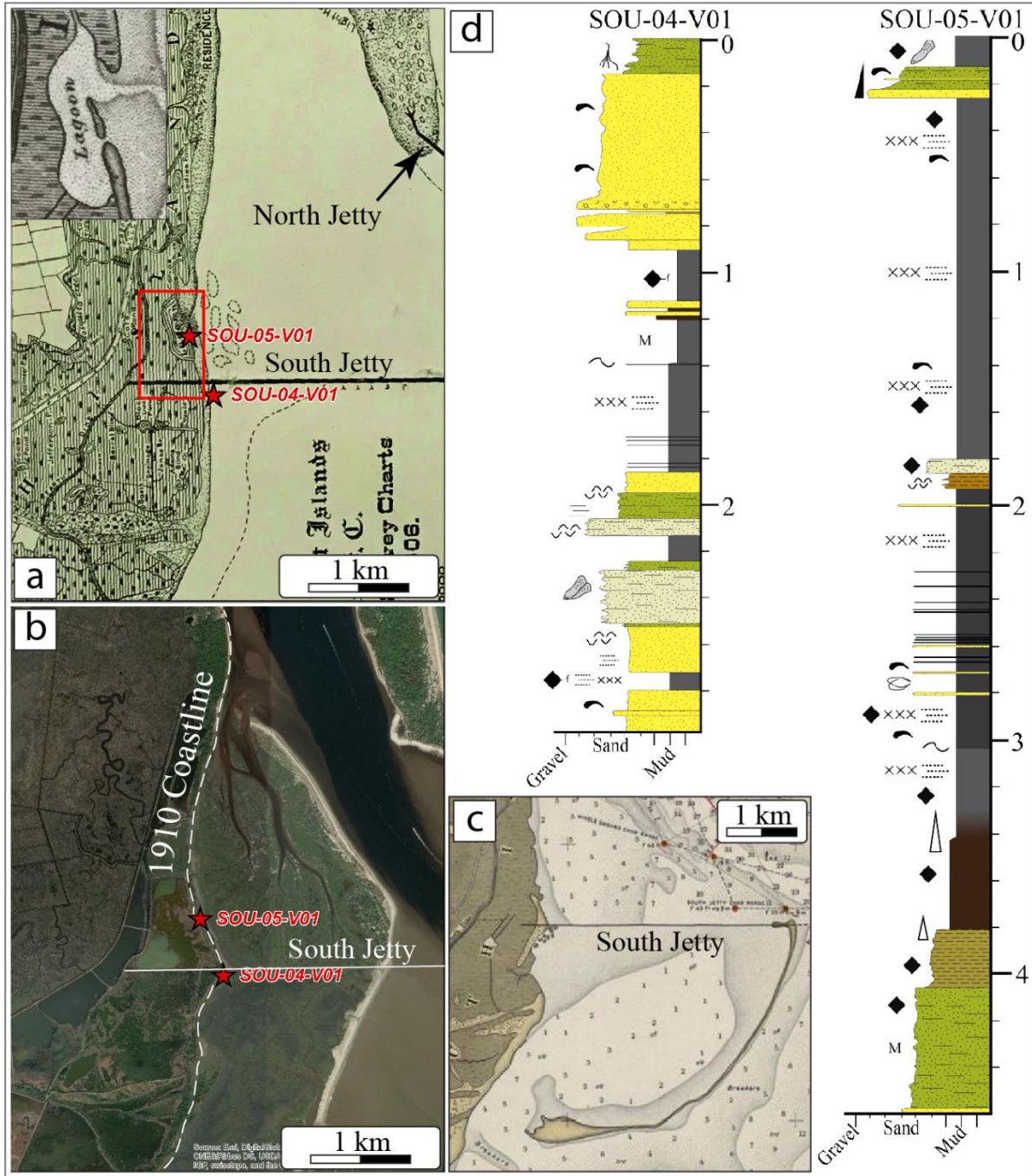


Figure 4.11 (South Island Jetty). South Island jetty and growth of a barrier-backbarrier system over the last 120 yrs. **a)** Map of the coast of South Island from around 1910 showing the location of a lagoon and the shoreline adjacent to the southern jetty. **b)** Present day configuration of South Island. The shoreline has moved more than a kilometer to the east and a backbarrier salt marsh has

developed between the modern and the 1910 shorelines. **c)** United States Coastal and Geodetic Survey nautical chart from 1929 showing the location of the newly-developed barrier offshore of South Island. **d)** Logs of cores taken from historical coastline. SOU-04-V01 records phases of high-energy and low-energy deposition that are the result of dynamic coastal geomorphology. The upper-most rooted muddy sands likely formed as the shoreface stabilized commensurate with the developing barrier-backbarrier system. The vertical succession in SOU-01-V05 preserves the depositional record of the infilling of the coastal lagoon shown in Fig. 11a and overlying marsh deposition. See Figure 3 for location.

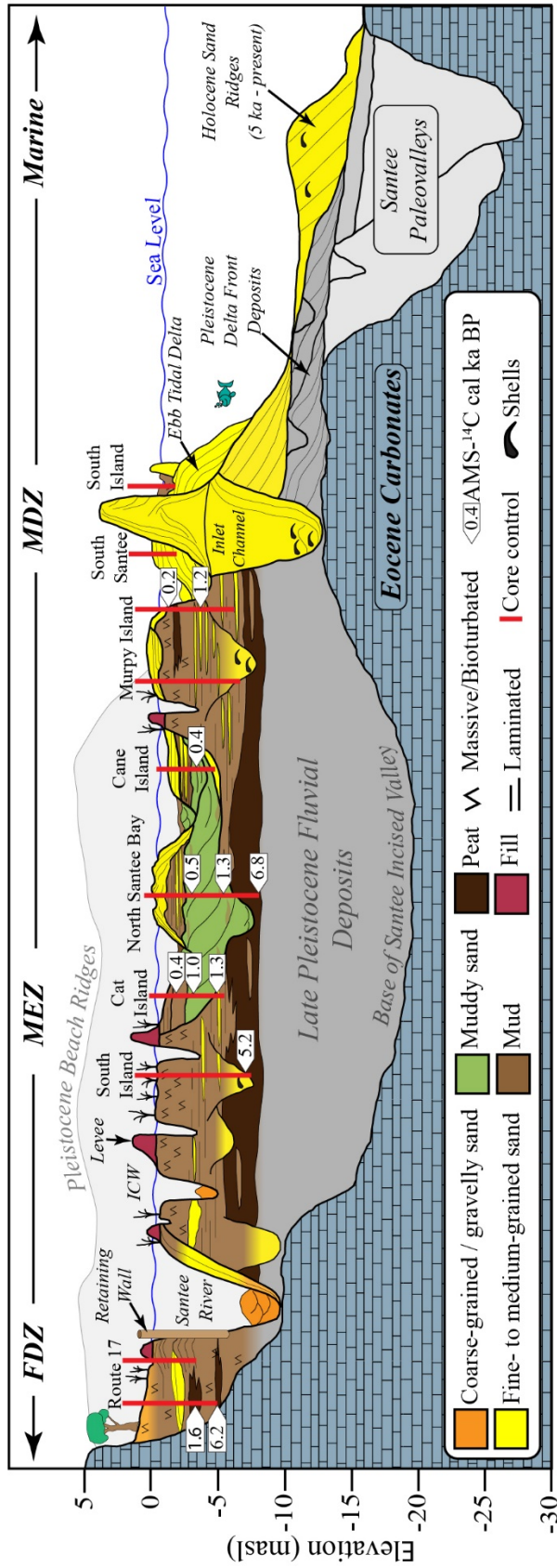


Figure 4.12. Stratigraphic panel summarizing the distribution of key subsurface and surficial elements documented within the Santee Delta plain. Numeric labels are AMS-¹⁴C ages in cal ka BP. Offshore stratigraphy is from Long and Hanebuth (2020). Basement morphology is based on new sediment cores, previously-existing boreholes from the USGS and SCGS, and Eckard (1986).

Core Name	Surface Elevation (masl)	Sample Core Depth (m)	Modern Delta Plain Zone	Raw ¹⁴ C Age (yr BP)	Lab Error (yr)	Calibrated Median ¹⁴ C Age (cal yr BP)	2σ Age Error (yr)	Material
CAN-01-V01	0.0	3.53	MDZ (T)	510	30	530	52	shell
CAN-02-V01	0.0	3.00	MDZ (T)	598	48	601	63	shell
CAT-01-V01	-1.0	1.07	MEZ (C)	534	47	551	71	wood
CAT-01-V01	-1.0	2.76	MEZ (C)	1,305	48	1,239	91	shell
CAT-01-V01	-1.0	3.25	MEZ (C)	1,902	48	1,846	114	shell
CAT-01-V01	-1.0	5.00	MEZ (C)	1,430	48	1,334	64	shell
CDR-01-V01	0.0	2.87	MDZ (C)	688	48	648	71	shell
CDR-01-V01	0.0	3.44	MDZ (C)	873	47	788	108	shell
CDR-01-V01	0.0	3.88	MDZ (C)	3,400	35	3,646	125	wood
CDR-04-V01	-1.0	2.66	MDZ (C)	1,127	48	1,037	119	shell
MRP-01-V01	1.5	0.70	MDZ (M)	174	47	173	121	wood
MRP-01-V01	1.5	1.28	MDZ (M)	5,255	35	6,015	126	wood
MRP-01-V01	1.5	3.30	MDZ (M)	1,130	30	1,027	105	shell
NSB-10-V01	-0.5	1.26	MEZ (C)	550	30	555	60	shell
NSB-10-V01	-0.5	2.17	MEZ (C)	1,050	30	957	63	shell
NSB-10-V01	-0.5	3.02	MEZ (C)	1,340	30	1,280	60	shell
NSB-10-V01	-0.5	3.64	MEZ (C)	5,185	35	5,942	54	wood
NSB-10-V01	-0.5	4.12	MEZ (C)	5,797	48	6,596	120	wood
NSB-10-V02	-0.5	0.38	MEZ (C)	118		0	0	shell
NSB-10-V02	-0.5	5.19	MEZ (C)	5,880	40	6,702	113	wood
SCI-01-V01	1.0	0.54	FDZ (F)	186	47	177	116	wood
SCI-01-V01	1.0	3.00	FDZ (F)	5,244	48	6,009	132	wood
SCI-02-V01	1.0	0.85	FDZ (F)	1,842	47	1,777	127	wood
SCI-02-V01	1.0	2.60	FDZ (F)	5,595	48	6,371	86	wood
SOU-01-V01	0.5	5.46	MEZ (M)	4,470	35	5,161	23	wood

Table 4.1. AMS-¹⁴C data from sediment cores. Modern zones refer to those defined here as Fluvial-dominated (FDZ), Mixed-energy (MEZ), and Marine-dominated (MDZ) zones and within these zones, cores were recovered from channels (C), marshes (M), floodplains (F), and tidal flats (T).

Chapter 5

Integration of Results and Conclusions

INTRODUCTION

Using the results and conclusions from previous chapters, the processes that ultimately control the stratigraphy can be better understood providing the context for a broader understanding of the regional development of the Santee River delta. These processes are organized into three general categories: 1) allogenic processes of regional or global influence (Fig. 1.2); 2) autogenic processes that are intrinsic to the depositional system; and 3) anthropogenic processes develop in response to human activity and typically act on a local scale but collectively may have regional or global influence. These processes are not mutually exclusive, and depositional trends within an environment can be influenced by various combinations of all three.

Allogenic processes influence depositional patterns across sedimentary systems by controlling changes in sediment supply, accommodation, and topographic or bathymetric gradients (Beerbower 1964; Reading and Levell 2006). These processes include changes in sea level, tectonic movement, and climatic variability (Beerbower, 1964; Cecil, 2003; Reading and Levell, 2006). They generally operate over time scales ranging from decadal climatic oscillations to tectonic cycles of hundreds of millions of years (Fig. 1.2b) (Maslin et al. 2001; Willard et al. 2005; Miall 2010; Romans et al. 2016). Quaternary climate variability has been shown to have had a significant influence on Atlantic Coastal Plain depositional systems (Willard et al. 2005; Leigh 2006; Swezey 2020, see discussion in Chapter 4) and therefore has undoubtedly influenced deposition within all three study areas. However, we do not isolate a specific climatic contribution to depositional history

Autogenic processes are those that are intrinsic to a depositional system (Beerbower 1964) and control depositional patterns within that system as they include fluvial and estuarine channel migration and avulsion, migration of bedforms, bars, and inlets, as well as delta-lobe switching (Cecil, 2003). These processes are aperiodic and typically operate over relatively short time scales ranging from nearly instantaneous events to millennial-scale processes (Fig. 1.2b) (Cecil 2003; Miall 2010; Romans et al. 2016).

Significant anthropogenic influences on deposition systems within the study area began during the early 18th century, coinciding with European colonization of eastern North America (Lewis 1979; Espenshade 1989; McCarney-Castle 2010). They continue to the present day. Agricultural land use, dam construction, and coastal modifications influence surface erosion, sediment transport, as well as natural wetland processes and habitats.

SEA LEVEL

Throughout the Quaternary, changes in eustatic sea level driven by numerous glaciations coupled with regional subsidence and uplift have resulted in a spatially variable record of RSL change along the east coast of the United States. Estimates of RSL during this period range from approximately -100 to + 5 m, relative to current sea level (Fig. 2.8). More recently, during the late Holocene, eustatic sea-level rise in the western Atlantic is estimated to be between 1.47 - 0.93 mm a⁻¹ (Toscano and MacIntyre 2003) while RSL along the coast of South Carolina has risen at a rate of between 0.72 - 0.8 mm a⁻¹ (Van De Plassche et al. 2014). The difference between the two is attributed to continued uplift of the Cape Fear Arch (Van De Plassche et al. 2014). Changes in RSL throughout the Quaternary have influenced the stratigraphic record in three primary ways: 1) it controls regional topographic and bathymetric gradients, 2) controls the position of the shoreline and associated depositional systems over time, and 3) it controls accommodation.

Sea Level-controlled Regional Gradient

Changes in regional gradient within fluvial valleys associated with falls in RSL commonly lead to incision of the newly-exposed continental shelf by large rivers leading to the development of incised valleys, a response driven by the re-establishment of a graded or equilibrium profile within these fluvial systems (Mackin 1948; Schumm and Ethridge 1994; Posamentier and Vail 1988; Catuneanu 2006; Holbrook et al. 2006). Chapter 2 describes the development of two incised valleys associated with the Santee River (Figs. 2.6, 2.7, and 2.10). The paleovalleys are the Bulls Bay paleovalley and the Santee incised valley, both of which were formed by the Santee River during the periods of RSL fall in the late Pleistocene. Subsequently, under conditions of rising RSL, their incised valleys became filled as fluvial and paralic environments migrate landward along with the associated shoreline. Channels of smaller coastal plain and tidal rivers and creeks also infilled, resulting in the paleochannels that are common in the subsurface stratigraphy across the region (Chapter 2 and 3; Fig. 2.10a).

Shoreline Position

Evidence of changes in the position of the shoreline associated with both across-shelf progradation and transgressive barrier-backbarrier development is provided in Chapters 2 and 3, respectively. Several episodes of across-shelf progradation of fluvial-influenced deltaic shoreface deposits in response to falling sea level is documented in Chapter 2. Despite limited control on the ages of these deposits, they are likely of late Pleistocene age (Fig. 2.3). Preservation of these types of deposits are rare in this setting (Field and Trincardi 1991) and have not been previously documented in this region.

Chapter 3 documents the preservation of numerous paleochannels and paleovalleys that developed during the late Pleistocene and Holocene along the modern-day inner continental shelf.

Paleochannels of different ages crosscut one another resulting in complex paleovalley configurations of overlapping paleochannels (Fig. 3.6, 3.7, and 3.8). These paleovalleys are the result of the development of backbarrier channels during different sea level cycles. Welded barrier systems are found along the modern coast, consisting of remnants of Pleistocene barrier islands forming the cores of Holocene barrier islands (Hayes 1994; Weems et al. 2014), and they offer a reasonable analogue for how this process may have worked. This configuration has resulted in modern backbarrier channels developing in the same area as older Pleistocene backbarrier channels (Weems et al. 2014). With continued RSL rise, wave and tidal ravinement may remove much of the barrier island deposits; however, the low-lying, mud-rich backbarrier paleochannels have a higher preservation potential.

One of the more common stratigraphic units documented in Chapters 2 and 3 are relatively thin (< 3-4 m), internally-transparent, sheet-like deposits interpreted as transgressive sand sheets (Figs. 2.5, 2.6, 2.7, 2.9, and 3.7). They are interpreted as products of shoreface erosion and deposition by waves during rising RSL (Swift, 1975). Based on sediment-core data (Fig. 3.5), these sand sheets consist of moderately- to well-sorted, coarse-grained, and often shelly sand. AMS-14C analysis indicate that much of the material has been re-worked from older deposits (Fig. 3.5, Table 3.1).

The influence of late Holocene RSL rise on the Santee delta is described in Chapter 4 where fluvial floodplain deposits, lying at a depth of ~5 mbsl, are overlain by delta plain deposits of the modern system. This would indicate a rise in RSL of approximately 5 m over the last 5,000 years, approximately 1 mm yr⁻¹, within the range of estimated rates of RSL rise for the South Carolina coast (Van De Plassche et al. 2014).

Accommodation

Accommodation in marine environments generally lies between wave base and the sea floor (Jervey 1988; Catuneanu 2006). Rising RSL or subsidence of the basin floor, caused by either tectonic influences or compaction increases accommodation, while falling RSL or seafloor uplift decreases accommodation. The zonation of the shoreface-shelf profile is based on the distinction between fairweather- and storm-wave base (Reading and Collinson 2006); however, this distinction can be complicated by local bathymetry and regional oceanographic conditions (Peters and Loss 2012).

The narrow, low-gradient continental shelf offshore of the Georgia Bight has a maximum depth of approximately 50 m (Fig. 1.1). Peters and Loss (2012) integrated oceanographic data collected by buoy's in the western Atlantic Ocean and concluded that the modal wavelength for this region is approximately 120 m, corresponding to an estimated wave base of 60 m. This suggests that sediments on the sea floor across most of the continental shelf in this region are regularly subjected to reworking by waves. Coupled with wave and tidal ravinement (Catuneanu, 2006), this general lack of accommodation has contributed to the development of widespread composite erosional (6th order) surfaces as described in Chapter 2 (Fig. 2.4, 2.5, 2.6, 2.7, and 2.9; Table 2.2).

TECTONICS AND STRUCTURE

As summarized in the introduction of Chapter 2, the east coast of United States is a passive margin characterized by regional trends in uplift and subsidence related to isostatic adjustments and changes in dynamic topography and by local fault movement (Scholle, 1979; Baldwin et al., 2006; Rowley et al., 2013; Doar, 2014; Van De Plassche et al., 2014). These factors have influenced deposition in two ways: they 1) influence regional gradients, and 2) create local, fault-related accommodation.

Tectonically-controlled Regional Gradient

Two broad, basement-involved tectonic elements, the Cape Fear Arch (CFA) and southeast Georgia Embayment (SGE), have influenced regional gradients and Coastal Plain depositional systems throughout the Quaternary (Scholle 1979; Hayes 1994; Weems 2002; Baldwin et al. 2006, Van De Plassche et al. 2014) (Fig. 3.9). As described in Chapter 3, Hayes (1994) defined a series of geomorphological compartments that he attributed to large-scale tectonism, sediment supply, hydrodynamic regime, and local tectonic influences. Tectonic uplift throughout the Quaternary has led to the relatively high, structurally-influenced regional gradient of the lower Coastal Plain of northern to central South Carolina (Hayes 1994). This increased gradient has resulted in lower long-term accommodation and the preservation of a thin Quaternary stratigraphic package onshore (Colquhoun et al., 1983; Hayes, 1994) and offshore (Long 2018; Alexander et al. 2019; Chapter 2). Conversely, down-warping and subsidence to the south, within the SGE, has led to increased long-term accommodation and the preservation of a thicker Quaternary section in southern South Carolina and Georgia onshore (Hayes 1994; Colquhoun 1995) and offshore (Long 2018; Alexander et al. 2019). The extension of this trend into the offshore along the inner shelf and its influence on both the thickness of the Quaternary stratigraphic section and the architecture of Quaternary paleoincisions is described in Chapters 2 and 3 and summarized in Figures 2.9 and 3.10.

Local structure

As summarized in Chapter 2, localized fault movement has influenced fluvial and paralic environments across the Coastal Plain of the southeastern United States during the Quaternary (Marple and Talwani 2000; Bartholomew and Rich 2012). Several examples of this influence are described in Chapters 2 (Fig. 2.7) and 4. Considering its location and orientation relative to the

Bulls Bay paleovalley and the incised valley of the Santee River, activity along the Oceda fault system may have played a role in the evolution of this system as described in Chapter 2. Closer to the modern coast, the Eocene-age Santee Limestone crops out along the southern margin of the Santee incised valley while the base of the valley lies at an approximate depth of 20 – 25 mbsl (Fig. 2.10a). This relief was likely caused by incision by the Santee River during the Pleistocene and earliest Holocene; however, the prevalence of faults within the Santee Limestone (Fig. 1.3) suggests that local structure may influence the elevation of the pre-Quaternary basement beneath the Santee delta plain and inner continental shelf.

AUTOGENIC PROCESSES

Autogenic processes are those that influence local (i.e. intrabasinal) depositional trends. They are the result of sediment-transport dynamics, they are instantaneous, and they are randomly distributed in both time and space (Cecil 2003; Hajek and Straub 2017). These processes have influenced the stratigraphic record within the study area in several specific ways.

Paleoincisions fill in response to both intrinsic processes such as channel abandonment, and, as discussed above, extrinsic processes such as RSL rise. Chapter 3 provides several examples of paleovalley architecture resulting from infill and renewed incision with backbarrier channels that occurred during the late Holocene (Fig. 3.7). As described in Chapter 3, channel discharge within these environments can vary significantly in response to channel volume increase through headward erosion or channel capture (Zeff 1988; Hughes 2012). These processes can lead to increased channel erosion. Lateral channel migration or avulsion, however, can lead to channel infill or abandonment.

The strongly heterogenous sediment distributions present in modern and ancient, mixed-energy depositional environments are the result of complex, local morphodynamics. Several examples of these distributions are presented in Chapters 3 and 4. Depositional facies change rapidly as the relative influences of local currents (fluvial, tidal, or wave-induced) interact with regional and local topography, bathymetry, and channel orientation. The mixed-energy zone of Chapter 4 (Fig. 4.8) and many of the mud-rich and heterolithic sediment cores from paleochannels presented in Chapter 3 (Figs. 3.3 and 3.5) provide evidence of this type of variability.

Delta plain channels are prone to avulsion in response to changes in local gradients and discharge (Reading and Collinson 2006). Erosion associated with the development of these channels in the Santee system is likely responsible for the apparent time gap observed from the cores recovered associated with the research described in Chapter 4. In the North Santee Bay, estuarine/backbarrier channel deposition began just prior to 1.3 cal ka BP and disconformably overlie freshwater peats deposited between 5.9 and 6.7 ka cal BP (Fig. 4.9). Along the southwestern margin of the North Santee River mixed-energy tidal flat facies that were deposited ~ 3.6 cal ka BP were recovered in the CDR-01-V01 core (Table 4.1), suggesting that this channel may be older than the broad channel associated with the North Santee Bay.

Chapters 3 and 4, provide examples of the influence that underlying stratigraphy can have on channel development. The elevation of the Santee Limestone beneath the Santee delta plain ranges from ~25 mbsl (Eckard et al. 1986) to several meters above sea level where it crops out along the southwestern bank of the Santee incised valley (Chapter 4, Figs. 4.3, 4.5, and 4.12). In several locations where the channel floor of the modern Santee River is scoured to depths in excess of 10 m, high-resolution bathymetric data coupled with Chirp sub-bottom profiles and grab samples indicate that the Santee Limestone defines the base of channel thalwegs (Fig. 4.6). These

locations are near Goat Island, Doar Point along the North Santee River, and the confluence of Minim Creek and the North Santee River (Fig. 4.3). The meandering nature of the North Santee River in this location is likely related to the resistant nature of the Santee Limestone (Fig. 4.3). This relationship between the modern river morphology and the underlying stratigraphy is similar to that described within the paleochannel networks offshore of Kiawah Island in Chapter 3. Figure 3.7 clearly shows that the maximum depth of paleochannels is associated with a specific stratigraphic horizon, likely to its mechanical properties.

Autogenic processes are not limited only to fluvial or backbarrier settings. Morphodynamic feedbacks associated with tides and waves, particularly those generated by storms, can shape deposits along the continental shelf. The sand ridges found offshore of the Santee delta described in Chapter 2 are one example of these deposits. Pendleton et al. (2017) summarized the main hypotheses related to the formation of the shelf sand ridges that are found along the U.S. mid-Atlantic inner shelf. These hypotheses state that sand ridges are either relict shoreface-associated deposits abandoned during the Holocene transgression or are actively forming under modern, post-transgressive, hydrodynamic conditions with ridge progradation driven by the offshore deflection of storm-related currents (Pendleton et al. 2017). Snedden et al (2011) proposed that shelf sand ridges offshore of New Jersey developed through a combination of the two components summarized by Pendleton et al. (2017) with transgressed shoreface-associated deposits serving as a local sediment source which is subsequently reworked by oceanographic processes to form prograding sand ridges. The sand ridges defined in Chapter 2 have a cusped morphology that roughly parallels the shape of the inboard coastline (Fig. 2.4) which contrasts with the generally linear, shore-oblique morphology of sand ridges elsewhere along the shelf. AMS-¹⁴C dates and

AAR ages from Core SC-BOEM-2015-VC24 and Chirp sub-bottom profiles offshore of Cape Romain indicate that this feature has prograded over the past ~ 4.7 kyr (Fig. 2.3).

ANTHROPOGENIC MODIFICATIONS

The widespread clearing of coastal woodlands and the construction of canals and embankments in the mid-18th century associated with rice cultivation has left an indelible imprint on the modern depositional environment. Additionally, agricultural land use associated with European settlers in the early 18th century and the construction of large dams in the mid-20th century had significant impacts on fluvial sediment flux (McCarney-Castle et al. 2010). Mixed-energy tidal flats, while fairly common in the subsurface, are absent in the modern system, likely a function of channel embankment. Floodplain sedimentation is limited to areas where embankments are no longer actively maintained, inhibiting the systems natural ability to aggrade as modern sea level continues to rise. Channel embankments also limit the ability of channels to migrate laterally, influencing the Holocene stratigraphic record. Although the timing is loosely constrained by AMS-¹⁴C dating, a significant shift in sedimentation style occurred throughout the North Santee Bay at some point after ~ 530 cal yr BP (± 52) which may coincide with and be a result of the drastic changes made to the delta plain roughly 250 yrs ago. Along the coast of South Island two large jetties constructed in 1909 altered nearshore circulation and has led to the deposition of roughly 7.5 km² of saltwater marsh on the southern margin of the Winyah Bay inlet (Fig. 4.11). The construction of the Atlantic Intracoastal Waterway has altered the natural circulation of the Santee and Winyah Bay systems, connecting Winyah Bay, North Santee Bay, the North Santee River, and the South Santee River. Hockensmith (2014) found that the salinity varies at the intersections of these channels with the AIWW throughout the tidal cycle.

CHAPTER 6

Future Work

The conclusions from the studies presented here provide the foundation for additional focused research. Each of the projects suggested below are subsidiary to the research presented in Chapters 2, 3, and 4 and addresses questions that have arisen from these findings.

STUDIES ASSOCIATED WITH CHAPTER 2

Holocene Sand Ridge Complexes

Cusate sand ridges (Fig. 2.4) appear to be morphologically, and potentially, genetically different than those found in other regions which display straight-to-oblique ridge orientation. The main questions to be addressed are: 1) what is the temporal relationship of sand-ridge successions across the shelf, 2) what controls their cusate morphology, 3) what is the source of the sand, and 4) what influence does the variable substrate (hardbottom, Pleistocene cohesive or consolidated sediments, mobile sand) in the region exert on the genesis and evolution of sand ridges?

Addressing these questions would require looking at sediment-transport dynamics at two different scales: 1) A regional-scale, focusing on 2 or 3 sites distributed across the continental shelf applying a high-resolution approach similar to that used in the 2015 BOEM ASAP project; and 2) a local-scale, involving high-resolution continuous monitoring and repeated surveys of short-term modifications in a representative sub-area. The two goals are to 1) establish a conceptual, process-based, semi-quantitative sedimentary model to better understand sediment transport within these sand ridge systems; and 2) use the new detailed data set in a following step for quantitatively simulating the local hydrodynamic and sediment-dynamics conditions that are involved in

formation and transformation of the sand-ridge succession. The results will be compared to those of other studies focused on sand ridge systems along the US east coast (Swift 1975a; Swift et al. 1984; Goff 2009; Snedden et al. 2011; Pendleton et al. 2017).

Pleistocene deltaic deposits

The identification of Pleistocene delta-front deposits (seismic facies PGt) offshore of the Santee River is significant in that these deposits record the progradation of a moderate-sized, fluvial delta across the Atlantic continental shelf. The distribution, morphology, composition, and age of these deposits can inform reconstructions of changes in relative sea level as a function of sediment supply, accommodation, and eustatic sea level. The high-resolution seismic data set that is currently available and was interpreted in Chapter 2 (Fig. 2.5) is adequate to document the general distribution and internal architecture of these deposits, but their morphological, detailed stratigraphic architecture, composition, and age remain poorly-defined.

Answering these questions will require the acquisition of new data to be completed in two phases. The first phase consists of the targeted acquisition of closely-spaced (< 100 m) high-resolution seismo-acoustic (Chirp) data where these deposits have already been identified, which is an area of approximately 650 km². The second phase consists of the acquisition of sediment cores to determine the composition and ages of these river-influenced deltaic deposits. Core locations will be determined from Chirp profiles and should sample the full range of recognized features including topsets, foresets, bottomsets, 4th-order onlap boundaries, and paleochannels. Initial dating should be done via AMS-¹⁴C analysis; however, given the uncertainty of the age range of ages other methods may be required (i.e. OSL).

Santee River Paleovalleys

Understanding the spatial distribution, morphology, and periods of activity of the onshore incised valleys of the Santee River is important for two specific reasons. First, understanding how and why the Santee River has altered its course throughout the Quaternary can shed light upon the regional controls that influence Coastal Plain morphology. The northerly migration of the Santee from its most southern position near the modern Edisto River (Weems et al. 1994), through an intermediate position (The Bulls Bay Paleovalley of Chapter 2), to its current position is counter to the southerly migration of the Pee Dee River as interpreted by Baldwin et al. (2006). Second, the morphology of the incised valley of the modern Santee River likely influences the morphology of the modern fluvial system (Chapter 4); therefore, defining the morphology of valley floor can be important for understanding the morphology of the modern fluvio-deltaic system of the Santee.

To address these topics, additional borehole, sediment core, and geophysical data are required. Onshore delineation of the Bulls Bay paleovalley is based on data from boreholes drilled by both the South Carolina Geological Survey and the United States Geological Survey. The distribution of these data in most parts of the Coastal Plain are adequate for mapping of these subsurface features with the exception of the Shulerville 7.5-minute quadrangle in Berkeley County, SC. This is a key region between the bifurcation point of the Santee and Bulls Bay valleys near Jamestown and the onshore data near the coast of Bulls Bay. Additional boreholes within this quadrangle will help to constrain the location of the Bulls Bay paleovalley. Figure 2.7a is a borehole cross-section across both the Bulls Bay Paleovalley and Santee Incised Valley. Recovery of sediment cores from locations offset to existing boreholes should provide material from the lower sections of these valleys that is suitable for OSL dating, providing an estimate of when these valleys were active. We have suggested a potential connection between local fault activity along

the Oceda Fault system and the establishment of Santee Incised Valley and constraining the age of this valley could also indicated when this fault system became active.

Offshore Paleovalleys

We have identified several paleovalleys in the subsurface of the inner continental shelf offshore of the Santee Delta and Bulls Bay (Fig. 2.10). The distribution of available seismic data and lack of core control in the vicinity of these features prohibits their detailed characterization. Two important questions remain related to these offshore paleovalleys: 1) Are the interpreted trends in both the Santee and Bulls Bay Paleovalley show in Figure 2.10 accurate? and 2) when were these valleys last active? Both questions address the spatial and temporal relationships between the onshore paleovalleys of the Santee River and the offshore paleovalleys.

To answer these questions about the offshore paleovalleys requires the acquisition of new geological and geophysical data. New geophysical data should include both Chirp and HRS data acquired in a similar way to that of the NF0404 data set that targeted the paleovalley of the Pee Dee River offshore. The NF0404 was acquired by a collaboration between NOAA and CCU and followed the trend of the Pee Dee paleovalley offshore with a dense grid of valley-parallel and cross-valley profiles. In addition to geophysical data, sediment cores should be recovered at regular intervals or where significant changes occur within the paleovalley systems. Sediment cores provide valuable information regarding the depositional environments and ages of the paleovalley-filling sedimentary successions.

Basement Structure

The conclusions from all three research topics suggest that the morphology and structural features (i.e. faulting and folding) associated with the pre-Quaternary basement within the study

area have influenced Quaternary depositional systems; a trend that continues into modern times. To resolve the details of the pre-Quaternary section the Georgetown Pilot-Deep Seismic Study was completed between 2016 and 2018 in collaboration with SCGS and the University of Hamburg (Germany). This study was the first attempt at imaging the deeper sections of the stratigraphy within the Santee Delta and offshore from Cape Romain to Winyah Bay. The results of the study were mixed because of environmental and equipment complications. Offshore, we successfully imaged the southerly-dipping and faulted Eocene Santee Limestone, the onlapping of Oligocene and Miocene sections on the Eocene, as well as the thin Quaternary section (Fig. 1.3). Future work related to this study would focus on continued data acquisition offshore to both extend the widely-spaced existing profiles to the north and to fill in over areas of particular interest (e.g. areas of increased structural complexity or large paleovalley systems).

STUDIES ASSOCIATED WITH CHAPTER 3

Age Control

Continued work is needed to constrain the ages and timing related to the development and abandonment of paleochannels and paleovalleys in areas where geophysical data provide a good control on the stratigraphic relationships. Existing AMS-¹⁴C data indicate three periods of paleochannel development during the Quaternary across the region, however, the oldest of these periods contains samples that exceed the reliability of AMS-¹⁴C analysis (> ~ 47 ka). Additional sampling of existing cores for geochronological analysis employing methods with a longer time span would greatly increase our understanding of the timing of development of these systems and the forcing mechanisms that drive that development.

Under-represented Paleochannels

From the results of integrated core and Chirp data, 52 % of the paleochannels and the majority of sediment cores reported in Chapter 3 contain predominantly mud-rich, tidally-influenced backbarrier deposits that are associated with distinctive seismic characters. The next most common type of paleochannels contain seismically-transparent fill (CHt) and are under-represented in sediment cores. Cores that were recovered from these systems range from entirely mud-rich to entirely sand-rich (Fig. 3.5). Analysis of additional cores from these paleochannels could provide a means of distinguishing between muddy and sandy CHt, a potentially significant issue sand resource assessment.

While several types of paleochannels are well-represented in both Chirp and core data, laterally-accreting paleochannels (CHa) represent a distinct type of paleochannel fill. They are rare in Chirp data and have not been cored. Similar facies have been documented from fluvial, estuarine, and backbarrier environments where they represent the deposits of point bars that formed along the margins of sinuous estuarine channels or tidal inlets due to lateral migration (Dalrymple et al. 1992; Dalrymple et al. 2012; Hughes 2012; Fitzgerald and Miner 2013). Examples of this type of paleochannel occur within the subsurface offshore of Cape Romain and should be the target of future coring programs to begin to answer the question of why this type of channel fill is so uncommon.

STUDIES ASSOCIATED WITH CHAPTER 4

Floodplain Stratigraphy

Historical maps indicate that the main distributary channels of the Santee Delta have been mostly stable since at least 1773 (Cook 1773; Bradford 1838). While the channel margins were stabilized soon after this time, the lateral mobility of these channels during the late Holocene prior

to ~250 years ago is completely unknown. Understanding how these channels migrate and avulse addresses the overall stability of the channels, morphologies of the channel margins and floodplains, all of which influence the distribution of sediment across the delta plain and onto the delta front.

The floodplain cross-section shown in Figure 4.7 shows the vertical transition from poorly-drained floodplain deposits to well-oxidized deposits within the FDZ of the delta plain. This succession is a result of the change from saturated, low-oxygen conditions that prevailed prior to rice field construction to the well-drained, exposed conditions that followed these changes. A 1.5-m thick, fining-upwards sand-rich unit was deposited as either an overbank sheet (i.e. crevasse splay) or within a relatively shallow floodplain channel. Currently there are no sediment cores from the mixed-energy region of the delta plain. We are currently planning to recover sediment cores in between the existing widely-spaced cores as well as from new transects oriented both parallel and perpendicular to the existing transect. In addition to sediment cores, ground-penetrating radar (GPR) should be used along the core transects to define floodplain stratigraphy. Early in the project our group collaborated with Dr. Eric Wright (CCU) to collect GPR profiles along the artificial embankments on South Island, the only areas of the MER floodplains suitable for this kind of acquisition. Our results were hindered by the thick accumulation of artificial fill that formed the substrate of these roads. Future GPR acquisition should target the FDR floodplains between these embankments during the periods when they are exposed.

Pleistocene Fluvial Deposits and the Holocene Transition

The basal paleovalley sedimentary succession within the Santee Incised Valley is reported to consist of either compositionally-immature, fluvial sand and gravel deposited within fluvial channels during the late Pleistocene (Eckard 1986) or as muddy floodplain deposits (Payne 1970).

Existing borehole or core descriptions are commonly simplified with vertical resolutions of decimeters to meters (Payne, 1970; Eckard, 1986). The base of Holocene deposits that overlie these Pleistocene deposits are commonly marked by thick peat deposits that were deposited between 5 – 7 ka (Fig. 12, Research Topic 3). This peat layer has proven to be impenetrable in many of our sediment cores, preventing us from sampling the Pleistocene section of the incised valley fill.

Future work should focus on recovering sediment cores from the Pleistocene fluvial succession and, more specifically, the Pleistocene-Holocene transition. Constraining both the nature of the fluvial transition as well as the age of this transition can help to constrain the stratigraphic evolution of the incised valley fill. Several important aspects of this transition are unknown: 1) is there a progressive change in fluvial style preserved within the Pleistocene; 2) did the flooding associated the Holocene transgression occur in phases or is it preserved as a discrete interval; and 3) how do Pleistocene fluvial deposits compare to modern fluvial deposits of the Santee River?

North Santee Bay Circulation

As shown in Figure 4.9 and described in Chapter 4, sediment core and Chirp data indicate an abrupt change in lithology that is the result of either a dramatic decrease in depositional energy or an increase in suspension deposition within the North Santee Bay at some time following ~500 cal yr BP. Detailed bathymetric data from an Army Corps of Engineers survey prior to the completion of the Pinopolis and Santee dams indicate that the large oblique bar within the North Santee Bay (NSB-10 of Chapter 4) was approximately the same size and shape in 1935 as it is today. The upper unit of this bar consists of cross-bedded sands that overly the laminated muddy facies (Fig. 4.8b) which marks the change in circulation mentioned above. Along the seaward edge

of Cane Island, sediment cores contain this same muddy facies overlain by sandy wave-influenced tidal flat deposits. The change from laminated mud facies to the bar-top sand and sandy tidal flat deposits marks a change in conditions from relatively low to relatively high depositional energy. These sedimentological data suggest that whatever conditions were responsible for the accumulation of thick muddy deposits within the North Santee Bay had ended prior to 1935. Additional cores may provide datable material closer to the basal contact of the muddy deposits and the implementation of additional dating techniques may provide an upper limit to this interval.

REFERENCES

- Aburawi, R. M. (1968). *Sedimentary Facies of the Holocene Santee River Delta*. University of South Carolina.
- Allen, G. P., & Posamentier, H. W. (1994). Transgressive Facies and Sequence Architecture in Mixed Tide- and Wave-Dominated Incised Valleys: Example from the Gironde Estuary, France. In R. W. Dalrymple, R. L. Boyd, & B. A. Zaitlin (Eds.), *Incised-Valley Systems: Origin and Sedimentary Sequences*. SEPM Special Publication No. 51 (pp. 225–241). Tulsa, OK: The American Association of Petroleum Geologists.
- Allen, J. R. L. (1970). *Physical Processes of Sedimentation* (4th ed.). London: George Allen & Unwin.
- Allen, J. R. L. (1983). Studies in Fluvial Sedimentation: Bars, Bar-complexes and Sandstone Sheets (low-sinuosity braided streams) in the Brownstones (L. devonian), Welsh Borders. *Sedimentary Geology*, 33(4), 237–293.
- Anderson, B., & Miglarese, J. (1982). *An Ecological Characterization of South Carolina Wetland Impoundments*. Technical Report Number 51. Charleston, SC.
- Anthony, E. J., Marriner, N., & Morhange, C. (2014). Human influence and the changing geomorphology of Mediterranean deltas and coasts over the last 6000 years: From progradation to destruction phase? *Earth-Science Reviews*, 139, 336–361.
- Aptim Environmental & Infrastructure, I. (2017). *Inventory of Potential Beach Nourishment and Coastal Restoration Sand Sources on the Atlantic Outer Continental Shelf, Atlantic Sand Assessment Project (ASAP), Final Report of Findings*. Atlantic Sand Assessment Project (ASAP Final Report of Findings, Contract Number M14PC00006. Saint Petersburg, FL.

- Auerbach, L. W., Goodbred, S. L., Mondal, D. R., Wilson, C. A., Ahmed, K. R., Roy, K., ... Ackerly, B. A. (2015). Flood risk of natural and embanked landscapes on the Ganges-Brahmaputra tidal delta plain. *Nature Climate Change*, 5(2), 153–157.
- Bain, R. L., Hale, R. P., & Goodbred, S. L. (2019). Flow Reorganization in an Anthropogenically Modified Tidal Channel Network: An Example From the Southwestern Ganges-Brahmaputra-Meghna Delta. *Journal of Geophysical Research: Earth Surface*, 124(8), 2141–2159.
- Baldwin, W. E., Morton, R. A., Putney, T. R., Katuna, M. P., Harris, M. S., Gayes, P. T., ... Schwab, W. C. (2006). Migration of the Pee Dee River system inferred from ancestral paleochannels underlying the South Carolina Grand Strand and Long Bay inner shelf. *Geological Society of America Bulletin*, 118(5–6), 533–549.
- Bartholomew, M. J., & Rich, F. J. (2012). Pleistocene shorelines and coastal rivers: Sensitive potential indicators of Quaternary tectonism along the Atlantic Coastal Plain of North America. *Recent Advances in North American Paleoseismology and Neotectonics East of the Rockies*, 493(02), 17–36.
- Beerbower, J.R. (1964). Cyclothems and Cyclic Depositional Mechanisms in Alluvial Plain Sedimentation. In Merriam, D.F. (ed.) *Symposium on Cyclic Sedimentation: Kansas Geological Survey, Bulletin 169*, p. 31-42.
- Berné, S. (2000). Architecture, dynamics and preservation of marine sand waves (large dunes). In *Marine Sandwave Dynamics, International Workshop* (pp. 25–28). Retrieved from
- Bhattacharya, J.P. (2006). Deltas. In *Facies Models Revisited* (pp. 237–292).

- Bhattacharya, Janok P., & Walker, R. G. (1992). Deltas. In R. G. Walker & N. . James (Eds.), *Facies Models, Response to Sea Level Change* (1st ed., pp. 157–179). St. Johns, Newfoundland: Geological Association of Canada.
- Blatt, H., Middleton, G., & Murray, R. (1972). *Origin of Sedimentary Rocks* (1st ed.). Englewood Cliffs, NJ: Prentice-Hall.
- Blum, M. D., Martin, J., Milliken, K., & Garvin, M. (2013). Paleovalley systems: Insights from Quaternary analogs and experiments. *Earth-Science Reviews*, 116, 128–169.
- Bradford, T. G. (1838). *Map of South Carolina*. Office of the District Court of Massachusettes. 1 Sheet.
- Carter, H. H. (1909). *Plan of the Shooting Preserve of the Santee Club*.
- Castle, J. W., & Miller, R. B. (2000). Recognition and hydrologic significance of passive-margin updip sequences: An example from Eocene coastal-plain deposits, USA. *Journal of Sedimentary Research*, 70, 1290–1301.
- Cattaneo, A., & Steel, R. J. (2003). Transgressive deposits: A review of their variability. *Earth-Science Reviews*, 62(3–4), 187–228.
- Catuneanu, O. (2006). *Principles of Sequence Stratigraphy* (1st ed.). Amsterdam, The Netherlands: Elsevier.
- Catuneanu, O., Galloway, W. E., Kendall, C. G. S. C., Miall, A. D., Posamentier, H. W., Strasser, A., & Tucker, M. E. (2011). *Sequence Stratigraphy: Methodology and Nomenclature*. *Newsletters on Stratigraphy*, 44(3), 173–245.
- Charles, A. D. (2016). *Intracoastal Waterway*. *South Carolina Encyclopedia*, University of South

- Carolina, Institute for Southern Studies. 1 pp.
- Charlton, R. (2008). *Fundamentals of Fluvial Geomorphology* (1st ed.). New York, NY: Routledge.
- Chaumillon, E., Féliès, H., Billy, J., Breilh, J. F., & Richetti, H. (2013). Tidal and fluvial controls on the internal architecture and sedimentary facies of a lobate estuarine tidal bar (The Plassac Tidal Bar in the Gironde Estuary, France). *Marine Geology*, 346, 58–72.
- Childers, D. P., Madsen, J. A., Krantz, D. E., & Deliberty, T. L. (2019). Constraining the Geometry of Subsurface Paleochannels beneath Delaware Bay and the Mid-Atlantic Inner Continental Shelf. *Journal of Coastal Research*, 35(3), 590.
- Christie-Blick, N. (2012). Geological time conventions and symbols. *GSA Today*, 22(2), 28–29.
- Collinson, J. D. (2006). Alluvial Sediments. In H. G. Reading (Ed.), *Sedimentary Environments: Processes, Facies and Stratigraphy* (3rd ed., pp. 37–83). Malden, MA: Blackwell Science Ltd.
- Colquhoun, D. J. (1961). *Wicomico Shoreline in Orangeburg, Dorchester, and Berkeley Counties, South Carolina*. Columbia, SC.
- Colquhoun, D. J. (1962). *On Surficial Sediments in Central South Carolina- A Progress Report*. Columbia, SC.
- Colquhoun, D. J. (1995). A review of Cenozoic evolution of the southeastern United States Atlantic coast north of the Georgia trough. *Quaternary International*, 26(C), 35–41.
- Colquhoun, D. J., Bond, T. A., & Chappel, D. (1972). Santee Submergence, Example of Cyclic Submerged and Emerged Sequences. *Geological Society of America Memoir* 133, 475–485.
- Colquhoun, D. J., & Brooks, M. J. (1986). *New Evidence from the Southeastern U.S. for Eustatic*

- Components in the Holocene Sea Levels. *Geoarchaeology: An International Journal*, 1(3), 275–291.
- Cook, J. (1773). A Map of the Province of South Carolina with all the Rivers, Creeks, Bays, Inlets, Islands, Inland Navigation, Soundings, Time of High Water on the Sea Coast, Roads, Marshes, Ferrys, Bridges, Swamps, Parishes, Churches, Towns, Townships, County, Parish,. 1 sheet. London.
- Cooke, C. W. (1936). Geology of the Coastal Plain of South Carolina. USGS Bulletin 867. 218 pp.
- Cooper, J. A. G. (1993). Sedimentation in A River Dominated Estuary. *Sedimentology*, 40, 979–1017.
- Cronin, T. M., Thunell, R., Dwyer, G. S., Saenger, C., Mann, M. E., Vann, C., & Seal, I. R. (2005). Multiproxy evidence of Holocene climate variability from estuarine sediments, eastern North America. *Paleoceanography*, 20(4).
- Cronin, Thomas M., Szabo, B. J., Ager, T. A., Hazel, J. E., & Owens, J. P. (1981). Quaternary climates and sea levels of the U.S. atlantic coastal plain. *Science*, 211(4479), 233–240.
- Dalrymple, R.W., Mackay, D. A., Ichaso, A. A., & Choi, K. S. (2012). Processes, Morphodynamics, and Facies of Tide-Dominated Estuaries. In R. A. Davis & R. W. Dalrymple (Eds.), *Principles of Tidal Sedimentology* (pp. 79–107). Springer Science + Business Media.
- Dalrymple, R.W., Zaitlin, B. A., & Boyd, R. (1992). Estuarine_Facies Models: Conceptual Basis and Stratigraphic Implications. *Journal of Sedimentary Petrology*, 62(6), 1130–1146.

- Dalrymple, Robert W., Boyd, R. L., & Zaitlin, B. A. (1994). History of Research, Valley Types and Internal Organization of Incised-Valley Systems: Introduction to the Volume. In Robert W. Dalrymple, R. L. Boyd, & B. A. Zaitlin (Eds.), *Incised-Valley Systems: Origin and Sedimentary Sequences*. SEPM Special Publication No. 51 (pp. 3–11). Tulsa, OK: Society for Sedimentary Geology.
- Dalrymple, Robert W., & Choi, K. (2007). Morphologic and facies trends through the fluvial-marine transition in tide-dominated depositional systems: A schematic framework for environmental and sequence-stratigraphic interpretation. *Earth-Science Reviews*, 81(3–4), 135–174.
- Dashtgard, S. E., & La Croix, A. D. (2015). Sedimentological trends across the tidal-fluvial transition, Fraser River, Canada: A review and some broader implications. In *Fluvial-tidal Sedimentology* (1st ed., Vol. 68, pp. 111–126). Elsevier B.V.
- Davis, Richard A, Knowles, S. C., & Bland, M. J. (1989). Role of hurricanes in the Holocene stratigraphy of estuaries; examples from the Gulf Coast of Florida. *Journal of Sedimentary Research*, 59(6), 1052–1061.
- Denny, J. F., Baldwin, W. E., Schwab, W. C., Gayes, P. T., Morton, R., & Driscoll, N. W. (2007). Morphology and Texture of Modern Sediments on the Inner Shelf of South Carolina's Long Bay from Little River Inlet to Winyah Bay. U.S. Geological Survey Open File Report 2005-1345, 2005(1345).
- Denny, J. F., Schwab, W. C., Baldwin, W. E., Barnhardt, W. A., Gayes, P. T., Morton, R. A., ... Voulgaris, G. (2013). Holocene sediment distribution on the inner continental shelf of northeastern South Carolina: Implications for the regional sediment budget and long-term

- shoreline response. *Continental Shelf Research*, 56, 56–70.
- Desjardins, P. R., Buatois, L. A., & Mángano, M. G. (2012). Tidal Flats and Subtidal Sand Bodies. In *Developments in Sedimentology* (Vol. 64, pp. 529–561). Elsevier B.V.
- Doar III, W. R. (2014). The Geologic Implications of the Factors that Affected Relative Sea-level Positions in South Carolina During the Pleistocene and the Associated Preserved High-stand Deposits. University of South Carolina.
- Doar III, W. R., & Kendall, C. G. S. C. (2014). An Analysis and Comparison of Observed Pleistocene South Carolina (USA) Shoreline Elevations with Predicted Elevations Derived from Marine Oxygen Isotope Stages. *Quaternary Research*, 82, 164–174.
- Donnelly, J. P., Butler, J., Roll, S., Wengren, M., & Webb, T. (2004). A backbarrier overwash record of intense storms from Brigantine, New Jersey. *Marine Geology*, 210, 107–121.
- Durán, R., Guillén, J., Rivera, J., Lobo, F. J., Muñoz, A., Fernández-Salas, L. M., & Acosta, J. (2018). Formation, evolution and present-day activity of offshore sand ridges on a narrow, tideless continental shelf with limited sediment supply. *Marine Geology*, 397(October 2017), 93–107.
- Durica, J. T., Hanebuth, T. . . J., & Long, J. H. (2019). Local Hydrodynamics Controls on the Distribution of Bedforms in the Santee River Delta. In *Geologic Society of America, Southeastern US Section Meeting*. Charleston, SC.
- Eckard, T. L. (1986). *Stratigraphy and Depositional History of the Santee River Delta, SC*. University of South Carolina.
- Eckard, T. L., Hayes, M. O., & Sexton, W. J. (1986). *Deltaic Evolution During a Major*

- Transgression. Field Trip No. 6 Guide, SEPM Third Annual Midyear Meeting.
- Engelhart, S. E., Peltier, W. R., & Horton, B. P. (2011). Holocene relative sea-level changes and glacial isostatic adjustment of the U.S. Atlantic coast. *Geology*, 39(8), 751–754.
- Engineers, U. S. W. D. C. of. (1903). Annual Reports of the War Department for the Fiscal Year Ended June 30, 1903, Volume X. Washington, D.C.
- Espenshade, C. T., & Brockington, P. E. (1989). An Archeological Study of the Minim Island Site: Early Woodland Dynamics in Coastal South Carolina. Atlanta, GA.
- Feldman, H., & Demko, T. (2015). Recognition and prediction of petroleum reservoirs in the fluvial/tidal transition. In *Fluvial-tidal Sedimentology* (1st ed., Vol. 68, pp. 483–528). Elsevier B.V.
- Fenies, H., & Faugères, J. C. (1998). Facies and geometry of tidal channel-fill deposits (Arcachon Lagoon, SW France). *Marine Geology*, 150(1–4), 131–148.
- Field, M. E. (1980). Sand Bodies on Coastal Plain Inner Shelves: Holocene Record of the U.S. Atlantic Inner Shelf off Maryland.
- Field, M. E., & Trincardi, F. (1991). Regressive coastal deposits on Quaternary Continental Shelves: Preservation and Legacy. In *SEPM Special Publication No. 46: From Shoreline to Abyss* (pp. 107–122).
- Fitzgerald, D. M., & Miner, M. D. (2013). Tidal Inlets and Lagoons along Siliclastic Barrier Coasts. In *Treatise on Geomorphology* (Vol. 10, pp. 829–837).
- Flemming, B. W. (2000). The role of grain size, water depth and flow velocity as scaling factors controlling the size of subaqueous dunes. In *Marine Sandwave Dynamics*, International

- Workshop (pp. 55–61).
- Flemming, B. W. (2012). *Geology, Morphology, and Sedimentology of Estuaries and Coasts*. Treatise on Estuarine and Coastal Science (Vol. 3). Elsevier Inc.
- Friedrichs, C. T. (2012). Tidal Flat Morphodynamics: A Synthesis. In B. W. Flemming & J. D. Hansom (Eds.), *Treatise on Estuarine and Coastal Science* (Vol. 3, pp. 137–170). Elsevier Inc.
- Galloway, W. E. (1975). Process Framework for describing the morphologic and stratigraphic evolution of deltaic depositional systems. In M. Broussard (Ed.), *Deltas: Models for Exploration* (pp. 87–98). Houston, TX: Houston Geological Society.
- Gayes, P. T., Scott, D. B., Collins, E. C., & Nelson, D. D. (1992). A Late Holocene Sea Level Fluctuation in South Carolina. *SEPM Special Publication*, No. 48(48).
- Ghinassi, M., Alpaos, A. D., Gasparotto, A., Carniello, L., Brivio, L., Finotello, A., ... Cantelli, A. (2018). Morphodynamic evolution and stratal architecture of translating tidal point bars : Inferences from the northern Venice Lagoon (Italy). *Sedimentary Geology*, (65), 1354–1377.
- Gibling, M. R. (2006). Width and Thickness of Fluvial Channel Bodies and Valley Fills in the Geological Record: A Literature Compilation and Classification. *Journal of Sedimentary Research*, 76(5), 731–770.
- Giosan, L., Constantinescu, S., Filip, F., & Deng, B. (2013). Maintenance of large deltas through channelization: Nature vs. humans in the Danube delta. *Anthropocene*, 1, 35–45.
- Giosan, L., & Goodbred, S. L. (2007). Deltaic Environments. In *Encyclopedia of Quaternary*

Sciences (p. 12). Elsevier.

- Gonzalez-Villanueva, R., Perez-Arlucea, M., Costas, S., Bao, R., Otero, X. L., & Goble, R. (2015). 8000 Years of Environmental Evolution of Barrier-lagoon Systems Emplaced in Coastal Embayments. *The Holocene*, 1–16.
- Goodbred, S. L., & Saito, Y. (2012). Tide-dominated deltas. In R. A. Davis & R. W. Dalrymple (Eds.), *Principles of Tidal Sedimentology* (pp. 129–149). Springer Science + Business Media.
- Green, A. N. (2009). Palaeo-drainage, incised valley fills and transgressive systems tract sedimentation of the northern KwaZulu-Natal continental shelf, South Africa, SW Indian Ocean. *Marine Geology*, 263(1–4), 46–63.
- Hajek, E.A., and Straub, K.M. (2017). Autogenic Sedimentation in Clastic Stratigraphy. *Annual Review of Earth and Planetary Sciences*, 45, 681-709.
- Harris, M. S., Gayes, P. T., Kindinger, J. L., Flocks, J. G., Krantz, D. E., & Donovan, P. (2005). Quaternary Geomorphology and Modern Coastal Development in Response to an Inherent Geologic Framework: An Example from Charleston, South Carolina. *Journal of Coastal Research West Palm Beach*, 21, 49–64.
- Harris, M. S., Sautter, L. R., Johnson, K. L., Luciano, K. E., Sedberry, G. R., Wright, E. E., & Siuda, A. N. S. (2013). Continental shelf landscapes of the southeastern United States since the last interglacial. *Geomorphology*, 203, 6–24.
- Hathaway, J. C., Schlee, J. S., Poag, C. W., Valentine, P. C., Weed, E. G. A., Bothner, M. H., ... Schultz, D. M. (1976). Preliminary Summary of the 1976 Atlantic Margin Coring Project of the U.S. Geological Survey. USGS Open File Report 76-844, (November), 217.

- Hawkes, A. D., Kemp, A. C., Donnelly, J. P., Horton, B. P., Peltier, W. R., Cahill, N., ... Alexander, C. R. (2016). Relative sea-level change in northeastern Florida (USA) during the last ~8.0 ka. *Quaternary Science Reviews*, 142, 90–101.
- Hayes, M. O. (1991). Geomorphology and sedimentation patterns of tidal inlets. A review. *Coastal Sediments '91*; Volume 2, (April), 1343–1355.
- Hayes, M. O. (1994). The Georgia Bight Barrier System. In Richard A. Davis (Ed.), *Geology of Holocene Barrier Island Systems* (pp. 233–304). Springer-Verlag.
- Hayes, M. O., & Fitzgerald, D. M. (2013). Origin, Evolution, and Classification of Tidal Inlets. *Journal of Coastal Research*, (69), 14–33.
- Hayes, M. O., Sexton, W. J., Colquhoun, D. J., & Eckard, T. L. (1993). Evolution of the Santee/Pee Dee Complex, South Carolina, USA. In R. Kay & O. T. Magoon (Eds.), *Deltas of the World* (pp. 54–64). American Society of Civil Engineers.
- Heller, P. L., Wentworth, C. M., & Poag, C. W. (1982). Episodic post-rift subsidence of the United States Atlantic continental margin. *Geological Society of America Bulletin*, 93(5), 379–390.
- Hickin, E. J. (2004). Sediment transport. In *River Hydraulics and Channel Form*.
- Hockensmith, B. L. (2004). Flow and Salinity Characteristics of the Santee River Estuary , South Carolina. South Carolina Department of Natural Resources: Water Resources (Vol. 35).
- Hodge, J. A. (1977). Erosion of the North Santee River Delta and Development of a Flood-Tidal Complex. University of South Carolina.
- Hoitink, A. J. F., Nittrouer, J. A., Passalacqua, P., Shaw, J. B., Langendoen, E. J., Huismans, Y., & van Maren, D. S. (2020). Resilience of River Deltas in the Anthropocene. *Journal of*

- Geophysical Research: Earth Surface, 125(3), 1–24.
- Holbrook, J. (2001). Origin, genetic interrelationships, and stratigraphy over the continuum of fluvial channel-form bounding surfaces: An illustration from middle Cretaceous strata, Southeastern Colorado. *Sedimentary Geology*, 144(3–4), 179–222.
- Hopkins, E. M. (1971). Origin of capes and shoals along the southeastern coast of the united states: Discussion. *Bulletin of the Geological Society of America*, 82(1), 59–66.
- Horwitz, M. H., & Wang, P. (2005). Sedimentological Characteristics and Internal Architecture of Two Overwash Fans From Hurricanes Ivan and Jeanne. *Gulf Coast Association of Geological Societies Transactions*, 55, 342–352. Retrieved from
- Howard, J. D., & Frey, R. W. (1973). Characteristic Physical and Biogenic Sedimentary Structures in Georgia Estuaries. *AAPG Bulletin*, 57(7), 1169–1184.
- Hoyt, J. H., & Henry Vernon J. (1971). Origin of capes and shoals along the southeastern coast of the united states. *Bulletin of the Geological Society of America*, 82(1), 59–66.
- Hughes, Z. J. (2012). Tidal Channels on Tidal Flats and Marshes. In R.A. Davis & R. W. Dalrymple (Eds.), *Principles of Tidal Sedimentology* (pp. 269–300). Springer Science + Business Media.
- Hupp, C. R., Pierce, A. R., & Noe, G. B. (2009). Floodplain geomorphic processes and environmental impacts of human alteration along coastal plain rivers, USA. *Wetlands*, 29(2), 413–429.
- Ichaso, A. A., & Dalrymple, R. W. (2009). Tide- and Wave-generated Fluid Mud Deposits in the Tilje Formation (Jurassic) Offshore Norway. *Geology*, 37(July), 539–542.

- Jalon-Rojas, I., Schmidt, S., & Sottolichio, A. (2015). Turbidity in the fluvial Gironde Estuary (southwest France) based on 10-year continuous monitoring: Sensitivity to hydrological conditions. *Hydrology and Earth System Sciences*, 19, 2805–2819.
- Johnson, S. M., & Dashtgard, S. E. (2014). Inclined heterolithic stratification in a mixed tidal-fluvial channel: Differentiating tidal versus fluvial controls on sedimentation. *Sedimentary Geology*, 301, 41–53.
- Kana, T. W., Traynum, S. B., Gaudiano, D., & Kaczowski, H. L. (2013). The Physical Condition of South Carolina Beaches 1980-2010. *Journal of Coastal Research*.
- Kapsimalis, V., Masse, L., & Tastet, J. P. (2004). Sediment Transport in European Estuarine Environments. In P. Ciavola & M. Collins (Eds.), *Sediment Transport in European Estuarine Environments* (Vol. Special Is, pp. 1–12). Bologna, Italy: *Journal of Coastal Research*.
- Kemp, A. C., Horton, B. P., Corbett, D. R., Culver, S. J., Edwards, R. J., & van de Plassche, O. (2009). The relative utility of foraminifera and diatoms for reconstructing late Holocene sea-level change in North Carolina, USA. *Quaternary Research*, 71(1), 9–21.
- Kim, W., Paola, C., Swenson, J.B., and Voller, V.R. (2006). Shoreline Response to Autogenic Processes of Sediment Storage and Release in the Fluvial System. *Journal of Geophysical Research*, 111, 1-15.
- Kjerfve, B. (1976). The Santee-Cooper: A study of Estuarine Manipulations. *Estuarine Processes*, 1(36), 79–89.
- Kjerfve, B. . b, & Greer, J. E. . b. (1978). Hydrography of the Santee River during moderate discharge conditions. *Estuaries*, 1(2), 111–119.

- Kjerfve, B., Micher, W. K., & Gardner, L. R. (1994). Impacts of climate change in estuary and delta environments. *Impacts of Climate Change on Ecosystems and Species*, (August 2015), 31–43.
- Knighton, D. (1998). *Fluvial Forms & Processes*. New York, NY: Oxford University Press Inc.
- Kopp, R. E., Horton, B. P., Kemp, A. C., & Tebaldi, C. (2015). Past and future sea-level rise along the coast of North Carolina, USA. *Climatic Change*, 132(4), 693–707.
- La Croix, A. D., & Dashtgard, S. E. (2014). Of sand and mud: Sedimentological criteria for identifying the turbidity maximum zone in a tidally influenced river. *Sedimentology*, 61(7), 1961–1981.
- Leckie, R. M., & Olson, H. E. (2013). Foraminifera As Proxies for Sea-Level Change on Siliciclastic Margins. In H. E. Olson & R. M. Leckie (Eds.), *Micropaleontologic Proxies for Sea-Level Change and Stratigraphic Discontinuities*. SEPM Special Publication No. 75 (pp. 5–19). Society for Sedimentary Geology.
- LeGrand, H. E. (1961). Summary of Geology of Atlantic Coastal Plain. *AAPG Bulletin*, 45(9), 1557–1571.
- Leigh, D. S. (2006). Terminal Pleistocene braided to meandering transition in rivers of the Southeastern USA. *Catena*, 66(1–2), 155–160.
- Lewis, K. E., University of South Carolina. Institute of Archeology and Anthropology., & South Carolina. Dept. of Parks Recreation and Tourism. (1979). Hampton, Initial Archeological Investigations at an Eighteenth Century Rice Plantation in the Santee Delta, South Carolina. Research Manuscript Series, (no 151), 124 p.

- Lockhart, M. A. (2017). From Rice Fields to Duck Marshes : Sport Hunters and Environmental Change on the South Carolina Coast , 1890 – 1950 by. University of South Carolina.
- Long, A.M. and Hill, J.(2016). The influence of inherited topography and/or tectonics on paleo-channel systems and incised valleys offshore of South Carolina. American Geophysical Union Fall Conference, abstract #EP13B-1035
- Long, J. H. (2018). BOEM South Carolina Offshore Vibracore Description and Seismo-acoustic Integration Project: Summary. Columbia, SC.
- Long, J. H. (2019). BOEM Georgia Offshore Vibracore Description and Seismo-acoustic Integration Project Summary.
- Long, J. H., & Hanebuth, T. J. J. (2020). The Quaternary Stratigraphic Architecture of a Low-Accommodation, Passive-Margin Continental Shelf (Santee Delta Region, South Carolina, U.S.A). *Journal of Sedimentary Research*, *In Press*.
- Longhitano, S. G., Mellere, D., Steel, R. J., & Ainsworth, R. B. (2012). Tidal depositional systems in the rock record: A review and new insights. *Sedimentary Geology*, *279*, 2–22.
- Luciano, K., Howard, C. S., Wehmiller, J. F., Alexander, C. A., Long, J. H., Harris, M. S., ... Barbeau, D. (2019). Sedimentary Petrology and Geological Framework Investigations in the Southeastern U . S . Outer Continental Shelf. Final Report of Findings: Announcement M14AC00012. Prepared for the Department of Interior, Bureau of Ocean Energy Management. 34 pp.
- Luciano, K.E. (2010). Impacts of Underlying Stratigraphy, INlet Formation, and Geomorphology on Coastal Sediment Dynamics: Capers Inlet Quadrangle, SC (USA). Masters Thesis, The

College of Charleston.

- Luciano, Katherine E., & Harris, M. S. (2013). Surficial geology and geophysical investigations of the Capers Inlet, South Carolina (USA) 7.5-Minute Quadrangle. *Journal of Maps*, 9(1), 115–120.
- Mackin, J. (1948). Concept of the Graded River. *Geological Society of America Bulletin*, 59 (5), p. 463-512.
- MacNeil, S. (1949). Pleistocene Shore Lines in Florida and Georgia. Geological Survey Professional Paper 221-F. Washington, D.C.
- Marple, R. T., & Talwani, P. (2000). Evidence for a buried fault system in the Coastal Plain of the Carolinas and Evidence for a buried fault system in the Coastal Plain of the Carolinas and Virginia — Implications for neotectonics in the southeastern United States. *Geology*, 112(2), 200–220.
- Maslin, M., Stickley, C., and Ettwein, V. (2001). Holocene Climate Variability. *Encyclopedia of Ocean Sciences*, 1992, p. 1210-1217.
- Matteucci, T. D., & Hine, A. C. (1987). Evolution of the Cape Fear Terrace: A Complex Interaction Between the Gulf Stream and a Paleoshelf Edge Delta. *Marine Geology*, 77(3–4), 185–205.
- Mattheus, C. R., & Rodriguez, A. B. (2014). Controls on Lower-Coastal-Plain Valley Morphology and Fill Architecture. *Journal of Sedimentary Research*, 84, 314–325.
- Matthews, T. D., & Shealy, M. H. (1982). A Description of the Salinity Regimes of Major South Carolina Estuaries.
- Mayewski, P. A., Rohling, E. E., Stager, J. C., Karlén, W., Maasch, K. A., Meeker, L. D., ... Steig,

- E. J. (2004). Holocene climate variability. *Quaternary Research*.
- McCarney-Castle, K., Voulgaris, G., & Kettner, A. J. (2010). Analysis of Fluvial Suspended Sediment Load Contribution through Anthropocene History to the South Atlantic Bight Coastal Zone, U.S.A. *The Journal of Geology*, 118, 399–415.
- Meade, R. H., & Meade, R. H. (1982). Sources , Sinks , and Storage of River Sediment in the Atlantic Drainage of the United States Published by : University of Chicago Press Stable. *Journal of Geology*, 90(3), 235–252.
- Mellet, C. L., Hodgson, D. M., Plater, A. J., Mauz, B., Selby, I., & Lang, A. (2013). Denudation of the continental shelf between Britain and France at the glacial- interglacial timescale *Geomorphology Denudation of the continental shelf between Britain and France at the glacial – interglacial timescale. Geomorphology*, 203(July 2014), 79–96.
- Miall, A. D. (1985). Architectural-Element Analysis : A New Method of Facies Analysis Applied to Fluvial Deposits. *Earth-Science Reviews*, 22, 261–308.
- Miall, A. D. (1992). Alluvial Deposits. In R. G. Walker & N. P. James (Eds.), *Facies Models Revisited - Response to Sea Level Change* (1st ed., pp. 119–142). St. Johns, Newfoundland: Geological Association of Canada.
- Miall, A. D. (2010). *The Geology of Stratigraphic Sequences* (2nd ed.). Heidelberg, Dordrecht, London, New York: Springer-Verlag Berlin Heidelberg.
- Miall, A. D. (2014). The Facies and Architecture of Fluvial Systems. In A. D. Miall (Ed.), *Fluvial Depositional Systems* (pp. 9–69). Springer International Publishing.
- Mitchum Jr, R. M. (1977). *Seismic Stratigraphy and Global Changes of Sea Level Part Eleven:*

Glossary of Terms Used in Seismic Stratigraphy. In Charles E. Payton (Ed.), AAPG Memoir 26: Seismic Stratigraphy-Applications to Hydrocarbon Exploration (1st ed., pp. 205–221). Tulsa, OK.

Mitchum Jr, R. M., Vail, P. R., & Sangree, J. B. (1977). Seismic Stratigraphy and Global Changes of Sea Level, Part 6: Stratigraphic Interpretations of Seismic Reflection Patterns in Depositional Sequences. In C.E. Payton (Ed.), AAPG Memoir 26: Seismic Stratigraphy-Applications to Hydrocarbon Exploration (pp. 117–133). Tulsa, OK: The American Association of Petroleum Geologists.

Molina, M., McCarthy, J., Wall, D., Alley, R., Cobb, K., Cole, J., ... Shepard, M. (2014). What We Know-The Reality, Risks, and Response To Climate Change. AAAS “What We Know.”

Moslow, T. F., & Tye, R. S. (1985). Recognition and characterization of Holocene tidal inlet sequences. *Marine Geology*, 63(1–4), 129–151.

Moucha, R., Forte, A. M., Mitrovica, J. X., Rowley, D. B., Quéré, S., Simmons, N. A., & Grand, S. P. (2008). Dynamic topography and long-term sea-level variations: There is no such thing as a stable continental platform. *Earth and Planetary Science Letters*, 271(1–4), 101–108.

Muhs, D. R., Wehmiller, J. F., Simmons, K. R., & York, L. L. (2003). Quaternary sea-level history of the United States. *Developments in Quaternary Science*, 1(C), 147–183.

Mullin, P. R. (1973). *Facies of North Santee Inlet*. University of South Carolina.

Nixon, Z. (2004). *Wetland Vegetation Change in the Santee River Delta*. The Nature Conservancy: Report. Columbia, SC.

Nordfjord, S., Goff, J. A., Austin, J. A., & Sommerfield, C. K. (2005). Seismic geomorphology of

- buried channel systems on the New Jersey outer shelf: Assessing past environmental conditions. *Marine Geology*, 214(4), 339–364.
- Nummedal, D., & Fischer, I. A. (1978). Process-Response Models for Depositional Shorelines: The German and the Georgia Bights. In *Proceedings of the 16th Conference on Coastal Engineering* (p. 17). Hamburg, Germany.
- Orton, G. J., & Reading, H. G. (1993). Variability of Deltaic Processes in Terms of Sediment Supply, with Particular Emphasis on Grain Size. *Sedimentology*, 40, 475–512.
- Otvos, E. G. (2000). Beach ridges - definitions and significance. *Geomorphology*, 32(1–2), 83–108.
- Parsons, B., Swift, D. J., & Williams, K. (2003). Quaternary Facies Assemblages and Their Bounding Surfaces, Chesapeake Bay Mouth: An Approach to Mesoscale Stratigraphic Analysis. *Journal of Sedimentary Research*, 73(5), 672–690.
- Patterson, B. G., Cooney, T. W., & Harvey, R. M. (1996). Sediment Transport and Deposition in Lakes Marion and Moultrie , South Carolina, 1942-1985. U.S. Geological Survey Water-Resources Investigations Report 95-4236.
- Payne, M. W. (1970). *Geomorphology and Sediments of the Santee Delta*. University of South Carolina.
- Peltier, W. R. (1999). Global sea level rise and glacial isostatic adjustment. *Global and Planetary Change*, 20(2–3), 93–123.
- Pendleton, E. A., Brothers, L. L., Thieler, E. R., & Sweeney, E. M. (2017). Sand ridge morphology and bedform migration patterns derived from bathymetry and backscatter on the inner-

continental shelf offshore of Assateague Island, USA. *Continental Shelf Research*, 144(June), 80–97.

Peters, S.E. and Loss, D.P. (2012). Storm and Fair-weather Wave Base: A Relevant Distinction? *Geology*, 40 (6), p. 511-514.

Pettijohn, F. J., Potter, P. E., & Siever, R. (1987). *Sand and Sandstone* (2nd ed.). New York, NY: Springer Science + Business Media.

Popenoe, P., Henry, V. J., & Idris, F. M. (1987). Gulf trough - the Atlantic connection. *Geology*, 15(4), 327–332.

Popenoe, Peter. (1985). Cenozoic Depositional and Structural History of the North Carolina Margin from Seismic-Stratigraphic Analysis.

Posamentier, H. and Vail, P. (1988). Eustatic Controls on Clastic Deposition II-Sequence and Systems Tracts Models. In *Sea-level Changes: An Integrated Approach*, SEPM Special Publication No. 42, p. 125-154.

Potter, P. E. (1967). Sand Bodies and Sedimentary Environments: A Review. *AAPG Bulletin*, 51(3), 337–365.

Reading, H. G., & Collinson, J. D. (2006). Clastic Coasts. In H. G. Reading (Ed.), *Sedimentary Environments: Processes, Facies and Stratigraphy* (3rd ed., pp. 154–232). Malden, MA: Blackwell Science Ltd.

Reading, H. G., Levell, B. K., Collinson, J. D., Talbot, M. R., Allen, P. A., Kocurek, G. A., ... Orton, G. J. (2006). *Sedimentary Environments: Processes, Facies and Stratigraphy*. (H. G. Reading, Ed.).

- Reinick, H. E., & Singh, I. B. (1980). *Depositional Sedimentary Environments* (2nd ed.). Berlin: Springer-Verlag.
- Reynaud, J. Y., & Dalrymple, R. W. (2012). Shallow-marine tidal deposits. In *Principles of Tidal Sedimentology*.
- Richards, H. G. (1967). Stratigraphy of the Atlantic Coastal Plain Between Long Island and Georgia: Review. *AAPG Bulletin*, 51(12), 2400–2429.
- Riggs, S. R., Cleary, W. J., & Snyder, S. W. (1995). Influence of inherited geologic framework on barrier shoreface morphology and dynamics. *Marine Geology*, 126(1–4), 213–234.
- Roach, A. (2017). *Geological Framework of the Continental Shelf of South Carolina Winyah Bay : Paleodrainage , Transgressions and Essential Fish Habitat*. Unpublished MS thesis, Coastal Carolina University.
- Romans, B.W., Castellort, S., Covault, J.A., Fildani, A., and Walsh, J.P. (2016). Environmental Signal Propagation in Sedimentary Systems. *Earth-Science Reviews*, 153, p. 7-29
- Rovere, A., Raymo, M. E., Mitrovica, J. X., Hearty, P. J., O’Leary, M. J., & Inglis, J. D. (2014). The Mid-Pliocene sea-level conundrum: Glacial isostasy, eustasy and dynamic topography. *Earth and Planetary Science Letters*, 387, 27–33.
- Rowley, D. B., Forte, A. M., Moucha, R., Mitrovica, J. X., Simmons, N. a., & Grand, S. P. (2013). Dynamic topography change of the eastern United States since 3 million years ago. *Science*, 340(6140), 1560–1563.
- Ruby, C. H. (1981). *Clastic Facies and Stratigraphy of a Rapidly Retreating Cuspate Foreland, Cape Romain, South Carolina*. University of South Carolina.

- Schumm, S. A., & Ethridge, F. G. (1994). Origin, Evolution, and Morphology of Fluvial Valleys. In Robert W. Dalrymple, R. L. Boyd, & B. A. Zaitlin (Eds.), *Incised-Valley Systems: Origin and Sedimentary Sequences*. SEPM Special Publication No. 51 (pp. 11–29). Tulsa, OK: SEPM (Society for Sedimentary Geology).
- Schwartz, R. K. (1982). Bedform and Stratification Characteristics of Some Modern Small-scale Washover Sand Bodies. *Schwartz, 1982. Sedimentology*, 29, 835–849.
- Sexton, W. J., & Hayes, M. O. (1996). Holocene deposits of reservoir-quality sand along the central South Carolina coastline. *AAPG Bulletin*, 80(6), 831–855.
- Sexton, W. J., Hayes, M. O., & Colquhoun, D. J. (1992). Evolution of Quaternary Shoal Complexes Off the Central South Carolina Coast. *Quaternary Coasts of the United States*, 48, 161–172.
- Shen, Z., Wright, E., Loh, B., & Mauz, B. (2017). Resolving the Controversy of Pleistocene Shoreline Deposits in the Lower Coastal Plain in Northeastern South Carolina. In 2017 GSA Southeastern Section Meeting (p. Oral Presentation).
- Smith, D. G., Hubbard, S. M., Leckie, D. A., & Fustic, M. (2009). Counter point bar deposits: Lithofacies and reservoir significance in the meandering modern peace river and ancient McMurray formation, Alberta, Canada. *Sedimentology*, 56(6), 1655–1669.
- Smoak, E. (2016). Small Mud and Sand Filled Paleochannels Offshore Charleston , SC. University of South Carolina.
- Snedden, J. W., & Dalrymple, R. W. (1999). Modern Shelf Sand Ridges: From Historical Perspective To a Unified Hydrodynamic and Evolutionary Model. In K. M. Bergman & J. W.

- Snedden (Eds.), *Isolated Shallow Marine Sand Bodies: Sequence Stratigraphic Analysis and Sedimentological Interpretation*, SEPM Special Publication No. 64 (pp. 13–28). Tulsa, OK.
- Snedden, J. W., Tillman, R. W., & Culver, S. J. (2011). Genesis and Evolution of a Mid-Shelf, Storm-Built Sand Ridge, New Jersey Continental Shelf, U.S.A. *Journal of Sedimentary Research*, 81(7), 534–552.
- Stanley, D. J., & Warne, A. G. (1994). Worldwide Initiation of Holocene Marine Deltas by Deceleration of Sea-Level Rise. *Science*, 265, 228–231.
- Stanley, D. J., & Warne, A. G. (1997). Holocene Sea-Level Change and Early Human Utilization of Deltas. *GSA Today*, 7(12), 1–6.
- Stedman, S., & Dahl, T. E. (2008). Status and Trends of Wetland in the Coastal Watersheds of the Eastern United States 1998-2004.
- Stephens, D. G. (1973). *Sedimentary and Faunal Analyses of the Santee River Estuaries*. University of South Carolina.
- Stephens, D. G., Van Nieuwenhuise, D. S., Mullin, P., Lee, C., & Kanes, W. H. (1976). Destructive phase of deltaic development; North Santee River delta. *Journal of Sedimentary Petrology*, 46(1), 132–144. <https://doi.org/10.1306/212f6ed8-2b24-11d7-8648000102c1865d>
- Suter, J. R. (2006). Facies Models Revisited : Clastic Shelves. In *Facies Models Revisited*. SEPM Specialial Publication SEPM No. 84 (pp. 339–397). Tulsa, OK.
- Swezey C.S. (2020) Quaternary Eolian Dunes and Sand Sheets in Inland Locations of the Atlantic Coastal Plain Province, USA. In: Lancaster N., Hesp P. (eds) *Inland Dunes of North America. Dunes of the World*. Springer, Cham

- Swift, D. J. (1975). Tidal sand ridges and shoal-retreat massifs. *Marine Geology*, 18(3), 105–133.
- Swift, D. J., Mckinney, T. F., Stahl, L., Key, V., & Florida, M. (1984). Recognition of Transgressive and Post-Transgressive Sand Ridges on the New Jersey Continental Shelf: Discussion. In *SEPM Special Publication 34: Siliclastic Shelf Sediments* (pp. 25–36).
- Swift, D. J., Phillips, S., & Thorne, J. A. (1991). Sedimentation on Continental Margins, IV: Lithofacies and depositional Systems. In D. J. P. Swift, G. F. Oertel, R. W. Tillman, & J. A. Thorpe (Eds.), *Shelf Sand and Sandstone Bodies: Geometry, Facies, and Sequence Stratigraphy. Special Publication Number 14 of the International Association of Sedimentologists* (1st ed., pp. 89–152). London: Blackwell Scientific Publications.
- Switzer, A. D., & Jones, B. G. (2008). Large-scale Washover Sedimentation in a Freshwater Lagoon from the Southeast Australian Coast: Sea-level Change, Tsunami or Exceptionally Large Storm. *The Holocene*, 18(5), 787–803.
- Syvitski, J. P. M., Kettner, A. J., Overeem, I., & Hutton, E. W. H. (2009). Sinking Deltas due to Human Activities. *Nature Geoscience*, (January 2014), 681–686.
- Taylor, M., & Stone, G. W. (2013). Beach-Ridges: A Review. *Journal of Coastal Research*, 12(3), 612–621.
- Tessier, B. (1998). Tidal Cycles: Annual Versus Semi-lunar Records. In C. A. Alexander & R. A. Davis (Eds.), *Tidalites: Processes and Products*, *SEPM Special Publication No. 61* (pp. 69–74). Tulsa, OK: Society for Sedimentary Geology.
- Thieler, E. R., Foster, D. S., Himmelstoss, E. A., & Mallinson, D. J. (2014). Geologic framework of the northern North Carolina, USA inner continental shelf and its influence on coastal

- evolution. *Marine Geology*, 348, 113–130.
- Torres-garcia, L. M. (2014). *Flow Dynamics in the Transition Zone from Estuarine Tidal to Fluvial Regime in the Santee River, SC, USA*. University of South Carolina.
- Torres, R. (2017). Channel geomorphology along the fluvial-tidal transition, Santee River, USA. *GSA Bulletin*, 129(11/12), 1681–1691.
- Toscano, M. A., Kerhin, R. T., York, L. L., Cronin, T. M., & Williams, S. J. (1989). Quaternary stratigraphy of the inner continental shelf of Maryland. Report of Investigations No. 50.
- Toscano, M. A., & Macintyre, I. G. (2003). Corrected western Atlantic sea-level curve for the last 11,000 years based on calibrated 14C dates from *Acropora palmata* framework and intertidal mangrove peat. *Coral Reefs*, 22(3), 257–270.
- Vakarelov, B. K., & Bruce Ainsworth, R. (2013). A hierarchical approach to architectural classification in marginal-marine systems: Bridging the gap between sedimentology and sequence stratigraphy. *AAPG Bulletin*, 97(7), 1121–1161.
- Van De Plassche, O., Wright, A. J., Horton, B. P., Engelhart, S. E., Kemp, A. C., Mallinson, D., & Kopp, R. E. (2014). Estimating tectonic uplift of the Cape Fear Arch (south-eastern United States) using reconstructions of Holocene relative sea level. *Journal of Quaternary Science*, 29(8), 749–759.
- Walker, R. L., & Tenore, K. R. (1984). Growth and Production of the Dwarf Surf Clam *Mulinia lateralis* (Say 1822) in a Georgia Estuary. *Gulf Research Reports*, 7(4), 357–363.
- Warner, J. C., Armstrong, B., Sylvester, C. S., Voulgaris, G., Nelson, T., Schwab, W. C., & Denny, J. F. (2012). Storm-induced inner-continental shelf circulation and sediment transport: Long

Bay, South Carolina. *Continental Shelf Research*, 42, 51–63.

Weems, R. E., Gohn, G. S., & Houser, B. B. (1987). Additions and Revisions to the Auger Hole Records for the Cainhoy and Charleston Quadrangles, South Carolina.

Weems, R. E., & Lemon. (1999). Geology of the Bethera, Cordesville, Huger, and Kittredge Quadrangles, Berkeley County, SC. Weems and Lemon.

Weems, R. E., & Lemon, E. M. (1985). Detailed Sections from Auger Holes and Outcrops in the Cainhoy, Charleston, and Fort Moultrie Quadrangles, South Carolina. USGS Open File Report 85-378.

Weems, R. E., Lemon, E. M., Gohn, G. S., & Houser, B. B. (1985). Detailed Sections from Auger Holes and Outcrops in the Ladson, Moncks Corner, Mount Holly, and Stallville Quadrangles, South Carolina.

Weems, R. E., Lemon, E. M., Gohn, G. S., & Houser, B. B. (1987). Detailed Sections from Auger Holes and Outcrops in the Clubhouse Crossroads, Johns Island, Osborn, and Ravenel Quadrangles, South Carolina. USGS Open File Report 87-661.

Weems, R. E., Lemon, E. M., Nelson, M. S., Gohn, G. S., & Houser, B. B. (1987). Detailed Sections from Auger Holes and Outcrops in the Pringletown, Ridgeville, Summerville Northwest, and Summerville Quadrangles, South Carolina. USGS Open File Report 87-524, (December).

Weems, R. E., & Lewis, W. C. (1997). Detailed Geologic Sections from Auger Holes in Northeastern Charleston County, South Carolina, east of 79 45 West Longitude. US Geological Survey Open-File Report 97-712-A (Vol. Open-File). Reston, VA.

- Weems, R. E., & Lewis, W. C. (2002). Structural and tectonic setting of the Charleston, South Carolina, region: Evidence from the Tertiary stratigraphic record. *Bulletin of the Geological Society of America*, 114(1), 24–42.
- Weems, R. E., Lewis, W. C., & Lemon, E. M. (2014). Surficial Geologic Map of the Charleston Region, Berkeley, Charleston, Colleton, Dorchester, and Georgetown Counties, South Carolina (Vol. USGS Open-).
- White, R. E. (1987). *Introduction to the Principles and Practice of Soil Science*.
- Willard, D.A., Bernhardt, C.E., Korejwo, D.A., and Meyers, S.R. (2005). Impact of Millennial-scale Climate Variability on Eastern North American Terrestrial Ecosystems: Pollen-based Climatic Reconstruction. *Global and Planetary Change*, 47, p. 17-35.
- Williams, H. F. L. (2015). Contrasting styles of Hurricane Irene washover sedimentation on three east coast barrier islands: Cape Lookout, North Carolina; Assateague Island, Virginia; and Fire Island, New York. *Geomorphology*, 231, 182–192.
- Wilson, C., Goodbred, S., Small, C., Gilligan, J., Sams, S., Mallick, B., & Hale, R. (2017). Widespread infilling of tidal channels and navigable waterways in the human-modified tidal delta plain of southwest Bangladesh. *Elementa*, 5.
- Wright, E., Kruse, S., Forman, S. L., & Harris, M. S. (2017). Millennial Scale Development of a Southeastern United States Spit. *Journal of Coastal Research*, 342, 255–271.
- Zecchin, M., Catuneanu, O., & Caffau, M. (2019). Wave-ravinement surfaces: Classification and key characteristics. *Earth-Science Reviews*, 188(November 2018), 210–239.
- Zeff, M. L. (1988). Sedimentation in a salt marsh-tidal channel system, southern New Jersey.

Marine Geology, 82(1–2), 33–48.

Zhang, X., Dalrymple, R. W., & Lin, C. M. (2018). Facies and stratigraphic architecture of the late Pleistocene to early Holocene tide-dominated paleo-Changjiang (Yangtze River) delta. *Bulletin of the Geological Society of America*, 130(3–4), 455–483.

Appendix A. Sediment Core Inventory

Core Name	Length (m)	Core Type	Area
ACN-PC-01	2.23	Push Core	Santee Delta
ACN-PC-02	0.80	Push Core	Santee Delta
CAN-01-V01	3.84	Vibracore	Santee Delta
CAN-02-V01	3.92	Vibracore	Santee Delta
CAT-01-V01	5.40	Vibracore	Santee Delta
CDR-01-V01	3.82	Vibracore	Santee Delta
CDR-01-V02	4.74	Vibracore	Santee Delta
CDR-02-V01	1.00	Vibracore	Santee Delta
CDR-04-V01	4.63	Vibracore	Santee Delta
GA-BOEM-2015-VC01	4.76	Vibracore	Cumberland Island
GA-BOEM-2015-VC03	5.03	Vibracore	Cumberland Island
GA-BOEM-2015-VC05	5.37	Vibracore	St. Simons Island
GA-BOEM-2015-VC06	5.43	Vibracore	St. Simons Island
GA-BOEM-2015-VC07	5.30	Vibracore	St. Simons Island
GA-BOEM-2015-VC09	5.73	Vibracore	Ossabaw Island
GA-BOEM-2015-VC11	4.91	Vibracore	Ossabaw Island
GA-BOEM-2015-VC11A	1.53	Vibracore	Ossabaw Island
GIO-PC-01	1.83	Push Core	Santee Delta
MRP-01-P01	0.60	Push Core	Santee Delta
MRP-01-P02	0.50	Push Core	Santee Delta
MRP-01-P03	0.55	Push Core	Santee Delta
MRP-01-P04	0.60	Push Core	Santee Delta
MRP-01-P05	0.50	Push Core	Santee Delta
MRP-01-V01	4.23	Vibracore	Santee Delta
MRP-02-V01	6.04	Vibracore	Santee Delta
NSB-10-V01	4.23	Vibracore	Santee Delta
NSB-10-V02	5.22	Vibracore	Santee Delta
NSB-22-V01	3.85	Vibracore	Santee Delta

NSB-22-V02	3.05	Vibracore	Santee Delta
NSR-11-V01	0.30	Vibracore	Santee Delta
NSR-30-V01	4.50	Vibracore	Santee Delta
NSR-PC-01	1.12	Push Core	Santee Delta
NSR-PC-02	1.52	Push Core	Santee Delta
SC-BOEM-2015-VC01	5.55	Vibracore	Hilton Head
SC-BOEM-2015-VC04	5.79	Vibracore	Kiawah Island
SC-BOEM-2015-VC06	6.10	Vibracore	Kiawah Island
SC-BOEM-2015-VC07	5.49	Vibracore	Kiawah Island
SC-BOEM-2015-VC14	5.49	Vibracore	Kiawah Island
SC-BOEM-2015-VC15	5.18	Vibracore	Kiawah Island
SC-BOEM-2015-VC18	5.79	Vibracore	Kiawah Island
SC-BOEM-2015-VC19	5.49	Vibracore	Kiawah Island
SC-BOEM-2015-VC20	6.10	Vibracore	Kiawah Island
SC-BOEM-2015-VC21	5.79	Vibracore	Kiawah Island
SC-BOEM-2015-VC22	5.39	Vibracore	Cape Romain
SC-BOEM-2015-VC23	2.66	Vibracore	Cape Romain
SC-BOEM-2015-VC24	5.36	Vibracore	Cape Romain
SC-BOEM-2015-VC25	0.91	Vibracore	North Myrtle Beach
SC-BOEM-2015-VC26	3.05	Vibracore	North Myrtle Beach
SC-BOEM-2015-VC27	3.05	Vibracore	North Myrtle Beach
SC-BOEM-2015-VC28	1.52	Vibracore	North Myrtle Beach
SC-BOEM-2015-VC29	1.22	Vibracore	North Myrtle Beach
SC-BOEM-2015-VC30	0.91	Vibracore	North Myrtle Beach
SCI-01-V01	3.40	Vibracore	Santee Delta
SCI-01-V02	1.93	Vibracore	Santee Delta
SCI-02-V01	3.04	Vibracore	Santee Delta
SCI-03-V01	4.16	Vibracore	Santee Delta
SOU-01-V01	5.46	Vibracore	Santee Delta
SOU-02-V01	3.00	Vibracore	Santee Delta
SOU-03-V01	2.21	Vibracore	Santee Delta

SOU-03-V02	1.67	Vibracore	Santee Delta
SSR-10-V01	1.72	Vibracore	Santee Delta
SSR-30-V01	1.64	Vibracore	Santee Delta
SSR-PC-01	1.39	Push Core	Santee Delta
ACN-PC-01	2.23	Push Core	Santee Delta
ACN-PC-02	0.80	Push Core	Santee Delta

Appendix B. Related Reports and Project Summaries

Bureau of Ocean Energy Management (BOEM) Projects

Long, J.H., 2018, SCGS-BOEM South Carolina Offshore Vibracore Description and Seismo-acoustic Integration Project: Summary Report. 49 pp.

Long, J.H., and Venherm, C., 2019, BOEM Georgia Offshore Vibracore Description and Seismo-acoustic Integration Project Summary Final Report. 42 pp.

Alexander, C., **Long, J.H.**, and Venherm, C., 2019, Geospatial Sand Resource Assessment for Georgia Coastal Recovery and Resiliency-Phase II, Resource Identification, Delineation, and Management Practices Agreement M14AC00005: Georgia Cooperative Agreement. Draft Technical Report to Bureau of Ocean Energy Management, 83 pp.

Luciano, K., Howard, S., Wehmiller, J., Alexander, C., **Long, J.H.**, Harris, S.M., Corbett, D.R., Conery, I., Mallinson, D., and Barbeau, D., 2019. Sedimentary Petrology and Geological Framework Investigations in the Southeastern U.S. Outer Continental Shelf. Final Report of Findings to the Bureau of Ocean Energy Management, Announcement M14AC00012. 34 pp.

South Carolina Geological Survey (SCGS) Projects

Hanebuth, T.J.J. and **Long, J.H.**, 2019, Santee Point Quadrangle Mapping, Final Report. Project Summary Report to the South Carolina Geological Survey. 9 pp.

Hanebuth, T.J.J., **Long, J.H.**, and Lüdmann, T., 2019, Georgetown Pilot-Deep Seismic Study. Project Summary Report to the South Carolina Geologic Survey. 12 pp.

Continental Slope of Uruguay and Argentina Research Cruise, Sedimentology Group

Kasten, S., Schwenk, T., Aromokeye, D., Baques, M., Baumann, K.-H., Bergenthal, M., Bösche, J., Bozzano, G., Brune, R., Bülden, J., Chiessi, C.M., Coffinet, S., Crivellari, S., Dehning, K., Dohrmann, I., Dröllner, M., Düßmann, R., Durica, J.T., Frederichs, T., Garcia Chaporí, N., Gonzalez, L., Hanebuth, T.J.J., Hilgenfeldt, C., Hüttich, D., Jones, C.K., Klann, M., Klar, S., Klein, T., Kockisch, B., Köster, M., Lantzsich, H., Linowski, E., **Long, J.H.**, Melcher, A.-C., Ogunleye, O.J., Pereyra, N., Rehage, R., Riedinger, N., Rosiak, U., Schmidt, W., Schnakenberg, A., Spieß, V., Steinmann, L., Thieblemont, A., Volz, J., Warnke, F., Warratz, G., Wenau, S., Zonneveld, K.A.F., 2020, Dynamics of sedimentation processes and their impact on biogeochemical reactions on the continental slope off Argentina and Uruguay (MARUM) Cruise No. SO260/Leg 1 & Leg2, 195 pp.

Appendix C. Conference Presentations

Long, J.H. and Hanebuth, T.J.J., 2017, Late Quaternary stratigraphic architecture of the Santee River Delta, South Carolina, U.S.A. Coastal & Estuarine Research Federation National Meeting, Providence, RI: Abstract B096.

Long, J.H. and Hanebuth, T.J.J., 2017, Late Quaternary stratigraphic architecture of the Santee River Delta, South Carolina, USA. American Geophysical Union, Fall National Meeting 2017, New Orleans, LA: Abstract #EP21B-1853.

Long, J.H., Hanebuth, T.J.J., and Lüdmann, T., 2018, Following the river: Quaternary valleys of the Santee River as integral components of a regional stratigraphic framework. American Geophysical Union, Fall Meeting 2018, Washington, DC: Abstract #EP21B-2221.

Long, J.H., Hanebuth, T.J.J., Alexander, C.A., and Luciano, K., 2019, A Quaternary stratigraphic framework for the Santee Delta region of the Atlantic Coastal Plain and Inner Continental Shelf, South Carolina, U.S.A.: Geological Society of America Abstracts with Programs, v. 51, no. 3, ISSN 0016-7592.

Long, J.H., Hanebuth, T.J.J., and Lüdmann, T., 2019, A Quaternary stratigraphic framework for the Santee Delta region of the Atlantic Coastal Plain and Inner Continental Shelf of South Carolina: Geological Society of America Abstracts with Programs, v. 51, no. 3, ISSN 0016-7592.

Luciano, K., Tweel, A., Harris, M.S., **Long, J.**, Howard, C.S., and Sanger, D., 2019, Estimating potential volumes and onshore compatibility of surficial and shallow sand resources on the near (3-8 nm) Outer Continental Shelf offshore of South Carolina: Geological Society of America *Abstracts with Programs*, v. 51, no. 3, ISSN 0016-7592.

Long, Joshua H. and Hanebuth, Till J.J., 2020, The Quaternary Stratigraphic Architecture of a Low Accommodation, Passive-Margin Shelf (Santee Delta, SC, U.S.A.), Geological Society of America Joint Northeastern Southeastern Regional Meeting, Reston, VA, Abstract 6-10. (*Cancelled*)

Shen, Z., Hanebuth, T.J.J., Muñoz, S., **Long, J.H.**, Larese-Casanova, P., and Fernandez, L., 2020, Source-to-sink mobilization of sediments and contaminants by Hurricane Florence, ECU and NCEM Hurricane Conference (*Cancelled*)